

**COMPUTATIONAL STUDY OF KLANG VALLEY'S
URBAN CLIMATOLOGY, AND URBANISATION
OF PUTRAJAYA CITY, MALAYSIA**

KENOBI ISIMA MORRIS, BEng.

**Thesis submitted to the University of Nottingham for the degree of
Doctor of Philosophy**

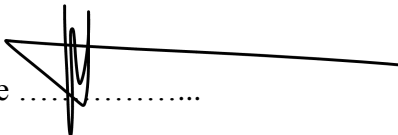
APRIL 2016

AUTHOR'S DECLARATION

I hereby declare that I am the sole author of this thesis and have performed all of the work presented herein. I also declare that this work has not been submitted in any form for another degree at any other university or institution of tertiary education.

All information derived from published or unpublished works of others have been duly acknowledged in the text and provided in the list of references.

Kenobi Isima Morris

Signature

Date: 20 April 2016

Abstract

Urbanisation is associated with physical modifications of land surfaces and climate of a given area. Studies of urbanisation effect on urban climate for Klang Valley region is below par. This research aims to bridge the gap by using a coupled *Weather Research and Forecasting (WRF) model with the NOAA Land Surface Model (NOAH) and Urban Canopy Model (UCM) – WRF/NOAH/UCM* to investigate the urban climatology of Klang Valley and the urbanisation of Putrajaya over a decade. In addition, evaluation of the garden city concept adopted in the development of Putrajaya city is also conducted. The model is first validated against a network of meteorological observations in the region to determine its suitability for urban climate investigations. Climatological variables (near-surface temperature, relative humidity, and wind speed) along with land use and land cover (LULC) changes; planetary boundary layer height (PBLH), and urban heat/cool islands (UHI/UCI) of the area are also investigated. The model evaluation shows good performance over the region. LULC changes demonstrates strong influence in thermal climatology variations. A mean maximum UHI intensity of ~ 4.2 °C was observed in the urban canopy-layer of the Klang Valley.

Results reveal that urbanisation of Putrajaya leads to 2-m temperature increase at the rate of ~ 1.66 °C per decade, with the area experiencing a mean UHI intensity of ~ 2.1 °C per day. Other climatological variables vary accordingly with the urbanisation processes.

Evaluation of the garden city concept indicates that the adopted concept causes a reduction in 2-m air temperature of the Putrajaya area, amounting to ~ 0.53 °C per day; with vegetation contributing more (~ 0.39 °C) to the daily reduction relative to water bodies (~ 0.14 °C). Location of the city in the tropics accustomed with high intensity of daily solar radiation masked the cooling potentials of the concept to some extent.

List of publications

Results of this thesis are published and presented in the following journals, conference proceedings:

Journal peer-reviewed articles:

K.I. Morris, A. Chan, M.C.G. Ooi, M.Y. Oozeer, Y.A. Abakr, K.J.K. Morris. Effect of vegetation and waterbody on the garden city concept: An evaluation study using a newly developed city, Putrajaya, Malaysia. *Computers, Environment and Urban Systems*, 58, pp. 39 – 51, 2016.

K.I. Morris, A. Chan, M.C-G. Ooi, S. Aekbal Salleh, Y.A. Abakr, M.Y. Oozeer. Numerical study on the urbanisation of Putrajaya and its interaction with the local climate, over a decade. *Urban Climate*, 16, pp. 1 - 24, 2016.

K.I. Morris, S. Aekbal Salleh, A. Chan, M.C.G. Ooi, Y.A. Abakr, M. Y. Oozeer, M. Duda. Computational study of urban heat island of Putrajaya, Malaysia. *Sustainable Cities and Society*, 19, pp. 359 – 372, 2015.

K.I. Morris, S. Aekbal Salleh, A. Chan, M.C.G. Ooi, Y.A. Abakr, M.Y. Oozeer, M. Duda. Integrating Weather Research and Forecasting Model, Noah Land Surface Model and Urban Canopy Model for Urban Heat Island Effect Assessment. *British Journal of Environment and Climate Change*, 5(3), pp. 231 - 253, 2015.

Conference and workshop presentations:

Morris, K.I. M.C-G. Ooi, A. Chan, Y.A Abakr, S.A. Salleh, M.Y. Oozeer, M. Duda. Numerical study on urban heat island of the city of Kuala Lumpur, Malaysia, using weather research and forecasting (WRF) model. *Urban Environmental Pollution 2014: Climate Change and Urban Environment*, 2014, Sheraton Centre, Toronto, Canada, pp. P2.05.

Morris, K.I. M.C-G. Ooi, A. Chan, Y.A Abakr, S.A. Salleh, M. Duda. Urban heat island of Putrajaya. In *Proceedings of 2nd Postgraduate Colloquium For Environmental Research 2013 (POCER2013)* held in Genting Highland, 28th – 29th June, pp. ID-083. Awana Hotels and Resorts, Genting Highland, Malaysia.

Morris, K.I. M.C-G. Ooi, A. Chan, Y.A Abakr, S.A. Salleh, M. Duda. Influence of Urbanisation on Urban Heat Island Effects in Putrajaya, Malaysia. In *Proceedings of 12th International Conference on Atmospheric Sciences and Applications to Air Quality* held in Seoul, 3rd – 5th June 2013, edited, Chung, Y.S. & Yoon, S.C., pp. S8-1. Seoul, Seoul National University and Korea Centre for Atmospheric Research.

Morris, K.I. M.C-G. Ooi, A. Chan, Y.A Abakr, S.A. Salleh. Urbanisation and Urban Heat Island (UHI): The Putrajaya case study. Poster presentations, *Malaysia Aerospace Mission Workshop*, March 18-22, 2013, KLTC Kuala Lumpur, Malaysia.

I dedicate this work to my late beloved sister, Eroli Precious Onyebuchi

(Nee Morris)

Acknowledgements

To God Almighty be the glory for the success of this PhD journey. It is Him who has granted me grace, unmerited favour and above all faithfulness during this period. I ascribe all honours and praises to Him.

I would like to express gratitude to my supervisors Prof. Andy Chan and Dr Yousif Abdalla Abakr. Their inspiration, enthusiasm, support and guidance during this period cannot be overstated. Regular meetings and Prof. Andy's philosophy of graduate student independence has enriched me scientifically and strengthened my self-sufficiency. Indeed, it has been a journey worth all its steps.

I am thankful to the Faculty of Engineering, University of Nottingham Malaysia Campus and again Prof. Andy Chan, for awarding me academic excellent scholarship during the program leading to this thesis. I would also like to acknowledge support through the e-Science fund of the Ministry of Science, Technology and Innovation (MOSTI) with contract number M0056.54.01, and the University of Nottingham for access to the University of Nottingham High Performance Computing Facility for part of the numerical calculations.

To Maggie and Yaasiin who have been wonderful research team members and their contributions to my research are unquantifiable. I am grateful for answering and replying my late night calls and chats, respectively. To Dr Siti A Salleh and Dr. Michael Duda, I am thankful for your support and assistance on land use classifications and WRF configurations, respectively.

To My friends and research colleagues: Otuami Obiga, George Edward G. Njoroge, Mohammed S. Haruna, Ejikeme R. Ezeigwe, Eliasu Mumuni and the endless list. I say thank you for being there when I needed you.

My family, you have been the best one could ever ask for and I am grateful for your encouragements and prayers all through this period. I thank God for blessing me with such a family.

Finally, and most importantly, my beautiful wife (Mrs. Kwami J K Morris), I am thankful for your patience, unconditional support, always being at my need and for being my editor-in-chief for all my manuscripts. You are the best. I love you.

Contribution of others:

Prof. Andy Chan is the principal supervisor of this work; directed and guided me all throughout the research. Dr. Yousif Abdalla Abakr is the secondary supervisor and his contributions are immeasurable. Ms. Maggie Chel Gee Ooi and Mr. Muhammad Yaasiin Oozeer are my research team members and were always available for brainstorming and discussion on model configurations. Dr Siti Aekbal Salleh of the Faculty of Architecture, Planning and Surveying, Universiti Teknologi MARA, Selangor, Malaysia, helped in land use and land cover classification, and guidance on ArcGIS usage. Finally, Dr. Michael Duda of the National Centre for Atmospheric Research, Boulder, Colorado, United States of America has assisted me greatly on WRF model and associated libraries installations and configurations.

List of Figures

Fig. 1:1. Schematic of different climate scales and vertical layers found in urban areas (Oke 2006)	12
Fig. 1:2. Schematic of the garden city concept surrounded by other self-contained and functioned garden cities (Howard 1898).....	15
Fig. 1:3. Housing at Letchworth garden city, Hertfordshire, England (TCPA 2011)..	16
Fig. 1:4. Thesis flowchart; showing a graphical representation of the relationship and dependence among the different chapters	19
Fig. 2:1. WPS flowchart (Source: http://www2.mmm.ucar.edu)	22
Fig. 2:2. Example of WRF domain configuration	23
Fig. 2:3. Share section of the <i>namelis.wps</i> file	26
Fig. 2:4. WRF system components (Skamarock & Klemp 2008)	28
Fig. 2:5. Simplified flowchart for WPS and WRF (source: http://ruc.noaa.gov/wrf/)	31
Fig. 2:6. NOAA/UCM in WRF	34
Fig. 2:7. Print screen of a sample of in-process WTOOLS land use on Google Earth Pro for grids/fields modifications	36
Fig. 2:8. Example of Klang Valley 2-m temperature and wind speed plot using NCL for 24th September, 2011 at 05 00 MST	36
Fig. 2:9. Netcdf4Excel example during operation.....	37
Fig. 2:10. Klang Valley encompassing Putrajaya and Kuala Lumpur (Malaysia Department of Statistics 2010).....	43
Fig. 3:1. Model domain configuration: (a) 3 one-way nested domain (top panel), and (b) finest domain (d03) terrain height and the map of Klang Valley (bottom panel). Water body along the Strait of Malacca has been masked.....	50
Fig. 3:2. Land-use-cover for: (a) MODIS (left panel) – used as the inaccurate urban representation of GKL (MURB) – left panel, and (b) Updated urban land surface with 2011 satellite data (URB) to represent the true surface characteristics of GKL – right panel.	52
Fig. 3:3. Average meteorological conditions of the study region for September 2011; Blue contour lines (Sea level pressure, hPa), black arrows (wind fields, ms-1),	

spread contour (relative humidity, %) and the area with shaded green boundary (Klang Valley).	57
Fig. 3:4. (a) The diurnal profile of anthropogenic heat used in the single-layer UCM (top left panel); the ratio to the peak value of each urban land-use-cover type. Peak values for each urban type are given in Table 3:1. Averaged model validation: (b) 2-m temperature (top right panel), (c) 2-m relative humidity (bottom left panel) and (d) 10-m wind speed (bottom right panel).....	60
Fig. 3:5. Averaged (a) PBLH in m (left panel), (b) Sensible heat flux – SH (middle panel), and (c) Latent heat flux – LH, for the simulated period (right panel). SH and LH are calculated in Wm^{-2}	62
Fig. 3:6. Averaged temporal variations of meteorology of the GKL: (a) Sensible heat flux (Wm^{-2}) – top left panel, (b) latent heat flux (Wm^{-2}) – top right panel, (c) Planetary boundary layer height (m) – bottom left panel, and (d) 2-m relative humidity (%) – bottom right panel.....	63
Fig. 3:7. Averaged wind field (ms^{-1}) above the simulated domain demonstrating local sea and land breezes at fully developed stages: (a) land-sea breeze (left panel) and (b) sea-land breeze (right panel). LT is the Malaysian Local Time used in this study	67
Fig. 3:8. Spatiotemporal variation of relative humidity above the surface during: (a) morning (left panel), (b) daytime (middle panel) and (d) nighttime (right panel)	69
Fig. 3:9. Averaged temporal variations of: (a) 2-m temperature (left panel) and (b) canopy layer urban heat island (URB+AH minus NOURB), in $^{\circ}C$ (right panel). The bottom panels represent the spatial distribution and variation of the simulated average (a) 2-m temperature in $^{\circ}C$ (left panel) and 2-m urban heat island intensity (right panel). “D” in the UHII legend substitutes URB+AH – because of limited space accommodate URB+AH.	70
Fig. 3:10. Average spatial distribution and temporal changes of 2-m temperature and urban heat island intensity. Top panels represent temperature during: (a) morning (left), (b) daytime (middle) and (c) nighttime (right), while bottom panels represent UHII during: (d) morning (left), (e) daytime (middle) and (f) nighttime (right). “D” on the legend of each case is used to substitute URB+AH, due to limited space on the each plots.	71
Fig. 4:1.(a) Klang Valley showing Putrajaya and Kuala Lumpur (Top panel). (b) Putrajaya precincts (bottom panel)	84
Fig. 4:2. WRF model domain configuration (image to the left) and terrain height for the finest domain (d04) and Putrajaya Map	85
Fig. 4:3. Model validation for near-surface urban climate variables; (a) 2-m air temperature, (b) model biases for 2-m temperature, (c) 2-m RH, (d) model biases for RH, (e) 10 m wind speed, and (f) model bias for 10 m wind speed.....	95

Fig. 4:4. (a) Putrajaya meteorological station - CAC 053 and (b) mean wind speed prediction and error bars for the finest domain (d04)	98
Fig. 4:5. Mean predictions of Putrajaya meteorological station (d04) for; (a) 2-m temperature and (b) 2-m RH	99
Fig. 4:6. Land use and land cover for 1999 (top left), 2003 (top right), 2007 (lower left) and 2011 (lower right).....	101
Fig. 4:7. Percentage; (a) coverage of each land use class and (b) change of each land use class from the preceding year	102
Fig. 4:8. Model simulated mean surface energy components.....	106
Fig. 4:9. Mean diurnal profile of surface energy components for 1999	108
Fig. 4:10. (a) 2-m air temperature and (b) changes in 2-m temperatures for the years experimented.....	109
Fig. 4:11. Mean WRF 2-m temperature for 1999 (upper left), 2003 (upper right), 2007 (lower left), and 2011 (lower right)	111
Fig. 4:12. Mean model 10-m wind speed for 1999 (upper left), 2003 (upper right), 2007 (lower left), and 2011 (lower right)	114
Fig. 4:13. Mean simulated relative humidity for 1999 and 2011.....	115
Fig. 4:14. Mean annual (a) PBLH and (b) urban - rural UHII, for each year considered	116
Fig. 4:15. Mean simulated nurban UHI for (a) 1999 - upper left, (b) 2003 - upper right, (c) 2007 - lower left and (d) 2011 - lower right.....	121
Fig. 5:1. Putrajaya: (a) WRF domain configuration, (b) Land use, (c) Terrain height and (d) zoomed in d02 and d03.....	131
Fig. 5:2. Model evaluation for Putrajaya station (d03) from 0100 MST for 48 h	138
Fig. 5:3. (a) Putrajaya with grid cells and (b) mean diurnal T2m over Putrajaya during the investigated period	139
Fig. 5:4. (a) Land use and land cover coverage for each of the simulated cases, and mean surface energy balance components for: (b) case 1, (c) case 2 and (d) case 3	141
Fig. 5:5. Mean diurnal profile of urban fraction-induced difference in meteorological variables between the experimented scenarios and the control conditions of the area: (a) T2m, (b) RH2m, (c) PBLH and (d) Q2m.....	143

Fig. 5:6. Mean diurnal variations of 2-m temperature over Putrajaya; (a) images to the left (case 1), (b) middle (case 2) and (c) images to the right (case 3)	146
Fig. 5:7. Evaluation of vegetation and waterbody on T2m. (a) case 2-1 (effect of waterbody) and (b) case 3-1 (effect of vegetation)	149
Fig. 5:8. (a) UHI estimation and (b) PBLH for the different scenarios tested.....	150
Fig. 5:9. Simulated spatiotemporal variations of UHI: (a) case 1, (b) case 2 and (b) case 3.....	152
Fig. 5:10. Mean simulation spatiotemporal difference in Q2m due to changes in urban fraction: (a) case 2-1 (left) and (b) case 3-1 (right).....	154
Fig. 0:1. Depiction of the ARW η coordinate system (Skamarock et al. 2008)	197

List of Tables

Table 1:1. Chronological evaluation of urban climate effect approaches (Mills (2014)	10
Table 3:1. Urban surface parameters used in the UCM for each urban land-use-cover type (Shahidan et al. 2012; Salleh et al. 2012; Ahmed et al. 2015; Salleh et al. 2015). Data obtained from literature are supplemented with data from onsite observations, GIS, geospatial techniques, and google earth.	55
Table 3:2. Measurement site metadata	56
Table 3:3. Statistical summary of model validation for the different experiments.....	59
Table 4:1. Stations metadata.....	86
Table 4:2 Model evaluation statistics for near surface variables.....	96
Table 4:3. Summary of different land use and land coverage categories of Putrajaya.	99
Table 4:4. Reclassified land use and land cover coverage of Putrajaya area.....	103
Table 4:5. Changes in land use and land cover of the Putrajaya external boundaries	104
Table 4:6. Summary of mean surface energy budget components from model simulations	104
Table 4:7. Summary of 2-m temperature for each year	112
Table 4:8. Mean summary of WRF simulated Relative humidity	114
Table 4:9. Properties of lulc categories used in the model (Chng et al. 2010; Salleh et al. 2013; Tehrany et al. 2013)	117
Table 5:1.Observational sites metadata	137
Table 5:2. Model evaluation for 2-m temperature (°C) on d02 and d03 from 0100 MST for 48 h.....	137
Table 5:3. Model evaluation for 2-m Relative humidity (%) on d02 and d03 from 0100 MST Or 23/09/2011 for 48 h	138
Table 5:4. Mean surface energy balance components for the different scenarios during the study period.....	141

ABSTRACT	i	
list of publications	ii	
acknowledgements	iv	
list of figures	vii	
list of tables	xi	
1 Introduction	1	
1.1 Urbanisation	1	
1.2 Urban climatology	6	
1.3 Green city and garden city concept (GCC)		13
1.4 Objectives	16	
1.4.1 Aim	16	
1.4.2 Specific objectives	16	
1.5 Significance of the study	17	
1.6 Thesis Outline	18	
2 Methodology and analytical tools descriptions		21
2.1 WRF Pre-processing System (WPS)		21
2.1.1 Geogrid (geogrid.exe)	23	
2.1.2 Ungrib (ungrib.exe)	24	
2.1.3 Metgrid (metgrid.exe)	25	
2.2 Weather Research and Forecasting (WRF) model		26

2.2.1	Advanced Weather Research and Forecasting (ARW) model - WRFARW	28
2.2.1.1	Real (real.exe)	29
2.2.1.2	Wrf (wrf.exe)	30
2.3	NOAH Land Surface Model (NOAH LSM)	31
2.4	Urban Canopy Model (UCM)	32
2.5	Other Post-processing, GIS and analysis tools	33
2.5.1	ArcGIS	34
2.5.2	WTOOLS	35
2.5.3	Google Earth Pro	35
2.5.4	NCAR Command Language (NCL)	36
2.5.5	NetCDF4Excel	37
2.5.6	OriginPro	38
2.6	Input and validation data	38
2.6.1	Input data	38
2.6.1.1	NCEP Final analysis (FNL) data	38
2.6.1.2	Static Geographic data	39
2.6.2	Meteorological data	40
2.7	Study location	40

2.7.1	Klang Valley	41
2.7.2	Putrajaya	42
2.8	Conclusions	43
3	Evaluation of NOAH LSM/UCM coupled to WRF, and study of urban climatology of Klang Valley	45
3.1	Introduction	46
3.2	Study design	48
3.2.1	Study area	48
3.2.2	Model and experimental design	50
3.3	Model validation, results and discussions	58
3.3.1	Model validation	58
3.3.2	Results and discussions	62
3.3.2.1	Urban surface energy balance and PBLH	62
3.3.2.2	Wind speed	66
3.3.2.3	Relative humidity	67
3.3.2.4	2-m temperature and urban heat island	69
3.4	Conclusion	74
4	Urbanisation of Putrajaya and its interactions with the local climate	76
4.1	Introduction	77
4.2	Methodologies	81

4.2.1	Background information and study site description	82
4.2.2	Meteorological data	86
4.2.3	Model details, numerical settings and experimental design	87
4.3	Model evaluation	91
4.3.1	Near-surface urban climate parameters	93
4.4	Results and Discussions	99
4.4.1	Land use and land cover data sets	99
4.4.2	Surface energy balance	104
4.4.3	2-m air temperature	108
4.4.4	Relative humidity and wind speed	112
4.4.5	PBLH and UHI	115
4.5	Conclusions	121
5	Computational evaluation of the garden city concept adopted in the development of a tropical city - Putrajaya, Malaysia	124
5.1	Introduction and background information	125
5.2	Study area description and planning concept	128
5.2.1	Study area	128
5.2.2	PC planning concept	130
5.3	Methodology and model evaluation	131

5.3.1	WRF/Noah/UCM	133
5.3.2	Numerical settings and model initialisation	134
5.3.3	Model validation	136
5.4	Results and discussions	139
5.4.1	Surface energy balance	140
5.4.2	T2m and RH2m	142
5.4.3	UHI	149
5.5	Conclusions	154
6	Conclusion	156
6.1	Suggestions for further studies	158
	References	161
	Appendix	190

Chapter 1

1 Introduction

1.1 Urbanisation

Urbanisation is the process by which rural communities grow and expand into urban cities, and by extension conurbation. The earliest reported record of urbanisation was the ancient city of Mesopotamia during the period 4300 – 3100 BCE (Mark 2014). It is induced by humans because of migration and strives for better living conditions and survival. The process of urbanisation is associated with changes in political, economic, social, and environmental dynamics (Davis 1955).

The world is currently confronted with the vague yet significant problems posed by urbanisation to the environment (Dodman 2009). Our environment is changing; urban cities lower atmospheres and water bodies are polluted (Satterthwaite 2009; Huang et al. 2013), canopy layer temperatures are on the rise (Jones et al. 2008; Qu et al. 2013), farm and agricultural lands are altered to urban forms (Winfield 1973; Zhou et al. 2004; Marcotullio et al. 2008; Schneider et al. 2009), increased energy consumption and emission (S. Wang et al. 2014), surface energy balance – especially sensible heat and precipitation are modified in urban areas thus, perturbation in spatial variability in thunderstorm occurrence (Lin et al. 2008; Shem & Shepherd 2009; Miao et al. 2010), increase in population density of urban areas resulting from rural and

peri-urban migration thereby exacerbating the pressure on the limited resources to sustain urban metabolism (Newman 1999; Kennedy et al. 2007; Kennedy et al. 2011). According to Pidwirny (2006) “*climatologists have measured about up to 10% more rainfall in urban areas. This increase may be due to the combined effect of particulate air pollution and increased convective uplift. Air pollution may enhance rainfall by increasing the number of condensation nuclei through the atmospheric addition of smoke and dust particles. The additional generation of heat within the city increases the number of convection currents over that surface. Convection is required to initiate the development of thunderstorms*”. The impact of urbanisation is not only felt on the climatological and environmental perspectives but also in behavioural sense. Hence, urbanisation has been linked with altered human behaviour (Widodo 2012; Salleh et al. 2012). For instance, increased crime rate is reported in Soh's (2012) and Montoya (2015) modelling of the relationship between crime rate and urbanisation in the Netherlands.

The accompanying problems with urbanisation are speculated to escalate. In 2008, for the first time in human history, human population residing in urban areas was reported to exceed that in the rural areas, with projections for continual increase in urban residents (Heilig 2012; United Nations 2014). The noticed overshoot in urban population was predicted in 1955 by Davis (1955); where he states emphatically “*that the process of urbanisation has moved rapidly in the entire world since 1800, and the peak is not yet in sight*”. This increase in population is expected to come from developing countries such Brazil, China, Indonesia, India, Mexico and Nigeria (United Nations 2014).

Urbanisation rates vary globally relative to a country's population. United States of America (USA) and the United Kingdom (UK) have higher urbanisation rates compared to other countries (New World Encyclopedia 2010). However, they have far less annual urban growth rates since a smaller proportion of their population still reside in the rural areas. Examples of cities that have experienced high growth rate in the last three decades include: Seoul, South Korea; Lagos, Nigeria; Beihai, China; Ghaziabad, India; Sana'a, Yemen; Kabul, Afghanistan; Bamako, Mali; and Dar es Salaam in Tanzania (Heilig & United Nations 2012).

Urbanisation in Malaysia started in earlier centuries before the arrival of the British colonial era (18th century). Prior to the British era, urban settlement in the form of empire was mainly concentrated in the Melaka region that has already established kingdom and leadership (Hadi et al. 2011). During the British era, urban centres were primarily occupied by colonial masters and serve as administrative centres to administer law and order to sustain the exploitation of tin and rubber production, in addition to the provision of goods and services (Hadi et al. 2011). The British marked urbanisation in Malaysia was followed by the pseudo-urbanisation phase, characterised by rural youths (mostly male) migration to the urban centres to seek for limited jobs. This took place after the second World War (Hirschman 1976). The most prominent urbanisation transition witnessed in Malaysia was the outcome of the New Economic Policy (NEP), 1970 and subsequent developmental policies that follow the NEP, 1970. The growing extent of the mega-urban regions stretching from Bernam river basin on the Perak-Selangor border to the Linggi river basin bordering Negeri Sembilan (Gullick 2003) and Melaka, and the

further expansion of the Klang Valley (Yaakob et al. 2010; Masron et al. 2012).

Urbanisation in Malaysia is defined and gazetted by the Department of Statistics, and used in the Population Census of 1970, 1980, 1991, and 2000. It defines urban area as having a population of 10,000 or more and/or gazetted area with their adjoining built-up areas and combination of both areas having a total population of 10,000 or more (Malaysia Department of Statistics 2010). A study conducted by Masron et al. (2012) on the spatial distribution of urban cities in Malaysia using analysis of geographical information system (GIS) from 1957 - 2000, shows that there has been about 400% increase in urban settlement resulting from cities sprawling from existing urban cities to cities from pure vegetated areas such as the Putrajaya city (Moser 2010; Chin 2006; Morris et al. 2015b). Penang, Melaka, the Klang Valley (Kuala Lumpur, Shah Alam, Petaling Jaya, Subang Jaya, Putrajaya, Cheras, Kajang, Selayang Baru), Johor Baru, Ipoh, Negeri Sembilan, Kuantan, George Town, etc., are some of the cities that have experienced tremendous urban expansion and increased population in the past 40 years (Department of Statistics Malaysia (DSM) 2010; Masron et al. 2012).

Industrialisation and urbanisation are intertwined in the case of Klang Valley expansion and continual urban growth. Rural Malays and Chinese migration to the Valley for better paychecks and living conditions triggered an extension of already developed urban cores in the region, such as Kuala Lumpur, especially in the 1970s (Choo & Taylor 1986). Most of the migrants could only afford to reside in the peripherals of the existing urban cores which prompt the development and further expansion of the peripherals (e.g., TTDI

Jaya in Shah Alam, Selangor, Kampung Haji Abdullah Hukom in Kuala Lumpur, and Subang Jaya in Selangor) to accommodate the migrating population into the region (Choo & Taylor 1986; Yusoff 2007).

The attitude of migrants opting to reside in outskirts and peripherals of cities caused a slowdown in the projected population of major Malaysian cities (Shuid 2004). For instance, Kuala Lumpur recorded 1.29 million population according to the 2000 population census, 0.9 million shortfalls of *Kuala Lumpur Structure Plan 2000* initiated in 1984 (Dewan Bandaraya Kuala Lumpur 2000) projection. Shuid (2004) in his study on *Urbanisation and housing in Kuala Lumpur City Centre* opined that failure of Kuala to achieve projected population was not wholly due to rural migrants behaviour to reside in peripherals of the cities because of their prevailing economic situations but urban dwellers migrating to the city's outskirt for cheaper and yet comfortable housing and living conditions.

Putrajaya, a city within the Klang Valley, on the other hand, could be described as a city without urban history (Kho & Low 1998; Chin 2006; Moser 2010; Morris et al. 2015a). Unlike other urban city resulting gradually as a result of human migration in search of good and healthy living conditions, industrialisation, proximity to seaports and other viable reasons to attract labour migration (Karl et al. 1988; Hill 1995; Yaakob et al. 2010), Putrajaya emergence was solely the idea of Dr. Tun Mahathir, former Prime Minister of Malaysia in the mid-1980s. He conceived an idea of building a city to represents Malaysia culture, pride, independence and departure from the colonial master and self-sufficiency (Moser 2010). This is reflected in the landmarks and Malay laden architectures that emblemise the city. In the early

1990s the then densely populated palm and rubber farm formerly part of the Selangor statutory control was seceded to the government to be the newly federal capital – administrative (Chin 2006). The nascent city in the late 1990s, however, metamorphosed to today's celebrated garden and intelligent city. Its population has grown from less than 3000 in 1995 to approximately 70,000 as reported by the 2010 population census (Malaysia Department of Statistics 2010). Detail descriptions of the Putrajaya are given in Chapters 4 and 5 while the Klang Valley Chapter 3 of this report.

1.2 Urban climatology

Because of changes of natural land cover and soil surfaces, urban cities have a profound impact on the immediate overlying and surrounding atmosphere. Modifications in urban form have direct impacts on gaseous emission, alteration of thermal heating budget, urban heating, air pollution, urban boundary layer (UBL) modifications, water vapour availability, and materials that attend to human activities (urban metabolism) (Elgin & Oyvat 2013; Henderson & Venables 2009; Han et al. 2014; Kennedy et al. 2011). **Urban climatology** is the field of climatology that deals with urban effect on the immediate overlying, surrounding, and the atmosphere at large, and application of this knowledge to improve urban planning, design, provide guidelines for urbanisation and development to mitigate the associated problems of urbanisation. Urban climatology and meteorology are often interchanged in their usage. Though similar, they differ in temporal coverage. Urban climatology is not a standalone field as it incorporates aspects of many different fields ranging from meteorology, climatology, architecture, urban

design, air pollution science, biometeorology, and other related disciplines. It is noteworthy that each of these disciplines has its own established focus and developed distinct tools and methodologies suitable for their interests (Mills 2014; Hebbert 2014). Thus, most of the knowledge drawn from different disciplines that form the body of urban climatology is still fragmented and in its infancy stage with an effort to assimilate and put together a field of study with coherence in the process (Mills 2006; Mills 2014).

The fundamental motivation in the field of urban climatology is drawn from Albert Kratzer statement of purpose in his doctoral thesis – *Climate of Cities (Das Stadtklima)* (Kratzer 1956); “*Only when we possess sufficient knowledge of the bright and dark sides of city climate are we in a position to use this information and to formulate a technique for city construction based on considerations of climate. Yet something is already accomplished when we realise that we do not have to accept city climate simply as a fact but can influence it*”.

The scientific history of urban climatology can be traced to Luke Howard first publication on *The Climate of London* which contained continuous daily surface observations of London from 1801 (Howard 1818b), where he deduced the changing trend of London overlying thermal climate relative to its rural to the tune of $\sim 1.579^\circ$. Though the work could hardly be criticised because of the limited data and temporal coverage of the observations available, it is however not deterministic in its estimations of London (urban temperature, T_U) and suburbs (rural temperature, T_R) thermal variations (ΔT_{U-R}) and non-representative of the cities but the vantage of London and the outside London where the stations were situated (Mills 2014). Howard’s work established the

premise of the difference that exists between urban and rural thermal climates resulting from differential urbanisation processes which could hardly be disputed. It was not until the early 1970s that Lowry (1977) developed an empirical approach and formulated the problems inherent in examining the *urban effect* on the overlying atmosphere. He identified three different components in any set of measurements; (1) the background climate, (2) the effects of the local climate, and (3) the effects of the local urbanisation.

$$\Delta T_{U-R} = T_U - T_R \quad \text{Eq. 1:1}$$

In an ideal investigation of the urban effect on the thermal condition measured (Eq. 1:1), there should be continuous set observations prior to and after urbanisation processes, thus, the unique contribution of urban effect on the climatology could easily be identified and extracted. However, Howard's pilot studies and most observational studies today (Howard 1818a; Howard 1820; Grimmond 2006; Mirzaei & Haghghat 2010; Arnfield 2003) are based on *urban* and *rural* sites designations in pre-existing urban and rural conditions. This, however, could hardly be avoided owing to the limitation in awareness of the *urban effect* on the local and regional weather and climate 40 – 60 years ago. Hence, observational study of the *urban effect* could be conducted and its impact estimated by accurately planning and designing the techniques to be used prior to the development of any city. For instance, the city of Putrajaya, Malaysia, could have served the best purpose since it was built from originally farm and agricultural lands.

Evolution of the approaches used in studying the urban climatology is classed here into two eras; prior to 1970s and after the 1970s. Prior to 1970s,

most of the studies done on the subject were in Central Europe within the context of landscape studies and microscale climatology (Mills 2014). For example, Geiger's first publication on the subject "*The climate near ground*" which appeared in German language in 1927 but only published in English language during the mid-1960s (Geiger 1965; Gloyne & Geiger 1967). Geiger (1965) studies were followed by Kratzer (1956) comprehensive studies on the *Climate of Cities* published in German in 1937 and appeared in English in the late 1950s. Relatively, there were fewer studies on these topics elsewhere. A decade later, Balchin & Pye (1947), investigated the *local effect* (including that of towns) in Britain, Sundborg (1950) studied the urban heat island (UHI) around the city of Lund in Sweden with great effort to understand the effect at the city scale; Okita (1960) in Japan during winter to understand the wind speed variable and observe the urban effect across Asahikawa city, and Chandler's work on *Climate of London* in 1965 and reprinted by Oke (2009) marked the urban climate evolving trend prior to the 1970s.

After the 1970s there shows a significant increased awareness of the *urban effect* on the city climate and a subsequent increase in number of investigators with changing perspectives (Mills 2014). This period is dominated by studies in the Anglo-American region populated by physical geographers and thus adoption of quantitative and systematic approaches to the research on urban climate. Examples of such studies are Myrup (1969); Oke (1973); Johnson et al. (1973); Lowry (1974); Terjung & Louie (1974); Terjung (1976); Oke (1976); Nunez & Oke (1977); Lowry (1977b); Oke (1981); Oke (1982); Arnfield (1982); and Oke (1984). The current state of urban climatology is dominated by numerical modelling of urban environment with

more dependence on computer processing power (Hebbert 2014). Improved computer power has caused improvements in the scale and sophistications of computer models, development of new models to accommodate microscale phenomena, urban surface (Chen et al. 2004), land cover descriptions (Chen et al. 1996; Mitchell et al. 2005), material properties and geometry and functions that defined different types of urban neighbourhood (Tewari et al. 2007; Chen et al. 2011; Wang et al. 2015). Furthermore, improvements in urban scale climatology due to computer modelling have been matched with developments in modelling hierarchy of climate scales (see Fig. 1:1); from global to regional, and to mesoscale, now capable of including the presence of cities to varying degrees, for example (Masson 2000; McCarthy et al. 2010; Gsella et al. 2014; Chen et al. 2014)

Table 1:1. Chronological evaluation of urban climate effect approaches (Mills (2014))

Time period	Approach
1900	Observation and description of urban effects using conventional meteorological equipment (thermometers, hygrometers, etc.)
1960	Move toward measurement of 'process' variables – radiation, sensible and latent heat exchanges. The use of statistical methods to summarise and generalise results
1970	Application of conventional (micro-)meteorological theory to urban climates. Use of energy budget as a framework to explain the urban effect. Observation of process variables: radiation, estimated fluxes. Use of computer modelling techniques. More rigorous definition of urban 'surface', urban scales and observing urban effects
1980	Adoption of an experimental approach: Select common urban forms (streets become canyons). Use of scaled-physical models and direct measurement of fluxes
1990	Relationships between real urban forms and climate effect. Urban field projects examined by research teams. Generalizations based on a range of settlements
2000	Development of realistic urban climate models. Employment of novel techniques for examining urban climate

Table 1:1 highlights and summarises development and approaches used in investigating the urban climate effects prior to and after the 1970s. While Fig. 1:1 shows the different climate spatial scales in urban climate studies. The urban boundary layer – the lower layer of the atmosphere in direct interactions with the earth surface (Stull 1988; Barlow 2014). This is another aspect of

urban climatology that has drawn considerable attention in recent times (e.g., Oke 1995; Arnfield 2003; Tong et al. 2005; Salamanca et al. 2011; Pichelli et al. 2014; Barlow et al. 2014; Barlow 2014). Fig. 1:1 describes and distinguishes between the three scales of effect and as well highlights the processes that dominate in each of these scales.

From the nascent stage and today growing interest in the field of urban climatology, tropical countries (especially Malaysia and Singapore) have seen little effort trying to understand the urban effect on local and region climates. Probably the first documented English published literature in the field of urban climatology in the tropics was Nieuwolt (1966) research on *The urban microclimate of Singapore* between 1964/65 followed by Sham Sani pioneering studies in Malaysia (Sani 1972; 1973; 1980; 1984b, 1986; 1990; 1991b; 1993; 1994; 1998). In 1972, Sani conducted a short-term (2 days) study to investigate the climate of Kuala Lumpur, Malaysia, and observed that the core was generally warmer and drier than the rural surroundings (Sani 1972). These findings were later confirmed by additional mobile measurements (Sani 1973). This gave rise to Sani continual interest and other related studies in urban climate of the region.

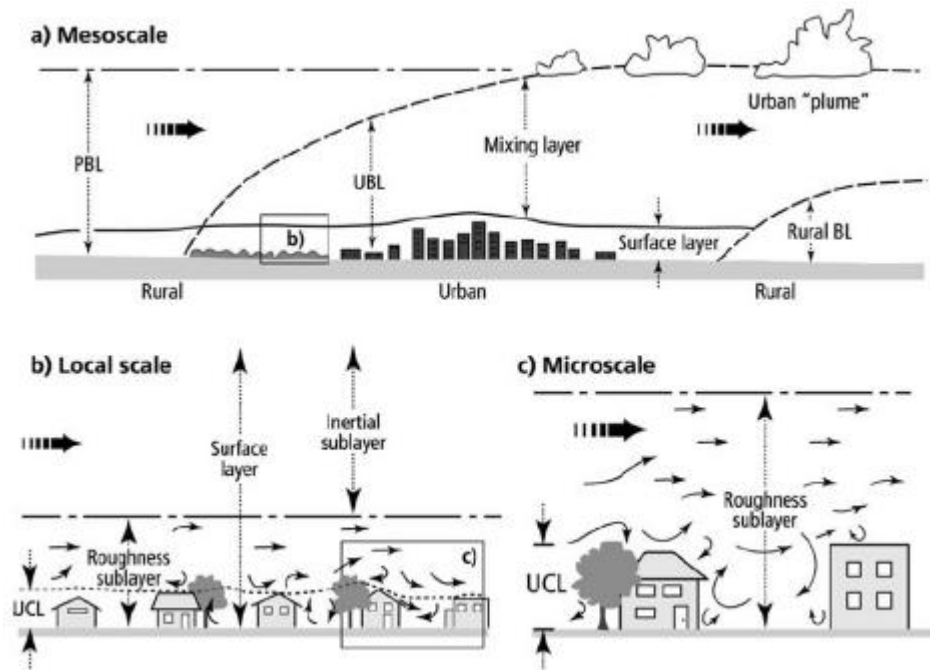


Fig. 1:1. Schematic of different climate scales and vertical layers found in urban areas (Oke 2006)

Summary of a decade research conducted in Malaysia from Sani (1972) pioneering investigation on the UHI of Kuala Lumpur is reported in Sani (1983). The investigation paved the way for future research (e.g., Sani 1984a, 1994, Ahmad et al. 2009, Ahmad et al. 2010, Ibrahim & Samah 2011, Elsayed 2012, Yusuf et al. 2014) in urban climate with emphasis on UHI formation around Kuala Lumpur. Further studies note increase in maximum UHI intensity (UHII) between 1972 and 1980 and reduced significance of wind speed in controlling night-time UHII (Sani 1990; Sani 1991a) relative to mid-latitude cities (Chow & Roth 2006). He argued that mindfulness of these findings in design and building of urban cities will reduce the resulting influence of urbanisation in the region (Sani 1991b).

Despite the few studies to understand the urban climate in the region (Klang Valley), most of which have been concentrated in the Kuala Lumpur axis with emphasis on UHI formation. As of the time of reporting, only three

studies (Chng et al. 2010; Tehrany et al. 2013; Shaharuddin et al. 2014) have been conducted on urban climate over the region with limited scope on the urban climatology. For instance, Chng et al. (2010) numerically investigate the impact of improved land use on MM5 predictions with latent effort on the climatological parameters of the region; Tehrany et al. (2013) on the other hand, used remote sensing approach to investigate variations in urban land use of the region on the land surface temperature; while Shaharuddin et al. (2014) study was on the impact of UHI on thermal comfort of Klang Valley. However, relative to urban climate studies over the Valley, there is proliferation of air pollution and air quality studies (e.g., Lodhi et al. 1997; Awang et al. 2000; Hashim et al. 2004; Azmi et al. 2010; Varikoden et al. 2011; Juneng et al. 2011a; Juneng et al. 2011b; Singh 2014; Ahamad et al. 2014; Jamhari et al. 2014; Rahman et al. 2015). The flooding of air quality and pollution studies is likely due to the consistent haze occurrence over the Valley's atmosphere caused by transboundary transport of smoke resulting from bush burning within Malaysia and neighbouring countries (such as Indonesia and Thailand) (Othman et al. 2014; Ashfold et al. 2015). Deficiency in the investigation and understanding of the general urban climate of Klang Valley has necessitated the current study to bridge the knowledge gap. In this study, urban climate parameters not limited to air temperature are investigated.

1.3 Green city and garden city concept (GCC)

The quest for a better urban environment without environmental problems associated with urbanisation and industrialisation is one of the motivated factors for the adoption of sustainable urban planning. This has become

imperative due to different factors: urban inhabitants, government, and strong advocates from climatologists in the mid and late 20th century such as Helmut Landsberg in his famous and undying list of meteorological principles (Landsberg 1973) that must begin to penetrate the annals of planning process of urban environment. For instance, reduction in in-town automobile emissions; increase green space for evapotranspirational cooling and run-off reduction; halt in building on flood plains; not sacrificing shade trees for traffic flow; recognising urban heat as a potential health hazard; and mindfulness of aggravating the outdoor heat load through reliance on indoor air-conditioning (Landsberg 1973). These efforts result in the green concept integrated into city design and planning practices in use around the globe today as demonstrated in recent literature (Caruso et al. 2015; Haaland & van den Bosch 2015)

The garden city concept proposed by Sir Ebenezer Howard (Howard 1898) in 1898 was inspired by Edward Bellamy's *Utopian novel "looking Backward: 2000 – 1887"* (Bellamy 1888). It is an urban planning approach where cities are planned to be, self-contained communities surrounded by greenbelts, and containing carefully balanced residential areas, industry and agriculture (see Fig. 1:2). The concept has influenced some cities around the globe during the 20th centuries such as; Baldwin Hills Village in Los Angeles and Walkerville, Ontario, in Canada (New World Encyclopedia 2010). French Dakar city, Senegal (Bigon 2012); Chengdu, China (Zhao 2012) and the recently developed city of Putrajaya in Selangor, Malaysia (Moser 2010; Morris et al. 2015a; Morris 2016). Fig. 1:3 is an example of a street view of implemented GCC in Hertfordshire, England.

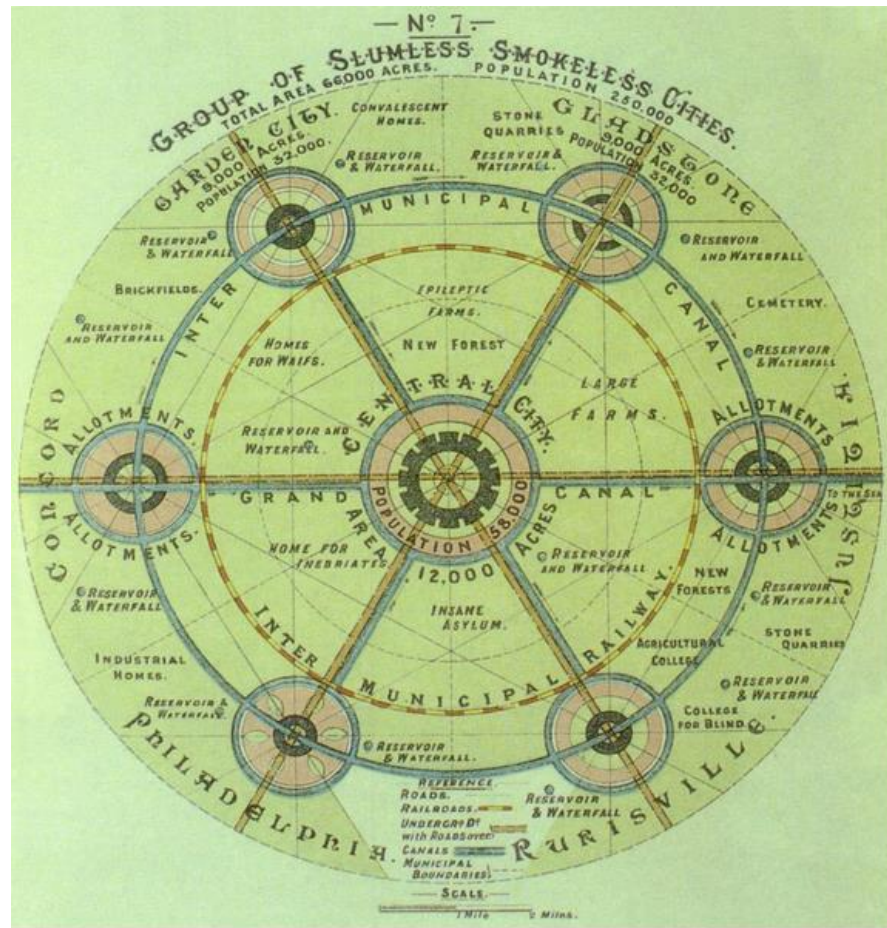


Fig. 1:2. Schematic of the garden city concept surrounded by other self-contained and functioned garden cities (Howard 1898)

Despite the growing popularity and adoption of the concept from its inception to today current strive for better urban environmental and climatic conditions, there is no existing scientific literature with dedicated studies on evaluation of the GCC in mitigating problems posed by urbanisation and industrialisation in cities, which is the primary objective of its adoption. Thus, the present study aims to evaluate the concept using the nascent tropical city of Putrajaya recently developed from a pure farm and agricultural lands, from 1995 to 2011 as a case study. The study also investigates individual contributions of some of the natural elements (water and greenery) integrated into the concept to the overall thermal performance of the garden city approach

in reducing the urban thermal conditions of Putrajaya. This is achieved by comparing the present urban climate of the city with other neighbouring tropical cities and numerically manipulating the land cover of the Putrajaya city to represent different scenarios that enable investigation of the different natural elements implemented during the development of the city.



Fig. 1:3. Housing at Letchworth garden city, Hertfordshire, England (TCPA 2011)

1.4 Objectives

1.4.1 Aim

To computationally study the urban climatology of Klang Valley and urbanisation of Putrajaya City, Malaysia.

1.4.2 Specific objectives

1. To evaluate Weather Research and Forecasting (WRF) model suitability for urban climate study in Klang Valley region.
2. To investigate the urban climate of Klang Valley using WRF.

3. To study the microclimate of Putrajaya city and investigate the existence of urban heat island in the city.
4. To investigate climate and environmental changes accompanying the urbanisation of Putrajaya.
5. To evaluate the effectiveness of the adopted garden city concept in the development of Putrajaya city to mitigate elevated thermal conditions associated with urbanisation; with emphasis on two natural elements (greenery and water body) integrated into the concept.

1.5 Significance of the study

1. Experimental and data collection cost which could linger into months and cost millions of dollars, as well as spatial coverage limitations inherent with *in-situ* studies, could be reduced by successful implementation of the coupled WRF/NOAH LSM/UCM models (freeware) in the area.
2. Findings of this study will help urban planners, designers, ecologists, environmental scientists, governmental and non-governmental bodies in proper planning, updating of current guidelines and design methods for building sustainable and livable urban cities.
3. The study will help economists make reliable decisions when embarking on green city projects.
4. The study outcomes will provide platforms for future urban climate research in the region.
5. Knowledge of spatial and temporal variations of UHI and solar intensity in the region are necessary for urban pedestrians.

6. Results of the study, especially on the garden city concept evaluation are necessary to justify the cost and sustainable aim of the Putrajaya City.
7. Spatial and temporal variations of a city thermal climate and boundary layer depth influence pollution dispersion greatly. Thus, readily available information is necessary should there be a need to model the spread of any outbreaks in the city. Here, the study findings will bridge this gap.
8. Findings of this study will help in urban and evolving cities planning, formulation of urban development strategies and evaluation of existing policies on urban development towards mitigation of urbanisation induced problems.

1.6 Thesis Outline

This thesis is structured into six independent yet intertwined chapters (see Fig. 1:4); with Chapter 1 and 2 serving as a prelude to Chapter 3, 4 and 5. Chapter 6 summarises and concludes the different conclusions of Chapter 3, 4, and 5. Each Chapter (3, 4, and 5) has a brief introduction and literature review pertaining to the subject being investigated fused under the heading “*Introduction*”. Methodology and numerical settings for each chapter are also highlighted with justification for each choice where necessary.

Chapter 1 gives an overview of relevant selected literature in the field of study, starting from a global scope to regional before narrowing to the area of interest. Finally, it highlights the objectives and significance of the study.

Chapter 2 introduces the different numerical techniques/models combined to conduct the research. In addition, statistical and other tools employed in this current study are also described in this chapter. Chapter 2 is concluded with brief descriptions of the investigation areas, research materials, and input data.

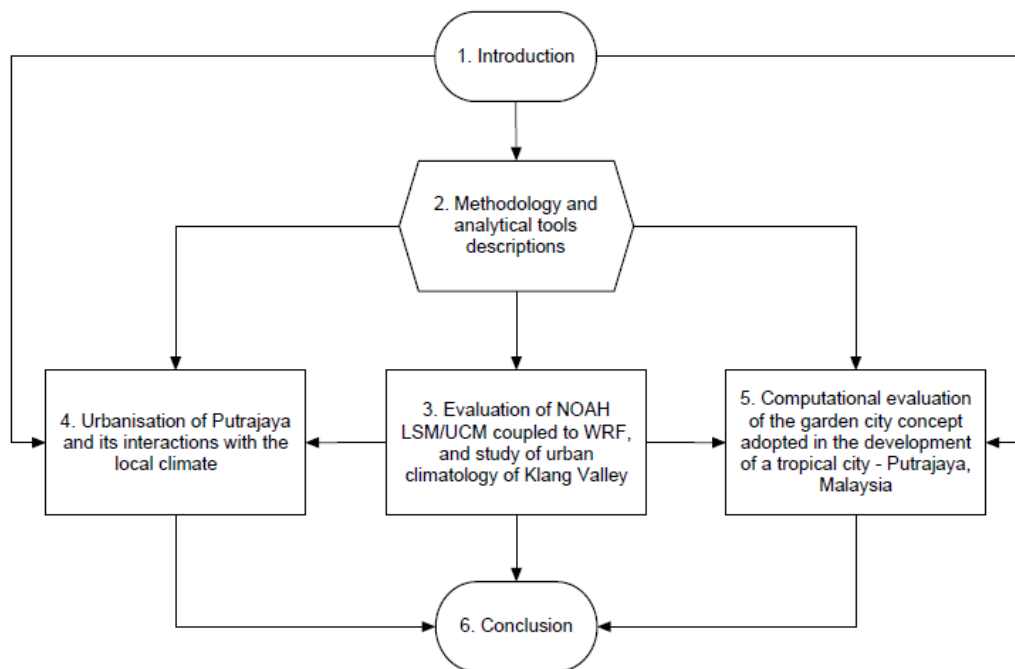


Fig. 1:4. Thesis flowchart; showing a graphical representation of the relationship and dependence among the different chapters

Chapter 3 gives detailed physics and dynamics descriptions of the different models used, their coupling and numerical settings/parameterisations to represent the study location in the model. Coupled model (WRF/NOAH/UCM) evaluation and climatology of Klang Valley is also investigated here. This chapter is concluded by summarising the different investigation conducted herein.

Chapter 4 highlights the urbanisation of Putrajaya city and how the local climate has adapted to the surface and thermal changes that have taken place.

Model evaluation for the location is conducted as well as investigation on climatological parameters variations with the urbanisation processes with a final section concluding the chapter.

Chapter 5 details a computational evaluation of the garden city concept and some of the natural elements employed during the development of Putrajaya. PBLH, RH and urban heating variations with the different scenarios considered are also investigated in this chapter.

Finally, Chapter 6 concludes the different conclusions of the different chapters and with some suggestions on possible future studies in the region.

Chapter 2

2 Methodology and analytical tools descriptions

Summary

This section of the report details the different techniques and tools adopted to achieve the set aims and objectives of this research. Weather Research and Forecasting (WRF) model, NOAA Land Surface model (NOAHLISM), and Urban Canopy Model (UCM) are used for the numerical integration, handling of land surface fluxes and account for urban roughness, drag, inhomogeneity, and land cover variations induced forcing, respectively. ArcGIS, WTOOLS, Google Earth Pro, and FORTRAN scripts are used for land use and land cover preparation and implementation, while NCAR Command Language (NCL), NetCDF4Excel, OriginPro, are used for data analysis and result presentations. Brief and concise information on the study locations are detailed in this section of the report.

2.1 WRF Pre-processing System (WPS)

The WRF Preprocessing System (WPS) is a set of programs (*geogrid.exe*, *ungrib.exe*, and *metgrid.exe*) whose collective role is to prepare input data to the *real* program for real-data simulations. Each of the programs performs distinctly one stage of the preparation: the *geogrid* defines model domains and interpolates static geographical data to the grids; the *ungrib* extracts meteorological fields from GRIB-formatted files; while the *metgrid*

interpolates horizontally the meteorological fields extracted by the *ungrib* program to the model grids defined by *geogrid* program. It is noteworthy that vertically interpolation of meteorological fields to the WRF vertical levels (*eta*) is performed by the *real* program (Wang et al. 2012).

Fig. 2:1 shows the flowchart of the WPS programs. Each of the individual WPS programs reads parameters from a common file “*namelist.wps*” (see sample on Appendix 1) as depicted in the Fig. 2:1. The *namelist.wps* file has separate namelist records for each of the programs separated by the slash symbol (/) and a shared namelist record, which defines parameters that are used by more than one WPS program. Note that the individual programs need their respective tables to function. These tables provide additional control over the operations of each program, though they generally do not need to be changed by the user. The purpose, contents, and format of these tables are documented in the WRF user’s guide (Wang et al. 2012). The WPS program used in this study is installed on Linux operating system on personal computers and the University’s clusters both in the United Kingdom (UK) and Malaysia Campus. Build mechanism for the WPS is similar to the build mechanism used by the WRF model.

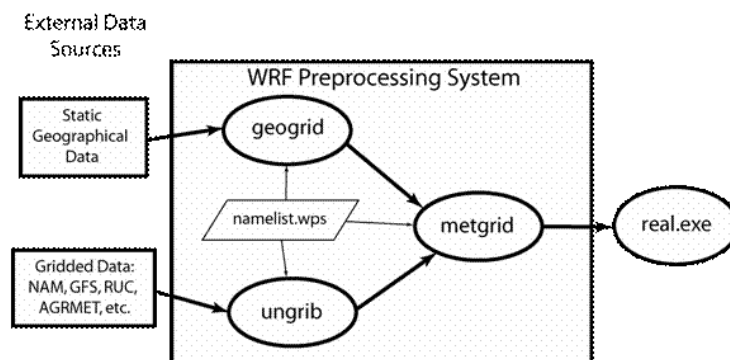


Fig. 2:1. WPS flowchart (Source: <http://www2.mmm.ucar.edu>)

2.1.1 Geogrid (geogrid.exe)

The primary purpose of the geogrid is to define the simulation domains, and interpolate various terrestrial data sets to the model grids. The simulation domain (see Fig. 2:2) is defined using information specified by the user in the geogrid's section of the *namelist.wps*. By default, and in addition to computing latitude and longitudes for every grid point, geogrid will interpolate land use category, soil categories, terrain height, monthly vegetation fraction, annual mean deep soil temperature, monthly albedo, maximum snow albedo, and slope category to the model grids. Global data sets for each of these fields can be downloaded from the MMM website (MMM 2015).

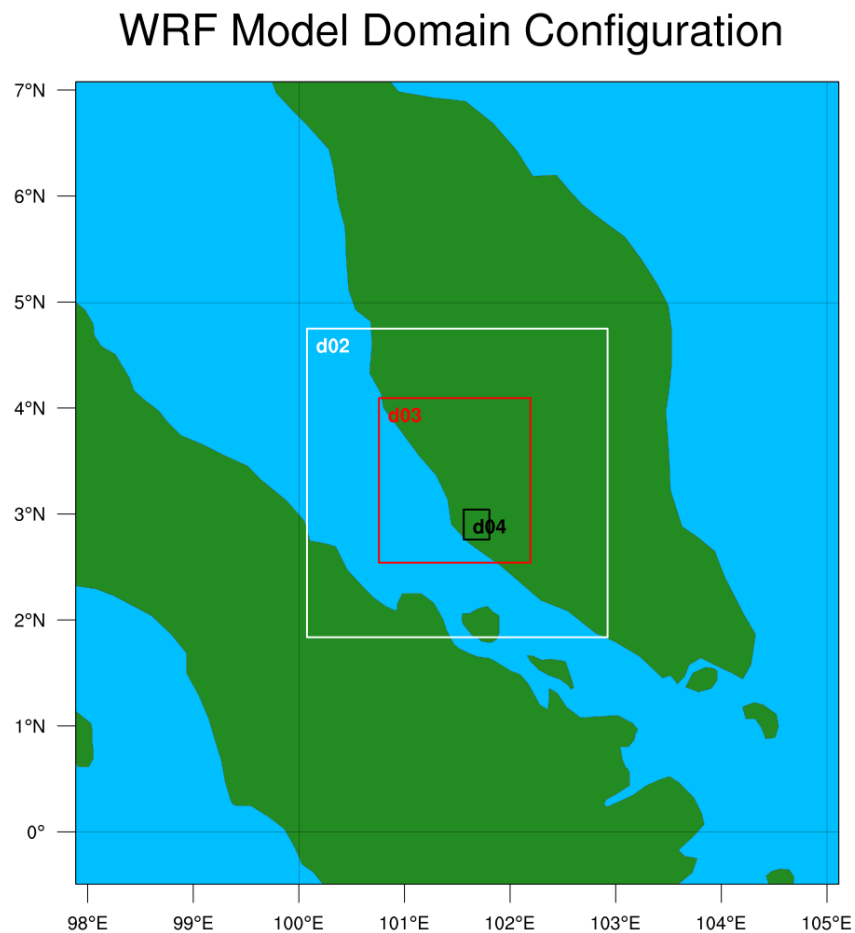


Fig. 2:2. Example of WRF domain configuration

Apart from interpolating the default static terrestrial fields, the *geogrid* program is able to interpolate most of the continuous and categorical fields to the simulation domains. For example, new and additional data sets can be interpolated to the simulation domain through the use of the table file, *GEOGRID.TBL* (see Appendix 2). The *GEOGRID.TBL* defines the fields that will be produced by *geogrid* program. The *GEOGRID.TBL* also specifies the interpolation methods to be used for each field, as well as the file system location where each data for the set fields are located (Wang et al. 2012). Furthermore, outputs from *geogrid* program are written in WRF input and output (I/O) application program interface (API) format, and thus, by specifying the Network Common Data Form (NetCDF) I/O format, *geogrid* writes its output in NetCDF. This can later be visualised using external software packages such as *ncview* and Read/Interpolate/Plot (RIP4) - a Fortran program that utilises the NCAR Graphics System Plot Package suite of plotting routines for creating plots, primarily from mesoscale model output (MMM 2015).

2.1.2 Ungrib (ungrib.exe)

Like the *geogrid.exe* program, the *ungrib* program reads GRIB files data, decodes (degribs) them, and then writes the data in a simple file format – WPS that is understood by the *metgrid.exe* program, called the intermediate format. GRIB files contain time-varying meteorological fields, and are typically from other regional or global model, such as NCEP's North America Mesoscale (NAM) or Global Forecast System (GFS).

Because the GRIB files typically contain more fields than are needed to initialise WRF, thus the *Vtable* (see Appendix 3 for example of the *Vtable*) defines which fields from the numerous fields of the GRIB files that are to be extracted and then write into the intermediate file format understood by the *metgrid.exe* program. The *Vtable* template for GRIB model output files used in this research is provided with the *ungrib* software. Detail descriptions of the fields in the *Vtable* can be found on the WRF-ARW User's Guide V3, "creating and editing *Vtable*" section (Wang et al. 2012).

2.1.3 Metgrid (metgrid.exe)

The *metgrid* program horizontally interpolates intermediate file format meteorological data that are extracted by the *ungrib* program onto the simulation domains defined by the *geogrid* program. These interpolated *metgrid* outputs are then ingested by the *real.exe* program. The range of dates to be interpolated by *metgrid* program is defined in the "share" section of the *namelist.wps* file (see Fig. 2:3). The date ranges are specified for each simulation domain. This is because the function of the *metgrid* program, like that of the *ungrib* program, is time-dependent. This program (*metgrid*) of the WPS is run each time a new simulation is initialised.

Control over how each meteorological field is interpolated is provided by the *METGRID.TBL* file (see Appendix 4). The *METGRID.TBL* like the *GEOGRID.TBL* file provides one section for each field, and within a section, it is possible to specify options such as the interpolation methods to be used for the field, the field that acts as the mask to be used for masked interpolations,

and the staggering (e.g., U, V in ARW; H, V in NMM) to which a field is to be interpolated.

Also, outputs from *metgrid.exe* are written in the WRF I/O API format. Hence by selecting the NetCDF I/O format, *metgrid.exe* can be made to write its output in NetCDF for easy visualisation using external software packages (Wang et al. 2012).

```
&share
wrf_core = 'ARW',
max_dom = 3,
start_date = '2011-09-22_00:00:00', '2011-09-22_00:00:00', '2011-09-22_00:00:00', '2011-01-30_12:00:00',
end_date = '2011-09-24_18:00:00', '2011-09-24_18:00:00', '2011-09-24_18:00:00', '2011-02-15_18:00:00',
interval_seconds = 21600,
io_form_geogrid = 2,
opt_output_from_geogrid_path = '/home/ezakm2/kenobi/',
debug_level = 0,
/
```

Fig. 2.3. Share section of the *namelis.wps* file

2.2 Weather Research and Forecasting (WRF) model

The Weather Research and Forecasting (WRF) Model is a next-generation mesoscale numerical weather prediction (NWP) system (Skamarock & Klemp 2008) designed to serve both atmospheric research and operational forecasting needs. Numerical weather prediction refers to the simulation and prediction of the atmosphere with a computer model. The model has two dynamical cores: a data assimilation system, and a software architecture allowing for parallel computation and system extensibility. The model serves a wide range of meteorological applications across scales from meters to thousands of kilometres (Wang et al. 2012). Development of the WRF began in the latter part of the 1990s and was a collaborative partnership principally among the National Centre for Atmospheric Research (NCAR), the National Oceanic and

Atmospheric Administration (represented by the National Centres for Environmental Prediction (NCEP) and the (then) Forecast Systems Laboratory (FSL)), the Air Force Weather Agency (AFWA), the Naval Research Laboratory, the University of Oklahoma, and the Federal Aviation Administration (FAA) (MMM 2015).

In addition, the WRF system comes with two dynamical solvers, referred to as the ARW (Advanced Research WRF) core developed and maintained by the MMM Laboratory (MMM 2015) and the NMM (Non-hydrostatic Mesoscale Model) which was developed by the National Centres for Environmental Prediction (NCEP) and supported by the Developmental Testbed Centre (DTC) (NCEP & DTC 2015). WRF allows researchers to generate atmospheric simulations reflecting real and ideal scenarios using real data (observations, analyses) and idealised conditions, respectively. WRF offers operational forecasting a flexible and robust computationally-efficient platform while providing recent advances in physics, numeric, and data assimilation contributed by developers across the broad research community. WRF is currently in operational use at NCEP, AFWA, and other forecasting centres across the globe (MMM 2015).

Fig. 2:4 shows the principal components and flowchart depicting the functionality of the components of the WRF modelling system. The software framework provides infrastructure that houses the dynamic solvers, physics packages that interface with the solver, programs for initialisation and other software components of the model (WRF) (Skamarock et al. 2008).

The WRF model open source and community-based development has enabled a growing research and operational community of users worldwide,

with over 30,000 registered users in over 150 countries (<http://www.wrf-model.org/index.php>). The WRF-ARW dynamic core is used in this study because of its extensive application in different spheres of research and real-time forecasting throughout the world (Morris et al. 2015b; Martins et al. 2015; Li et al. 2016). Refer to Appendix 7 for basic equations calculated by the WRF model.

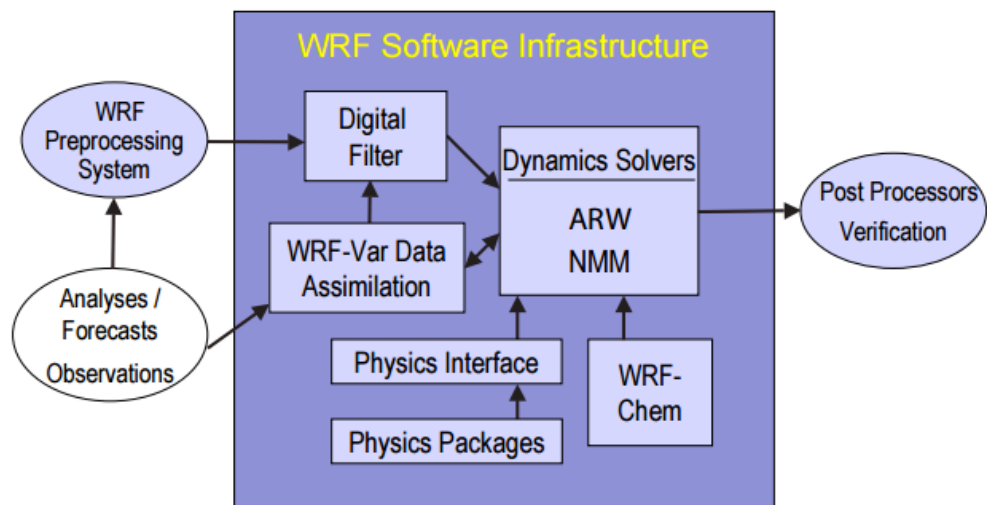


Fig. 2:4. WRF system components (Skamarock & Klemp 2008)

2.2.1 Advanced Weather Research and Forecasting (ARW) model - WRFARW

The advanced WRF here refers as ARW is a fully compressible, Eulerian mass coordinate non-hydrostatic with a run-time hydrostatic option. ARW is a regional climate model that solves the conservative equations of mass, momentum and energy on terrain-following coordinates, and with option of multiple nesting to enhance resolution over area of interest (Skamarock et al. 2008). It is a next-generation numerical weather prediction model with advanced dynamics, physics, and numeric schemes. The terrain-following hydrostatic pressure coordinate system with permitted vertical stretching used

by the model is proposed by Laprise (1992). Arakawa C grid staggering is used for horizontal discretisation. The model equations are conservative for scalar variables. Other features of the model includes the time split third order Runge-Kutta (RK3) integration scheme (Skamarock & Klemp 2008) for model integration, higher order advection schemes and complete Coriolis, curvature and mapping terms. The model is widely used for urban hydrology and meteorology (Chen et al. 2011; Li et al. 2013). More information about the model and its different governing equations can be obtained on the NCAR ARW Technical note (Skamarock et al. 2008).

Like the WPS, the ARW has two important executable programs (*real.exe* and *wrf.exe*) generated during the model installation process. The *real.exe* program handles real-data and model initialisation, while the *wrf.exe* program executes the simulation integration and calculation of all the physics and dynamics options specified.

2.2.1.1 Real (*real.exe*)

The *real.exe* program is a real-data initialisation and pre-processor to the WRF model (*wrf.exe*) program and takes in pre-processed data from the WPS program – *metgrid.exe* which provides each atmospheric and static field with fidelity appropriate to the chosen grid resolution for the model. Other functions of the *real.exe* program include but not limited to;

- Compute a base state/reference profile for geopotential and column pressure
- Initialise meteorological variables such as potential temperatures and vapour mixing ratio
- Interpolates data to the model's vertical coordinate

- Initialise static fields for the map projection and the physical surface
- Read data from the *namelist.input* file (see Appendix 5)
- Allocate space for the requested domain, with model variables specified at run-time
- Generate initial condition files (*wrfinput* and *wrfbdy*) to be used by the model executable program (*wrf.exe*)
- Read meteorological and static input data from WPS
- Prepare soil fields for use in the model (usually, vertical interpolation to the required levels for the specified land surface scheme)
- Check to verify that land use, soil categories, land mask, soil temperature, sea surface temperature (SST) are all consistent with each other
- Ensures that multiple input time periods are processed to generate the lateral boundary conditions required unless processing a global forecast.
- Ensures that 3 D boundary data (such as vertical and horizontal components of velocity, potential temperatures, vapor mixing ratio, and total geopotential are properly coupled with the total column pressure

2.2.1.2 *Wrf (wrf.exe)*

The ARW executable file handles the model numerical integration and computes the varying physics and dynamics options of different real simulation scenarios conducted on the model, using the initial and boundary conditions from the *real.exe* program. The *real.exe* program runs the model simulation with run-time selected *namelist.input* (see Appendix 5) options (such as

physics choices, time-step, length of simulation, and type of nesting) and outputs history and restart files which could be used to initiate the program at a later time. A simplified flowchart of the WPS and WRF interactions and dependence is depicted in Fig. 2:5

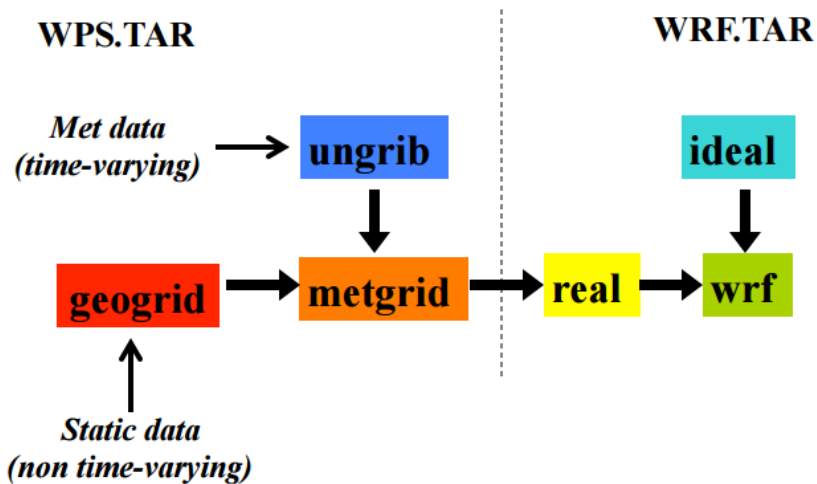


Fig. 2:5. Simplified flowchart for WPS and WRF (source: <http://ruc.noaa.gov/wrf/>)

2.3 NOAH Land Surface Model (NOAH LSM)

The updated NOAH LSM is a surface-hydrology and one-dimensional model that describes land surface characteristics (e.g., land cover parameters), states (temperature, soil moisture, and soil temperature, snow depth, snow, leaf area, water equivalent), and fluxes (surface energy balance outgoing components, water content flux, evapotranspiration, photosynthesis, and canopy water content) as a function of space and time (Chen & Dudhia 2001). The model has a single-canopy layer with multi-soil layers of different thickness (10, 30, 60, and 100 cm); 10 and 100 cm being the top and bottom layers, respectively. Thus the total depth of the NOAH LSM is 2 m, with the upper and lower layers of the soil serving as the root zone depth and reservoir with gravity drainage, respectively (Giannaros et al. 2013). Furthermore, NOAH LSM is formulated

based on diurnal varying Penman potential evaporation approach; a multi-layer soil model, surface hydrology, frozen ground physics and a modestly complex canopy resistance parameterisation (Chen et al. 1996; Chen et al. 1997; Chen & Dudhia 2001; Ek 2003). Prognostic variables in NOAH include liquid water, ice, and temperature in the soil layers; water stored in the vegetation canopy; and snow water equivalent stored on the ground (Chen et al. 2011). One basic function of the NOAH LSM is to provide surface sensible heat and latent heat fluxes and surface skin temperature as lower boundary conditions for coupled atmospheric models.

2.4 Urban Canopy Model (UCM)

The simple single-layer urban canopy model (SLUCM) original developed by Kusaka et al., (2001) and later modified by Tewari et al., (2007) is a two-dimensional urban model that parameterises urban canopy geometry effects such as increased drag, trapping of solar shortwave radiation and turbulent generation when coupled to atmospheric models. The SLUCM considers building height, roof and road width, and assuming street canyon of infinite length. It also considers solar trapping and reflection of radiation and shadowing effects. Thus, energy, mass, and momentum transfer between urban environment and the atmosphere could be calculated by computing surface temperatures and heat fluxes of roof, wall, and road within the study domain.

In the current study, urban modelling resources are channelled onto the coupling the urban canopy model with NOAH in WRF which is made possible the urban fraction parameter (F_{urb}), the urban fraction parameter represents the proportion of impervious surfaces in the WRF subgrid scale. For any given

grid cell in the WRF domain, the NOAH model calculates surface fluxes and temperature for urban vegetated areas (e.g., trees, parks, open grassland, etc.), while the UCM provides the fluxes for anthropogenic surfaces. The total grid scale sensible heat fluxes could be estimated using (Eq. 2.1), where Q_H is the total sensible heat flux from the surface to the WRF model lowest atmospheric layer, F_{veg} is the fractional coverage of natural surfaces (vegetation), such as grassland, shrubs, crops, and trees in cities, F_{urb} is the fractional coverage of impervious surfaces (i.e. percentage of the urban area with urban surfaces coverage), such as buildings, roads, and railways. Q_{Hveg} is the sensible heat flux from NOAH for natural surfaces, and Q_{Hurb} is the sensible heat flux from the UCM for artificial surfaces (such as roads, buildings, pavements and other engineered surfaces). Grid-integrated latent heat flux, upward longwave radiation flux, albedo, and emissivity are estimated in the same way. Surface skin temperature is calculated as the averaged value of the artificial and natural surface temperature values, and is subsequently weighted by their areal coverage (Chen et al. 2011). The coupling of the NOAH LSM/UCM in WRF is represented pictorially in Fig. 2:6.

$$Q_H = F_{veg} \times Q_{Hveg} + F_{urb} \times Q_{Hurb}, \quad \text{Eq. 2:1}$$

2.5 Other Post-processing, GIS and analysis tools

This section of the report gives brief highlights of some of the post-processing software/tools employed in analysing and preparing the model outputs.

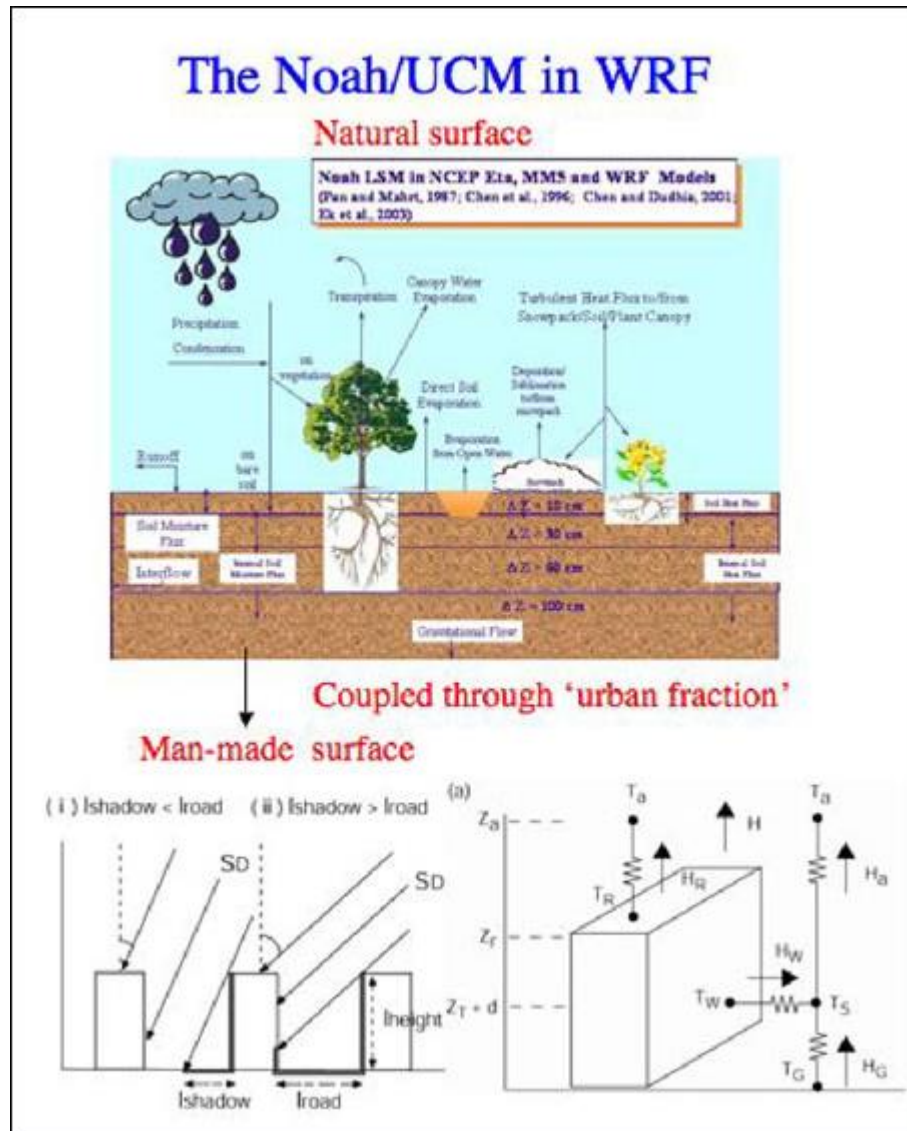


Fig. 2.6. NOAH/UCM in WRF (Source: http://ral.ucar.edu/lar/2007/goal_1/priority_4.php)

2.5.1 ArcGIS

ArcGIS is geographic information system (GIS) software for working with maps and geographic information (Kennedy 2000; ArcGIS 2015). It is also used creating and using of maps, analysing map information, compiling geographic data, and other range of geographic applications. In the current research, the ArcGIS V10.2.2 is employed in creating of maps, shapefiles, land use classification, geo-referencing of ARW output results graphics and

selection of data for analysis. Some of its applications will be seen in the subsequent chapters of this report.

2.5.2 WTOOLS

WTOOLS (Nuss 2011) is a program to display, modify WRF grid Information, land use, and soil type categories using Google Earth. The program runs on Java NetCDF library. Here the program is applied in modifying the land use and land cover dataset employed in this study to properly represent the ground truth of the location in conjunction with the ArcGIS software (see Fig. 2:7 for a sample of WTOOLS converted Land use to KML format for modification on Google Earth).

2.5.3 Google Earth Pro

Google Earth Pro is a virtual globe, map and geographic information program that enable exploration of the Earth's surfaces. The program displays satellite images of varying resolution of the earth surface, thereby allowing users to view cities and houses to the recognizable resolution. Identification of particular locations, land cover and urban characteristics of Klang Valley and Putrajaya city are conducted in support of the program. The Google Earth also serves as the platform for the modification of land cover; soil type and geographical information of the static input dataset of the WRF model to represent the real or existing conditions of the area using the WTOOLS (see Fig. 2:7).

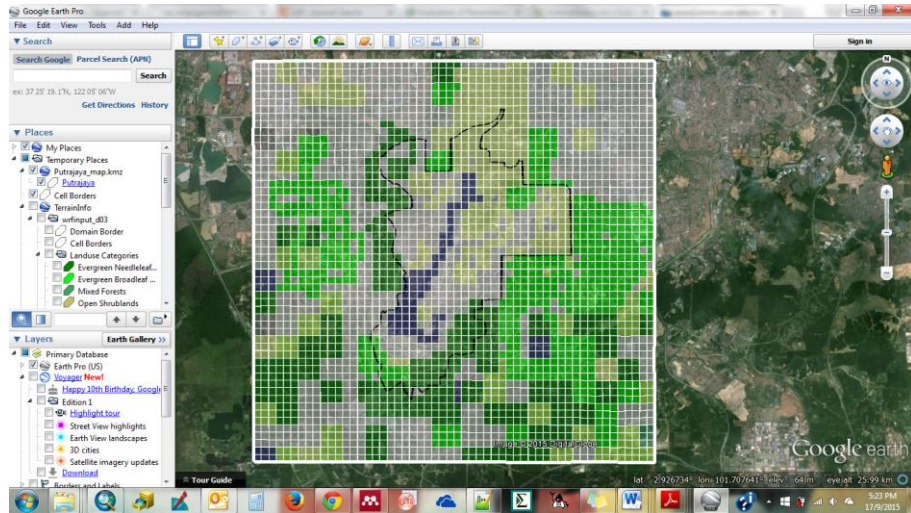


Fig. 2:7. Print screen of a sample of in-process WTOOLS land use on Google Earth Pro for grids/fields modifications

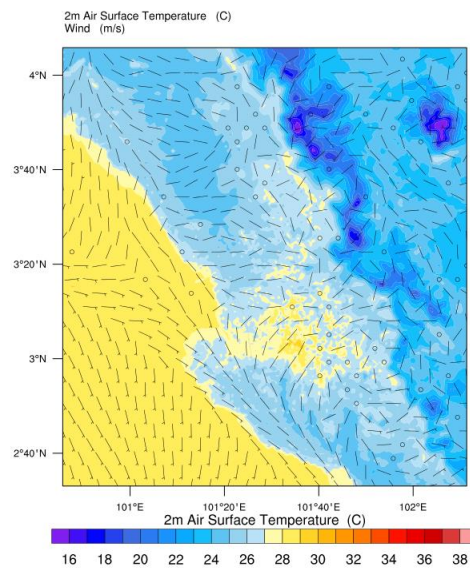


Fig. 2:8. Example of Klang Valley 2-m temperature and wind speed plot using NCL for 24th September, 2011 at 05 00 MST

2.5.4 NCAR Command Language (NCL)

The NCAR command Language (NCL) is a gratis interpreted language designed by the National Centre for Atmospheric Research (NCAR) for the purpose of scientific visualisation and processing of data from atmospheric and regional models such as the WRF, MM5 (NCAR 2015). The language is robust, portable and important of all, it is free and available a binaries or open

source. This language can produce high-quality graphics (see Fig. 2:8). A sample of the script for determining the nearest model grid for a particular location is shown in Appendix 6. The NCL can read data in different formats; NetCDF, HDF4, GRIB, binary and ASCII data.

2.5.5 NetCDF4Excel

NetCDF4Excel is an excel add-in designed for Excel running with the Microsoft Windows operating system. This add-in allows NetCDF data to be open in excel to read/write access. This add-in is used in the extraction of WRF data and averaging over the model domain for different analyses of parameters of interest (Netcdf4excell 2014). The add-in gives the user opportunity to specify the parameter to be extracted, the range of time, position (using latitude and longitude), and vertical levels for 3D variables. See Fig. 2:9 on the appearance of the add-in during operation

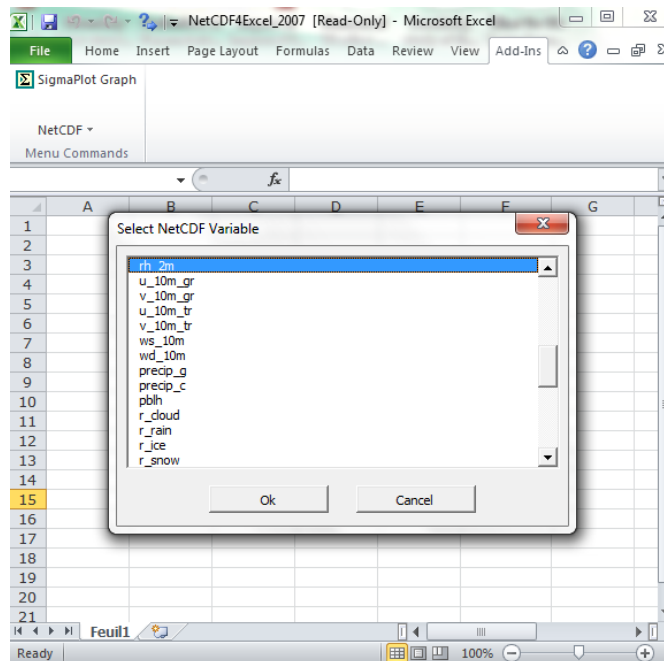


Fig. 2:9. Netcdf4Excel example during operation

2.5.6 OriginPro

This is proprietary computer software for interactive scientific graphing and data analysis. It is licensed and produced by OriginLab Corporation and operate on Microsoft Windows platforms. Data analyses in the software include statistics, curve fitting, signal processing and peak analysis. OriginPro can directly import files in different formats such as Excel, NetCDF, ASCII, etc. and export the plotted graphs to various image file formats such as JPEG, GIF, EPS, and TIFF (OriginLab 2013).

In summary, the different software applied in this study enables pre-processing of input data, numerical calculations (simulations) of data, post-processing of simulated results, and presentation of the processed results in acceptable formats as presented herein this thesis.

2.6 Input and validation data

2.6.1 Input data

To initiate the coupled WRF/NOAH/UCM, various input data such as the initial and lower boundary conditions, static geographic, and atmospheric forced data are needed. These data come from different sources which are discussed in subsequent section.

2.6.1.1 NCEP Final analysis (FNL) data

The NCEP FNL (Final) Operational Global Analysis data are (1.0 ° x 1.0 °) grids prepared operationally every six hours. This FNL is from the Global Data Assimilation System (GDAS), which continuously collects observational data from the Global Telecommunications System (GTS), and other sources, for several analyses (NCEP et al. 2000). The FNLs are model according to the

Global Forecast System (GFS) which NCEP uses, but however, the FNLs are prepared about an hour after the GFS is initialised. The FNLs delayed is necessary so that more observational data can be used. The GFS is run earlier in support of time-critical forecast needs and uses the FNL from the previous 6-hour cycle as part of its initialisation.

The analyses are available on the surface, at 26 mandatory and other pressure levels from 1000 millibars to 10 millibars, in the surface boundary layer and at some sigma layers, the tropopause, and a few others. Parameters include surface pressure, sea level pressure, geopotential height, temperature, sea surface temperature, soil values, ice cover, relative humidity, u- and v-winds, vertical motion, vorticity and ozone (NCEP et al. 2000).

2.6.1.2 Static Geographic data

The default static geographic dataset (USGS 24-category) used in WRF model is based on 1-km Advanced Very High Resolution Radiometer (AVHRR) data obtained from 1992 to 1993 (Chen, Yang, & Zhu, 2014). The alternative dataset (MODIS 20-category) is based on 1-km Moderate Resolution Imaging Spectroradiometer (MODIS) data obtained in 2004 (Chen et al. 2014). However, both datasets to a certain degree lack good representation of the extent of urbanisation and anthropogenic surface modifications that have taken place from when they were obtained in most of the regions; for example Klang Valley (Chng et al. 2010). Apart from lack of good representation, the datasets consider only a single urban land category, and has thus been reported to have failed in reproducing the urban effects on local climate caused by surface inhomogeneity in urban areas (Chen et al. 2014). This necessitates the need for new datasets to be implemented in the different case studies that are conducted

in this report. Combination of the functions of ArcGIS, Google Earth Pro, WTOOLS and some FORTRAN coding makes achieving this possible. This will be properly discussed in each section of the reported with application of the above mentioned utilities.

2.6.2 Meteorological data

Numerical studies come with ample information of spatial and temporal coverage, historical and future research (forecasting). However, numerical models need observed data to validate and tune its performance to the desired accuracy. Thus, meteorological data are often used as the benchmark for a given model. In this research, to evaluate the performance of the coupled model, physics and dynamic options, improved land use and land cover dataset, the influence of modified surface characteristics and anthropogenic heat releases, several meteorological data are used to validate the models at different scenarios considered in this research. These data for model validation are obtained from Malaysia Department of Environment (DOE) and online repository (<http://www7.ncdc.noaa.gov/CDO/cdo>) of the National Climate Data Centre (NCDC). More details on these data and the specific locations selected are provided in each of the chapters of this report.

2.7 Study location

This work concentrates on the urban climatology of the Klang Valley area, Putrajaya city urbanisation and interaction with the surrounding local climate, adaptability of the city and finally evaluation of the adopted green model in the Putrajaya development. In addition, the existence of more meteorological sites

and urban conurbation relative to other regions of the country makes the valley a more suitable area for the WRF model validation and thermal climate studies.

2.7.1 Klang Valley

Klang Valley (sometimes referred as Greater Kuala Lumpur – GKL) is an urban conurbation in Western Malaysia, encompassing the federal capital of Kuala Lumpur, its recently developed administrative capital, Putrajaya and its suburbs, and adjoining cities and towns in the state of Selangor. It is geographically delineated to the North and North-East by Titiwangsa Mountains and Strait of Malacca to the West (see Fig. 2:10) with equatorial climate of type Koppen *Af* (Kottek et al. 2006). GKL is typified by tropical rainforest and near-uniform monthly mean temperature and high humidity. The conurbation drives the Malaysian industry and commerce, and is home to about 7.2 million inhabitants. According to the Malaysian Department of Statistics, the area has recorded the highest rate of urbanisation within the past decade. GKL has a developed urban morphology comparative with the surrounding states. Most of the developments are associated with high-rise and mid-rise estates for residential and business needs, causing a proportional decreased in farm and forest land. Notable among the areas are, east of Selangor, Putrajaya, Subang Jaya, Petaling Jaya and some parts of Kuala Lumpur outskirts. Interlinking of neighbouring suburbs, cities and towns, and a highly developed road network, with many crisscrosses within the metropolis has made inter-commuting by cars more convenient for commercial and industrial purposes. The choice of people applying the roads with cars has led to Klang Valley

notorious high traffic jams, that often span kilometres of expressway; causing driving during peak hours exhausting.

Furthermore, the valley is situated few degrees off north of the equator and covers an area of approximately 8236 km², with a hilly terrain characterised by humid and hot weather all year round. Rainfall hardly follows a consistent pattern and averages 2-3 m in a year, with more frequent heavy falls during the monsoon season, depositing about 10 to 30 cm within few hours (Bunnell 2002). Proximity to the equator exposes the area to high solar radiation accounting to about 6.1 hours of sunshine per day all year round, hence the hot and humid climate experienced.

2.7.2 Putrajaya

Putrajaya is a planned administrative capital of Malaysia built to accommodate the growing size of the federal government ministries and national level civil servants. It is structured to accommodate all diplomatic activities for the country and to showcase the nation's modernisation agenda (Moser 2010). Putrajaya is located in the Klang Valley, 25 km south of Kuala Lumpur (see Fig. 2:10) and lies on coordinates 2°55'00" N 101°40'00" E with an approximate area of 49 km² which was previously covered by vegetation, rubber and oil palm plantation. Located few degrees north of the equator with an average elevation of 30 m, Putrajaya is a typical tropical city and sits on a hilly terrain. Rainfall averages 2-3 m in a year and falls heavily during the monsoon season, depositing about 10 to 30 cm within few hours (Bunnell 2002). Low variable canopy layer temperature during the year with an annual mean maximum of ~27.5 °C and mean minimum of ~25 °C. Relative humidity

supplied. Input data description and their respective sources are discussed. Furthermore, brief information on the Klang Valley conurbation and the Putrajaya city are supplied. Finally, the coupling of the NOAH LSM/UCM in the WRF is made possible through the urban fraction parameter.

Chapter 3

3 Evaluation of NOAH LSM/UCM coupled to WRF, and study of urban climatology of Klang Valley

Summary

A coupled modelling system (WRF/NOAH/UCM) is used to investigate the environmental conditions of a tropical conurbation in Malaysia. Parameterisation of anthropogenic heat and updated land-use-cover (of the area derived from satellite data) reveals improvement in model performance. Urbanisation has caused spatiotemporal variations on meteorological parameters of the area, such as increased planetary boundary layer height (PBLH), sensible heat flux (SH), canopy layer temperature (T2m), but decrease in relative humidity (RH2m) and latent heat flux (LH). Another impact of urbanisation over the area is the modifications of the surface energy components, which affect the diurnal temperature range (DTR) over rural (7.58 °C) and urban (6.03 °C) surfaces. T2m and UHI decrease radially away from the urban centre while RH2m and urban dry island (UDI) exhibit the opposite behaviour. Maximum urban heat island intensity (UHI) of 4.2 °C is found in the commercial district of the conurbation. The effect of urbanisation on the magnitude of diurnal UHI cycle is significant (at 95% level) during morning and nighttime, meanwhile, the spatial distribution and temporal changes of UHI is dominated by solar radiation during daytime. The influence of wind

system is also observed on the spatiotemporal variation of the meteorological conditions over the area; especially along the coastline bordering Strait of Malacca (by sea-land breezes) and the Titiwangsa mountain range (by mountain-valley breezes).

3.1 Introduction

Accurate representation of surface properties is essential in meteorological models such as the National Centre for Atmospheric Research (NCAR) Weather Research and Forecasting (WRF) Model and the 5th generation Pennsylvania State University/NCAR Mesoscale Model (MM5), for accurate capturing of local, regional and mesoscale circulations induced by land surface forcing (Chen & Dudhia 2001). MM5 and WRF depend on atmosphere-land surface coupling to predict basic climatic parameters: temperature, relative humidity, precipitation and wind speed (Niu et al. 2011; Li et al. 2013).

Cities contribute significantly on local and regional scale meteorology. The morphological dynamics, as well as thermal and radiative properties of urban surfaces, have a direct impact on the surface energy exchange, which is different relative to those observed in natural soils and vegetation (Oke 1988). Temperature gradient develops between cities and their surroundings: this is more significant at nighttime under clear and calm meteorological conditions, and this is known as the urban heat islands (UHI). UHI has been studied in different cities such as New York (Gaffin et al. 2008), Beijing (Jiang et al. 2014), Lagos (Ayanlade & Jegede 2015), Singapore (Wong & Yu 2005) and Putrajaya (Morris et al. 2015a).

One prominent characteristic of meteorological models used in urban climatology, for example, WRF, is the inclusion of anthropogenic heat (AH) associated with energy consumption from different sources within cities as input to the model. Human activities especially in industrial and urban areas contribute greatly to atmospheric heat and urban pollution. Their spatio-temporal distribution and evolution can be greatly influenced by urban thermodynamic and dynamic processes above cities. AH also, can originate through consumption of electricity and heating fuels needed in buildings or industrial activities; combustion of fuels from vehicular traffic, and other activities associated with human metabolism. Effect of anthropogenic heat release on meteorological models and urban climate studies have been reported in different studies: such effect as modification of the evolution of diurnal urban boundary layer (Atkinson 2003; Chen et al. 2009) and spatio-temporal variation of UHI.

Compared to other regions, tropical urban climate has been understudied, especially in Malaysia. Few investigations (Morris et al. 2015b; Salleh et al. 2015; Morris et al. 2016) have established links between the interactions of urbanisation and the overlying micrometeorology of the area. The effect of AH has not been included in related numerically studies conducted using the WRF in the area: thus, there is likely underestimation of the effect of urbanisation and the accuracy of the numerical predictions of the investigated locations. This study investigates the effect of land-use-cover and AH on the performance of the WRF model, and the meteorology of an urban conurbation, Klang Valley, in Malaysia and hopes to bridge this research gap. The urban land-surface interaction is represented by coupling a land surface model (NOAH

LSM) and an urban canopy model (UCM) to the WRF; this completes the land-surface and atmospheric thermodynamic and physical processes. The model is validated against a network of observation, followed by a discussion of simulation results.

3.2 Study design

3.2.1 Study area

The Klang Valley (sometimes referred as Greater Kuala Lumpur – GKL) is an urban conurbation in Western Malaysia. It encompasses the federal capital - Kuala Lumpur, the recently developed administrative capital – Putrajaya and the adjoining suburbs, cities and towns in the state of Selangor. The Klang Valley comprises of 40 districts, and is geographically delineated to the North and North-East by Titiwangsa Mountains, and Strait of Malacca to the West (Fig. 3:1). Its climate is characterised by equatorial climate type Koppen *Af* (Kottek et al. 2006). GKL is typified by tropical rainforest and near-uniform monthly mean temperature and high humidity (MMD 2015). The conurbation drives the Malaysian industry and commerce; is home to about 7.6 million people (26% of the country's population), and contributes about 41% of the country's gross domestic product (GDP) (Gambero 2013). According to the Malaysian Department of Statistics, the area has recorded the highest rate of urbanisation within the past decade. GKL has a developed urban morphology compared with the surrounding states.

GKL is situated a few degrees off north of the equator and lies in the western part of the Maritime Continent of Southeast Asian region. GKL covers an area approximately 8236 km², with a hilly terrain (towards the east)

characterised by humid and hot weather all year round. Rainfall hardly follows a consistent pattern and averages 2-3 m in a year, with more frequent heavy falls during the Northeast monsoon season, depositing about 10 to 30 cm within few hours (Bunnell 2002). Proximity to the equator exposes the area to high daily solar radiation accounting to ~6.1 hours of sunshine per day all year round. Northeast, Southwest and two inter-monsoonal seasons characterise the weather and meteorological conditions of the region. Annual mean temperature ranges 26.8 – 27 °C; ~26.2 and ~27 during the Northeast monsoon and Southwest monsoon respectively. Wind speed is generally light all year round, with annual mean relative humidity range of 63 – 68% (Shahidan et al. 2012; MMD 2015).

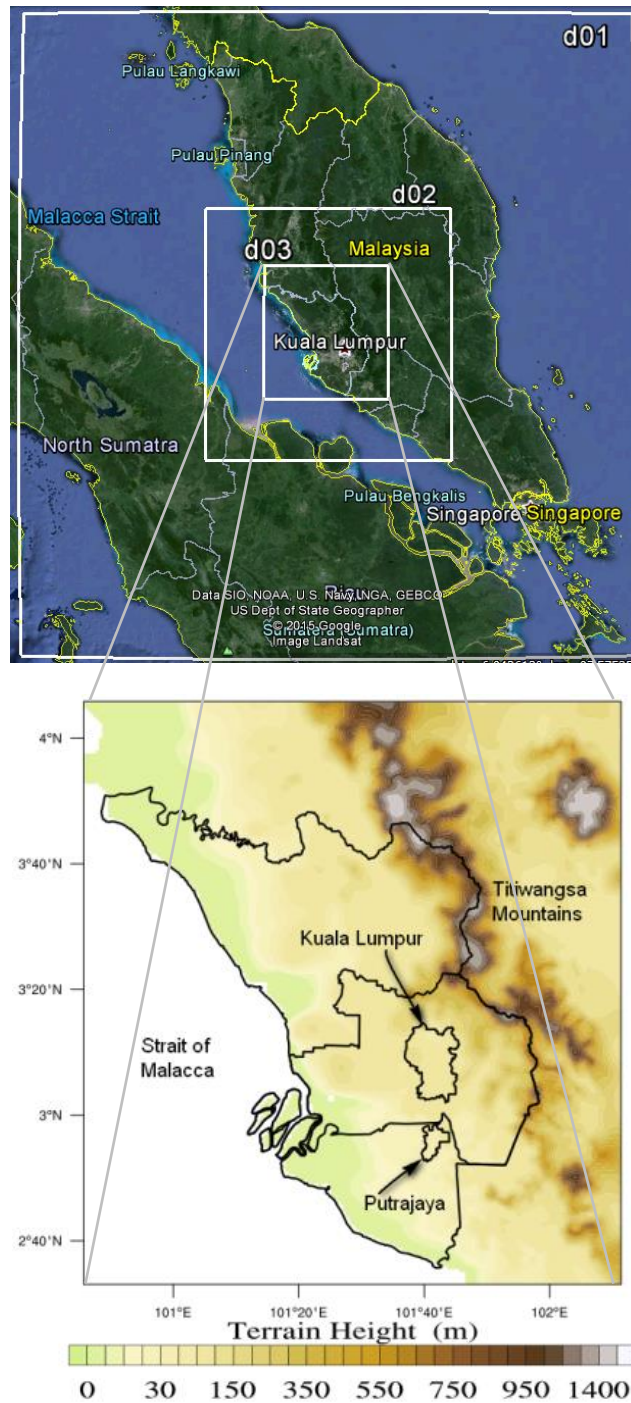


Fig. 3:1. Model domain configuration: (a) 3 one-way nested domain (top panel), and (b) finest domain (d03) terrain height and the map of Klang Valley (bottom panel). Water body along the Strait of Malacca has been masked.

3.2.2 Model and experimental design

Analysis of scarce meteorological observed data reveals a significant impact of urbanisation on local climate and the environment in some part of the Valley

(Sani 1984; Salleh et al. 2013; Shaharuddin et al. 2014). However, limited number of meteorological stations restricts detailed evaluation of associated impacts of urbanisation to the localised locations of the few meteorological stations. Thus, the use of proven numerical models such as the WRF is imperative to assess the possible surrounding and regional impact of urbanisation. For this study, the Advanced core of the WRF model system version 3.5.1: a next-generation mesoscale weather and regional climate numerical simulation system (Skamarock et al. 2008) is used. The WRF modelling system is coupled to a new generation single layer urban canopy scheme (UCM) and NOAA Land Surface Model (NOAH LSM) (Chen et al. 2011) – WRF/NOAH/UCM. This combination (WRF/NOAH/UCM) has been reported to reproduce meteorological conditions with minimum bias, and capable of capturing the impacts of urbanisation on near-surface meteorology and the diurnal evolution of urban boundary layer -UBL (Miao et al. 2009; Chen et al. 2011; Chen et al. 2014). Possibility to alter the default land surface components of the WRF model with up-to-date high resolution data of the region of interest makes the model more suitable for urban effect assessment.

Fig. 3:1 illustrates the domain configuration of the model and terrain distribution of the finest resolution (d03). A three one-way nested domain with an horizontal resolution of 25×25 km, 5×5 km, and 1×1 km, for d01, d02 and d03, are respectively configured to handle the numerical simulation of the area (Fig. 3:1). d01 covers Western Malaysian (South-West) and part of Indonesia. d02 the dominant geographical feature is the Strait of Malacca, while d03 covers the study area (Fig. 3:1). The model domain consists of 32 terrain-following vertical hydrostatic-pressure levels and is used to resolve

model's vertical layers for all domains; with model top at 100 hPa. Meanwhile, 16 of the levels are reserved below 850 hPa to further resolve turbulence and frequent changes of atmospheric variables within the lower boundary layer (PBL). Furthermore, the reserved 16 levels below 850 hPa would help to effectively account for the small-scale features near the Earth's surface.

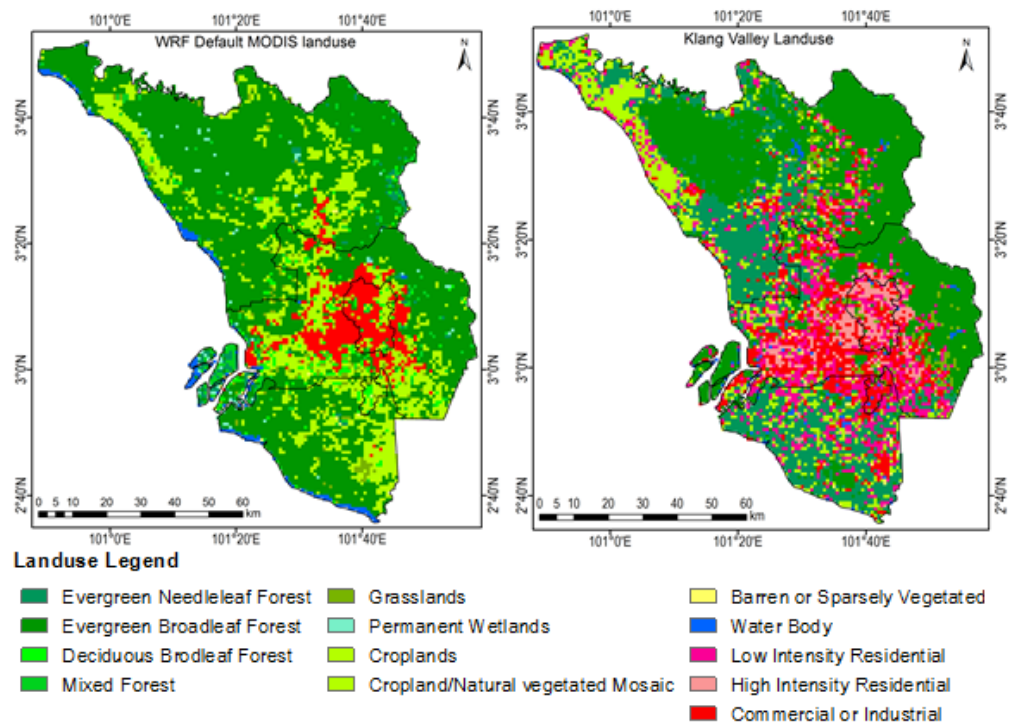


Fig. 3:2. Land-use-cover for: (a) MODIS (left panel) – used as the inaccurate urban representation of GKL (MURB) – left panel, and (b) Updated urban land surface with 2011 satellite data (URB) to represent the true surface characteristics of GKL – right panel.

WRF default MODIS land surface data is used for the 25 km (d01) and 5 km (d02) domain, to downscale Final (FNL) analysis ($1^\circ \times 1^\circ$) meteorological fields of the National Centre for Environmental Protection (NCEP), which are then laterally interpolated to be used as the initial and lateral boundary conditions for d03. For d03, four cases are designed for its land surface data: (1) MURB, (2) URB, (3) URB+AH and (4) NOURB. MURB represents inaccurate representation of the surface physical characteristics of the studied

area. The default WRF land-use data based on 2004 1-km Moderate Resolution Imaging Spectroradiometer (MODIS) data (Fig. 3:2a) are used to represent MURB case. For URB case, the accurate distribution of urban surfaces and natural vegetation is updated with 2011 Landsat satellite observations (Fig. 3:2b). The urban land-use type for URB is further classified into three different sub-classes (Low intensity residential – LIR, High intensity residential – HIR, and Commercial or industrial – COI) to account for variation in development density and different urban surface characteristics (Fig. 3:2b and Table 3:1). URB+AH represents the URB scenario plus AH parameterisation (Table 3:1); this is to account for the contribution of AH on the meteorology of the area. Finally, for the NOURB case, the urbanised surfaces are replaced with the domain nearest-neighbourhood grid vegetation type (i.e., an idealised scenario with the GKL area covered with natural vegetation). Comparison of the different dataset clearly indicates that rapid urbanisation has taken place over the GKL. To study the effect of urbanisation on GKL, URB+AH and NOURB are compared. It should be noted that urban parametrisation of the area is adapted from literature in the region (Table 3:1). Only case URB+AH has anthropogenic heat parameterisation. This is in line with Lowry (1977) and Oke (2006) concept of evaluating urban effects (i.e., simulating “*scenarios such that when present and absent*”). The no-urban scenario (NOURB) method of evaluating urbanisation effect (such as UHI) largely removes such effects as sea-land breezes, impacts of clouds, advection, heatwaves (Smogransky waves), and topography that may alter the surface temperature or other meteorological parameters (Bohnenstengel et al. 2011). This method (no urban) has been successfully implemented in various urbanisation effect

assessment studies (Li et al. 2011; Wang et al. 2014), and results corroborated with other methods.

The NOAH LSM parameterises the land surface processes (Chen & Dudhia 2001) through coupling with the UCM via urban fraction parameter. The urban fraction represents the proportion of impervious surfaces in the WRF grid scale. The updated NOAH LSM; a land surface-hydrology model provides surface sensible and latent heat fluxes, account for sub-grid fluxes and skin temperature, as lower boundary conditions to the boundary layer scheme of the WRF. The single layer UCM on the other hand, has a simplified two-dimensional urban geometry approach, considering building height, roof and road width, and assumed street canyons of infinite length. UCM includes trapping and shadowing effects, and reflection of radiation, defined by the street canyon dimensions and orientation, as well as the solar azimuth angle. Therefore, by computing surface temperatures and heat fluxes of road, roof, and wall, it is possible to calculate the energy and momentum transfer between an urban environment and the atmosphere (Chen et al. 2011). The coupling of the single-layer UCM with the NOAH LSM completes the urban surface energy balance by calculating fluxes from the vegetated portion of the urban surface in a given grid cell.

Model planetary boundary layer (PBL) is handled by the Yonsei University (YSU) scheme (Hong et al. 2006). The YSU is considered to performed well in high resolution urban climate applications when combined with the coupled NOAH/UCM (Morris et al. 2016). Other physics parameterisations include a long-wave Rapid Radiative Transfer Model (RRTM) (Mlawer et al. 1997), a short-wave radiation scheme based on Dudhia

cloud radiation scheme (Dudhia 1989) and a surface-layer scheme based on the Monin-Obukhov similarity theory. The WRF single-moment six-class (WSM-6) microphysics scheme is applied to all domains (Hong et al. 2004; Dudhia et al. 2008). However, Kain-Fritsch convective cumulus parameterisation scheme (Kain 2004) is only applied to d01 and d02, since model horizontal resolution for d03 is sufficiently refined to resolve updrafts and downdrafts. Also, the explicit microphysics is assumed to reasonably resolved convection for d03 (Skamarock et al. 2008; Li & Pu 2009).

Table 3:1. Urban surface parameters used in the UCM for each urban land-use-cover type (Shahidan et al. 2012; Salleh et al. 2012; Ahmed et al. 2015; Salleh et al. 2015). Data obtained from the literature are supplemented with data from onsite observations, GIS, geospatial techniques, and google earth.

Urban Parameters	Low Intensity Residential	High Intensity Residential	Commercial or Industrial
Mean Building height (m)	8	12.5	14
Standard deviation of building height (m)	1	4	5
Building roof width (m)	9	11	11
Road width (m)	5	14	21
Maximum Anthropogenic heat ($W m^{-2}$)	12	19	79
Urban Fraction	0.68	0.75	0.89
Volumetric heat capacity of roof ($MJ m^{-3} K^{-1}$)	1.20	1.20	1.20
Volumetric heat capacity of building wall ($MJ m^{-3} K^{-1}$)	1.40	1.40	1.40
Volumetric heat capacity of ground (road) ($MJ m^{-3} K^{-1}$)	1.68	1.68	1.68
Thermal conductivity of roof ($W m^{-1} K^{-1}$)	0.67	0.67	0.67
Thermal conductivity of building wall ($W m^{-1} K^{-1}$)	0.80	0.80	0.80
thermal conductivity of ground (road) ($W m^{-1} K^{-1}$)	1.32	1.32	1.32
Surface albedo of roof	0.20	0.20	0.20
surface albedo of building wall	0.20	0.20	0.20
surface albedo of ground (road)	0.11	0.11	0.11
surface emissivity of roof	0.90	0.90	0.90
surface emissivity of building wall	0.90	0.90	0.90
surface emissivity of ground (road)	0.93	0.93	0.93

Due to lack of sufficient buildings data for the cities in the area, the single-layer UCM is used to parameterise a typical urban area in the region (Table 3:1). Thus, I acknowledged the likely uncertainties the uniform parameterisation of the urban canopy for the urban areas might impose on the numerical simulations results. Also, the influence of aerosols is not considered

because of the lack of observed data and related information. Though this will reduce the complexity of the model calculations and computational cost, it could as well impact on the overall magnitude of the simulation bias. Anthropogenic heat and aerosols release in urban areas have been reported to modify the urban energy balance and radiation processes of urban areas in other cities (Chen et al. 2009).

The effect of urbanisation on thermal conditions of the environment has been reported to be evident during days with cloudless, calm wind and without precipitation (Heisler & Brazel 2010). Southwest monsoonal flows associated with drier conditions relative to the northeast monsoon in the region (MMD 2015) brings about conditions favouring urbanisation impact assessment as highlighted in the later. In addition, the availability of few monitored observed data (air temperature, relative humidity and wind speed) (Table 3:2) with limited missing observations by the Department of Environment Malaysia (Jabatan Alam Sekitar) is among the reason for the choice of September 2011 for this study. This period shows calm synoptic coinciding with the withdrawal of the Southwest monsoon of the region; characterised by southwesterly winds, calm weather, low wind speeds and humid conditions (Fig. 3:3) typical of Peninsular Malaysia (Oozer et al. 2016).

Table 3:2. Measurement site metadata

Station Name	Station ID	Latitude (°)	Longitude (°)	Elevation (m)
Nilai	DOE1	2.8030	101.797	32
Kelang	DOE2	3.0103	101.4081	4
Petaling Jaya	DOE3	3.1017	101.607	45
Shah Alam	DOE4	3.0850	101.533	53
Putrajaya	DOE5	2.9319	101.682	35

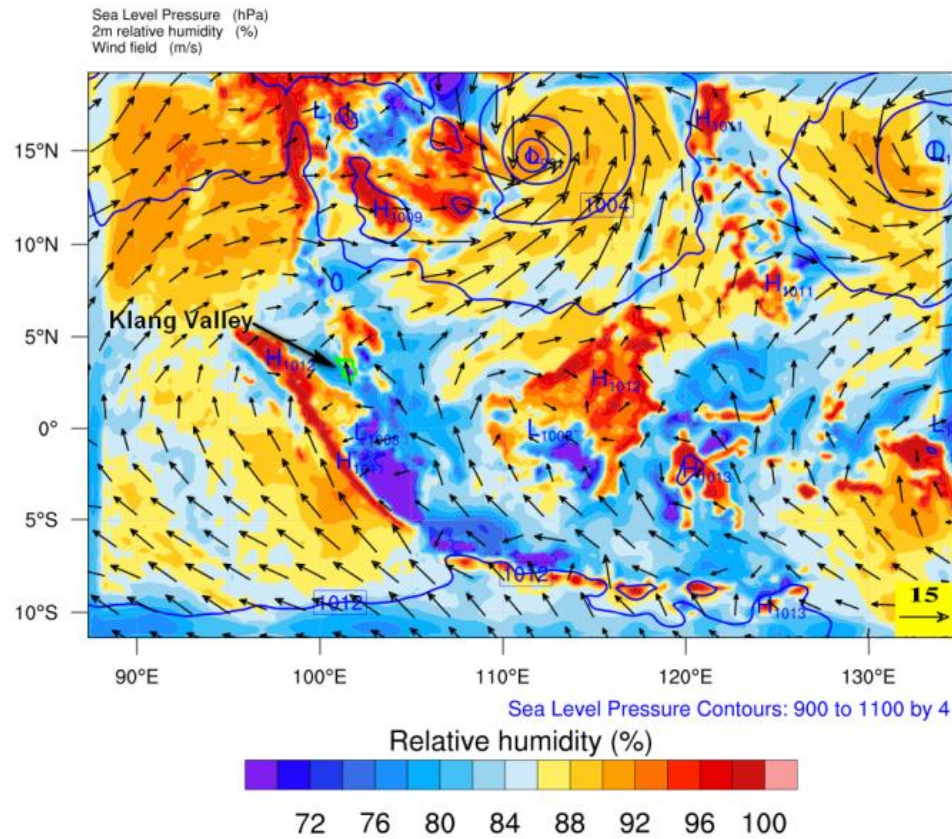


Fig. 3:3. Average meteorological conditions of the study region for September 2011; Blue contour lines (Sea level pressure, hPa), black arrows (wind fields, ms-1), spread contour (relative humidity, %) and the area with shaded green boundary (Klang Valley).

Manual correction is conducted on the observed data to replace three missing data (20110922_07, 20110924_11 and 20110926_21) with the observation time series mean. In total, 738 simulation hours are conducted and model's first 24 h used as spin-up time. Furthermore, a total of 113 h with observed precipitation from the simulation results are discarded before remaining simulated hours are averaged over a 24 h period for the analyses presented herein. Student's *t*-test at 95 and 99% confidence level is used to determine significance of results. Model validations and analyses are conducted on d03, except stated otherwise.

3.3 Model validation, results and discussions

3.3.1 Model validation

Atmospheric and mesoscale models have inherent limitation to accurately predict true ground observations. These inherent limitations may be due to the complexity of the physical characteristics of land, surface and atmosphere interactions simplified through different theoretical assumptions. Thus, validation of a numerical model (such as the WRF/NOAH/UCM) ability to reproduce observed meteorology of the area of interest before application in an investigation becomes a necessity. In this study, the model is validated against a network of monitored observations (Table 3:2) using four statistical tools: mean bias (MB), root-mean square error (RMSE), Pearson's correlation coefficient (*R*) and hit rate (HR). For 2-m temperature (T2m), relative humidity (RH2m) and wind speed (WS10m), 1.0 °C (Cox et al. 1998), 1.0 m/s (Kulkarni et al. 2008) and 5% (Lawrence 2005) are respectively applied as the desired accuracy (hit-rate).

Table 3:3 presents average statistical summary of WRF/NOAH/UCM validations against the observations for each of the land-use-cover data experimented, while Fig. 3:4 on the contrary, is a graphical demonstration of the comparison of averaged diurnal cycle of meteorological parameters against the observations. Overall the model performs well for 2-m temperature, relative humidity and wind speed. The model is able to reproduce the diurnal patterns of the meteorological parameters examined over the investigated area, with *R* values range of 66% to 90%, and *HR* range of 57% to 99%. NOURB and

MURB show the least diurnal trend agreement (R) and “yes” percentage, with the later performing better than the former.

Table 3:3. Statistical summary of model validation for the different experiments

Variables	Statistics	MURB	URB	URB+AH	NOURB
T2m (° C)	<i>MB</i>	-0.99	-0.16	0.20	-1.30
	<i>RMSE</i>	1.53	1.43	1.07	1.69
	<i>R</i>	0.84	0.83	0.86	0.90
	<i>HR</i>	0.81	0.85	0.86	0.71
RH2m (%)	<i>MB</i>	1.12	-4.97	-5.24	3.39
	<i>RMSE</i>	5.83	6.59	4.35	5.60
	<i>R</i>	0.82	0.82	0.84	0.87
	<i>HR</i>	0.69	0.64	0.71	0.57
WS10m (ms⁻¹)	<i>MB</i>	0.10	-0.06	0.10	0.11
	<i>RMSE</i>	0.49	0.46	0.40	0.48
	<i>R</i>	0.68	0.69	0.66	0.72
	<i>HR</i>	0.99	0.99	0.99	0.99

Cold bias of -0.16, -0.99 and -1.3 °C are observed for URB, MURB and NOURB, respectively while URB+AH shows a warm bias of 0.20 °C. Updating the terrestrial data in the WRF model and the inclusion of AH in the single-layer UCM to represent the true urban characteristics and thermodynamics of the study area yield an improved performance of the model by a 0.1 and 0.36 °C reduction in *RMSE* of 2-m temperature for URB and URB+AH, respectively (Table 3:3). For relative humidity, under-estimation of predicted forecast is observed for URB (-4.97%) and URB+AH (-5.24%), while over-forecasting is noted for MURB (1.12%) and NOURB (3.39%). Furthermore, AH parameterisation in the UCM also caused an improved model prediction of RH2m for URB+AH. However, the contrary is observed for RH2m when the land-use-cover is improved (Table 3:3). In the case of wind speed, the model has consistently overestimated the forecasted values, except for URB with a non-significant (at 95% level) underestimation of -0.06 ms⁻¹ (Table 3:3). Also, the influence of land-use and AH parameterisations on the

RMSE are less significant for wind speed relative to other meteorological parameters examined, except for URB+AH (Table 3:3).

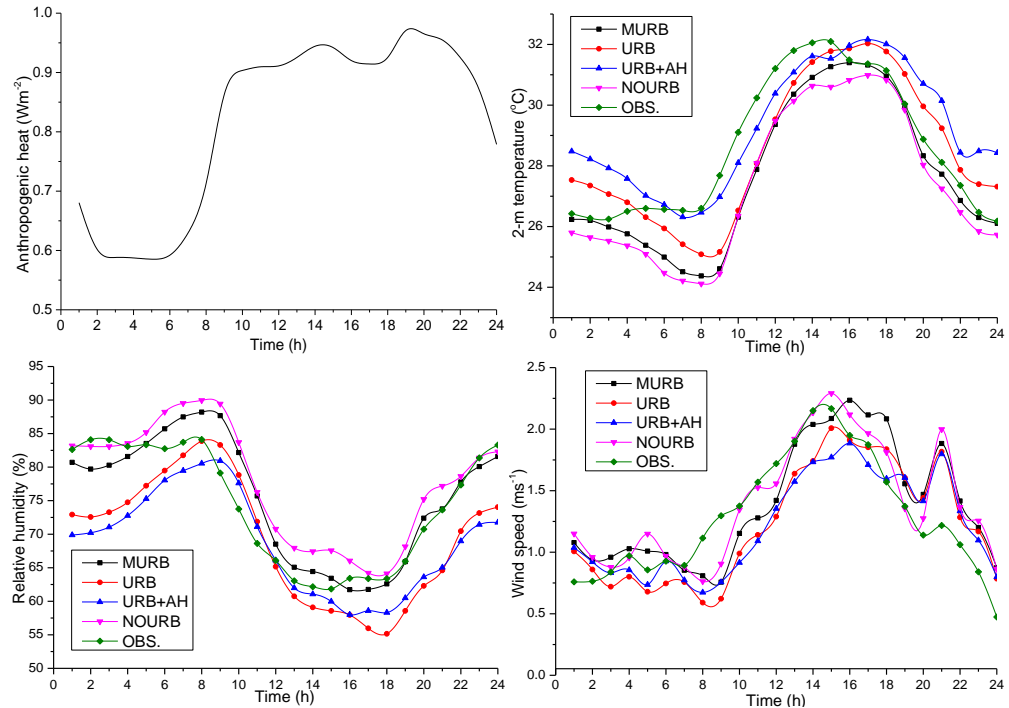


Fig. 3:4. (a) The diurnal profile of anthropogenic heat used in the single-layer UCM (top left panel); the ratio to the peak value of each urban land-use-cover type. Peak values for each urban type are given in Table 3:1. Averaged model validation: (b) 2-m temperature (top right panel), (c) 2-m relative humidity (bottom left panel) and (d) 10-m wind speed (bottom right panel).

The inclusion of AH to the WRF modelling system through the UCM adds to the sensible heat flux of the roof, road and wall surfaces, which makes up the total urban canopy sensible heat flux. This, of course, will change the canopy layer temperature of the urban environment and modifies other urban meteorological conditions (Fig. 3:4). Also, the improved terrestrial data will increase the surface fluxes accounted in the coupled model, through the NOAH/UCM, which integrates the different urban surface features into the energy balance and wind shear calculations. Furthermore, the NOAH/UCM takes into account the momentum sink over the entire building height, as well

as shadowing from building and the radiation trapping effect (reflection of radiations in the canopy layer). The influence of land-use and AH parameterisation on the overall model performance is clearly demonstrated diurnally in Fig. 3:4(a, b and c). For canopy layer temperature, improvement of the land-use data and AH additions caused an increase in surface temperature which reduces the cold bias observed for NOURB and MURB. AH role in improving model performance is more significant during morning to midday, 0600 – 1500 LT (LT - Malaysian Local Time), while the role of land-use update lasted from daytime to nighttime, 1200 – 2200 LT. The increase in T2m caused by land-use improvement and AH addition has a corresponding reduction in the relative humidity above the area, which led to model underestimation of the parameter. The somewhat expected effect of AH on RH2m is stronger during morning and nighttime (Fig. 3:4c). Also, the effects of land-use update and AH on wind speed is similar to that of relative humidity. Overall, land-use improvement (URB) and AH parameterisation (URB+AH) caused 6.5% and 25.2%; 13% and 34%; 6.1% and 13% changes in model performance (of *RMSE*) for T2m, RH2m and WS10m, respectively, with AH having an obvious greater effect. Hence, the coupled model could be considered to have performed significantly well for URB+AH. Except otherwise stated, results and analyses of the Klang Valley environment are conducted using the URB+AH case. Having established the model ability to reproduce air temperature, relative humidity, and wind speed, the coupled system is used to examine the effect of urbanisation on the spatial distribution and temporal changes on meteorology and urban heat island of the Klang Valley.

3.3.2 Results and discussions

3.3.2.1 Urban surface energy balance and PBLH

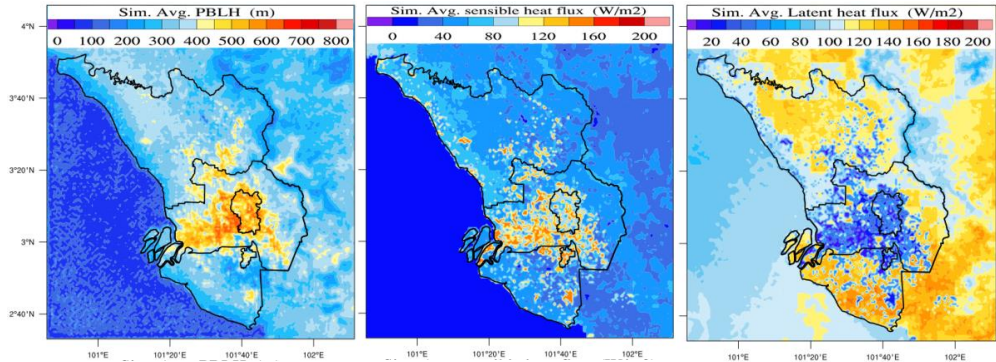


Fig. 3:5. Averaged (a) PBLH in m (left panel), (b) Sensible heat flux – SH (middle panel), and (c) Latent heat flux – LH, for the simulated period (right panel). SH and LH are calculated in Wm^{-2} .

Fig. 3:5 shows a simulated average of PBLH, sensible and latent heat fluxes above GKL area during the investigated period. Spatial variations of PBLH, LH and SH can be seen clearly on the model domain, with urban concentrated areas showing greater differences. LH and SH fluxes are observed to vary with urbanisation (Fig. 3:2b and Fig. 3:5). SH and LH variations for different land-use-cover types are also noticed. COI has an average heat flux of $149.9 \pm 120.5 \text{ Wm}^{-1}$ for SH, while the rural area (average of the vegetated classes) shows the least average flux for SH, with a mean magnitude of $56.6 \pm 84.6 \text{ Wm}^{-2}$. However, average fluxes (LH) of $(18 \pm 21.7 \text{ Wm}^{-2})$ and $(130.3 \pm 171.3 \text{ Wm}^{-2})$ are observed for COI and rural areas, respectively. Low surface albedo, specific heat capacity and moisture availability of urban surfaces are among the features that induce the observed spatial variability in surface fluxes between urban and rural areas. Conversion of vegetation to urban increases the accumulated heat transport away (SH) from urbanised surfaces. Conversely,

reduction in vegetation of urbanised area causes a decrease in the amount of moisture presence (from the soil and vegetation in the area due to evaporation) above the surfaces; hence limiting the amount of accumulated moisture transported away (LH) from the urbanised surfaces. The vegetated classes have fluxes with lower spatial gradient for both SH and LH. Nevertheless, advection of fluxes due to sea breezes during daytime induced a steep flux gradient in vegetated land-use types; this is detectable around the coasts, along the Strait of Malacca (Fig. 3:5). Also the complex interaction of sea-land breezes and mountain-valley breezes along the Titiwangsa mountain range creates flux gradients, especially, for LH. For the period considered in the current study, it is observed and expected that during daytime, solar irradiance dominates the domain surface energy fluxes.

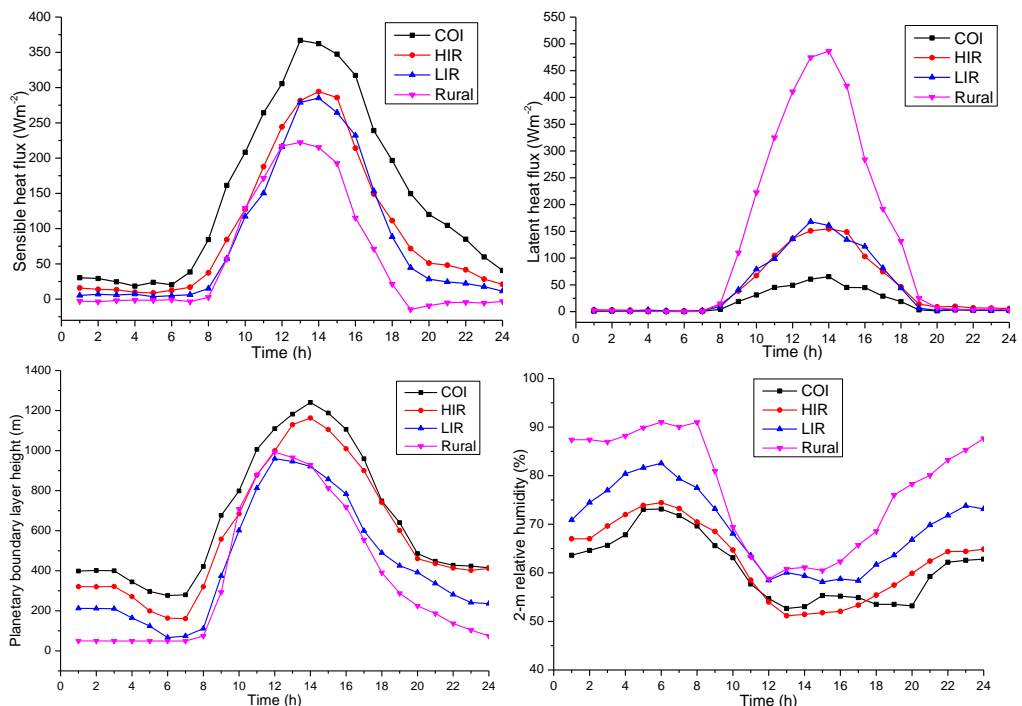


Fig. 3:6. Averaged temporal variations of meteorology of the GKL: (a) Sensible heat flux (Wm^{-2}) – top left panel, (b) latent heat flux (Wm^{-2}) – top right panel, (c) Planetary boundary layer height (m) – bottom left panel, and (d) 2-m relative humidity (%) – bottom right panel.

Urbanisation modifies components of the surface energy budget. This is clearly captured in Fig. 3:6b, during which the daytime latent heat flux over the rural area is clearly distinguished from the other urban surfaces. Obviously, presence of more vegetation, moisture availability and pervious soil in the rural area enhances increased phase changes above the area relative to the three urban classes. However, the rural area and the three urban classes maintain a stable profile of LH, with values between 0.2 and 9 m, during morning (0100 to 0700 LT) and nighttime (2000 to 2400 LT). Nonetheless, the SH benefits greatly from the increase in urban surfaces, which cause rapid changes in heat content of the surfaces during solar irradiance. This is evident in the distinction observed in the diurnal cycle of SH as shown in Fig. 3:6a. Prior to sunrise (0730 LT), low canopy layer fluxes effect a slow changes of the underlying surface temperature, which lead to an observed stable SH for the urban classes (between 4 and 31 Wm^{-2}) and rural area (between -1 and -4 Wm^{-2}). This is however different during daytime, where rapid evolution of SH (favoured by shortwaves solar radiation and atmospheric longwave fluxes) is observed. During this time (1000 – 1800), maximum values of SH (367, 294.4, 285.3 and 222.2 Wm^{-2} , for COI, HIR, LIR and rural, respectively) are observed. The effect of urbanisation on the surface energy exchange is expected to affect the local environment, especially, T2m, PBLH, RH2m and UHII.

PBLH is vital in weather and meteorology (especially in urban meteorology) for air pollution transport and dispersion modelling. During the period investigated, the PBLH shows variations in spatial distribution and temporal changes for the different land-use-cover types examined. The depth of the PBL is within few to hundreds of metres during morning and night time.

Conversely, the depth increases rapidly at daytime, with solar radiation. At daytime, the Earth's surface receives shortwave solar radiations and atmospheric longwave fluxes. These fluxes heat the surface and increase the surface temperature, and as a result cause vertical and horizontal transport of the heat fluxes (SH). Furthermore the increase in surface temperature results in an increase of evaporation processes of available surface moisture and transpiration from vegetation, which is then transported by wind (LH) into the lower boundary layer above the surface – canopy layer. These interactions of the thermodynamics of solar radiation, atmospheric longwave fluxes, and the sensible and latent heat fluxes affect the temporal growth of the PBLH (Fig. 3:6). On the other hand, the spatial distribution of the PBLH is influenced by variation in surface properties and sea-land breezes (Fig. 3:2b, Fig. 3:5 and Fig. 3:6), the latter having the least effect. Fig. 3:6c demonstrates that the evolution of the PBLH starts with minimum values (49.2, 66.3, 160.6 and 276.5 m for rural, LIR, HIR and COI, respectively) during morning (prior to onset of solar radiation, 0730 LT) and peak between 1200 LT and 1400 LT (991.9, 959.8, 1163.0 and 1240.5 m for rural, LIR, HIR and COI, respectively), after which a decline in PBLH growth is observed. During morning and nighttime, the three urban classes have a near-stable PBLH between 195 and 490 m, while the rural area has a shallow convective PBLH of 50 to 180 m.

COI consistently produced the maximum PBL, followed by HIR, and rural area the least, with corresponding averaged values of 653.1 ± 326.2 , 582.0 ± 322.0 and 361.5 ± 345.5 m. Higher percentage of urban fraction (89%) and AH (79 Wm^{-2}) of COI (Table 3:1) ensures that it has more fluxes above its surface and as well retains significant amount of heat energy during solar

radiation. The retained heat energy is then re-radiated into the urban canopy layer after sunset, providing the needed fluxes to maintain a deeper PBL height relative to the other classes (Fig. 3:5 and Fig. 3:6). In addition, the inclusion of AH to the model surface energy budget increases the available fluxes on the urban classes relative to the vegetated classes, with no AH parameterisation. Effect of AH on the PBLH is evident in Fig. 3:6c, especially, during morning and nighttime (Fig. 3:4b). From the average PBLH representation, Fig. 3:5a, and the land-use-cover spatial distribution (classification), Fig. 3:2b, it can be observed that the PBLH varies spatially, with decreasing magnitude in order of decreasing urban fraction. The effect of sea breeze is noticeable along the coastline of GKL.

3.3.2.2 Wind speed

Evolution of the wind speed over the area is significantly influenced by local circulations (sea-land breezes) caused by temperature gradient due to differential heating between land and sea. The GKL is coastal, thus, complex local circulations are inherent. These circulations drive local and regional air pollution transport, and boundary layer evolution. Sea breeze starts developing a few hours after the onset of daily solar radiation and becomes fully developed at 1500 LT (Fig. 3:7b), blowing south-westerly. At this time, the strength of the sea breezes is about 3 ms^{-1} , with a reduced magnitude over the urban area (especially, for HIR and COI), caused by increase obstruction from urban surfaces. From Kuala Lumpur, a downwind convergence is formed around northeast of the Klang Valley due to north-easterly mountain breeze induced by the low surface temperature (Fig. 3:9a) around the Titiwangsa mountain range. On the other hand, land breeze which started developing from 2200 LT

becomes developed at 0100 LT, with a weaker strength (relative to the sea breeze) blowing north-easterly from the Malay Peninsula to the strait of Malacca (Fig. 3:7a). In Fig. 3:7a, it is observed that the land breeze has a weak momentum and does not penetrate deep into the sea compared to the sea breeze. Convergence zones are formed around the southeast and northeast of GKL during the land breeze system. These convergence zones induce updrafts (not shown) of different magnitudes depending on the surface temperature around the area. Comparison of the NOURB case with the other cases reveals the effect of urbanisation on the evolution of sea/land breezes, with the stronger effect noticed for URB+AH, especially above the urban area.

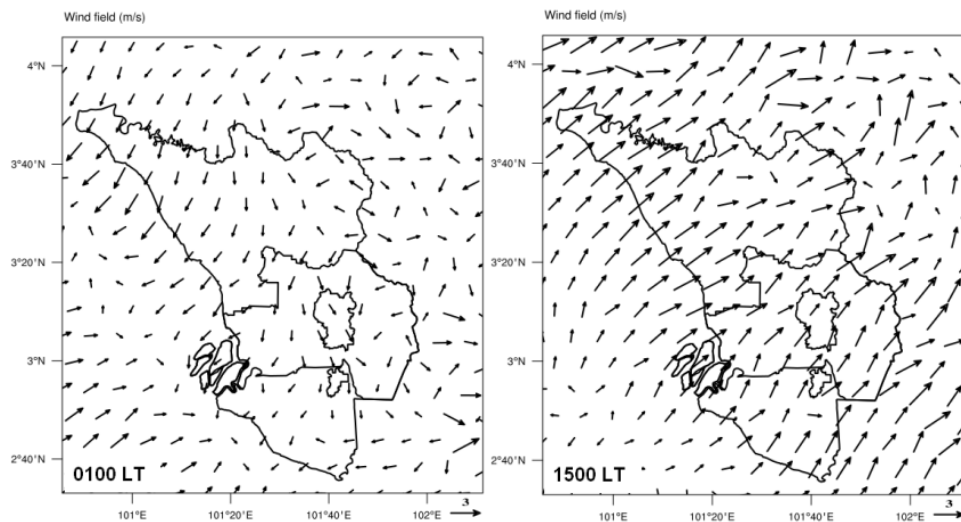


Fig. 3:7. Averaged wind field (ms^{-1}) above the simulated domain demonstrating local sea and land breezes at fully developed stages: (a) land-sea breeze (left panel) and (b) sea-land breeze (right panel). LT is the Malaysian Local Time used in this study

3.3.2.3 Relative humidity

Fig. 3:8 demonstrates the spatial distribution and temporal changes of relative humidity in the canopy layer of the examined domain. Urban dry island (UDI) – area with lower RH_{2m} relative to the surrounding environment, is formed above the urban surface, typical with human-engineered surfaces such as

cement, concrete and asphalt. These materials have water-proof like (impermeable) surfaces, with little/no available soil moisture compare to the rural surfaces. The rural surface is favoured with more vegetation, soil moisture and evapotranspiration. This is evident in the diurnal profile of RH2m as shown in Fig. 3:8. In addition to the impact of surface conversion, daily solar radiation has a direct effect on the RH2m. RH2m starts increasing after sunset to maximum values of 91, 82.6, 74.4 and 73.1% between 0600 and 0700 LT, for rural, LIR, HIR and COI, respectively, prior to sunrise (Fig. 3:6d). Meanwhile, RH2m commences a clear decrease in magnitudes to minimum values of 58.7, 58.1, 51.2 and 52.7% after sunrise, for rural, LIR, HIR and COI, respectively, between 1200 and 1600 LT. It is evident that increase in urban fraction decreases the surface relative humidity. A careful examination reveals averaged RH2m of 77.2 ± 11.5 , 69 ± 8.0 , 62.6 ± 7.7 and $61.2 \pm 6.7\%$ for the rural, LIR, HIR and COI, respectively. A quick comparison of the three simulated urban land-use-cover and the vegetation land-use-cover shows significant (at 95% level) urbanisation induced spatiotemporal effect on RH2m over the local environment (Fig. 3:6d and Fig. 3:8). The observed influence of urbanisation in decreasing RH2m is preponderant during morning (1100 – 1800 LT) and nighttime (2000 – 2400 LT) (Fig. 3:6d and Fig. 3:8a,c). Albeit small, the mean contrast between urban and rural RH2m shows that the city air is somewhat drier during daytime (Fig. 3:6d and Fig. 3:8b). Surface humidity is important for human thermal comfort and moisture processes, and as well influence on diurnal UHII evolution.

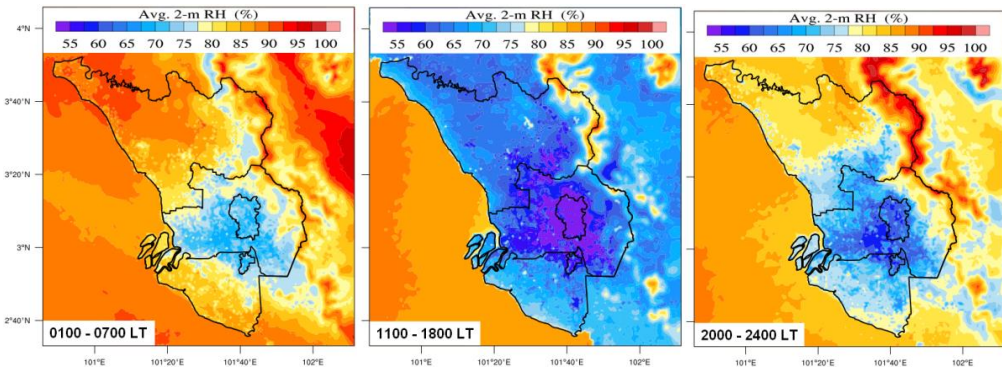


Fig. 3:8. Spatiotemporal variation of relative humidity above the surface during: (a) morning (left panel), (b) daytime (middle panel) and (d) nighttime (right panel)

3.3.2.4 2-m temperature and urban heat island

Fig. 3:9 shows the diurnal cycle of air temperature and UHI. Also, Fig. 3:10 shows spatiotemporal changes in magnitudes of T2m and canopy UHI, but with simulation results classified into three intervals (morning; 0100 – 0700 LT, daytime; 1100 – 1800 LT, and nighttime; 2000 – 2400 LT) distinguished by solar radiation occurrence. The canopy layer temperature, like other meteorological parameters, has temporal variation and spatial distribution with strong dependence on periodic (solar radiation and wind system) and human-induced forcing. T2m starts increasing spontaneously after sunrise to maximum magnitudes, somewhere between 1400 and 1600 LT, after which a decline is observed. Minimum and maximum T2m of 24.67 and ~ 33.0 °C are observed over the GKL area during the period of investigation on rural and urban (COI) surfaces, respectively. Averaged T2m of 30.10, 29.26, 28.27 and 27.85 are observed above COI, HIR, LIR and rural area, respectively (Fig. 3:9c). The water body on the Strait of Malacca is observed to maintain temperatures above the vegetated area during morning and nighttime; while the contrary is the case during daytime (Fig. 3:10). The impact of urbanisation on air

temperature in the GKL is reflected on the diurnal temperature range variation between the different land-use-cover types.

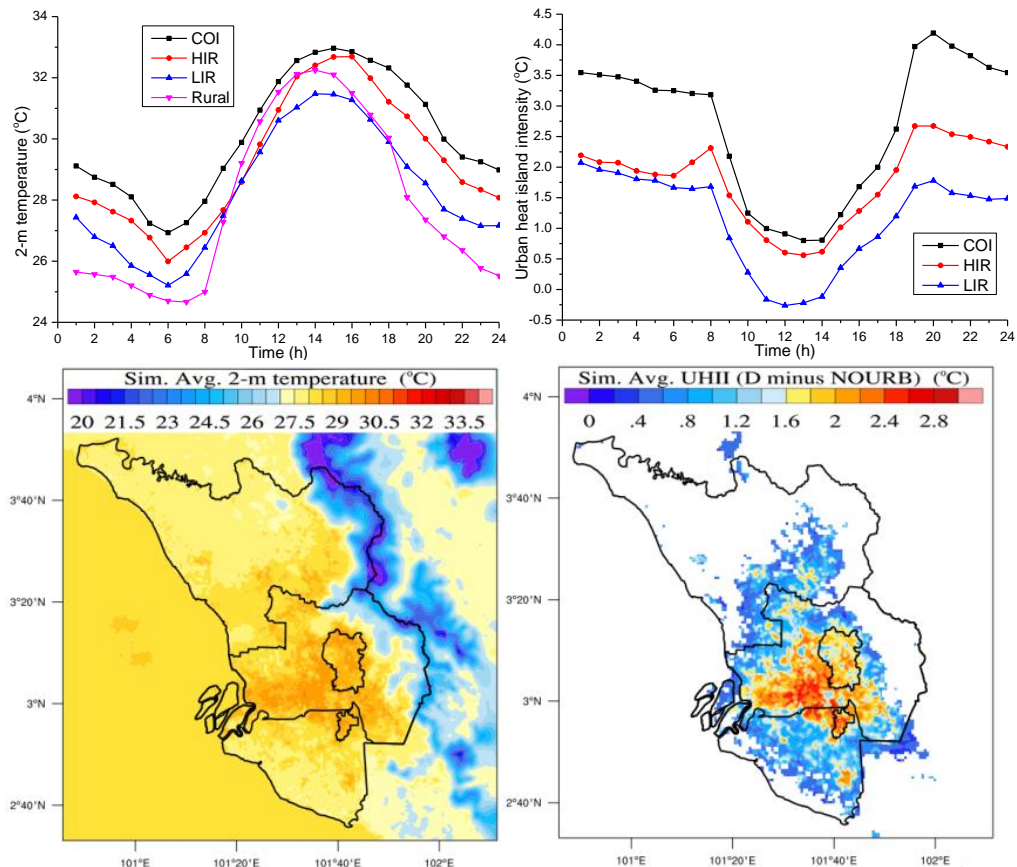


Fig. 3:9. Averaged temporal variations of: (a) 2-m temperature (left panel) and (b) canopy layer urban heat island (URB+AH minus NOURB), in °C (right panel). The bottom panels represent the spatial distribution and variation of the simulated average (a) 2-m temperature in °C (left panel) and 2-m urban heat island intensity (right panel). “D” in the UHII legend substitutes URB+AH – because of limited space accommodate URB+AH.

Diurnal temperature range (DTR) is a measure of the difference between maximum and minimum temperatures within a considered period. DTR is observed to decrease with increasing urbanisation of the area. COI with an urban fraction of 0.68 has a DTR of 6.03 °C, while the rural area has DTR of 7.58 °C. HIR and LIR have DTR of 6.27 and 6.70 °C, respectively. Urban surface materials are known for high thermal diffusivity and heat retention; thus, surface radiation losses/re-radiation of heat fluxes extend well after sunset

to nighttime and early morning. This causes increase in the minimum temperature of the urban surfaces and however, maintain little gains on the maximum temperature. This is evident in Fig. 3:9a, with an observed mean simulated minimum (maximum) T2m of 24.67 °C (32.25 °C) and 26.93 °C (32.96 °C) for the rural and urban surfaces, respectively.

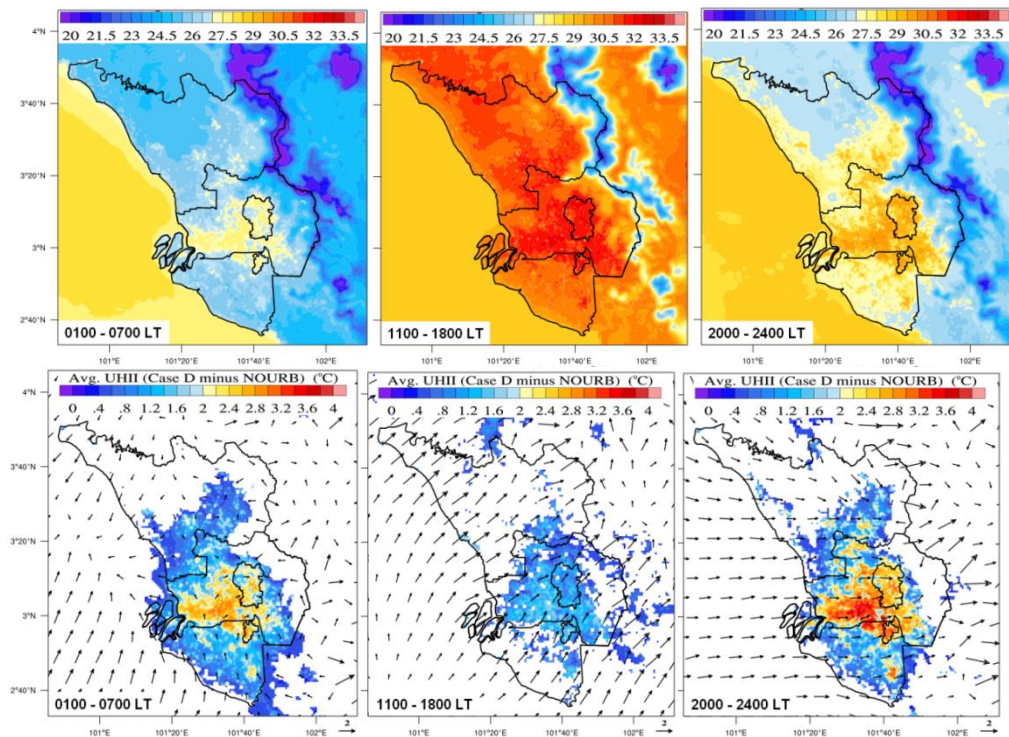


Fig. 3:10. Average spatial distribution and temporal changes of 2-m temperature and urban heat island intensity. Top panels represent temperature during: (a) morning (left), (b) daytime (middle) and (c) nighttime (right), while bottom panels represent UHII during: (d) morning (left), (e) daytime (middle) and (f) nighttime (right). “D” on the legend of each case is used to substitute URB+AH, due to limited space on the each plot.

The UHI (URB+AH – NOURB) above the GKL is estimated by subtracting the NOURB experiment from the URB+AH case. Results indicate that stronger effect of the phenomenon (UHI) is experienced during nighttime, with a prevailing maximum magnitude of ~4.20 °C and ~2.70 °C at 2000 LT in the commercial district and high urban intensity residential area of GKL, respectively (Fig. 3:10). On the other hand, low urban intensity residential

maintains a maximum magnitude of ~ 2.1 °C at 2400 LT (Fig. 3:10). Decrease in magnitudes of the UHI for the three urban land-use-cover types started after sunrise to minimum values between 1100 LT and 1400 LT. However, near-steady values of UHII are maintained between morning ($3.2 - 3.5$ °C, $1.8 - 2.2$ °C and $1.7 - 2.1$ °C for COI, HIR and LIR, respectively) and night-time ($3.5 - 4.2$ °C, $2.3 - 2.7$ °C and $1.5 - 1.8$ °C for COI, HIR and LIR, respectively). Overall, the urban area of GKL is warming more than the rural at ~ 1.9 °C per day; with COI contributing about 48% (2.68 °C) of the heating, while HIR and LIR contribute 32% (1.77 °C) and 20% (1.15 °C), respectively.

Spatial distribution of UHI is observed to be dependent on urban land-use type; this is preponderant during morning and nighttime. Thus, maximum warming of the area is found to decrease radially from COI to LIR in descending order of magnitudes (Fig. 3:2b and Fig. 3:10) for the three time intervals considered. However, this is less significant during daytime, because of the equal heating of rural and urban surfaces of GKL by solar radiations (Fig. 3:10e). This is evident in Fig. 3:9b and Fig. 3:10e, where the averaged UHII is least (1.07 , 0.81 and 0.04 °C for COI, HIR and LIR, respectively) significant (at 95 % level) relative to the other two intervals considered. During daytime, the Earth's surface is heated by direct solar radiation and atmospheric longwave fluxes, which dominates the fluxes over vegetated and urban landcover; this in effect reduces the thermal difference between urban and vegetated surfaces during daytime. This is however different during morning and nighttime, where most of the fluxes over vegetated and urban landcover are by re-radiation of absorbed fluxes. Conversion of vegetated areas to urban landcover modifies the urban energy exchange (Fig. 3:6a and b) and the

surface diffusivity (Salleh et al. 2013). Furthermore, urbanisation modifies the land surface thermal properties, such as surface albedo and heat capacity, which affect surface solar radiation absorption and retention rate. Meanwhile, radiation feedback in the canopy layer also plays an important role in surface energy budget. More shortwaves radiation is absorbed and trapped by the urban surfaces and buildings, which is then release at nighttime, leading to greater increase in the thermal difference between urban and vegetated areas. Low urban surface albedos and high heat capacity of urban landcover imply higher heat retention relative to the vegetated areas. It should be noted that while urbanisation induced effect of UHI on the environment is significant at the 95% and 99% confidence levels for COI and HIR, for the three windows (before, during and after solar radiation) investigated, significant effect (at 95% level) is nevertheless noted for HIR during morning and nighttime only.

Among factors observed to affect the UHI spatiotemporal changes during the study is the complex wind system of the tropical conurbation in GKL. The sea-land and mountain-valley wind system modifies the UHI greatly as can be noticed on both air temperature and UHI representation in Fig. 3:9 and Fig. 3:10. During daytime, sea breezes and mountain-valley winds resulting from differential surface heating cause the biggest forcing to the spatial variability of surface temperature. This is evident along the coastline and around the Titiwangsa mountain range. This period (1100 – 1800 LT) coincides with the initiation and full development of the sea breezes emanating from the Malacca Strait, and blows downwind lower air temperature above the water body. Conversely, during morning, surface fluxes are dominated by re-radiated heat and evapotranspiration above the urban surface. Nonetheless,

along the coastline and mountain range, land breeze and mountain breeze are observed to affect the temperature gradient during morning (0100 – 0700 LT), respectively.

3.4 Conclusion

In this study, high resolution numerical simulations are conducted to examine the impact of land-use and anthropogenic heat parameterisation on improving the performance of a coupled model system (WRF/NOAH/UCM). Urbanisation effect on the meteorology of the area is also investigated. Model validation shows model ability and suitability in reproducing the meteorological parameters over the area; thus judged fit for use in the current study. Results indicate that indeed parameterisation of AH and land-use-cover improved the model predictions of air and surface meteorology significantly, with AH showing greater effect. Environmental conditions of the area are observed to have been modified by urbanisation. For instance, mean relative humidity and latent heat flux decrease in urban areas relative to the rural surfaces. Nevertheless, impact of urbanisation is also observed to substantially increase the average values of PBL, SH, T2m and UHII during the period investigated; urban area having greater values relative to rural area.

Conversion of vegetated area to urban surface modifies the surface energy components and evolution of PBLH and UHII of the local environment. Decrease in canopy layer diurnal temperature range is observed to decrease in urban areas, with the effect more prominent within areas with high urban fractions. The effect of urbanisation on UHI of GKL is dominant after sunset, and continues to morning hours, before decreasing to minimum values during

daytime. Furthermore, spatial distribution and temporal changes of meteorological parameters are dependent on urbanisation intensity and periodic forcing such as solar radiation, sea-land breeze and mountain-valley breeze. Spatial distribution of parameters such as T2m, PBLH, SH and UHI are observed to decrease radially from the urban centre to the minimum values around the least developed areas of GKL. However, RH2m and LH increase radially away from the urban centre.

The simulations conducted have demonstrated the effect of urbanisation on the meteorology of the GKL environment. Increase/decrease in urban/vegetation is observed to be one of the contributing factors for increase in air temperature, formation of UDI and UHI in urban areas. This implies that to maintain an urban area with a moderate temperature, effort should be directed to increase the vegetation fraction in urban areas; this could be achieved by urban forestry and greening. Uniform parameterisation of urban canopy and non-aerosols parameterisation on the model may have had influence on the model validation, however, this influence is not expected to be significant on model overall solution. Also, the current study does not account for the impact of urban design and building configurations, but only assessed the effect of urbanisation on the meteorological parameters of the environment. Thus, to evaluate the impact of aerosols, urban design and building configuration, further studies need to be conducted.

Chapter 4

4 Urbanisation of Putrajaya and its interactions with the local climate

Summary

Land use and land cover changes, urban warming and changes in urban climate variables of a given location are some of the profound signatures of urbanisation. Putrajaya is a planned city built from a formerly vegetated farm and agricultural lands to a modern urban city. This study aims to investigate the chronological local urban climate changes that have taken place over a decade (1999 – 2011) of urbanisation using the NCAR Weather and Research Forecasting (WRF) model coupled to a numerically proven land surface and urban canopy model (NOAH/UCM). Up-to-date and accurate land cover dataset of the region implemented for each year is derived from LANDSAT images. Model results are evaluated against a network of observational studies in the region. 2-m air temperature, wind speed, relative humidity, planetary boundary layer height and urban warming of the area in each of the considered years are carefully examined. Solar radiation, urban surface induced variations in the urban surface energy balance components, and variations of the study area urban climatic variables are also investigated. Model results demonstrate good correlation and agreements with the observed data. 2-m air temperature performance is observed to be better relative to other variables evaluated.

Results show that 2-m temperature of the area is increasing at the rate of 1.66 °C per decade, while the prevailing urban heat island intensity (UHII) of the area is ~2.1 °C. The urban climate prognostic and diagnostic variables show good correlations with the urban surface modifications of the area from the original natural surfaces, except for wind speed which shows less variability to urbanisation. Furthermore, formation of urban cool islands is also noticed for 1999, 2007, and 2011. Near-uniform net all-waves radiations of the different years experimented conform to tropical city low climatic variability. Finally, the thermal conditions of the area exhibit spatial and temporal variations heavily induced by urbanisation.

4.1 Introduction

Human continual strive for better living conditions has caused rapid urbanisation and expansion of human inhabited areas, which have replaced previously natural farmland and vegetation with engineered surfaces. This has caused changes in the environment, prominent of which are the canopy-layer temperature and urban heating (Landsberg 1981). The underlying land use and land cover changes caused by urbanisation has impact on the thermal and dynamic properties of land surfaces (Zhang et al. 2010). Meanwhile increased urban environmental pollution associated with urbanisation is caused by rural-urban migration prompted by search for better living conditions and daily routine to sustain the urban population. The urban population needs huge urban energy resources to maintain the urban metabolism (Kennedy 2007; Wolman, 1965). However, consumption of urban heavily needed resources comes with

damning consequences on the environment through releases of anthropogenic heat (AH) and associated disposable human wastes (Marais et al. 2014).

Engineered materials and impervious surfaces such as asphalt, concrete, bricks, stones and bitumen, roads, low and high rise buildings, pavements, sidewalks and bridges (Wijeyesekera et al. 2012), have immense contributions to the alteration of urban surface energy balance (Arnfield & Grimmond 1998), urban boundary layer (Barlow 2014), and the urban climate (Zhang et al. 2009), urban roughness (Cao & Lin 2014) and reduction in sky view factor (Jusuf & Hien 2009). Farmland and vegetation are characterised with permeable surfaces, low surface roughness length, moderate albedo, high evapotranspiration and moisture availability (Taha 1997; Grimmond & Oke 1999), which have been reported to contribute positively in reducing surface thermal conditions of the immediate environment (Rosenfeld et al. 1998; Zhang et al. 2014). On the other hand, typical urban engineered surfaces are often dark materials with low surface albedo, high thermal conductivity, heat storage capacity and impervious surfaces (Ashtiani et al. 2014; Yang 2013; Taha 1997). This creates elevated thermal climate with accompanying consequences such as human discomfort (Tomlinson et al. 2011; Emmanuel & Krüger 2012), increased cost of heating for tropical cities all year round and summer for sub-tropical and middle latitude cities (Priyadarsini et al. 2008; Chow & Roth 2006), and air quality (Lai & Cheng 2009).

A recent study of Singapore environment by Li et al., (2013), shows induced effect of urbanisation on UHI formation and alteration of the urban boundary layer. UHI raises major health (Enete et al. 2014) and economic concern (Elsayed 2012) because of its associated daily elevated temperatures.

For instance, the number of deaths linked to heat stroke in Japan has outnumbered other natural causes such as typhoon and tornadoes (Fujibe 2009). In Japan, ambulances transport more than 10,000 people with heat stroke-related to the hospitals in the Tokyo metropolitan city in summer (Fire and Disaster Management Agency of Japan 2011). Furthermore, according to a case study in Japan, an increase in the daytime temperature by 1 °C during the summer increases daily maximum energy demand by about 1.9 GW in the Tokyo metropolitan area and its surroundings (Goto et al. 2004).

Many researches on urbanisation are channelled towards understanding the influence of urbanisation on the urban climate environment and synoptic processes (Jin et al. 2005), UHI (Rizwan et al. 2008), contributions of urban environments to global warming (Grimmond 2007), changes of precipitation (Shem & Shepherd 2009), urban surface run-off (Hamdi et al. 2011), and reduced evapotranspiration and moisture availability in cities (Jiang et al. 2015).

Relative to average global changes, urban areas have experienced more warming (Ren & Zhou 2014). Ren et al. (2008) carries a detailed analysis of data collected from 282 meteorological stations in Northern China, and discovers that urban warming has impacted prominently on the regional mean annual temperature series in the range of ~0.11 °C per decade. Urban warming has also impacted on the total annual mean surface air temperature change which was estimated to attain ~38% using the national basic reference station dataset. To further validate the influence of urban on global surface temperature, Jones et al. (2008) assessed possible urban influences using sea surface temperature data sets for Eastern Chinese mainland. Their investigation

reveals that urban associated warming over China is about 0.1 °C/decade during the period 1951–2004, with true climatic warming accounting for 0.81°C over this period. Jones et al. (2008) findings agree roughly with the discovery of Ren et al. (2008) on the contribution of urban warming to global surface temperature. Based on a reanalysis of global weather data from 1950–1999, Kalnay & Cai (2003) claims that half of the observed decrease in the diurnal temperature range in the continental United States is due to urban and other land use changes, and estimates 0.27 °C mean surface warming per century to have been due to land-use changes. This estimate is twice as the previous estimates based on urbanisation alone.

Despite the huge number of studies on the impact of urbanisation in other parts of the world, as of the time of reporting this study, only few studies (Sani 1980; Sani 1993; Elsayed 2012a) have been conducted in tropical regions like Malaysia to understand the induced impacts of urbanisation on the regional tropical climate. Most of the studies on urbanisation impact in the region are concerned with economic, social and cultural changes (Agus 1990; Hill 1995; Hew 2003; Yaakob et al. 2010; Gee 2011; Aziz et al. 2012; Shahbaz et al. 2015). However, there is a growing community on the study of UHI in Malaysia (Shaharuddin et al. 2014; Morris et al. 2015a; Morris et al. 2015b; Rajagopalan et al. 2014; Yusuf et al. 2014; Ahmed et al. 2015; Salleh et al. 2015). Malaysia being a tropical region (Proximity to the equator) is exposed to constant solar radiation exacerbating the UHI effect on its inhabitants. Lack of comprehensive investigation on the evolution and adaptation of urban climate (especially UHI) with urbanisation in tropical regions characterised by distinct climatic features relative to other climate zones and thus, non-

transferability of research outcomes (Köhler et al. 2002; Roth 2007) makes this current study imperative to understand tropical urban climate adaption to urbanisation, thermal interaction with the local climate and to bridge the knowledge gap.

Putrajaya, a recently planned and developed federal capital territory from a total farmland is selected to examine the impact of urbanisation growth and its interaction with the local climate over a decade (1999 – 2011). A planned city with ~85% completion in its development is suitable for climate research, offering the opportunity to formulate urban planning strategies to combat problems posed by urbanisation and its resulting UHI. Apart from the opportunity to combat problems posed by urbanisation, a planned city is a vital source of data on how temperature behaviour varies through the year. This is consistent with Memon et al. (2008) suggestion that future research should concentrate on urban design and planning parameters to mitigate thermal surge that is often associated with urbanisation. These will not only lead to a reduction in canopy layer temperature but the related economic, social and health problems of urbanisation. The induced conversion of rural farmland to urban land is carefully assessed on the significant changes effected on local urban climatic variables (near surface humidity, near-surface temperature, and wind speed) of the area using a numerical approach – Weather Research and Forecasting (WRF) model coupled to NOAA/UCM.

4.2 Methodologies

Different materials and methods are employed in this study to accommodate the different components and as well to replicate the urbanisation processes

that have taken place over the years. A derived land use and land cover dataset for each of the considered years (1999, 2003, 2007, and 2011) from LANDSAT imagery are adapted to MODIS 33-category classification system. Topography information of the area is also updated. Six hourly ($1.0^{\circ} \times 1.0^{\circ}$) Global Final (FNL) analysis data from NCEP (NCEP 2000) are used as initial and lateral boundary conditions for the simulations. Furthermore, a network of observational data is also used to validate the model performance first, before initiation of the case study simulations. Remote sense and Google Earth images are used for depiction and identification of locations for Land-use-land-cover (LULC) classifications. Finally, land surface characteristics for NOAH LSM and urban canopy model (UCM), are obtained from different scientific studies of the area (Thani et al. 2013; Shahidan et al. 2012; Salleh et al. 2013; Morris et al. 2015a) and governmental reports (Hashim et al. 2012).

4.2.1 Background information and study site description

Putrajaya is a planned administrative capital of Malaysia built to accommodate the growing size of the federal government ministries. It is structured to accommodate all diplomatic activities for the country and to showcase the nation's modernisation agenda (Moser 2010). Putrajaya is located in the Klang Valley, 25 km south of Kuala Lumpur (Fig. 4:1a) and lies on coordinates $2^{\circ}55'00''$ N $101^{\circ}40'00''$ E with an approximate area of 49 km^2 which was previously covered by vegetation, rubber and oil palm plantation. Located few degrees north of the equator with an average elevation of 30 m, Putrajaya is a typical tropical city and sits on a hilly terrain. Rainfall averages 2-3 m in a year and falls heavily during the monsoon season, depositing about 10 to 30 cm

within few hours (Bunnell 2002). Furthermore, the region is exposed to low variable canopy layer temperature throughout the year, with annual mean minimum and maximum of ~25 °C and ~27.5 °C, respectively. Relative humidity averages ~63% per annum with extended daily solar radiation with an average of 6 h per day. Winds are generally light and variable with speed ranging from 0 - 7.5 ms⁻¹ (Shahidan et al. 2012).

Development of the area started in the early 1990s with the first phase completed in 2006. The final phase of completion was slated to take place in 2012. Urbanisation attracts rural to urban migration and in some cases urban-urban migration. The lush nature of the newly constructed capital has caused migration to the area with a population of about 100,000 of the planned 350,000 residents currently living in Putrajaya. To reflect the country's pledge to adhere to environmental standards and the need to combat problems posed by urbanisation in other cities (Shem & Shepherd 2009; Elsayed 2012a; Jiang et al. 2015), ~38% of the total land area of Putrajaya is to be reserved for wetlands, green space, open space and water body (Chin 2006).

Putrajaya landscape is divided into two main areas; the core area comprising of five precincts (1, 2, 3, 4 and 5) and the peripheral areas consisting of 15 precincts. Putrajaya Boulevard divides the core area along its main axis. The Boulevard is designed for ceremonial purposes. It is 4.2 km long and 100 m wide and extends from the northeast to the southwest with symmetrical large-size federal government buildings. The current urban form of the Putrajaya Boulevard is classified as dispersed and lower density urban (Moser 2010) using the local climate zone (Stewart & Oke 2012) classification

system. The peripheral areas are located about 3 to 5 km from the central precinct with fourteen residential neighbourhoods (Chin 2006; Moser 2010).

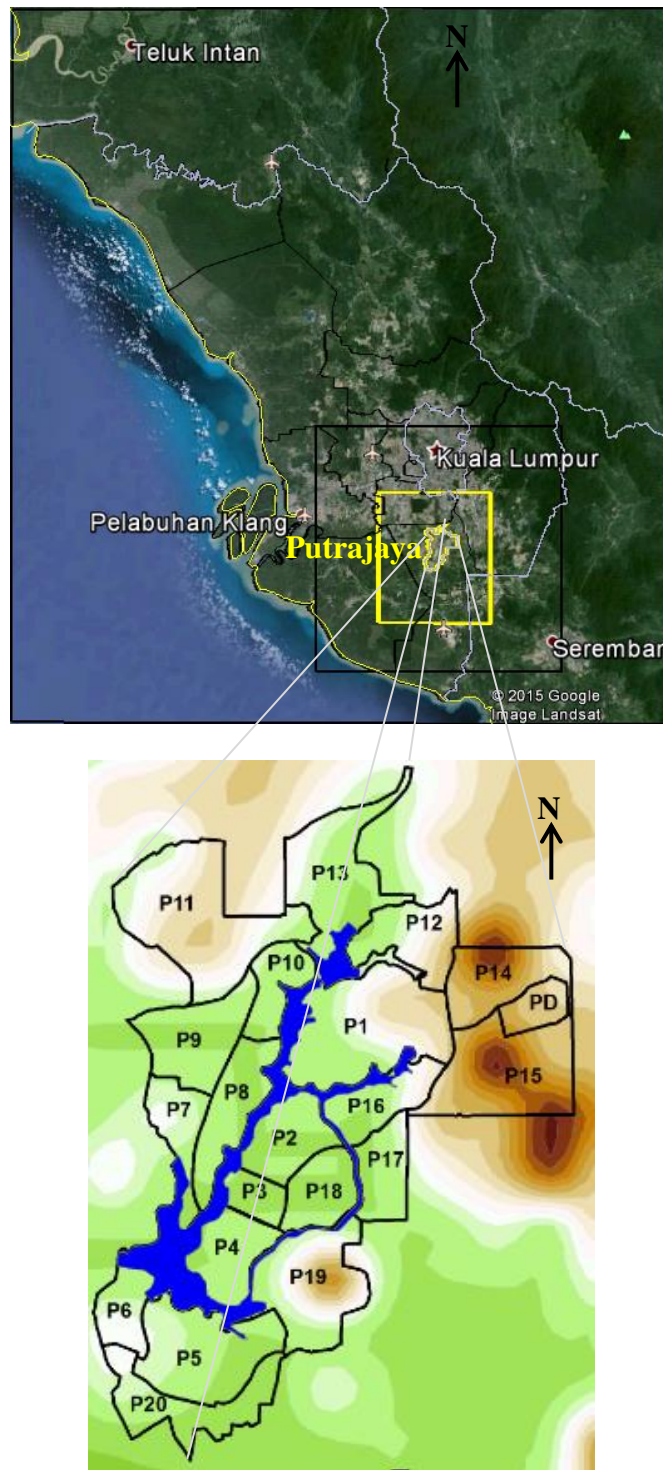


Fig. 4:1.(a) Klang Valley showing Putrajaya and Kuala Lumpur (Top panel). (b) Putrajaya precincts (bottom panel)

Putrajaya has seen rapid growth in urbanisation and development of infrastructures (see section 4.4.1). Wind flow, air temperature distribution, and exchange of momentum, heat and moisture in the city have all been affected by anthropogenic surface modifications that have taken place. Moreover, natural vegetation in the city, as well as environmental surface energy balance have been altered with greenery being replaced with asphalt-engineered surfaces (Wijeyesekera et al. 2012). Most of the materials used in the construction of roads, high-rise buildings, and recreational facilities have low reflectance and low surface albedo (Ahmed et al. 2015). In addition, the emissions from heavy-duty machinery, cars, and air conditioning units have only increased the environmental woes of Putrajaya. The urbanisation of the area has resulted in an increase in the population of people residing in the city and corresponding anthropogenic contributions (Moser 2010). It is thus interesting to observe the UHI development through urbanisation over the years starting almost from scratch.

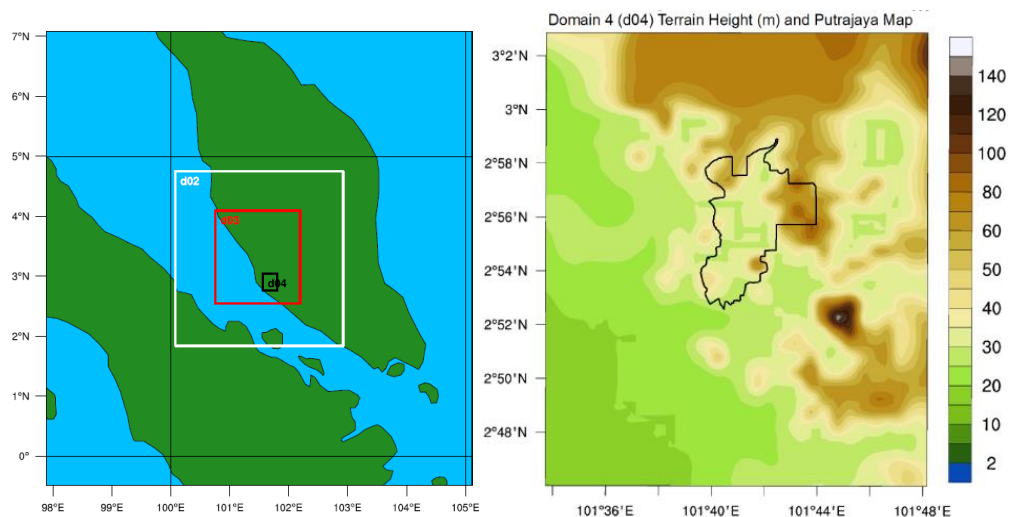


Fig. 4:2. WRF model domain configuration (image to the left) and terrain height for the finest domain (d04) and Putrajaya Map

4.2.2 Meteorological data

Table 4:1. Stations metadata

Station ID	Station Name	Location		Elevation (m) above MSL
		Latitude (°)	Longitude (°)	
PUTJ	Putrajaya	2.9319	101.6818	32.0
SUBJ	Subang	3.1167	101.5500	16.5
PETJ	Petaling Jaya	3.1000	101.6500	60.8
KLIA	KLIA Sepang	2.7333	101.700	16.3
NILA	Nilai	2.8208	101.8146	52.0
KLAN	Klang	3.0103	101.4081	4.00
PETY	Petaling Jaya	3.1102	101.7046	36.0
SHAH	Shah Alam	3.1050	101.5560	7.00
KUAL	KUALA LUMPUR INTL	2.7460	101.7100	21.0
R_1	-	2.917	101.599	25.0
R_2	-	2.903	101.604	27.0
R_3	-	2.914	101.599	24.0
R_4	-	2.92	101.596	23.0
R_5	-	2.906	101.604	17.0

A network of nine (see Table 4:1, *R_* in the table represents rural site) meteorological observational stations providing wind speed, air temperature and relative humidity from the Malaysia Department of Environment (DOE 2013) are used to validate the model and corroborate the model simulated outputs. A single observation station is located in the study location (d04) with 2009 as data commencement year. Thus, extensive model evaluation is carried using the third domain (d03) of the nested configuration, having nine of the hourly observational stations (see Fig. 4:2 and Table 4:1). The nine meteorological stations used are classified as urban sites.

30th of January to 15th of February is simulated for each year (1999, 2003, 2007 and 2011) to represent the urban climatic conditions and the urbanisation induced changes. The limited duration (17 days) simulated in this study represents the prevalent climatic conditions of the study site to an extent and is valid taking consideration of low seasonal climate variability typical of the tropics (Li et al. 2013), and also to reduce computational cost. February of

each year is known to have comparative low annual rainfall and at the same time among the months with the maximum monthly temperature (MMD 2015) which favours urbanisation studies. The duration is expected to somewhat represent the prevailing urbanisation induced urban climate conditions of the study area. For each considered year (duration), days with weak synoptic forcing favouring microclimatic investigations are selected for urban heating analysis. Weak synoptic forcing is preferable as it enables phenomena induced by physical characteristics of the local climate to be dominant.

Five rural sites (see Table 4:1) that meet the conditions for designation as rural in each year are selected for evaluation of urban and rural temperature difference (urban-rural UHI) of this study. Mean temperature values from the rural sites are used to compare with that obtained from urban sites. Rural sites are selected from locations few kilometres from the urban sites to reduce induced surrounding local climates due to advection and transport from nearby cities. Also, to minimise biases that could result from variations in topography features, a maximum 40 m elevation difference (see Table 4:1) is used as selection criterion between sites for correct UHI interpretation (Giannaros et al. 2013; Morris et al. 2015a).

4.2.3 Model details, numerical settings and experimental design

Simulation is conducted using Advanced Research WRF (ARW) dynamic core (Skamarock et al. 2008) coupled to NOAH land surface model (Chen & Dudhia 2001; Tewari et al. 2007) with the urban canopy model (Kusaka & Kimura 2004; Chen et al. 2011). This completes the connection of the land surface, urban surface and the overlying atmosphere and processes taking place

(Chen et al. 2011). Numerical model forcing fields such as large-scale atmospheric fields, sea surface temperature (SST) and initial soil parameters, including soil moisture and temperature, are derived from the NCEP 6 hourly ($1.0^{\circ} \times 1.0^{\circ}$ resolution) Global Final Analysis (FNL) data (NCEP 2000). These serve as the initial and lateral boundary conditions to the model. In addition, ingestion of sea surface temperature (SST) from NCEP 0.5° Real Time Global (RTG) analysis supplied the initial data for the model's non-prognostic field as lower boundary condition (Skamarock et al. 2008; Dudhia 2011).

Model domain comprises of a coarse (d01) and three one-way nested domain configurations (d02, d03, and d04) with horizontal grid resolution of 8.1, 2.7, 0.9, and 0.3 km respectively. The coarse domain covers the West Malaysia and path of Indonesia while d02 covers South-west Malaysia and the Strait of Malacca. D03 and d04 encompassed South-west of Klang Valley and the Putrajaya area with its surrounding cities, respectively.

The PBL is handled with the Yonsei University (YSU) scheme (Hong et al. 2006). A combination of YSU scheme with the coupled NOAH/UCM land surface model is considered to perform well in high resolution urban climate applications (Hong et al. 2006; Lin et al. 2008). Other physics parameterisations include a long-wave Rapid Radiative Transfer Model (RRTM) (Mlawer et al. 1997), a short-wave radiation scheme based on Dudhia cloud radiation scheme (Dudhia 1989) and a surface-layer scheme based on the Monin-Obukhov similarity theory. The WRF single-moment six-class (WSM-6) microphysics scheme is applied to all domains (Hong et al. 2004; Dudhia et al. 2008), while parameterisation of cumulus convection is completed using Kain-Fritsch scheme (Kain 2004).

WRF uses terrain-following hydrostatic-pressure vertical coordinate system proposed by (Laprise 1992) to resolve the vertical layers of the model PBL. In this study, 32 vertical levels are employed, 18 of which are reserved in the lower 2 km of the model to further resolve the lower atmosphere, while the model top layer is specified at 100 hPa. This is to accommodate frequent changes of atmospheric variables in the lower boundary layer and to handle the small scale features near the Earth's surface. However, the coarse vertical spacing of the sigma higher levels is to reduce computational cost (Chou 2011).

NOAH land surface model (LSM) is employed to parameterise the land surface processes (Chen & Dudhia 2001). The updated NOAH LSM is a land surface-hydrology model (Giannaros et al. 2013) which serves to provide surface sensible and latent heat fluxes, to account for sub-grid fluxes and skin temperature as lower boundary conditions to the boundary layer scheme of the WRF. The model (NOAH LSM) has a single-canopy layer with four soil layers of varying thicknesses (10, 30, 60 and 100 cm); 10 and 100 cm being the top and bottom layers respectively. This equates the total soil depth of the NOAH LSM to 2 m, with the upper and lower 1 m of the soil serving as the root zone depth and reservoir with gravity drainage respectively (Giannaros et al. 2013).

Single-layer UCM has a unique simplified two-dimensional urban geometry model, considering building height, roof and road width and assuming street canyons of infinite length. It also includes solar trapping and reflection of radiation and shadowing effects, which is determined by the street canyon dimensions and orientation, as well as solar azimuth angle. Thus,

energy and momentum transfer between urban environment and the atmosphere could be calculated by computing surface temperatures and heat fluxes of roof, wall and road within the considered area. In this study, the coupled NOAA/UCM model is modified (see section 4.4.5) to reflect the prevailing urban morphological and surface conditions of each year (Hashim et al. 2012; Shahidan et al. 2012; Aekbal et al. 2013; Thani et al. 2013; Qaid & Ossen 2014; Ahmed et al. 2015; Morris et al. 2015a; Morris et al. 2015b).

Four different cases (1999, 2003, 2007, and 2011) are simulated to investigate the impact of urbanisation in the area. Same simulation physics and dynamics configurations are applied for all cases except for static data (land use and land cover datasets) which are updated with each year accurate and up-to-date data. The model derived its initial urban and land use fields from the static datasets used. Putrajaya is centered on the finest (d04) model domain (see Fig. 4:2) to enable evaluation of convective and radiative interactions of climatological variables induced by the physical changes that have occurred within and outside the Putrajaya boundaries. A no urban scenario (nourban) (Li et al. 2013) is also simulated for each year to assess the urban heating of the area alongside the traditional urban-rural temperature difference technique. The no-urban case is achieved by replacing the urban fields of the accurately implemented land use and land cover dataset with the vegetation type of the nearest-neighbour grid. This is expected to reduce contamination of sites designated as rural or urban by surrounding heat fluxes through advection of surface convective and radiative fluxes. This way, the influence of surface modifications due to urbanisation is estimated.

4.3 Model evaluation

Numerical weather prediction (NWP) models are often associated with inherent biases resulting from model surface physics and atmospheric parameterisation (Hu et al. 2010), hence, there is a need to validate model simulated outputs against observational data to ascertain the model level of agreement with the observed data. In this study eight statistical tools; mean, mean bias error (MBE), mean absolute error (MAE) and root-mean-square error (RMSE), Pearson's coefficient of correlation (R), coefficient of determination (R^2), hit rate (HR), and index of acceptance (IOA) are employed to assess model's level of agreement with observed data, biasness, and degree of variation, magnitude of error and level of acceptance.

MBE measures the inclination of the model to *over (+)*- or *under (-)*-predict an event and does not provide insight to the magnitude of the typical error and hence could not be used as an indicator for accuracy (Moriasi et al. 2007; Wilks 2006). On the other hand, the MAE is an accuracy measurement and a typical magnitude of the predicted error (Wilks 2006). RMSE measure model accuracy and precision (Willmott et al. 1985) and aggregate the magnitudes of the errors in predictions for various time series into a single measure of predictive power associated with a model's prediction (Murphy 1988; Lundy et al. 2001). For MBA, MAE, and RMSE, reduction in magnitudes are always preferable.

Correlation measures the degree of covariance of bivariate data sets. R measures the strength and direction of a linear relationship (agreement) between the predicted and observed while R^2 measures the proportion of the

variance (fluctuation) of a predicted variable from the observed variable (Wilks 2006, pp.258–67). The coefficient of determination gives researchers the confidence to determine the degree of acceptability of predictions from a numerical model (Murphy 1995). R^2 ranges from 0 to 1, with higher values indicating less error variance (Santhi et al. 2001; Liew et al. 2003). R and R^2 are over-sensitive to high extreme values (outliers) and insensitive to additive and proportional differences between model predictions and measured data (Legates & McCabe 1999), thus, the need for normalised indexes such as the HR and IOA.

Hit rate is a reliable measure of model's performance and handles uncertainty in predicted values (Schlünzen & Katzfey 2003). This is evaluated by considering the fraction of “yes” event that was correctly predicted by the model (Wilks 2006). IOA was proposed by Willmott (1981) on his work “*on the validation of models*” to measure the degree to which a model prediction is free of discrepancy. It should be noted that IOA is not a measure of correlation or association in the formal sense. IOA varies between 0 and 1, with values of 1 signalling perfect agreement between predicted and observed results. Conversely, IOA of 0 connotes one of a variety of disagreements (Willmott 1981; Willmott 1982). It is noteworthy that index of acceptance is dimensionless, thus, relationship described by IOA should only be used to complement that described by other statistical tools (MBE, MAE, and RMSE).

For temperature, wind speed and relative humidity, ± 2 °C (Cox et al. 1998), ± 1.5 m/s (Kulkarni et al. 2008) and $\pm 5\%$ (Lawrence 2005) are the applied desired accuracy, respectively. These values are used to estimate the hit rate of the model predicted results. Model's variables are evaluated by stations

(see Table 4:1) and results of different stations aggregated to obtain mean values used in this analysis. Detailed performance for the different meteorological variables considered is discussed in subsequent sections.

4.3.1 Near-surface urban climate parameters

To evaluate model's ability to capture near-surface urban climate and to reproduce their diurnal characteristics, the model is evaluated against a network of observational data (see Table 4:1) for the simulated duration (390 h) with the first 28 h used as model spin up time. Observation sites used are classified as urban areas. Putrajaya is 8 h ahead of Coordinated Universal Time (UTC) which is the default time for the WRF model and NCEP analysis data used in this study. 16 00 h of 30th January 2000 UTC corresponds to 00 00 h of 31st January 2000 MST. Hence, simulated duration from 1st February to 15th February of each year is averaged over a 24 h for the purpose of this analysis. To ensure robustness of the model in simulating the urban climate of the area, d03 with more meteorological stations is selected for the model validation. Except otherwise stated model evaluation is carried out for the year 2011 using d03.

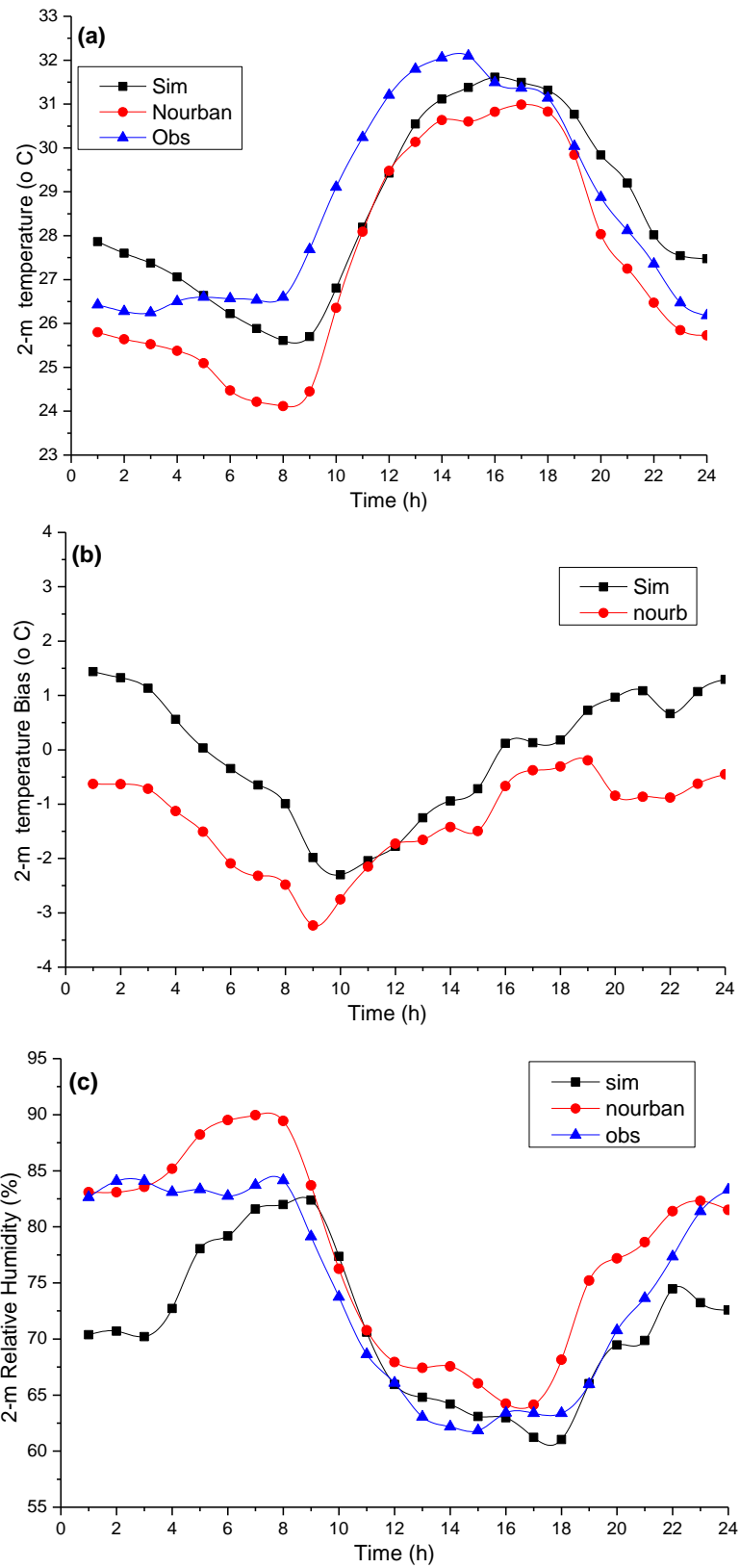


Fig. 4.3: (a, b and c) – see detailed description in the next page

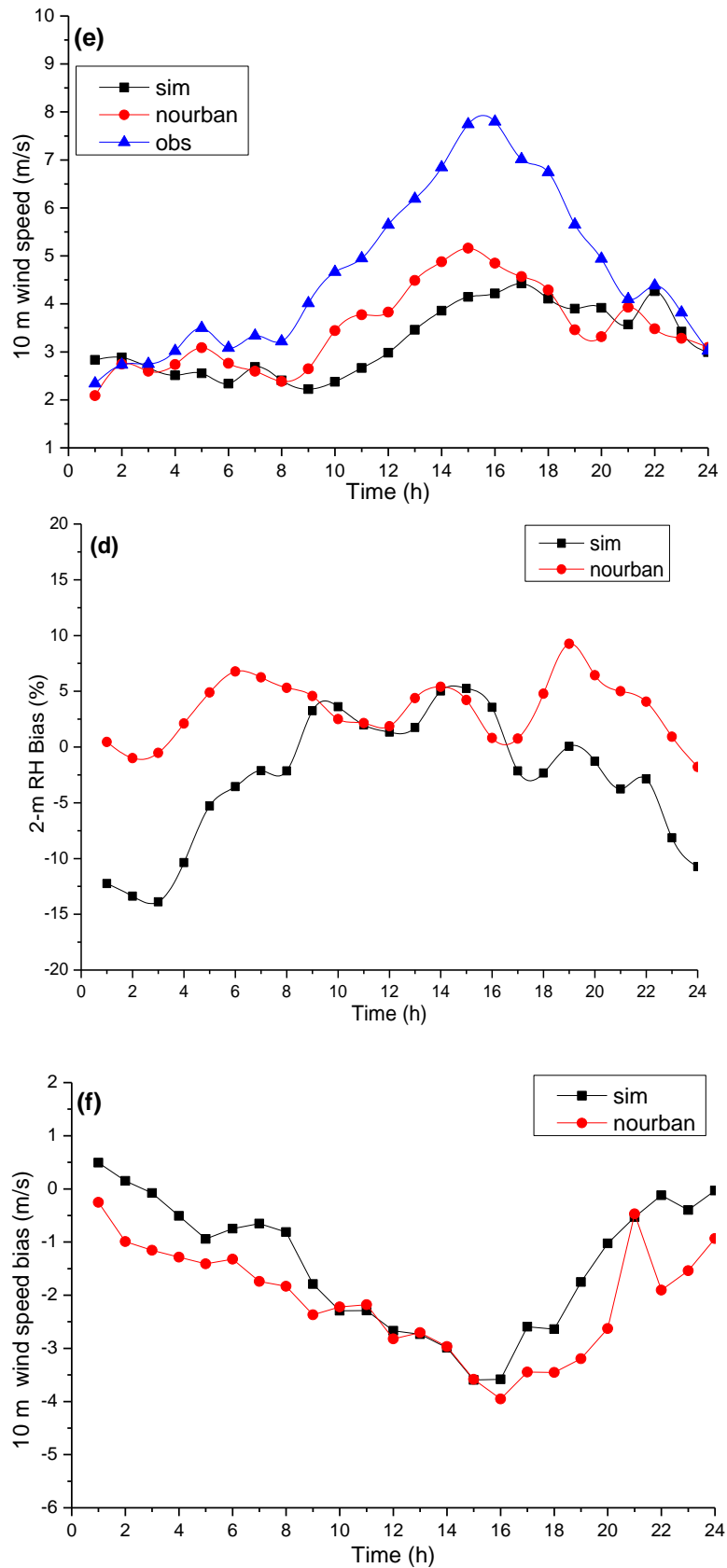


Fig. 4:3. Model validation for near-surface urban climate variables; (a) 2-m air temperature, (b) model biases for 2-m temperature, (c) 2-m RH, (d) model biases for RH, (e) 10 m wind speed, and (f) model bias for 10 m wind speed

The model reproduces the diurnal profile of 2-m air temperature with an error magnitude of 1.35 °C (RMSE) and mean bias error of -0.27 °C (see Fig. 4:3a and b, and Table 4:2). Hot biases are observed prior to and at the onset of solar shortwaves attenuation and continue to a peak value of ~1.4 °C by 24 00 h. However, the model shows cold biases during daytime. The hot biases are likely due to NOAH LSM underestimation of surface moisture availability while the cold biases could either have resulted from the unaccounted AH or UCM underestimation of surface re-radiated and reflected fluxes from building wall, roof and road in the urban canopy layer. Model performance for relative humidity on the other hand, shows some errors but is found to be consistent in predicting the diurnal trend, peak, and minimum values (see Fig. 4:3c). Maximum bias of ~-12% is obtained during the early hours between 01 00 and 02 00 MST for the accurate land use. Conversely, model accuracy in predicting RH is more pronounced during daytime with least biasness of ~-0.14%. RH simulation results for no-urban scenario seem to have produced the least overall error. This is expected considering its composition of high vegetation fraction and thus more moisture availability through evapotranspiration.

Table 4:2 Model evaluation statistics for near surface variables.

Statistical Tool	T2m (°C)	RH2m (%)	WS10m (m/s)
Mean WRF	28.35	68.84	3.22
Mean Obs.	28.62	74.37	4.65
MBE	-0.27	-5.53	-1.42
MAE	1.11	7.00	1.48
RMSE	1.35	6.83	1.22
R	0.84	0.79	0.66
R ²	0.70	0.62	0.44
HR	0.86	0.50	0.46
IOA	0.88	0.78	0.52

Wind speed is evaluated station by station and before averaging over the total number of stations considered. Results revealed that the wind speed has been consistently underestimated by the model for both accurate land use and no-urban scenario with maximum biases of ~ -3.78 and ~ -3.2 m/s, respectively (see Fig. 4:3 e,f and Table 4:2). Though with considerably good RMSE and MBE values, the indexes of performance are within average range (see Table 4:2). This disagreement in predicting wind speed has been reported in other studies, such as Liao et al. (2014) conducted in the Chinese Yangtze River Delta region, Liu et al. (2006) attempt to verified the model calculations in an urban area of Oklahoma city, USA, and Salamanca et al. (2011) investigation of the sensitivity of PBL evolution to different PBL schemes applying high resolution WRF/UCM+AH PBL.

To further validate the model performance before proceeding on the case study simulations, meteorological data from the single station (PUTJ) in the model finest domain (see Fig. 4:2 and Fig. 4:4a) are validated with the simulated outputs averaged over 24 h. PUTJ is located in a recreational open football field within an urban area, and data used for comparison are extracted from the nearest neighbouring grid cell (labelled CAC 053) about ~ 11 m from PUTJ (see Fig. 4:4a). Model results for 10 m wind speed, 2-m air temperature, and 2-m relative humidity demonstrate good correlation and agreement against the observations with mean absolute biases of ~ 0.74 ms^{-1} , ~ 1.1 $^{\circ}\text{C}$, and $\sim 4.3\%$, respectively, and mean values of ~ 3.4 ms^{-1} , ~ 28.4 $^{\circ}\text{C}$, and 68.2% , respectively (see Fig. 4:4b and Fig. 4:5). Fig. 4:4b, and Fig. 4:5 show mean predictions of the model climatological variables (black filled square boxes) and their biases (vertical bars). It is found that the model exhibits consistency

with diurnal trends observed for d03 urban climate, with improved marginal predictions for the finest domain. The improved model performance is somewhat expected since model calculates variables at a particular grid point by interpolating from the neighbouring grid cells, which in this case d04 has more grid cells relative to d03 per square km.

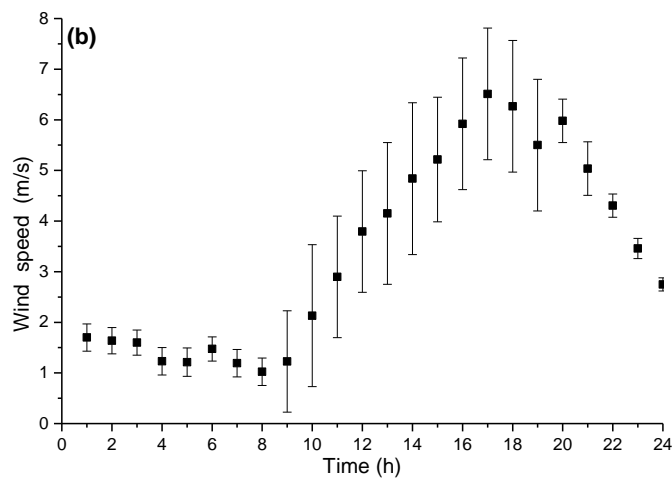


Fig. 4:4. (a) Putrajaya meteorological station - CAC 053 and (b) mean wind speed prediction and error bars for the finest domain (d04)

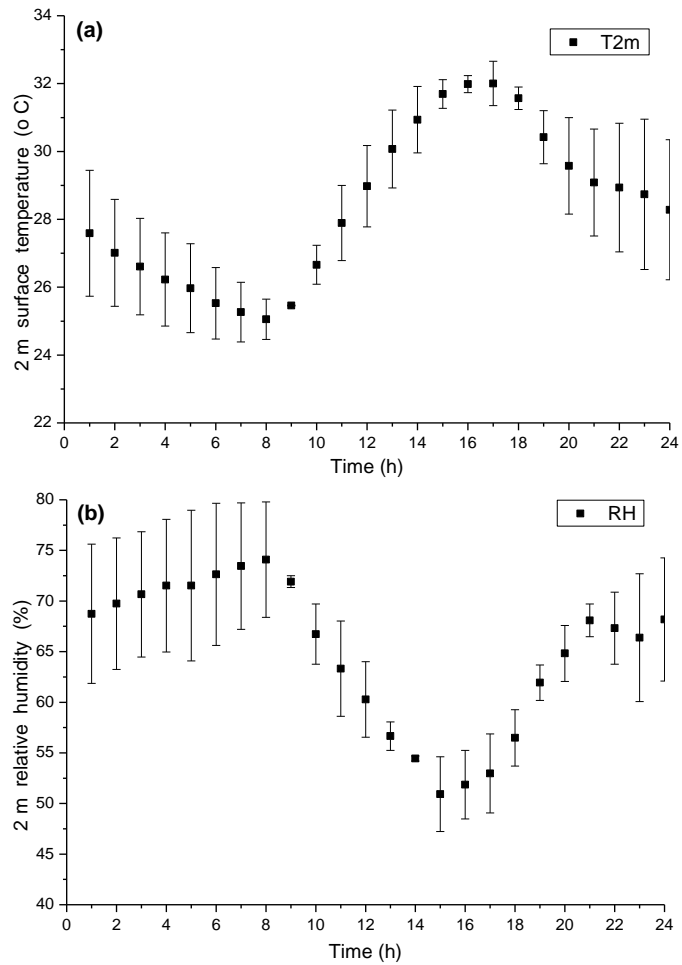


Fig. 4:5. Mean predictions of Putrajaya meteorological station (d04) for; (a) 2-m temperature and (b) 2-m RH

4.4 Results and Discussions

4.4.1 Land use and land cover data sets

Table 4:3. Summary of different land use and land coverage categories of Putrajaya.

LULC	1999 (%)	2003 (%)	2007 (%)	2011 (%)
Evergreen Needleleaf Forest	8.9	2.2	0.5	0.5
Evergreen Broadleaf Forest	13.1	4.1	6.6	5.0
Grassland and Shrubland	5.2	4.9	0.4	9.2
Cropland	13.5	6.7	6.4	6.9
Sparsely Vegetated	15.9	6.0	6.7	1.0
Water Body	0.6	4.8	5.4	5.5
Low Intensity Residential	25.8	14.5	24.9	32.0
High Intensity	4.3	7.6	12.5	12.7
Commercial/Industrial	12.2	49.2	36.5	20.8
Cloud Cover	0.3	0.0	0.0	6.4
Total	100	100	100	100

Transformation of agricultural and farm lands from vegetated and permeable soil to urban and semi-urban forms with impervious surfaces are some of the profound physical changes that characterise urbanisation. Changes in LULC interact differently with solar radiations which to a large extent determine the surface energy balance of the area. This is due to different physical and chemical characteristics of the constituent materials. Thus, it is pertinent to carefully identify the rural and urban lands with the associated characteristics in investigating the urban climate of the area and related phenomena, such as air temperature, surface moisture availability, relative humidity, and UHI, UCI and PBLH. In some countries, the government gazette and update the land use and land cover regularly. For instance, in the United States, federal and state agencies have assumed the task of developing Land Use and Land Cover (LULC) maps (Anderson et al. 1976). In Malaysia, different states and districts prepare and produce their respective LULC, most of which could hardly apply to scientific studies directly. In the current case, the land use and land cover maps of the area for the respective years are generated using ArcMap 10.2.2 from remotely sensed data before implementing into the WRF static data.

Table 4:3 shows changing coverage of the different land use classes applied over the Putrajaya area, while in Table 4:4 classes with similar physical characteristics area reclassified for easy analysis of the human-induced modifications that have taken place over the years. Furthermore, Table 4:5 shows changes that have occurred in the areas outside the Putrajaya boundaries but within the finest domain (d04) that houses Putrajaya. This is necessary to

access how the surrounding climates respond and influence the Putrajaya urban climate through vertical and horizontal advection of fluxes. Fig. 4:6 on the

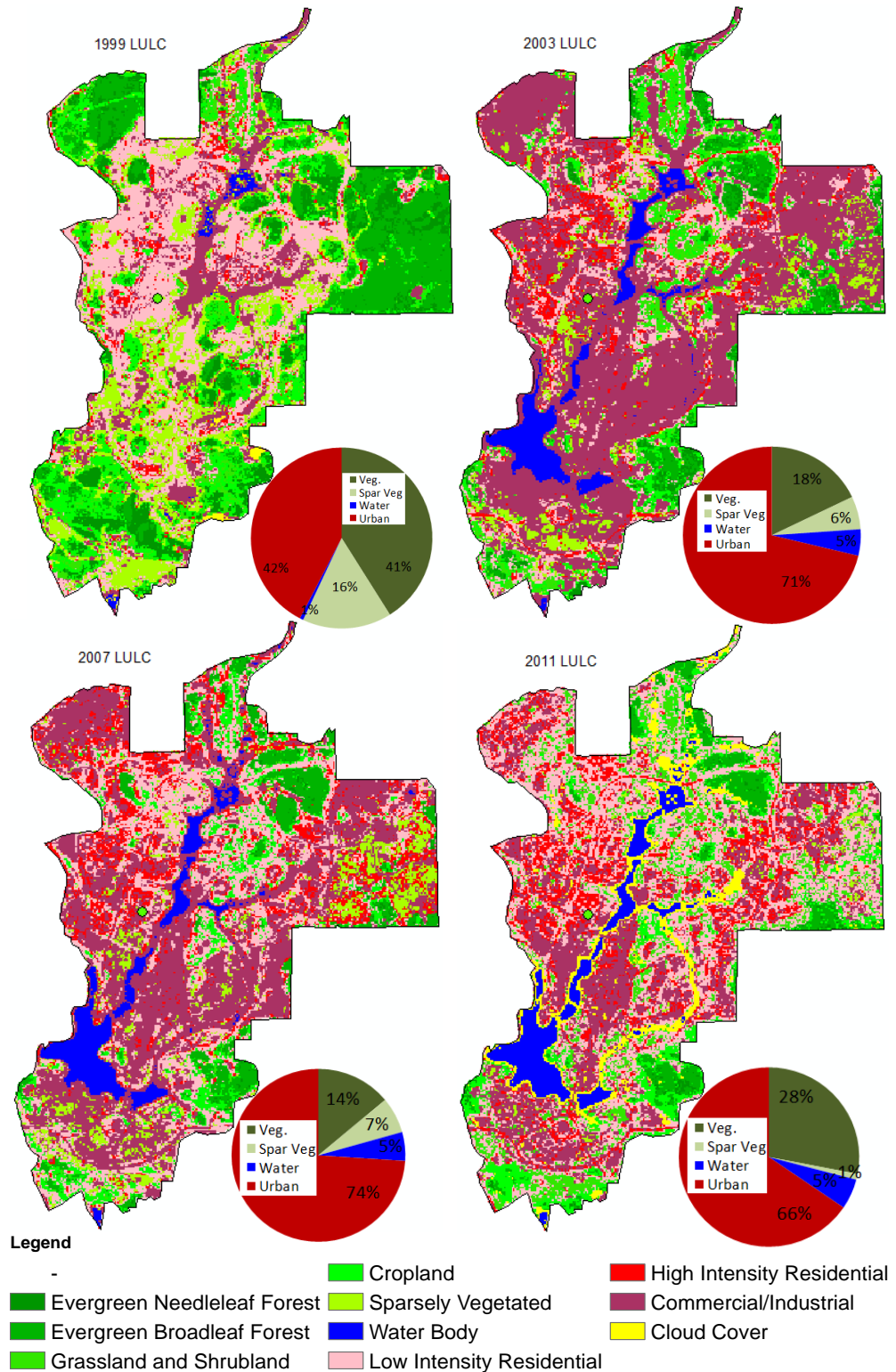


Fig. 4:6. Land use and land cover for 1999 (top left), 2003 (top right), 2007 (lower left) and 2011 (lower right)

other hand, presents the land use maps of Putrajaya and a visualised summary of the different class compositions for each year through pie charts positioned to the lower right of each LULC map. Fig. 4:7 (a and b) is a visual representation for the compositions of land use classes for different years and percentage of vegetated and natural greenery that are converted to urban surfaces and water body from the preceding years.

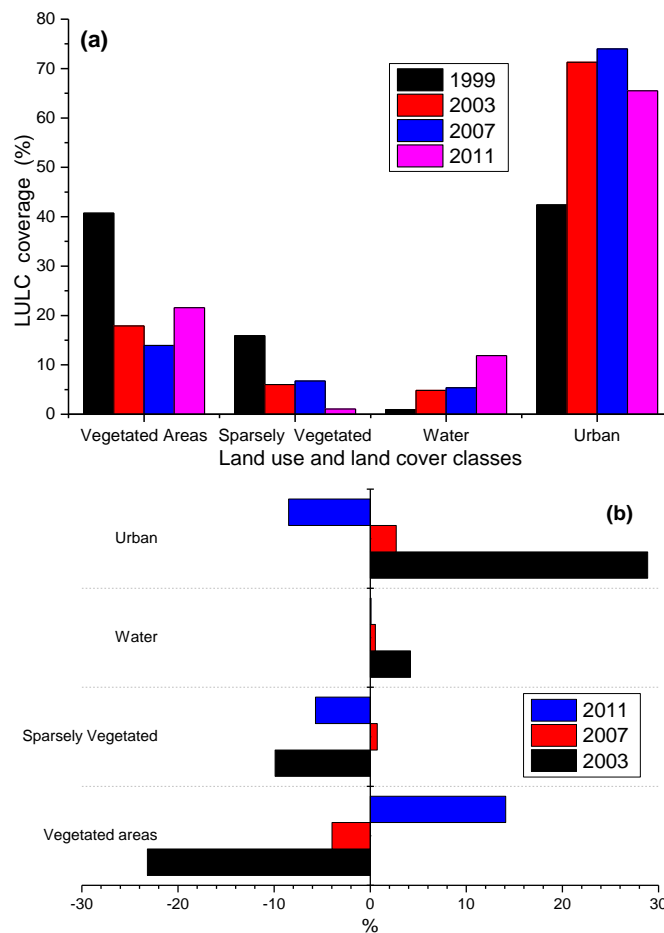


Fig. 4:7. Percentage; (a) coverage of each land use class and (b) change of each land use class from the preceding year

Urban land use class is the major benefactor of the human modification of the Putrajaya environment from natural greenery to urban engineered surfaces, followed by water body; from 42.4% to 65.5% and 0.6% to 5.5%, for urban and water classes, respectively, from 1999 to 2011. The main casualty of

the increased percentages experienced by urban and water body are the densely and sparsely vegetated land declining from 41.1% to 28.0% and 15.9 to 1.0%, respectively, from 1999 to 2011. Rapid decline in the level of greenery of the area is more prominent between 1999 and 2003, where 23.2% of vegetation and 9.9% of sparsely vegetated lands are converted to urban space and water body. Here, the urban land increased by ~29% and ~4.2% for water body (see Fig. 4:6 and Fig. 4:7). The sharp losses in forest areas and farm lands are attributed to rapid construction of the artificial lake, buildings, roads, urban pavements, and pedestrian path that are ongoing in the area.

Table 4:4. Reclassified land use and land cover coverage of Putrajaya area

LULC	1999 (%)	2003 (%)	2007 (%)	2011 (%)
Vegetation	41.1	17.9	13.9	28.0
Sparsely vegetated	15.9	6.0	6.7	1.0
Water body	0.6	4.8	5.4	5.5
Urban cover	42.4	71.3	74.0	65.5
Total	100	100	100	100

However, heavy deforestation witnessed between 1999 and 2003 were partly recuperated in 2011 through the beautification and greening exercise of the area carried out by the government in line with the green commitment. Densely vegetated areas increased by 14.1% (see Fig. 4:7b) whereas urban areas and sparsely vegetated land compensated for the increase noticed for vegetation by 8.5% and 5.7%, respectively. Note that sparsely vegetated could denotes clear land in some cases. Impact of land use and land cover variations over the investigated period on 2-m air temperature, RH, PBLH and UHI of the area are closely monitored in subsequent sections.

Table 4:5. Changes in land use and land cover of the Putrajaya external boundaries

LULC	1999 (%)	2003 (%)	2007 (%)	2011 (%)
Veg.	58.5	53.5	45.2	48.5
Spars. Veg	10.4	4.2	3.4	2.4
Water	1.0	0.9	1.9	1.8
Urban cover	30.2	41.4	49.5	47.3
Total	100	100	100	100

4.4.2 Surface energy balance

Table 4:6. Summary of mean surface energy budget components from model simulations

Year	Rural ¹			Suburbs ²			Urban ³		
	Q^*	Q_H	Q_E	Q^*	Q_H	Q_E	Q^*	Q_H	Q_E
1999 (W/m ²)	508.53	55.94	117.08	518.34	60.51	82.73	521.73	99.35	37.71
2003 (W/m ²)	506.99	57.99	112.18	516.80	69.56	84.80	522.20	120.44	12.71
2007 (W/m ²)	507.76	56.97	114.63	517.57	65.04	83.76	521.97	118.90	25.21
2011 (W/m ²)	507.76	53.43	111.52	519.42	72.16	68.99	519.02	111.08	31.67

The UCM estimates the surface temperature and heat fluxes from the roof, wall and road surface. It also calculates the momentum exchange between the urban surface and the atmosphere. If they are available, the UCM can take three different densities of urban development using special land-use categories (Skamarock et al. 2008). The surface energy balance depends on daily solar radiation and the physical properties of the constituent materials in which the investigated area physical surface is composed of. The surface energy balance explains in simple and precise context the role of surface characteristics and anthropogenic heating in near-surface climate, though, the anthropogenic component of Eq. 4:1 is not being considered in this study. Accurate prediction of surface energy balance is a primary requirement for atmospheric models

¹ Rural is the peripherals of the study area with more than 80% natural vegetation

² Suburb is the rural – urban fringe between the rural and urban areas

³ Urban in this context is the aggregate of the different urban classes contained in the land use/land cover classification

such as WRF, MM5, ECMWF and the JMA non-hydrostatic model. The surface energy balance for urban areas is represented as shown in Eq. 4:1.

$$Q^* + Q_F = Q_H + Q_E + \Delta Q_S. \quad \text{Eq. 4:1}$$

Where Q^* is the net all-wave radiations and Q_H turbulent sensible heat flux, while, Q_E , Q_F and ΔQ_S are latent heat fluxes, anthropogenic heat flux and the net heat storage flux, respectively (Li et al. 2013). It is noteworthy that the heat storage includes energy storage within the buildings, underlying soil and roads, and in some models the air space within the street canyon (Grimmond & Oke 1999). Due to non-availability of energy balance data of the study site, model validation on its predictability on energy balance data has not been performed in this current study. However, inference of the model capability is drawn from a study in Singapore by Li et al. (2013) on Singapore's tropical environment and interactions with the background atmosphere. Though, with limited data for extensive validation, Li et al. (2013) concludes that the model has performed fairly well on the estimation of energy balance data,

Singapore, a tropical country shares almost similar climatic conditions: humid and near-uniform monthly temperatures all year round with climate classification type Koppen *Af* (ZenTech 2010; WMO 2015), with the study area. Thus, it could be inferred that the model employed in this study could have performed well for surface energy balance data if validated since in both studies (Li et al. (2013) and the current study) the model has shown above average predictions in other simulated meteorological variables evaluated.

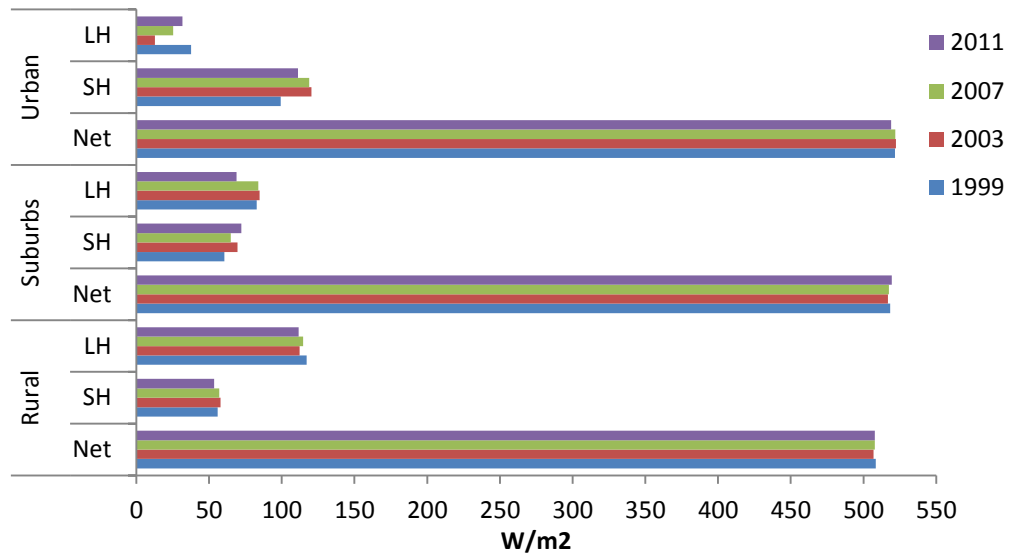


Fig. 4:8. Model simulated mean surface energy components

To investigate the surface energy adaptability to solar radiation for different surfaces, rural, suburb and urban are considered. In this study suburb refers to the rural-urban fringe. That is the transition zone between rural and urban areas (Hushak 1975; Weaver & Lawton 2001; Sullivan et al. 2004). Where urban in this context refers to the average for the different urban categories employed in this experiment over the study area, while rural is the mean for the rural sites considered. Table 4:6 and Fig. 4:8 show compressed summary of the surface energy balance averaged over the study site for each of the considered years. Likewise Fig. 4:9 is the surface energy balance components for 1999 averaged over the study area for 24 h period. For the purpose of analysis of the surface energy balance, sensible turbulent heat (SH) and latent heat (LH) are average over 24 h while the net all-wave radiation fluxes are averaged for 12 h of each day. This is justifiable since net all-wave radiation is heavily dependent on solar shortwave radiations and is only active for a period of ~12 h each day, starting from some minutes (~30 minutes) after

the onset of daily radiation (07 00 MST) and wanes gradually after solar shortwaves peak (~13 00 MST) to its extinction somewhere between (18 00 and 19 00 MST) of each day (see Fig. 4:9).

In Fig. 4:9, prior to sunrise (1 – 07 20 MST) and after sunset (19 30 – 24 00 MST), the surface energy balance fluxes is dominated by sensible and latent heat fluxes, however, shortwaves solar radiative fluxes dominate during daytime with sudden increase from 08 00 h to a mean peak value of 968 Wm^{-2} at about 13 00 h for 1999. This is somewhat consistent for the different durations experimented. However, for 2003 and 2007, during the absence of solar radiations window, SH is more dominant with minor contributions from LH for the urban areas, and considerate amount for the suburbs (see Fig. 4:8 and Table 4:6). Conversely, for the years considered LH shows more prominence relative to the SH for the rural areas and suburbs, except for 2011, where SH is observed to have more dominance with a mean value of $\sim 72.16 \text{ Wm}^{-2}$ against $\sim 68.98 \text{ Wm}^{-2}$ for LH. This is evidence of reduced vegetation caused by gradual development occurring around the Putrajaya suburbs (Feng et al. 2012).

During the solar radiation window, mean values of net all-wave radiations vary from $506.99 - 522.20 \text{ Wm}^{-2}$ (see Fig. 4:8 and Table 4:6) with the lower and higher margins associated with rural and suburbs, and urban areas, respectively. To an extent, this supports the hypothesis that the study area experiences a near-uniform solar heating and low climate variability all year round. During daytime, urban environment with engineered surfaces typified by dark materials and high thermal properties served as a heat reservoir to the incident solar radiation. Induced by propensity to ensure

thermal equilibrium between the urban environment and the overlying atmosphere, the stored heat energy at nighttime and early morning hours are meteorologically forced to reradiate to the overlying boundary layer through convective and radiative cooling; resulting in disproportionate availability of sensible and latent heat fluxes between urban classes and rural-urban developments (see Fig. 4:8, Fig. 4:9 and Table 4:6).

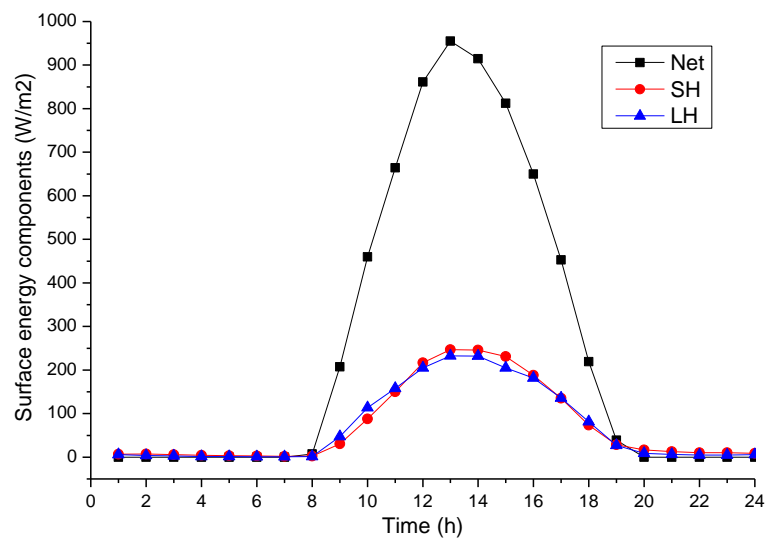


Fig. 4.9. Mean diurnal profile of surface energy components for 1999

4.4.3 2-m air temperature

From the WRF model simulations, it is observed that LH and SH responded very sensitively to changes in urban fraction of the urban categories. This is true since the coupled NOAH/UCM calculates latent fluxes from the vegetation fraction parameter, which is defined as the coverage of vegetation over a defined area (Hong et al. 2009). This has immense contribution in determining the urban climate, especially, relative humidity, mean urban canopy height temperature and UHI formation (Taha 1997).

Impact of urbanisation on the canopy layer temperature is assessed by comparing the rural, suburbs and urban temperatures variations for 1999, 2003, 2007 and 2011. Fig. 4:10 and Fig. 4:11 show the mean 2-m air temperatures and spatiotemporal changes for the experimented years for different urban intensities. It is observed that 2007 shows heating relative to other years considered with a mean maximum value of ~ 29.27 °C 2-m temperature (see Fig. 4:10) for the urban categories, followed by 2011 with a mean maximum value of ~ 28.93 °C.

The suburbs of Putrajaya showed a continuous increase for each year from a minimum value of 26.37 °C in 1999 to ~ 28.35 °C in 2011; the most prominent increase is noticed between 1999 and 2003 (see Fig. 4:10, Fig. 4:11 and Table 4:5). This is consistent with the observed variations in land use distribution between the same duration (see Fig. 4:6 and Fig. 4:7). The rural temperatures, on the other hand, show little variations ($\sim 0.06 - 0.22$ °C) during this period. The minor variations observed for the rural sites is consistent with expected natural climate variability and thus, could not be attributed to urbanisation induced effect (Jenkins 2009; Folland et al. 2001; Karl et al. 1995).

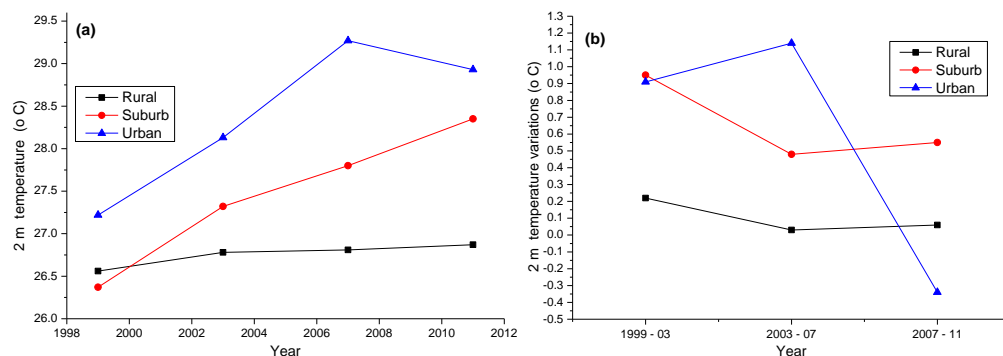


Fig. 4:10. (a) 2-m air temperature and (b) changes in 2-m temperatures for the years experimented

The urban temperatures show a strongly linked urbanisation induced increases from 1999 to 2007 and with an abrupt decline in magnitude for 2011, which corresponds to the gains made by the vegetation class during the later development of the area (see Fig. 4:6). During the development period of 1999 to 2007, most of the structural modifications and constructions of the area with materials typify with high thermal properties such as low surface albedo, high surface thermal conductivity and surface heat capacity are near completion. This is followed by the aesthetic and beautification exercise aimed at increasing the greenery and water body of the city. This caused about 14% increase in vegetation and a corresponding decrease in the sparsely developed land and areas previously considered urban (see Fig. 4:6) within the core precincts. Contrary to the variability of urban 2-m temperatures observed, the suburbs maintained a steady increase in its values. This could easily be explained by the corresponding changes that occurred in the suburbs of Putrajaya (see Table 4:5) during the same period. The increased 2-m temperatures from 1999 to 2007 and then a sudden attenuation from 2007 agrees well with Aekbal et al. (2013). It is attributed that the observed changes in intensities of UHI to the development approach adopted in the area, where pilot planting of trees and construction of parks and green recreational spaces were at the later stage of development.

Furthermore, it is observed that between 1999 and 2011, the temperature of Putrajaya has increased by a value of ~ 1.71 °C. Similarly, according to IPCC (2013) report on climate change, the global average air temperatures have increased by ~ 0.05 °C per decade in the period between 1998 and 2012 (McGrath 2014) far slower than the mean 0.13 °C recorded for the last

preceding five decades (IPCC 2007). It is vital to note that this increase in global average temperature have occurred within the same period considered by this study and thus, it is fair to state that the study reveals an increase of about $\sim 1.66\text{ }^{\circ}\text{C}$ per decade in air temperatures of Putrajaya city. This is largely due to urbanisation and surface modifications observed in the area (Ren et al. 2008).

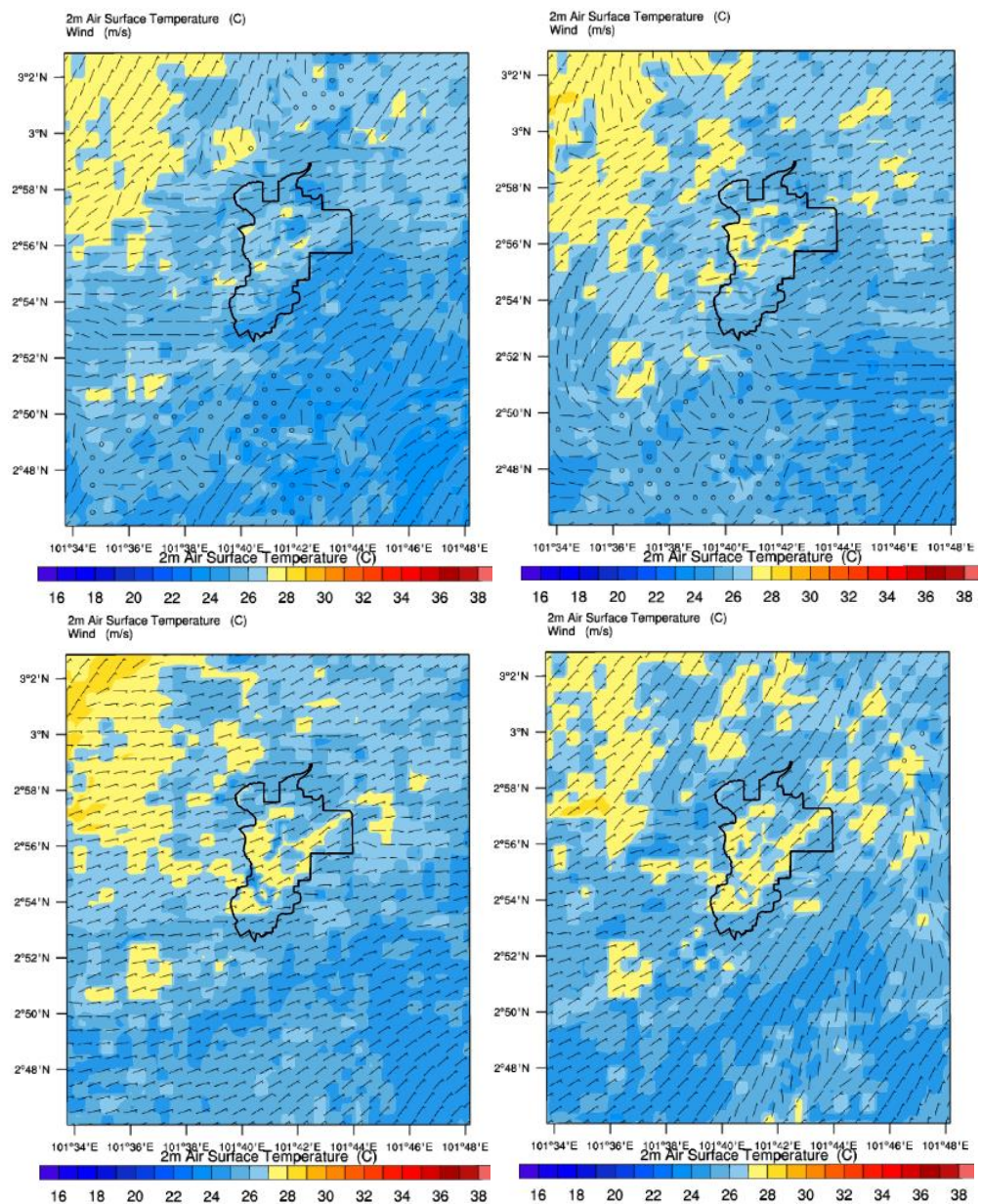


Fig. 4.11. Mean WRF 2-m temperature for 1999 (upper left), 2003 (upper right), 2007 (lower left), and 2011 (lower right)

Table 4:7. Summary of 2-m temperature for each year

Deve. Density	1999	2003	2007	2011	Δ 1999 - 03	Δ 2003 - 07	Δ 2007 - 11
Rural (°C)	26.56	26.78	26.81	26.87	0.22	0.03	0.06
Suburb (°C)	26.37	27.32	27.80	28.35	0.95	0.48	0.55
Urban (°C)	27.22	28.13	29.27	28.93	0.91	1.14	-0.34

4.4.4 Relative humidity and wind speed

Relative humidity shows the performance of evapotranspiration in a given area. Evapotranspiration is controlled by bulk stomatal resistance that is dependent on root zone soil moisture, photosynthetically active radiation, air temperature, and the relative humidity at the leaf surface. Grid aggregate vegetation and soil parameters are derived from fractional coverages of land use categories – urban fraction and soil texture types (Skamarock et al. 2008). Thus, urban fraction is an important parameter in determining the variability of the RH among the years considered. This is true in Fig. 4:13 and Table 4:8, where 1999 with the maximum vegetation fraction produces the highest relative humidity observed for the urban development class. Table 4:8 shows a summary of relative humidity averaged over the study duration, while Fig. 4:13 demonstrates mean diurnal behaviour of RH for rural, suburbs and urban area.

The RH of each year for the time considered shows low variability for the rural sites and suburbs, except for 2011 in the case of the suburbs. This abrupt divergence from the near-uniform pattern of the suburbs RH is caused by the observed surface modifications around the suburbs of Putrajaya (see Table 4:5). The decrease in the RH of the urban classes of the area from 1999 to 2007 (see Table 4:8) corresponds to increase urbanisation of Putrajaya from 42% in 1999 to 74% in 2007 (see Fig. 4:6). Nevertheless, a slightly observed increase of RH of the area in 2011 (see Table 4:8 and Fig. 4:13) corresponds

with the increase vegetation of ~14% associated with the beautification exercise embarked on in the area (see Table 4:4). In addition, the impact of replacing the vegetated and natural soil and surfaces of the area with engineered impervious surfaces, and interactions with the local climate is highlighted in Fig. 4:13, whereas in 1999 (see Fig. 4:13a) the rural and suburbs show similar diurnal trend without minor discrepancy during morning time. This is however contrary to the amplitude of RH observed in 2011. Here, though with similar diurnal profile, the discrepancy between rural and suburbs is more pronounced for both morning and night time (see Fig. 4:13b). This variability of the RH is attributed to the increased urban fraction and reduced vegetation resulting from the rapid urbanisation witnessed in the area.

During this study, 10 m wind speed is observed to show less variability and sensitivity to the urbanisation of the area (see Fig. 4:12). This could be attributed to less variability in building heights of the planned city and the model weak performance in predicting the wind environment of the area. This rather lacklustre in the model performance over Putrajaya could be improved with a dedicated *in-situ* and numerical study on the wind environment of the area. For each year, evidence of turbulence generated by the induced urbanisation effect of the Putrajaya area is noticed. The observed turbulence within the Putrajaya is however different with the immediate surrounding of the city.

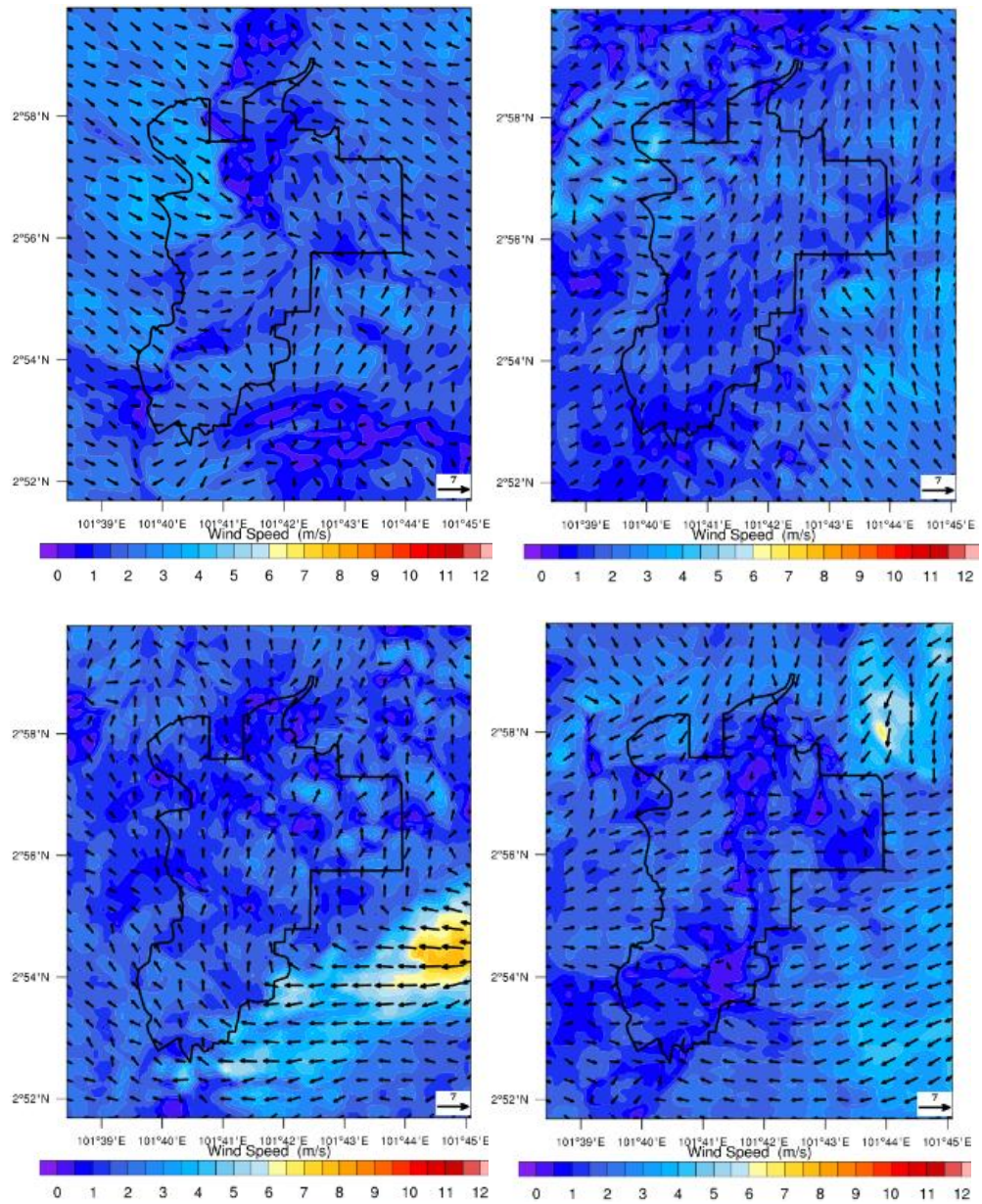


Fig. 4:12. Mean model 10-m wind speed for 1999 (upper left), 2003 (upper right), 2007 (lower left), and 2011 (lower right)

Table 4:8. Mean summary of WRF simulated Relative humidity

Year	Rural (%)	Suburb (%)	Urban (%)
1999	77.96	76.86	72.94
2003	77.10	75.33	64.74
2007	77.26	75.48	64.31
2011	77.12	72.17	67.56

4.4.5 PBLH and UHI

The urban PBLH and UHI are important variables of urban climate. Differential warming of the urban and rural areas resulting from the thermal alteration of the urban climate is known as the UHI (Morris et al. 2015a), while UHI is the temperature difference between the urban and rural areas. On the other hand, the lower turbulent atmospheric layer in direct interactions with the physical characteristics of the environment is referred as the PBL. The depth of the PBL is driven by aerodynamic drag caused by surface roughness, and convection associated with surface radiative forcing (Stull 1988). The surface energy budget with significant dependence on solar shortwaves radiations and partial urban surface re-radiated heat fluxes from urban heat sink during daytime, and total reliance on earth's surface fluxes at nighttime plays an immense role in determining the magnitude of the UHIs and PBLH (Jiang et al. 2008).

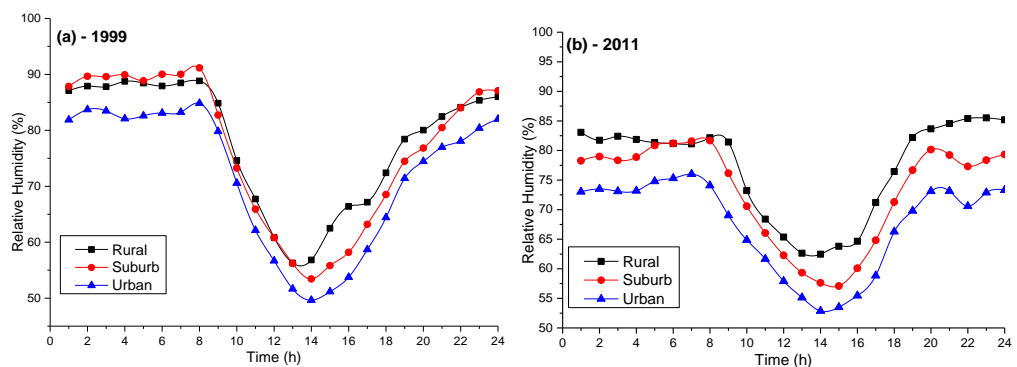


Fig. 4:13. Mean simulated relative humidity for 1999 and 2011

2-m air temperature (see Fig. 4:10), PBLH and UHI of the study area display similar trend; a gradual uphill slope from 1999 to peak value in 2007, and then a sudden downhill slope from 2007. The rural areas maintain a

consistent PBL depth with an average value of ~318 m through the years while Putrajaya suburbs show minor variations in PBLH with a sharp increase in 2011. The increased urbanisation witnessed from 2007 to 2011 around the Putrajaya peripherals is likely among the causative factors for the increased PBLH between 2007 and 2011. Conversely, variations in PBL depth is more significant for Putrajaya area, with a mean value of ~352 m for 1999 to a mean value of ~387 m in 2007, before responding to the increased vegetation in 2011 accordingly with an average value of ~370 m (see Fig. 4:14).

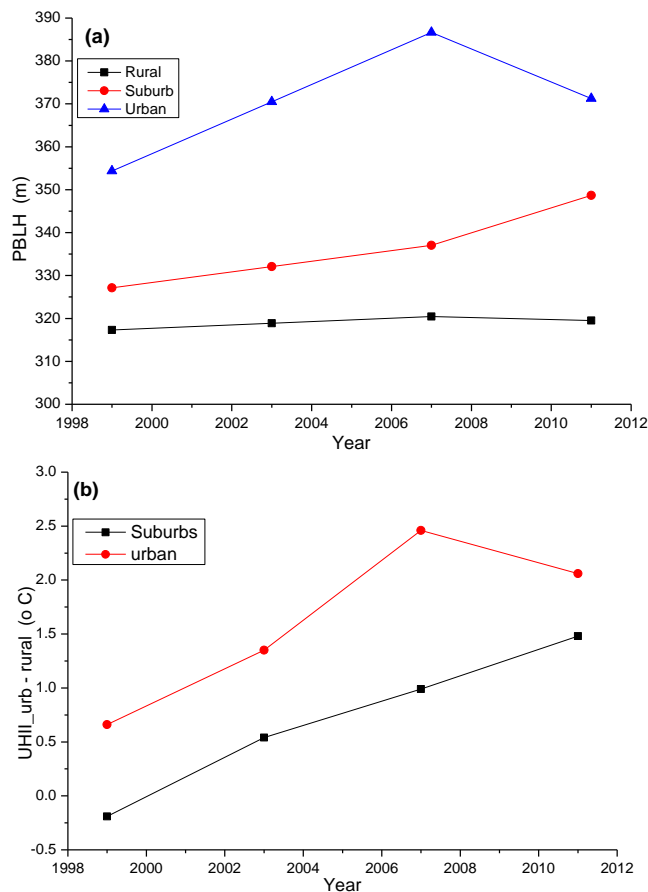


Fig. 4:14. Mean annual (a) PBLH and (b) urban - rural UHII, for each year considered

For the UHI estimation using the traditional temperature difference between urban and rural area, it is observed that 2007 shows a higher mean UHII of ~2.46 °C over the Putrajaya city while the least mean magnitude of

~0.66 °C is noticed in 1999. The suburbs and the study area demonstrate a positive correlation of mean UHII, with increasing magnitudes from 1999 for the simulated years, except for 2011, where the area responded accordingly with the improved vegetation fraction of the area from ~14% in 2007 to ~28% in 2011 (see Fig. 4:6 and Fig. 4:7). The alteration of the Putrajaya urban climate with the introduction of vegetation is likely to increase the evapotranspiration and moisture availability (see corresponding impact on RH, and Table 4:8) of the area, thereby inducing reduction in 2-m air temperature observed (see Fig. 4:10, Fig. 4:11 and Table 4:7).

Table 4:9. Properties of lulc categories used in the model (Chng et al. 2010; Salleh et al. 2013; Tehrany et al. 2013) .

Land use/land cover class	surface characteristics					
	ALB	SLM	SFE	SFZO	THERIN ($Jm^{-2}K^{-1}s^{-1}$)	SCFX
Evergreen Needleleaf Forest	0.12	0.3	0.95	50	4	3.33
Evergreen Broadleaf Forest	0.12	0.5	0.95	50	5	1.67
Deciduous Needleleaf Forest	0.14	0.3	0.94	50	4	2.86
Deciduous Broadleaf Forest	0.16	0.3	0.93	50	4	2.63
Mixed Forests	0.13	0.3	0.97	50	4	2.11
Closed Shrublands	0.22	0.1	0.93	5	3	1.56
Open Shrublands	0.2	0.15	0.95	6	3	2.14
Woody Savannas	0.22	0.1	0.93	5	3	1.56
Savannas	0.2	0.15	0.92	15	3	2
Grasslands	0.19	0.15	0.96	12	3	2.37
Permanent wetlands	0.14	0.42	0.95	30	5.5	1.32
Croplands	0.17	0.3	0.98	15	4	2.71
cropland/natural vegetation	0.18	0.25	0.98	14	4	2.56
Barren or Sparsely Vegetated	0.25	0.02	0.9	1	2	0.81
Water	0.08	1	0.98	0.01	6	0
Low Intensity Residential	0.1	0.17	0.97	80	3	1.67
High Intensity Residential	0.1	0.13	0.97	95	3	1.67
Industrial or Commercial	0.1	0.1	0.97	110	3	1.67

Table 4:9 shows the surface characteristics of the different land use and land cover classes applied during the configuration of the WRF model for each year. Surface albedo (ALBD), surface moisture availability (SLMO), surface emissivity (SFEM), surface roughness (SFZO), surface flux (SCFX), and

surface thermal inertia (THERIN) from the land use/land cover (LULC) datasets being implemented (Wang et al. 2012), determines the urban climate prognostic variables. Thus, increase in urban fraction of the area yields a corresponding surge in the thermal environment of the area as opposed to an increase in vegetation fraction (i.e. decrease in urban fraction). Furthermore, precincts in Putrajaya with substantial vegetation, especially, P13, P12, P15, P19, and P20 (see Fig. 4:1b) show less susceptibility to high thermal conditions (see Fig. 4:11). This is true since the vegetated classes have surface characteristics favouring low surface thermal climate, such as high albedo with mean value of ~ 0.18 , and mean surface moisture availability of ~ 0.27 , against ~ 0.11 of surface albedo and SLMO of ~ 0.13 , for the urban classes, respectively.

To further evaluate the UHI of the area, the nurban approach (Li et al. 2013) is employed. Fig. 4:15 shows the difference between the nurban scenario and the accurate simulations of the Putrajaya area for each year. The UHI development is consistent with the predicted magnitude using the conventional approach (Oke 1973). A maximum magnitude of ~ 2.3 °C is observed in 1999 towards precinct 9 and as well the formation of urban Cool Island (UCI) near precinct 10 with magnitude of ~ 0.3 °C, while precincts 6, 5, and 20 exhibited the least heating during the investigated period for 1999. Overall the mean magnitude of UHI over Putrajaya during 1999 is in the range of $\sim 0.7 \pm 0.1$ °C (see Fig. 4:15a). The significant surge in the conversion of natural materials to urban form during 1999 to 2003 is noticed in the thermal map (see Fig. 4:15b). Here surfaces that were originally grassland have been converted to urban areas (see Fig. 4:6) and thus the increase in the mean

magnitude of UHI observed ($\sim 1.3 \pm 0.2$ °C). It is noteworthy that no strong influence of the surrounding environment on the urban microclimate of Putrajaya is observed for 1999 and 2003 (see Fig. 4:15a and b).

The year 2007 and 2011, however, experienced significant induced influence of the surrounding urban microclimates resulting from urbanisation that occur simultaneously during the later development of area, where Putrajaya undergoes its transformation from agricultural and farmland to the prevailing urban conditions of 2007 and 2011 (see Fig. 4:15c and d). To the Northwest of Putrajaya, Taman Pinggiran Putra, Bandar Baru Bangi (Northeast) and Cyberjaya (West of Putrajaya) have all contributed significantly to the heating of the Putrajaya peripherals. Maximum magnitude of 4.2 °C and 3.8 °C of UHI are detected in 2007 and 2011, respectively. Meanwhile, UCI ranging from ~ 0.2 to ~ 0.4 °C are found near precincts 1, 2, and 10 for both 2007 and 2011. Overall, mean UHI magnitude of $\sim 2.3 \pm 0.1$ °C and $\sim 2.2 \pm 0.1$ °C are respectively found in 2007 and 2011. Both approaches employed in evaluating the urban heating of the Putrajaya area yielded similar outcome.

The magnitude of the urban heating over the Putrajaya area agrees well with previous UHI investigations conducted in the area (Shahidan et al. 2012; Ahmed et al. 2015; Morris et al. 2015a). Shahidan et al. (2012) and Ahmed et al. (2015) have conducted studies concentrated on the Putrajaya boulevard. The former in 2009 investigated the cooling effect of trees around the boulevard using experimented and numerical approaches, while the latter in 2012 studied the urban 2-m temperature behaviour and UHI effect of the Putrajaya Boulevard via pilot *in-situ* observations. UHI magnitude of 2.6 °C per month

and 2 °C per day were respectively observed. In addition, Morris et al. (2015a) conducted a preliminary numerical study to investigate the presence of UHI in the Putrajaya area for the year 2012. Their findings reveal that the Putrajaya area was heating at the rate of ~0.8 °C per day with temporal and spatial variations ranging from ~1.9 to ~3.1 °C. The current study has shown major improvement in the predictions of UHI. This is likely due to the improved classifications of the land use and land cover of the area, with urban built up area further sub-classified into three different categories according to their surface form, development and urban intensity (Chen et al. 2011).

The current study observed UHI (see Fig. 4:14b) however seems not to agree strongly with the observed magnitude of UHI (5.73, 6.75 and 5.91 °C for 1999, 2006 and 2009, respectively) from the research conducted by Aekbal et al. (2013) over Putrajaya core precincts on the contribution of surface albedo to the thermal conditions of the considered area using both *in-situ* observations and remote sense application. Though, both studies agreed well on the trend in the interactions of Putrajaya urban climate (e.g. 2-m air temperature) with urban fraction. To an extent, these magnitudes obtained by Aekbal et al. (2013) are on the high extreme relative to the maximum UHI reported by the other studies conducted in the area.

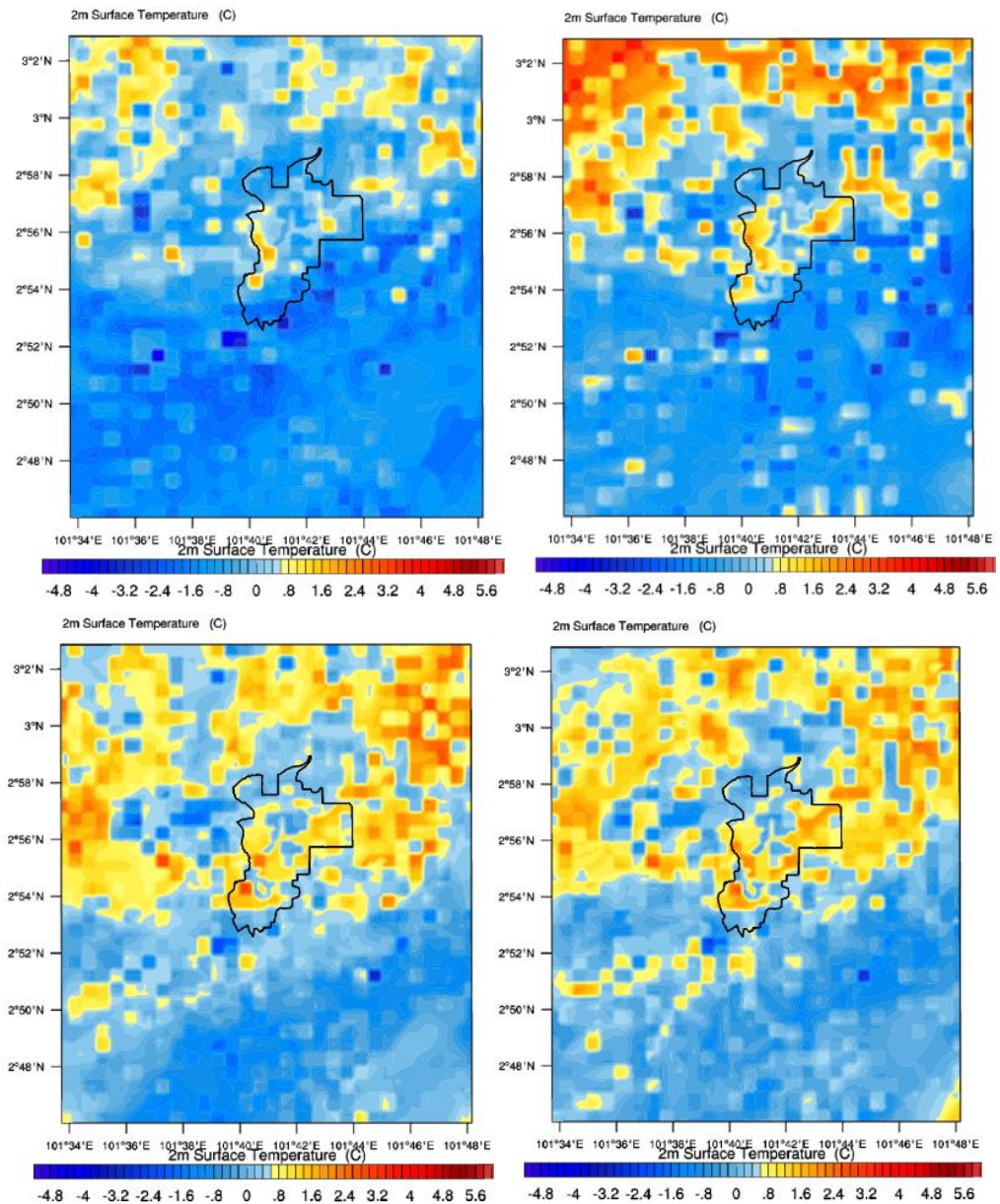


Fig. 4:15. Mean simulated nourban UHI for (a) 1999 - upper left, (b) 2003 - upper right, (c) 2007 - lower left and (d) 2011 - lower right

4.5 Conclusions

Model is evaluated against a network of observed data using eight statistical tools and the results show good agreement with the observed data, especially for 2-m air temperature. RMSE, MBE, and R^2 of 1.35 °C, -0.27 °C, and 0.7 °C; 6.83%, -5.53%, and 0.62%; 1.22 m/s, -1.42 m/s, and 0.44 m/s, are observed for 2-m temperature, relative humidity and wind speed, respectively.

The surface energy components and the urban climate of the study area responded accordingly to variations in the study area land use and land cover changes. The net all-wave radiation is near-uniform throughout the study durations. However, sensible and latent heats show more sensitivity to land use and land cover changes induced by the urbanisation processes of the area. Reduction in vegetation fraction of the area due to urbanisation leads to increase and decrease sensible and latent heat fluxes, respectively. The year 2007 exhibits the mean maximum temperature over the area (29.27 °C) while 1999 shows the mean minimum temperature (26.37 °C). On the other hand, RH and the PBLH vary according to the natural surface modifications; where the year 1999 with highest vegetation fractions (41%) exhibits the mean maximum RH of 72.94% and the least PBLH of ~352 m, and with 64.31% and ~387 m for RH and PBLH, respectively, for the year 2007 with the least vegetation fraction of 14%. Conversely, wind speed shows less sensitivity to the urbanisation of the area during the considered period.

The thermal urban climate of Putrajaya is successfully captured in this study. Model results show that 2007 has the maximum mean UHII of 2.46 °C while the least UHII (~0.7 °C) is noticed in 1999. In addition, UCI formation is also noted in 1999 with a mean magnitude of ~0.3°C, while that mean values of 2007 and 2011 vary from 0.2 to 0.4 °C. Current (2011) UHII of the study area is estimated as ~2.06 °C and 2.2 ± 0.1 °C using the conventional (urban – rural temperature difference) approach and the nourban technique, respectively. Both approaches show good agreement in the magnitude of heating of the area. Overall, the Putrajaya area is warming at the rate of ~1.66 °C per decade.

To improve the model performance in the area, caution and systematic planning is needed to collate climate data for model improvement. Also, new studies should be directed towards understanding model performance during intermonsoon seasons. Finally, results of this study will strengthen the limited resources in the area for future urban climate investigations.

Chapter 5

5 Computational evaluation of the garden city concept adopted in the development of a tropical city - Putrajaya, Malaysia

Summary

The garden city concept was adopted in the development of a new tropical city, Putrajaya, aimed at mitigating the effect of urban thermal modification associated with urbanisation, such as urban heat island (UHI). WRF/Noah/UCM coupled system was used to estimate the urban environment over the area and the individual thermal contributions of natural land use classes (vegetation and waterbody). A control experiment including all land use types describing the urban conditions of Putrajaya city agreed well with the observations in the region. A series of experiments was then conducted, in which vegetation and waterbody were successively replaced with an urban land use type, providing the basis for an assessment of their respective effect on urban thermal mitigation. Surface energy components, 2-m air temperature (T2m) and mixing ratio (Q2m), relative humidity (RH) and UHI intensity (UHII) showed variations for each land use class. Overall, an increase in urban surfaces caused a corresponding increase in the thermal conditions of the city. Conversely, waterbody and vegetation induced a daily reduction of 0.14 and 0.39°C of T2m, respectively. RH, UHI and T2m also showed variations with

urban fractions. A thermal reduction effect of vegetation is visible during mornings and nights, while that of water is minimally shown during daytime. However, during nights and mornings, canopy layer thermal conditions above waterbody remain relatively high, with a rather undesirable effect on the surrounding microclimate, because of its high heat capacity and thermal inertia.

5.1 Introduction and background information

At present, approximately 3.9 billion of the world population live in urban areas, which is expected to increase rapidly (United Nations 2014). This could be due to the rapid rural-to-urban migration of people in developing countries (e.g. China, Brazil, India, Indonesia, Nigeria and Mexico). Urban areas occupy <3% of the Earth surface (Liu et al. 2014) and the increase in the population of urban residents has exacerbated problems (e.g. waste management, increase in energy consumption, pollution and crowding) posed to the environment (Manning 2011). Achievements in urban climate research have produced thermal positive feedback of natural vegetation modification to urban engineered surfaces on the local and surrounding environment (Santamouris 2014). This has caused government and private urban developers to adopt and adhere to mitigation guidelines in developing new and expanding existing urban cities.

Urbanisation and relationship between the reduction in natural farmland and relative humidity (RH); increase of temperatures and significant urban heat island (UHI) effect; decrease of latent heat (LH) and increase of sensible heat (SH) fluxes; deterioration of visibility and urban heavy rainfall and local (regional) climate change are well established in the literature (Zhou et al.

2004; Hua et al. 2008; Yao et al. 2015). The impact of urbanisation is not only limited to the city scale, but also on regional climate change. Much effort is made to estimate the contribution of current and future urbanisation to regional climate change. For example, Chen & Frauenfeld (2015) estimated that urbanisation will lead to an increase of temperature of approximately 1.9°C in the regional areas of China, because of altered land–atmosphere interaction.

Wind flow; 2-m temperature (T2m) distribution and exchange of momentum, heat, and moisture in urban cities are affected by surface modifications caused by developments and increased human population. In addition, urban surface energy balance is altered because of the conversion of greenery to artificial materials often characterised by low surface albedo and high heat capacity. These materials are used in the construction of roads, pavements such as the large expanse boulevard in Putrajaya, Malaysia (Moser 2010), buildings and bridges. Most of these materials have low surface reflectance and albedo (Ahmed et al. 2015). In addition, the emissions from heavy-duty machinery, cars and other related equipment have only increased the environmental burden of city residents.

In order to mitigate the problems associated with urbanisation and anthropogenic contribution of thermal fluxes to the environment, the garden city concept (GCC) proposed by Sir Ebenezer Howard (Howard 1898), where cities are planned and built on undeveloped land with a garden concept, has been adopted in several cities such as the French Dakar city, Senegal (Bigon 2012); Maringa, Brazil (Macedo 2011); Chengdu, China (Zhao 2012); and the recently developed city of Putrajaya, Malaysia (Moser 2010; Morris et al. 2015a). This concept relies on the cooling properties of the different natural

land use composition of garden cities to effectively reduce the warming islands created by artificial surfaces typical of urban cities (Caruso et al. 2015).

Different studies have been conducted to investigate the cooling properties of various natural elements, such as the investigation on the effects of urban parks on the local urban thermal environment by Chang & Li (2014) and the study on the potential for UHI mitigation by green parking lots by Onishi et al. (2010). Similarly, a series of field measurement studies such as Jauregui (1990) shows thermal benefits of green zones, particularly urban parks in Mexico City. Observations in Chapultepec Park, Mexico City, show that during clear nights and light wind conditions the temperature is 2–3°C cooler than its urban surroundings, and it influences areas over a distance that is same as its width (2 km). Further details on studies conducted on the ability of urban greening to cool urban areas are empirically presented in Bowler et al. (2010).

Li et al. (2014) used Weather Research and Forecasting (WRF) model coupled with urban canopy model (UCM) to investigate the cooling impact of green and cool roof strategies on Baltimore–Washington metropolitan area during a heat wave event. Similarly, Papangelis et al. (2012) coupled WRF and UCM to assess the ameliorating thermal effect induced by green areas inside the warm urban microclimate of a densely populated coastal city of Athens, Greece.

Despite the continual adoption of the GCC and studies showing projected capacity of greenery and waterbody to reduce urban heating, there is no scientific study conducted on a city built with the GCC to assess its effectiveness (as a whole and its individual elements) in reducing urban

thermal climate. Thus, this study aims to bridge this gap by investigating the effect of the concept generally, and specifically the contribution of vegetation and waterbody to the overall performance, using a coupled numerical model (WRF/UCM) in a tropical city, Putrajaya, Malaysia. The study is modelled after Lowry's (1977) and Oke's (2006) concept of evaluating urban effects by simulating the presence or absence of these effects. Therefore, in order to assess the effects of the GCC and the individual effect of vegetation and waterbody, simulations for each were successively conducted when present and absent.

In general, this study discusses the effectiveness of the GCC in mitigating urban thermal climate effects associated with urbanisation. Section 5.2 highlights the planning concept adopted in the development of Putrajaya city (PC) and a brief description of the study area. Section 5.3 describes the coupled numerical models used, numerical settings and model initialisation and model configuration and evaluation against observations. Furthermore, Section 5.4 contains results and discussions for surface energy components, T2m, 2-m relative humidity (RH2m), UHI and 2-m mixing ratio (Q2m). This study ends with a summary of the study outcomes in Section 5.5.

5.2 Study area description and planning concept

5.2.1 Study area

Putrajaya is located in the Klang Valley region in Southeast Asia at 2°55'00" N 101°40'00" E and 25 km south of Kuala Lumpur (Fig. 5:1) with an approximate area of 49 km² previously covered by vegetation, that is, rubber and oil palm plantation. To the east, PC is bordered by Bangi, Cyberjaya to the west and

Dengkil to the north. Located few degrees north of the equator with an average elevation of 30 m, PC is a typical tropical city. Rainfall averages 2–3 m per year and falls heavily during the northeast monsoon season, depositing approximately 10–30 cm within few hours (Bunnell 2002). PC has low variable air temperature with an annual mean minimum and maximum of approximately 25 and 27.5°C, respectively. RH averages approximately 63% per annum in the area with extended daily average solar radiation of 6 h. Winds are generally light and variable with speed ranging from 0 to 7.5 m s⁻¹ (Shahidan et al. 2012).

The landscape of Putrajaya is divided into two main areas. The core comprises of five precincts (P1, P2, P3, P4 and P5), while the peripheral (residential neighbourhoods) areas consist of 15 precincts, located 2–5 km from the central precinct (Moser 2010). The Putrajaya Boulevard is one of the geographical landmarks of the city, with width and length of 100 m and approximately 4.2 km, respectively. The Boulevard forms the central spine linking the aforementioned five core precincts. In addition, the expansive Boulevard is designed for ceremonial purposes and embellished by four squares (dataran): Dataran Wawasan, Dataran Rakyat, Dataran Putrajaya and Dataran Gemilang. It extends from the northeast to the southwest with symmetrical large federal government buildings. Approximately 6.8 km² of artificial lake and wetlands in 23 parcels were reported to be created by flooding. The lake serves for both recreational and ecological functions, and provides a body of water maintained at a level safe for skin contact (but not for swimming). The lake helps mitigate floods and run-off with a wetland forming part of the lake (Kho & Low 1998). The current local climate zone (LCZ)

(Stewart & Oke 2012) of Putrajaya Boulevard could be classified as dispersed urban form, with low density (Moser 2010). Furthermore, PC comprises wide roads, sidewalks and parking lots. Currently, the city has a population of 100,000 people.

5.2.2 PC planning concept

The GCC was adopted in the development of PC. According to Howard (1898) ideals of a garden city, it should exhibit interrelationships between a country and city with the following unique characteristics: (1) size of the city should be predetermined and it should be built on a natural agricultural land; (2) the city should be surrounded by rural belt; (3) it should accommodate residents, industry and agriculture and (4) should have limited encroachment of the rural belt. Hence, in line with Howard (1898) ideals, 38% of PC total land area is reserved for recreational parks, gardens, adjacent wetlands, waterbody and open space (Fig. 5:1b and c). Vegetation and waterbody are integrated with the GCC to use their reported thermal reduction properties within urban microclimate, improve air quality (Hathway & Sharples 2012; Zhang et al. 2014) and replicate nature.

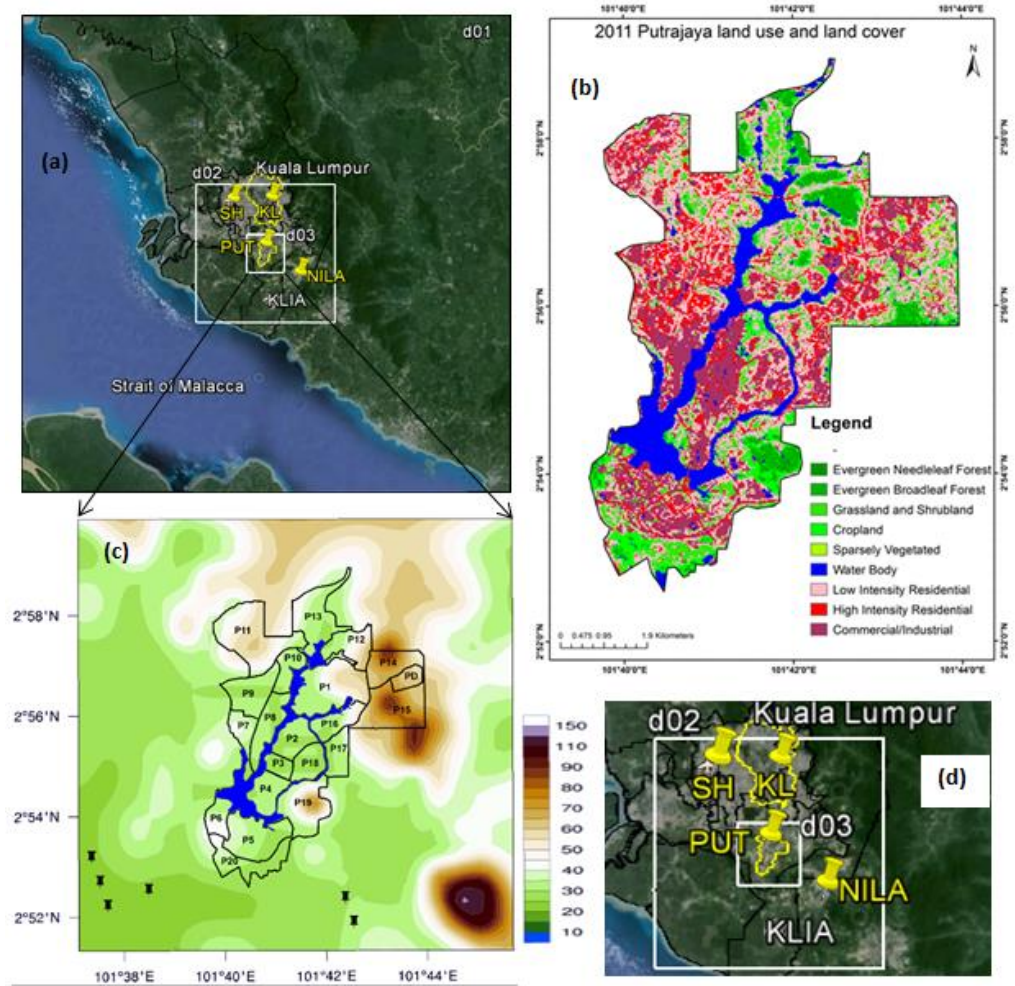


Fig. 5:1. Putrajaya: (a) WRF domain configuration, (b) Land use, (c) Terrain height and (d) zoomed in d02 and d03

5.3 Methodology and model evaluation

In order to assess the performance of the GCC in mitigating the effect of thermal positive feedback (such as UHI) on the urban and surrounding environment induced by urbanisation, a control case (case 1), two different experiments (cases 2 and 3) and an ideal case (non-urban) were successively simulated. Case 1 represents the up-to-date ground truth of the city while cases 2 and 3 represent scenarios with waterbody and vegetation of PC replaced with high-intensity residential urban surfaces, respectively. For the non-urban case, all urban surfaces of PC were replaced with their neighbouring grid vegetation

land use (to replicate agricultural land). Comparison of cases 2 and 3 against the control case enables estimation of the effect of waterbody and vegetation to the thermal mitigation of the GCC. Furthermore, the ideal case (non-urban) was used to evaluate relative changes in the urban environment of PC caused by the urbanisation of the area.

Accurate land use and land cover of the area (Fig. 5:1b) used as the model static geographic data were derived from remote sensing data of the area obtained from Landsat imagery. Furthermore, terrain information of the area (Fig. 5:1c) was updated accordingly. The accurate land use of waterbody and vegetation of PC were replaced for cases 2 and 3, respectively, with urban surfaces using WTOOLS (Nuss 2011). WTOOLS is used to display and modify WRF grid information using Google Earth. The International Geosphere–Biosphere Programme (IGBP) land cover classification system with three urban categories (low intensity residential, high intensity residential and commercial or industrial) (Fig. 5:1b) was adapted to account for the urban roughness inhomogeneity, variation in urban surface thermal properties and exchange of momentum and other physical processes in an urban area. The classification is suitable for the coupled Noah/UCM (Liu et al. 2006).

Anthropogenic heat release of the area was not parameterised in the UCM because of lack of data in the area. Land surface properties were defined as a function of the land use category. In order to represent the zero-order effects of urban surfaces and account for the land–atmosphere interactions, the bulk effects of urban area representation in the atmospheric model was adopted using the urban canopy parameterisation (Kusaka et al. 2001). Available surface information of Putrajaya was derived from recent studies and

government sources in the area (Shahidan et al. 2012; Gambero 2013; Salleh et al. 2013; Yusuf et al. 2014).

A mean roughness length of approximately 85 cm (Salamanca et al. 2010) was parameterised to represent turbulence created by roughness elements and induced drag from buildings. Surface albedo of urban and vegetated classes was assigned with approximately 0.11 and 0.18 (Salleh et al. 2013; Shahidan et al. 2012), respectively, to account for short-wave radiation trapping in the urban canyons and reduced heat sink effect in the vegetated areas. Volumetric heat capacity and the soil thermal conductivity of the area were set to $1.82 \text{ MJ m}^{-3} \text{ K}^{-1}$ and $1.66 \text{ W m}^{-1} \text{ K}^{-1}$ (Ahmed et al. 2015), respectively, to parameterise the large heat sink in the urban and underlying surfaces. Cases 1, 2 and 3 were parameterised with urban fractions of 0.66, 0.78 and 0.82, respectively. It is important to note that summation of urban and vegetation fractions is unity. However, for the non-urban land use categories, values of the properties as stated here but not specified are kept as default in the model. Parameterisation of the urban environment has been observed by Liu et al. (2006) and Chen et al. (2011) to enhance Noah/UCM significantly in representing the urban physical processes.

5.3.1 WRF/Noah/UCM

This study uses the WRF mesoscale model (Version 3.5.1) with integrated Advanced Research WRF (ARW) dynamic solver (Skamarock et al. 2008). This is a numerical weather prediction (NWP) and atmospheric simulation system used for research and forecasting. The study used the unified Noah land surface model (Noah LSM) (Chen & Dudhia 2001) coupled with single-layer

UCM (Tewari et al. 2007; Chen et al. 2011). The single-layer UCM has a simplified two-dimensional urban geometry approach considering building height, roof and road width, and assumes street canyons of infinite length. UCM includes trapping and shadowing effects and reflection of radiation, defined by the street canyon dimensions and orientation, as well as the solar azimuth angle. Therefore, by computing surface temperatures and heat fluxes of road, roof and wall, it is possible to calculate the energy and momentum transfer between an urban environment and the atmosphere. The coupling of the single-layer UCM with the Noah LSM completes the urban surface energy balance by calculating fluxes from the vegetated portion of the urban surface in a given grid cell.

5.3.2 Numerical settings and model initialisation

Numerical calculations were made for 66 h starting from 22 September 2011 using the coupled WRF/Noah/UCM with the first 16 h used as model spin-up time. Selected days for simulations showed clear cloudless skies, calm wind conditions, and absence of rainfall. These conditions favour strong UHI effect (Parker 2010). In the horizontal plain, three domains (d01, d02 and d03) using a one-way nesting approach were configured, leading to a high-resolution grid of 0.3 km, which covers the urban area of PC (Fig. 5:1). The coarse domain (d01) covers southwest Malaysia and Strait of Malacca, while d02 and d03 cover southwest of Klang Valley and PC area with its surrounding cities, respectively. The vertical plain of the domain has 32 terrain-following vertical levels to resolve the atmosphere with the model top level at 100 hPa, of which 18 levels near the surface and above the urban canopy layer (UCL) were

reserved to further resolve frequent variations of atmospheric variables and small-scale features near the Earth's surface. Initial and boundary conditions for the simulations are obtained from the National Centre for Environmental Prediction (NCEP) Global Final (FNL) Analysis ($1.0^\circ \times 1.0^\circ$) (NCEP et al. 2000).

The Yonsei University (YSU) scheme (Hong et al. 2006) was used as the planetary boundary layer (PBL). It is considered to perform better in high-resolution urban climate applications when combined with the coupled Noah/UCM (Lin et al. 2008). Other physics parameterisations include a long-wave rapid radiative transfer model (RRTM) (Mlawer et al. 1997), short-wave radiation scheme based on Dudhia cloud radiation scheme (Dudhia 1989) and surface layer scheme based on the Monin–Obukhov similarity theory. The WRF single-moment six-class (WSM-6) microphysics scheme is applied to all domains (Hong et al. 2004; Dudhia et al. 2008). However, cumulus convective parameterisation was not applied to any of the domain as model grids are sufficiently refined to resolve updrafts and downdrafts (Li & Pu 2009).

In this study, the coupled Noah/UCM model was modified to reflect the prevailing urban morphology and surface conditions using information derived elsewhere (Shahidan et al. 2012; Salleh et al. 2013; Thani et al. 2013; Qaid & Ossen 2015; Ahmed et al. 2015; Morris et al. 2015a; Morris et al. 2015b; Salleh et al. 2015; Morris et al. 2016). Similar simulation physics and dynamics configurations were applied to all simulated cases. The area of interest (PC) was centred on d03 (Fig. 5:1a and c) to enable convective and radiative interactions of urban environmental variables with their surrounding boundaries. Model finest domain (d03) is initialised through d02 initial and

lateral boundary conditions interpolated from d01. Similarly, the coarse domain (d01) boundary conditions were linearly interpolated from NCEP FNL 6-h data. Furthermore, the model derived its initial urban and land use fields from the static data sets used.

5.3.3 Model validation

NWP models are often associated with inherent biases resulting from model surface physics and atmospheric parameterisation. The need to validate model-simulated outputs against observational data is thus imperative to ascertain the model level of agreement with the observed data. In this study, seven statistical tools, mean, mean bias error (MBE), mean absolute error (MAE), root-mean-square error (RMSE), Pearson's coefficient of correlation (R), coefficient of determination (R^2) and hit rate (HR), were used to assess the level of agreement with observed data, biasness, degree of variation, magnitude of error and level of acceptance of the model. Temperature and RH of $\pm 2^\circ\text{C}$ (Cox et al. 1998) and $\pm 5\%$ (Lawrence 2005), respectively, were used to achieve the desired accuracy for HR estimation.

Model evaluation was conducted for d02 (Fig. 5:1) with four observational stations (see Table 5:1), and d03 for the only existing station situated in the area of interest. In order to ensure strong justification for the model performance over the region, the validation was first carried on d02 and then on d03, housing the PC. The yellow pushpins in Fig. 5:1d are the observational sites. Observed stations used are all classified as urban. Putrajaya station is located in an open field that is approximately 30 m from a residential vehicular road and 18 m from a pedestrian path typified by low-rise urban form

as physical characterisation using Stewart & Oke (2012) LCZ classification system. Observed data were obtained from Malaysia Department of Environment (DOE).

Table 5:1 shows metadata for meteorological observational stations used for model evaluation. Table 5:2 and Table 5:3 provide statistical summaries of the model performance of d02 for T2m and RH2m, respectively, for each station and the only station in Putrajaya (PUT_d03). On the contrary, Fig. 5:2 depicts the model diurnal profile for both canopy layer temperature and RH with their respective biases (red lines). The red vertical lines emanating from the magnitude of each square black-shaded box are the errors for each point.

Table 5:1. Observational sites metadata

Station ID	Station Name	Location		Elevation (m) above MSL
		Latitude (°)	Longitude (°)	
PUT	Putrajaya	2.9319	101.6818	32.0
NILA	Nilai	2.8208	101.8146	52.0
KL	Kuala Lumpur	3.1102	101.7046	36.0
SHA	Shah Alam	3.1050	101.5560	7.00

Table 5:2. Model evaluation for 2-m temperature (°C) on d02 and d03 from 0100 MST for 48 h

Station	Mean Sim.	Mean Obs.	MBE	MAE	RMSE	R	R ²	HR
PUT	28.42	28.61	-0.19	1.08	1.30	0.88	0.77	0.90
NILA	28.27	29.11	-0.84	1.11	1.11	0.90	0.81	0.85
KL	29.11	29.60	-0.49	1.03	1.14	0.88	0.78	0.88
SHA	28.86	28.97	-0.11	2.16	2.01	0.73	0.53	0.52
PUT_d03	28.52	28.61	-0.09	1.02	1.25	0.89	0.79	0.90

In d02, the model performed well for canopy layer temperature (T2m) with a mean RMSE and HR of approximately 1.4°C and 79% (Table 5:2). The diurnal profile was recreated with approximately 76% similarity with the observed data. Nevertheless, the model performance is less impressive for Shah Alam station with RMSE and HR of 2.01°C and 52%, respectively. RH

predictions are fair, but less significant than the performance observed for T2m (Table 5:2 and Table 5:3). However, model performance in d03 is relatively good with >90% and 73% of its predictions for T2m and RH2m (Fig. 5:2, Table 5:2 and Table 5:3), respectively, considered *yes event* for the set criteria.

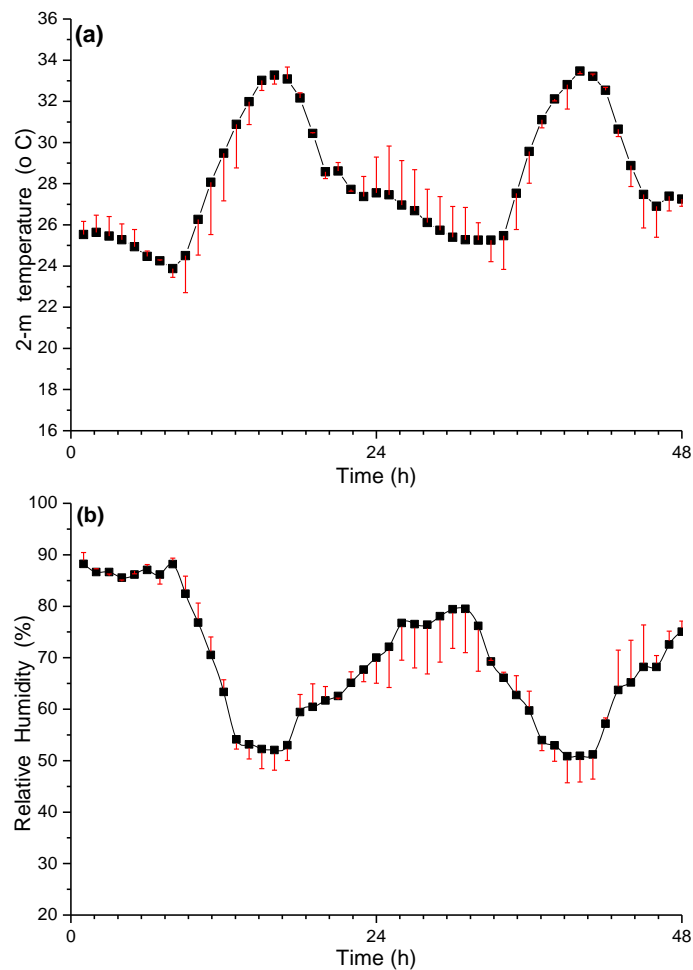


Fig. 5:2. Model evaluation for Putrajaya station (d03) from 0100 MST for 48 h

Table 5:3. Model evaluation for 2-m Relative humidity (%) on d02 and d03 from 0100 MST Or 23/09/2011 for 48 h

Station	Mean Sim.	Mean Obs.	MBE	MAE	RMSE	R	R ²	HR
PUT	66.16	69.65	-3.49	7.60	9.78	0.76	0.58	0.48
NILA	66.23	69.27	-3.04	8.76	11.17	0.61	0.37	0.42
KL	60.60	66.33	-5.73	7.30	9.00	0.89	0.79	0.58
SHA	61.48	71.52	-10.04	11.44	15.31	0.77	0.59	0.35
PUT_d03	68.79	69.65	-0.85	3.85	4.73	0.93	0.87	0.73

5.4 Results and discussions

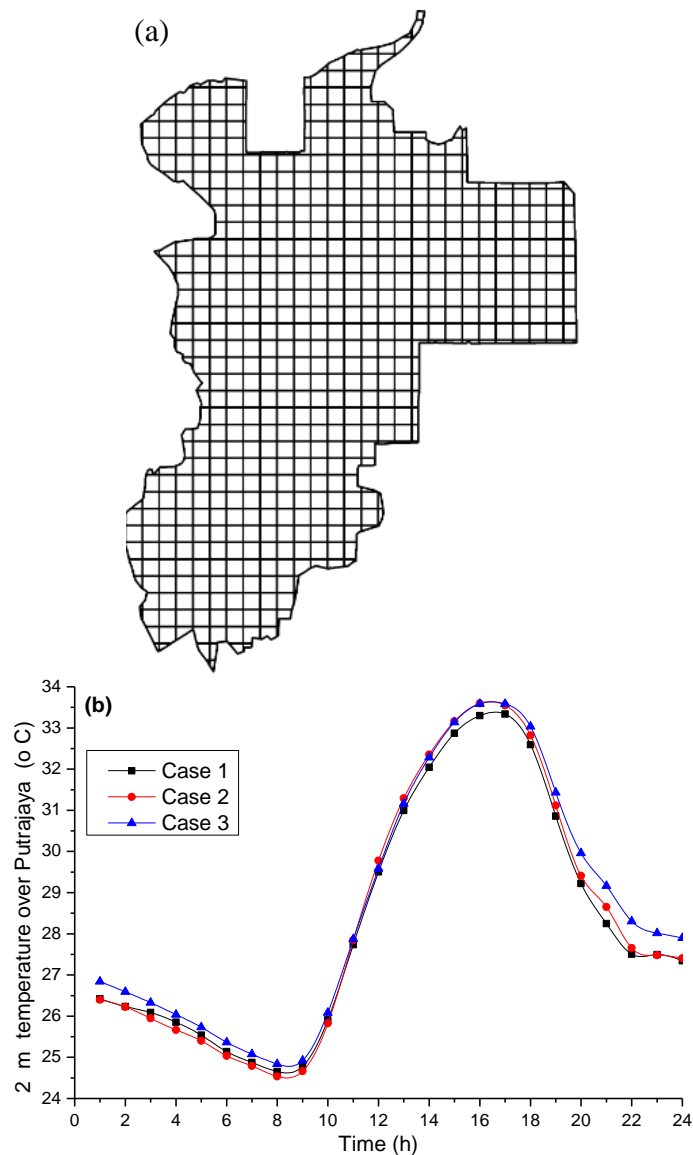


Fig. 5:3. (a) Putrajaya with grid cells and (b) mean diurnal T2m over Putrajaya during the investigated period

Model results and analyses are conducted for d03 only, except otherwise stated. Presented results are averaged over 513 grid cells (Fig. 5:3a) within PC for a 24-h temporal scale. Fig. 5:4a shows a graphical representation of reclassified land use and land cover for the three scenarios investigated. Vegetated land use classes were reclassified to greenery while urban classes

were reclassified to urban. Waterbodies and sparsely vegetated regions are left as originally classified. It is worth noting that sparsely vegetated areas depict clear lands with little or no greenery and are currently not used. The controlled case has waterbody, greenery and urban coverage of approximately 12%, 22%, and 66%, respectively (see Fig. 5:4a). In case 2, approximately 12% of waterbody was replaced with urban land use, thereby increasing the urban fraction of the area to approximately 77%, while vegetation was left same as the control case. However, in case 3, the waterbody was left as in the control case, while approximately 17% of the existing vegetation was replaced with urban land use. It is important to note that approximately 4.5% of the vegetation was left in case 3 to represent obtainable conditions in other urban cities. Thus, case 3 has the highest percentage of urban surfaces (~83%), followed by cases 2 and 1 the least (Fig. 5:4a). Modifications in land use composition of cases 2 and 3 are expected to have profound impact on the overlying thermal conditions of the PC.

5.4.1 Surface energy balance

The surface energy balance is mainly controlled by direct daily solar radiation cycle, from 0830 to 2030 MST (Fig. 5:4b, c and d), with minor contributions from evapotranspiration from vegetated areas; LH from changes in state of the fluids overlying the area; anthropogenic heat release; radiated and reflected fluxes from the ground surfaces and wall, roof and road. In this study, the effect of anthropogenic heat release is not accounted for because of lack of data in the area. Net SW represents net all-wave radiations, while SH and LH are sensible and latent heat fluxes, respectively. The composition of vegetation and

urban surface fraction in an area contributes immensely to the amount of moisture available and the overlying thermal conditions. Thus, it is important to analyse the behaviour of the surface energy balance for the different land use and land cover compositions of PC.

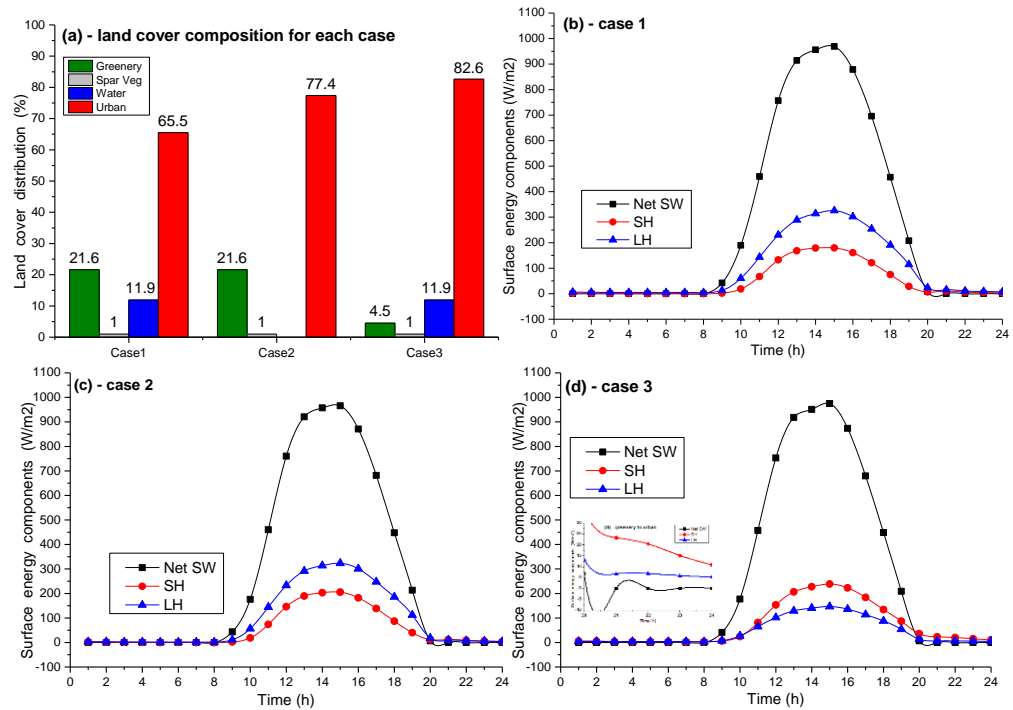


Fig. 5:4. (a) Land use and land cover coverage for each of the simulated cases, and mean surface energy balance components for: (b) case 1, (c) case 2 and (d) case 3

Table 5:4. Mean surface energy balance components for the different scenarios during the study period

Case No.	Average			Maximum			Minimum		
	Net SW	SH	LH	Net SW	SH	LH	Net SW	SH	LH
1 (W/m^2)	542.47	48.55	97.53	969.02	179.21	325.44	7.81	-0.37	4.23
2 (W/m^2)	541.89	55.57	95.07	965.79	205.30	323.54	6.65	-0.39	1.39
3 (W/m^2)	540.86	70.91	44.93	964.81	238.84	146.74	6.88	2.53	3.43

The net all-wave radiations for cases 1, 2 and 3 peaked at 1500 MST with 969.02, 965.79 and 964.81 $W m^{-2}$, respectively, with corresponding daily mean values of 542.47, 541.89 and 540.86 $W m^{-2}$. SH and LH of the different cases display non-uniform values as the net all-wave radiations. SH is influenced by

the reflected and radiated fluxes from solar radiation, while LH is influenced by the fraction of vegetation – evapotranspiration. This is evident in the graphical representation of the surface energy components (Fig. 5:4 and Table 5:4), where values of SH and LH, respectively, increase and decrease with increases in an urban fraction. This is true because the coupled Noah/UCM calculates the LH flux from the vegetation fraction parameter. For instance, case 1 (with an urban fraction of ~66%) has SH and LH magnitudes of approximately 49 and 98 W m⁻², respectively, whereas the corresponding figures for case 3 (with an urban fraction of ~83%) were approximately 71 and 45 W m⁻². It is observed in each case that direct solar radiation masked the contributions of SH and LH between sunrise (0720 MST) and sunset (1920 MST). However, before sunrise and after sunset, LH and SH dominate the fluxes overlying the area (Fig. 5:4b and c and the balloon sections of Fig. 5:4b, from 20 to 24 h, for more clarity).

5.4.2 T2m and RH2m

The effect of increased urban fractions on T2m over the area was observed to be profound during morning (0100–0800 MST) and night (1900–2400 MST) for both cases 2 and 3 with corresponding maximum magnitudes of approximately 0.41 and 0.91°C at 2100 MST (Fig. 5:5a); this was estimated by comparing each case with the control case (case 1). Temperature variations between cases 2 and 3 from Putrajaya real conditions (case 1) start during early morning and decline to minimum values during the late morning and daytime (Fig. 5:3b, Fig. 5:5a, Fig. 5:6 and Fig. 5:7). These declines in T2m difference

from the real conditions are then followed by a sudden increase in magnitudes of T2m variations (Fig. 5:3b and Fig. 5:5a).

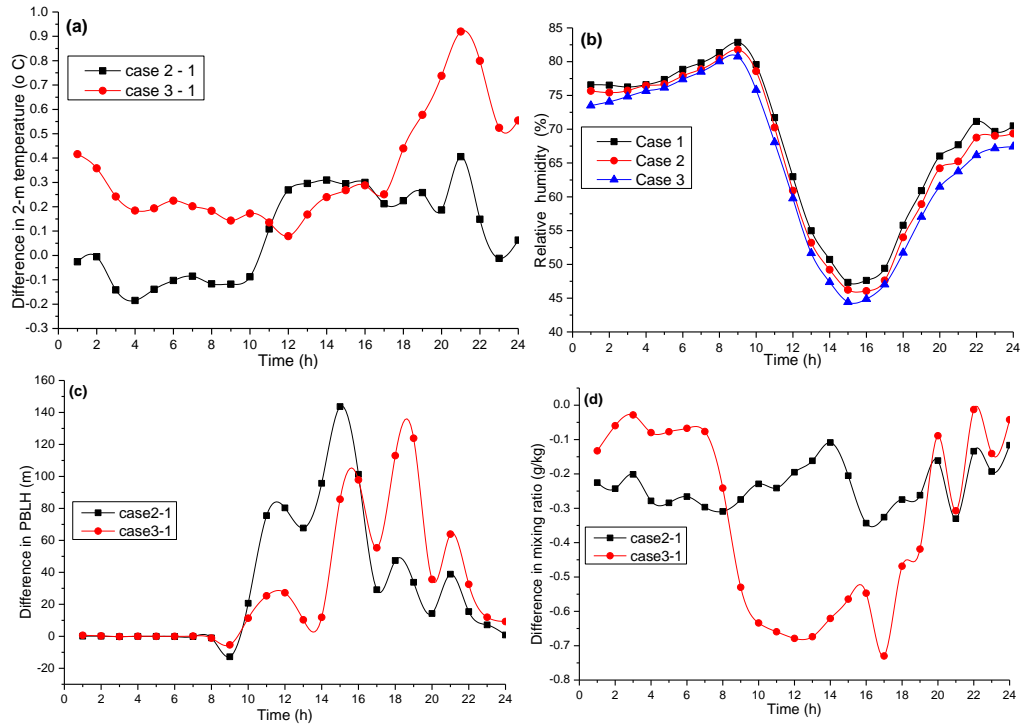


Fig. 5:5. Mean diurnal profile of urban fraction-induced difference in meteorological variables between the experimented scenarios and the control conditions of the area: (a) T2m, (b) RH2m, (c) PBLH and (d) Q2m

Case 3 shows a significant increase in induced thermal conditions of the area relative to case 1 with a mean magnitude of approximately 0.39°C , while case 2 showed a mean increase in magnitude of approximately 0.14°C relative to case 1 during the considered period. In Fig. 5:6, for cases 1 and 2, it is observed that regions with higher vegetation fraction show less heating before and after the incidence of direct solar radiation (see 0200 and 2400 MST, and Fig. 5:1). This is caused by high moisture availability resulting from evapotranspiration of areas with greenery (Vidrih & Medved 2013; Middle et al. 2014). Furthermore, the model has captured this behaviour as LH fluxes are estimated from vegetation fraction parameter. However, case 3 with

approximately 83% urban fraction does not indicate a similar trend for the same regions. Deviation in the trend of case 3 is caused by the increased urban fraction relative to cases 1 and 2 (Fig. 5:5d demonstrates the induced influence of increased urban fraction on the mixing ratios of cases 2 and 3, which depend on evapotranspiration).

Replacement of waterbody and vegetation with urban surfaces in cases 2 and 3, respectively, forms the basis for estimating their respective contributions in reducing the overlying thermal environment of the area. This, however, increases the urban fractions of cases 2 and 3. Each square kilometre of vegetation added to the Putrajaya area reduces the temperature by 0.047°C ; $0.39^{\circ}\text{C} \div (49 \text{ km}^2 \times 0.17)$. The observed effect of vegetation is however poor compared with other studies on the urban thermal cooling effect of vegetation (Vidrih & Medved 2013; Maimaitiyiming et al. 2014; Santamouris 2014). Shashua-bar & Hoffman (2000) concluded in their investigation of the different geometric configuration of greenery and tree shading that green area with little or no shading show reduction in cooling effect of 2.5°C compared with a configuration with proper shading. However, UCM scheme used in this study does not consider the individual effects of tree shading. In addition, other studies by Onishi et al. (2010) and Perini & Magliocco (2014) support the earlier conclusion of Onishi et al. (2010) on the effect of tree shading and configuration on the thermal cooling effect of vegetation in urban areas.

The poor performance of vegetation in the design of PC could be justified by Moser (2010) submission on the implementation of the adopted GCC in Putrajaya. He argued that rather than narrow streets that provide shade throughout the day, Putrajaya's wide and formal avenues expose pedestrians,

buildings and traffic to direct sunlight. However, these claims are plausible, but not strongly corroborated as the model implemented in this study adopts the bulk urban surface parameterisation approach, representing the model grid cell-averaged effect of building structures. In this approach, the UCM parameterises the ensemble features of the urban morphology, but not individual buildings, and street canyons are not explicitly represented (Brown & Williams 1998; Masson 2000; Martilli et al. 2002; Otte et al. 2004). Thus, Noah-MP coupled with the WRF/UCM and high-resolution observations of the PC are needed to strongly corroborate any claims on shading and configurations impact.

On the contrary, low performance of waterbodies in the area (0.024°C cooling effect per square kilometre of waterbody added to the area; $0.14 \div (49 \text{ km}^2 \times 0.119)$) was expected because of its high heat capacity and thermal inertia. It is observed in Fig. 5:6 (a and c) and Fig. 5:7 (a and b) that T2m above waterbody were relatively high after daytime, thereby yielding a mean negative effect of approximately 0.1°C from 01 00 to 10 00 MST. This is rather undesirable because of its aims of thermal reduction. This is further justified in Fig. 5:5a, Fig. 5:6 and Fig. 5:7, where replacing waterbody with urban areas shows little significance in the temperature difference between cases 1 and 2 (see from 2200 to 0200 MST). Fig. 5:7 shows the effect of waterbody and vegetation estimated by subtracting control case from the experimented ones. The observed rather negative influence of waterbody for the desired objectives in the development of the city are supported by a study conducted (Steenefeld et al. 2014) on the functionality of waterbodies in reducing T2m in the Netherlands. They observed that temperature above and

surrounding waterbodies have in fact increased during evening transition to daytime.

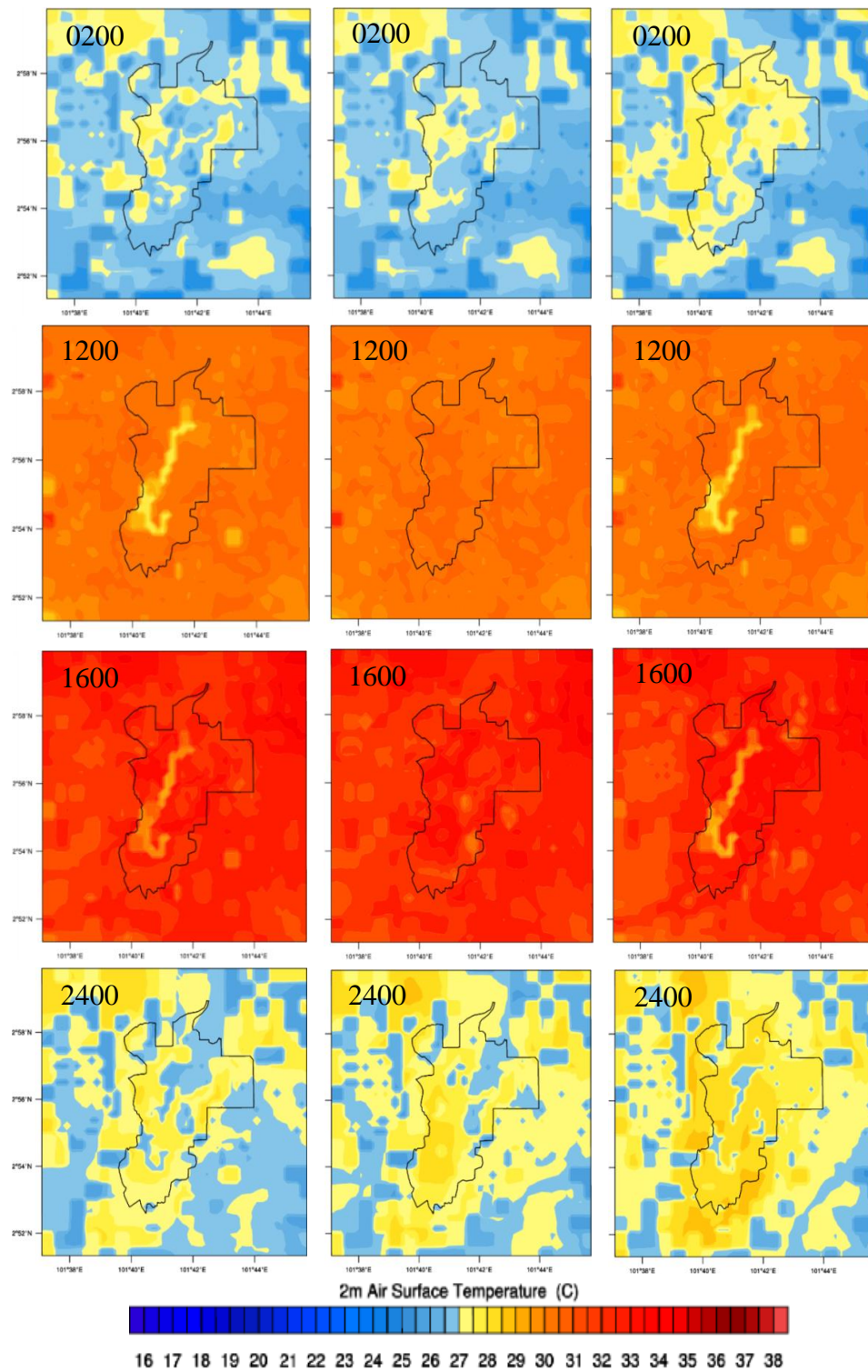


Fig. 5:6. Mean diurnal variations of 2-m temperature over Putrajaya; (a) images to the left (case 1), (b) middle (case 2) and (c) images to the right (case 3)

Fig. 5:6 and Fig. 5:7 show the diurnal and spatial changes in T2m that accompanied variations in urban fractions of the different cases considered. Induced thermal influence on the surroundings of Putrajaya was noted for each case. However, cases 2 and 3 showed significant influence on the surroundings, particularly before and after noon. The observed influences on the surroundings have likely resulted from slow advection of thermally forced convection. Non-uniform distribution of land use and land cover of the PC causes variations in heat fluxes of the area. This effect is more obvious in the absence of solar radiation (see Fig. 5:6 and Fig. 5:7 at 0200 and 2400 MST). Overall, combined cooling effects of the two natural elements integrated with the GCC caused a reduction in temperature of 0.53°C per day in the area.

For RH, case 1 (~68%) consistently shows a higher mean magnitude than cases 2 (~66.7) and 3 (~65.2%). Furthermore, all considered cases exhibited diurnal patterns with approximately 98% similarities; maintaining a near-uniform trend between 0100 and 0900 MST and then a sudden decline from 0900 MST to minimum values at 1500 MST, and then picks up from 1600 MST and continue on a steady increase to 2400 MST (Fig. 5:5b). This is consistent with the daily solar radiation cycle. RH depends on the amount of moisture available through convective evaporation and transpiration from vegetation in the area. The increase in the urban fraction of cases 2 and 3 showed the corresponding effects on the values of RH2m over the area, which start decreasing few minutes after the onset of sunrise and again start gaining magnitudes as the solar short-wave radiations start attenuating. During the study, it is observed that the mean simulated RH2m for the different scenarios maintained a consistent diurnal profile. However, marginal difference in RH2m

was noted for cases 1, 2 and 3; this difference was significant around regions with a high percentage of vegetation, which then influences the T2m overlying the regions.

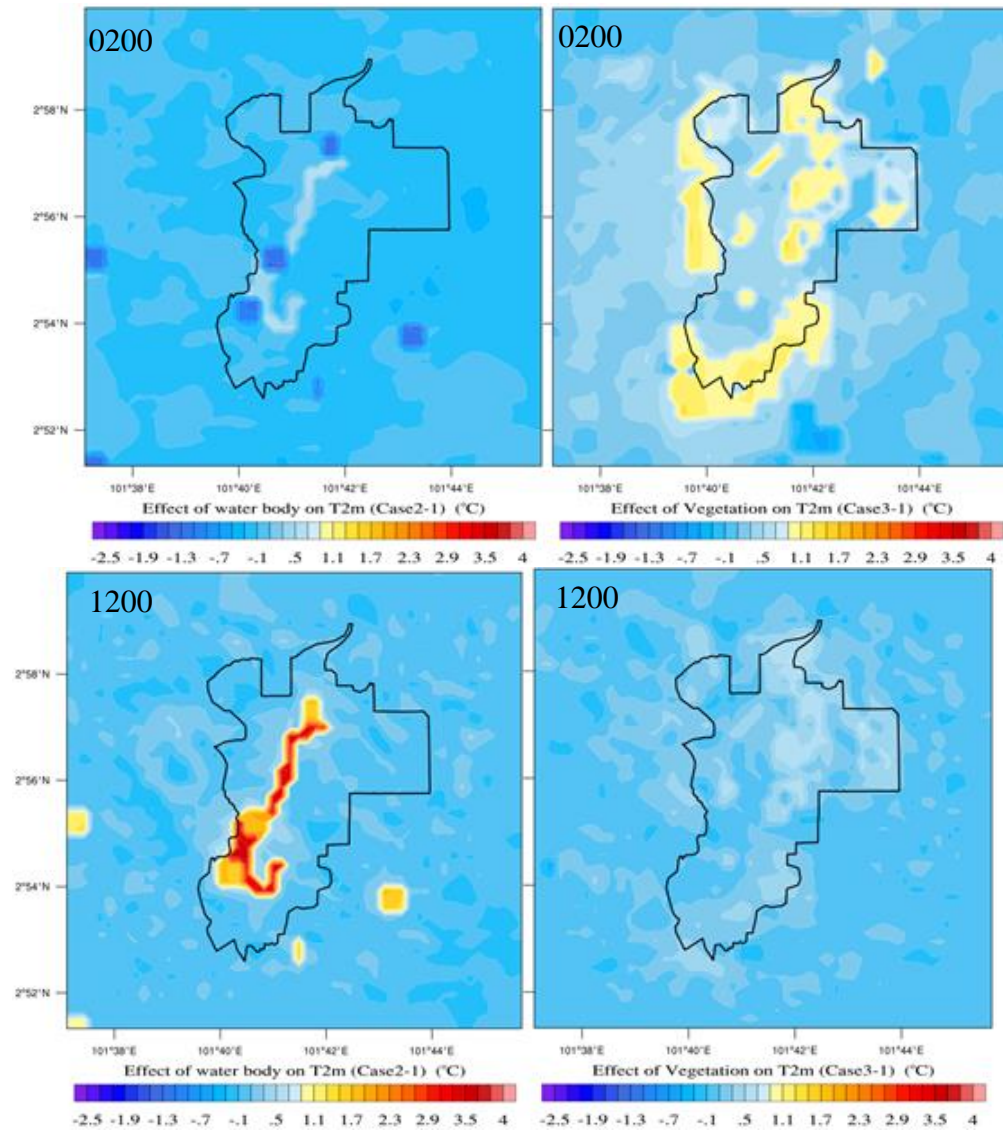


Fig. 5:7. See description in the next page

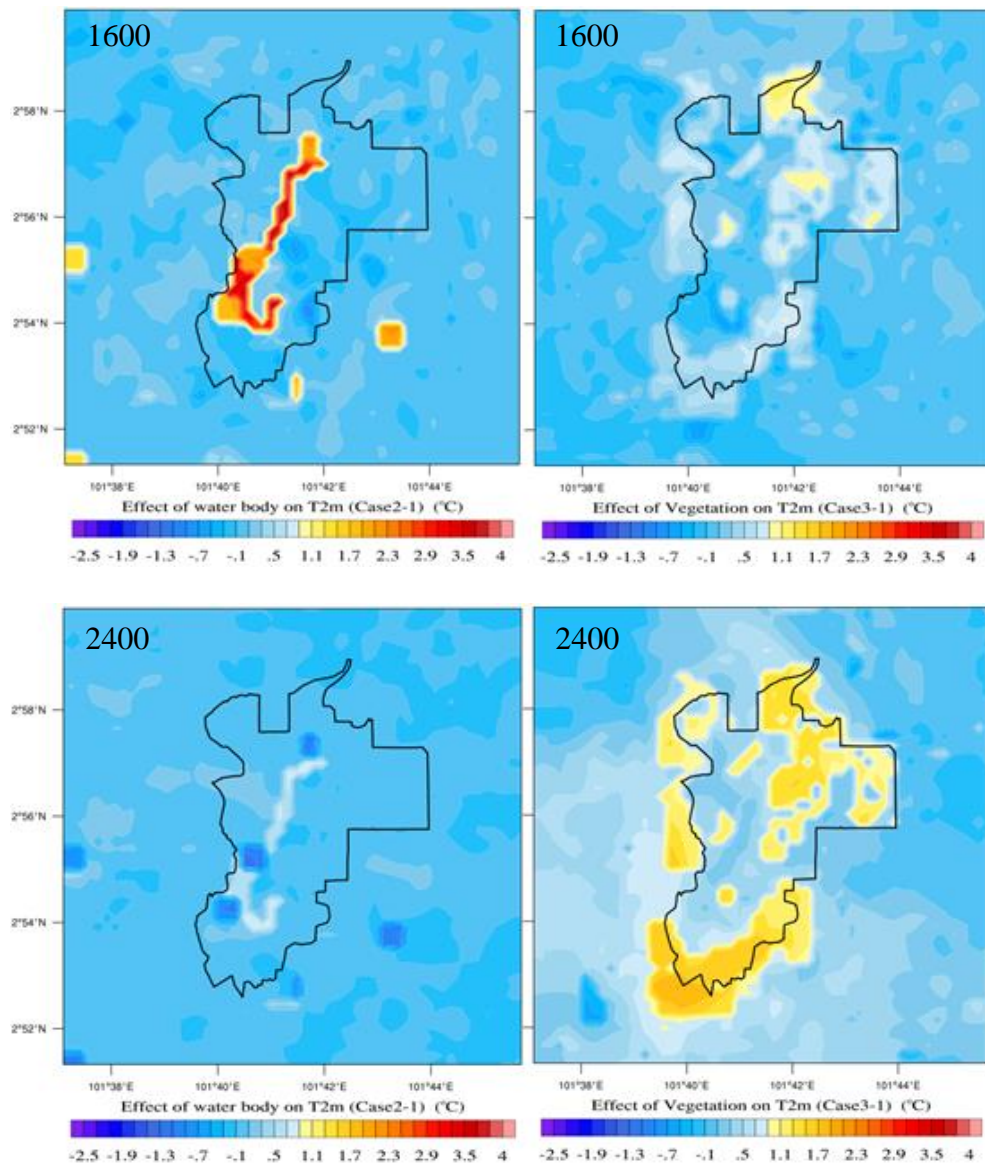


Fig. 5:7. Evaluation of vegetation and waterbody on T2m. (a) case 2-1 (effect of waterbody) and (b) case 3-1 (effect of vegetation)

5.4.3 UHI

The increase in urban fraction decreases the surface albedo and increases the amount of absorbed short-wave radiation fluxes during solar radiation. This would thereby cause an increase in the amount of heat to be radiated during morning and night. Because of land cover and surface differences between urban and rural areas, thermal microclimates over urban areas are usually warmer than the rural areas and countryside. The simultaneous differential

heating of surfaces in urban and rural areas is referred to as the UHI phenomenon.

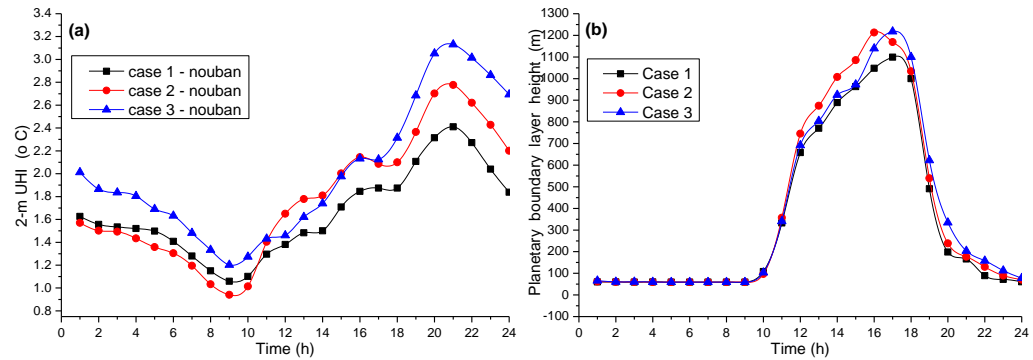


Fig. 5:8. (a) UHI estimation and (b) PBLH for the different scenarios tested

Similarly, the difference in T2m between urban and rural areas is known as the urban heat island intensity (UHII). Although the phenomenon is undesirable in some regions, particularly the tropics, it is important in cities located in the middle and high latitudes during winter (EPA 2009). During winter, an increase in the canopy layer temperature causes a reduction in energy demands for heating in middle- and high-latitude cities. In this study, the UHI is estimated by subtracting the ideal case (non-urban) from three different cases considered.

During daytime, urban surfaces retain a reasonable percentage of solar irradiance fluxes. Through natural convection and radiation processes, the retained thermal fluxes are radiated to the immediate overlying canopy layer; this is significant during nights (Fig. 5:4d and Fig. 5:8a). This leads to a canopy layer temperature difference between the urban and countryside/rural areas (Fig. 5:9). On the contrary, the rural areas are associated with high vegetation fractions, which imply higher plant respiration and transpiration, with higher moisture availability and RH of the canopy layer overlying the surfaces (Fig.

5:5b and d). This has a rather cooling effect on the lower boundary layer and thus reduction in the mean planetary boundary layer height (PBLH) of the area (Fig. 5:5c and Fig. 5:8b) (Rizwan et al. 2008; Norton et al. 2015); this is reflected on the mean PBLH over the PC for the three cases (~395, 388 and 359 m for cases 3, 2 and 1, respectively) considered in this study (Fig. 5:5b and d). It is observed in Fig. 5:8a that the intensities of heating for the different cases examined are temporally dependent, and showed a similar diurnal trend; decreasing from 0100 MST to minimum values at 0900 MST. The UHI magnitudes pick up momentum from 1000 and increase steadily to peak values at 2100 MST before embarking on the final attenuation in its magnitudes.

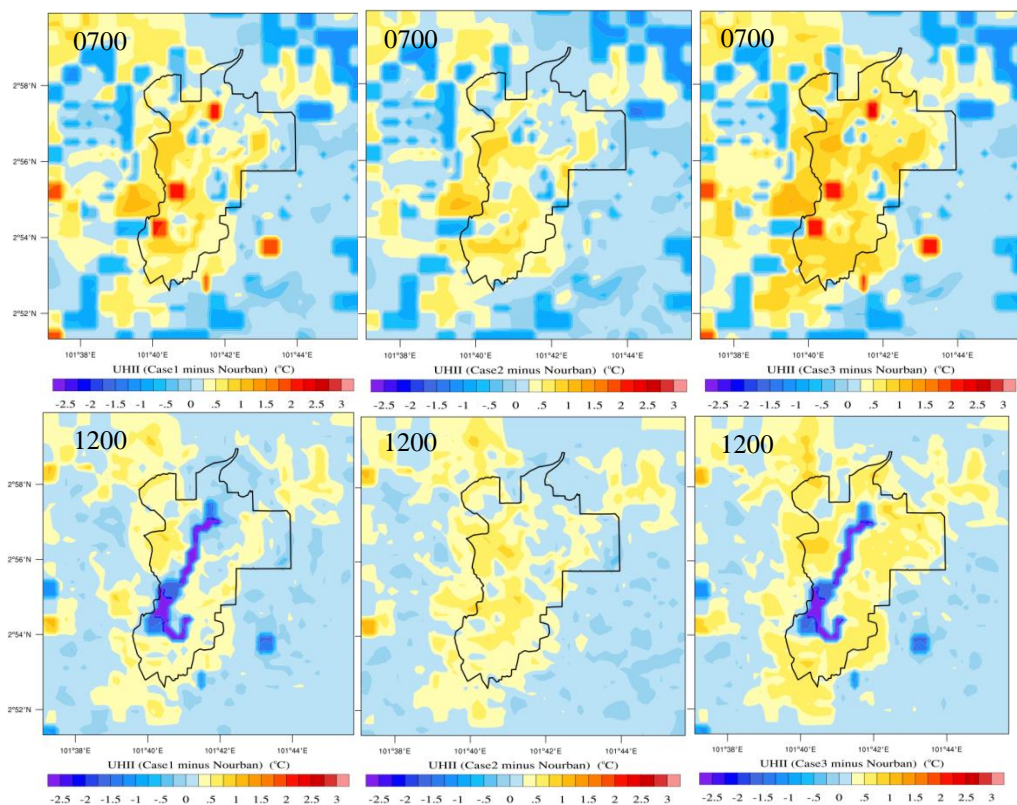


Fig. 5:9. See description in the next page.

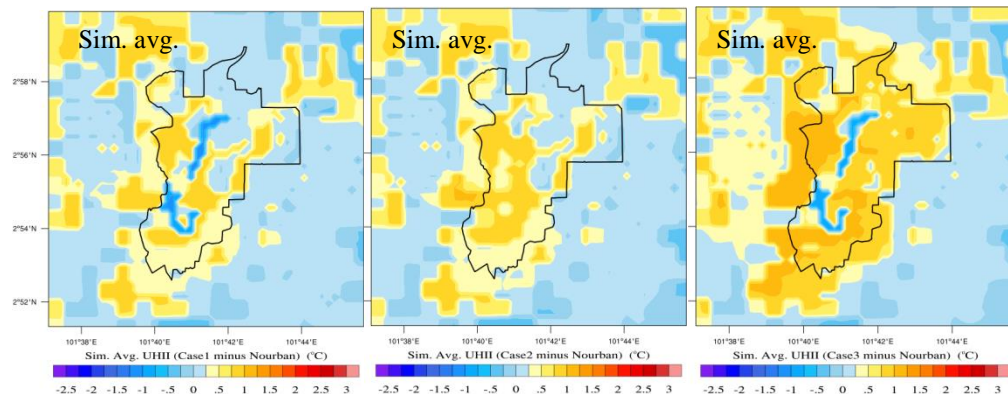


Fig. 5.9. Simulated spatiotemporal variations of UHI: (a) case 1, (b) case 2 and (b) case 3

On the basis of simulated cases, it is observed that increase in urban fractions caused intensification of UHI for cases 2 and 3 (Fig. 5:9). However, it is observed that replacing waterbody with urban surfaces (case 2) caused a reduction in UHI magnitude during morning hours (0100–1000 MST), despite the increase in urban fraction from approximately 66% to 78% (Fig. 5:8a). This effect is caused by the positive thermal feedback (extra heat fluxes) provided by waterbody in case 1 during the same window. This, however, reinforced early argument on the undesirable impact of waterbody, resulting from its high heat capacity and thermal retention properties; significantly, during night and early morning hours. During this period (morning and night), there is little or no influence of solar radiation, thereby making the influence of waterbody on the urban surface energy balance to be profound. Conversely, positive cooling effect of the waterbody is noted during daytime (1100–1600 MST), where replacing waterbody with urban surfaces increases the UHI by mean values of approximately 0.3 and 0.1°C higher than cases 1 and 3, respectively (Fig. 5:8a and Fig. 5:9). This positive influence of waterbody on the urban canopy thermal fluxes during daytime is also obvious in Fig. 5:6(a) and (c) at 1200 and 1600 MST, respectively. Between 1200 and 1600 MST, the daily solar

radiation is at its peak values, and hence, the urban heating is dominated by its fluxes. Nevertheless, positive influence of waterbody was observed. Furthermore, waterbodies showed an induced cooling effect on their local surroundings through slow advection (Fig. 5:6a and c at 1200 and 1600 MST). A higher depth of case 2 PBL relative to cases 1 and 3 (Fig. 5:8b) between 1200 and 1600 MST further validates the associated increase in overlying fluxes. This increase in fluxes is caused by the increase in the percentage of urban surfaces at the expense of waterbody, which exhibits thermal reduction property during daytime (Fig. 5:6a and c).

Mean UHI intensities of approximately 1.65, 1.79 and 2.04°C were observed for cases 1, 2 and 3, respectively. Minimum (~1.06, ~0.94 and ~1.20°C) and maximum (~2.41, ~2.78 and ~3.13°C) UHII were observed for cases 1, 2 and 3 at 0900 and 2100 MST (Fig. 5:8a), respectively. Furthermore, mean spatial variability of UHII over Putrajaya during the simulated period is shown in Fig. 5:9. Increase in extent and intensification of UHII in Fig. 5:9 during late night and morning hours for case 3 shows vegetation potential in reducing thermal conditions of the canopy layer. Fig. 5:10 also demonstrates the reduction in mixing ratios caused by increased urban fractions of cases 2 and 3. The increase in the percentage of urban surfaces in PC reduces the total land area reserved for vegetation and thus the LH fluxes. For case 2, the reduction in Q2m is localised over the area surrounding the waterbody. In addition, for case 3, the reductions in Q2m are obvious and more significant, and are not only limited to the areas where vegetation was converted to urban surfaces only, but also on the immediate surroundings (Fig. 5:10b). In addition, the effect of an increase in urban surfaces on Q2m during morning hours was

more significant relative to daytime. This reduction in Q2m corroborates the increase in heat fluxes observed for higher urban fractions relative to case 1.

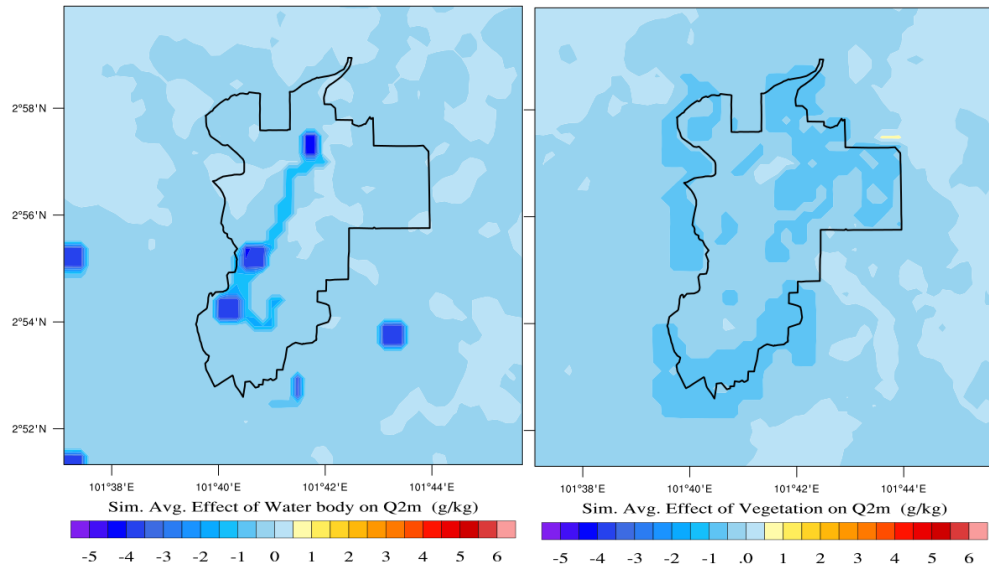


Fig. 5:10. Mean simulation spatiotemporal difference in Q2m due to changes in urban fraction: (a) case 2-1 (left) and (b) case 3-1 (right)

5.5 Conclusions

Coupled WRF/Noah/UCM was used to simulate the urban environment of Putrajaya using a one-way downscaling approach to investigate the effectiveness of the GCC adopted during the development of PC. Simulated results compared well with observational data. Surface energy balance analysis indicates that direct solar radiation predominates urban exchange of momentum, heat and water vapour during daytime. However, exchange of fluxes during night and early hours was controlled by reradiated absorbed fluxes from the area. SH and LH fluxes were observed to increase and decrease with increase in urban fraction, respectively.

Daily mean temperature reductions of 0.047 and 0.024°C per square kilometre of vegetation and waterbody added were observed, respectively.

However, effects of vegetation and waterbody were spatiotemporally dependent. During daytime, their cooling effects were masked by solar radiation. Nevertheless, they were partly visible during night and morning hours. Overall, an increase of urban surfaces was noted to increase T2m, UHI and PBLH. Conversely, an increase in urban surfaces also caused a reduction in Q2m and RH2m. Vegetation and waterbody were observed to contribute to T2m reductions of approximately 0.14 and 0.39°C, respectively, in the GCC. The pronounced cooling effect of water during daytime was predominated by the warming effect created during morning and night, because of its high thermal retention properties. On the contrary, vegetation showed consistent cooling effect during both mornings and nights.

UHIs showed spatiotemporal variations with urban fraction. The daily means (of UHI) of experimented cases with waterbody and vegetation replaced with urban surfaces were observed to be approximately 1.79 and 2.04°C, respectively while that of the control simulation was approximately 1.65°C. Thus, it can be concluded that increase in urban fraction caused an increase in UHI. In conclusion, waterbody and vegetation induced a daily reduction of T2m by 0.53°C over PC.

Findings of this study will help urban planners, designers, ecologists and governmental and non-governmental bodies to plan and update current guidelines and design methods for building sustainable and liveable cities.

Chapter 6

6 Conclusion

This research attempts to achieve four core research objectives: (1) to evaluate WRF configurations and suitability of the coupled WRF/NOAH/UCM model for Klang Valley urban climatology investigation, (2) to investigate the urban climatology of Klang Valley, (3) to study the local climate changes and adaptation to the urbanisation of Putrajaya, and (4) to evaluate efficacy of the garden city concept adopted during the development of Putrajaya city, using the available resources within the University of Nottingham.

Validation of the coupled WRF/NOAH/UCM model over the Klang Valley region against a network of meteorological observational stations demonstrates a good agreement and correlation. Investigation of Klang Valley urban climatology demonstrates the importance of land use and land cover (LULC) changes and anthropogenic heat (AH) ingestion into the model on predictions of urban climate variables in the region. Urban surface energy balance of the Valley is dominated by direct solar radiations during daytime, while trapped longwave radiation, re-emitted heat fluxes and anthropogenic heat releases are prominent during morning and nighttime. Mean maximum UHIIs of ~ 4.2 °C per day are observed in the Valley with diurnal variations closely tied to solar radiations. Regions of the Valley with low urban residential intensity experience moderate urban heat islands. This is due to the

high vegetation presence and thus high moisture availability (RH) relative to the other urban classes.

The urbanisation of Putrajaya city and its interaction with the local climate is conducted using the WRF coupled model. Climatology of the years: 1999, 2003, 2007, and 2011 were examined. Mean maximum and minimum warming of the area are found for 2007 and 1999, respectively. Conversely, the net all-wave radiation of the area (Putrajaya) maintains a near-uniform during the years considered; which conforms to low climate variability associated with the tropics, especially, Peninsular Malaysia. Diurnal variations of sensible and latent heats fluxes with their maxima and minima are consistent with the land cover modifications of the area. In addition, RH and PBLH exhibit variations according to the natural surface alterations and thermal variability induced by varying surface characteristics; where years with higher percentage of vegetation fractions show greater RH and low PBLH and vice versa. However, wind speed during the considered years for the urbanisation investigation shows less variability to urbanisation.

Adaptation of the microclimate phenomena (UHI and UCI) to urbanisation of Putrajaya area shows an interesting evolution with a reduction in the warming of the area found for 2011. Maximum and minimum UHIIs are observed for 2007 and 1999 with mean magnitudes of ~ 2.46 °C and ~ 0.7 °C, respectively while the area is currently (2011) warming with UHII of ~ 2.1 °C per day. Also, UCIs during the years considered vary from ~ 0.2 to ~ 0.4 °C. Investigation of the urbanisation processes that have taken place over the area reveals 2-m temperature of the Putrajaya city to be increasing at the rate of ~ 1.66 °C per day decade.

Results of the evaluation of the garden city concept indicate a ~ 0.53 °C reduction in 2-m temperature per day in the Putrajaya city. This outcome, however successful, in reducing the 2-m temperature of the city is below par expectations. Two prominent natural elements (water and vegetation) integrated into the concept reveal varying degree of diurnal performance. Vegetation shows more significant average performance (~ 0.39 °C) per day relative to water body (~ 0.14 °C). Proximity to the equator plays an important role on the magnitude of the mean cooling effect of each of the two natural elements investigated. Nevertheless, RH and PBLHs show consistent diurnal trends fairly influence by changes in urban and vegetation fractions, for the different scenarios considered in the investigation on the performance of the garden city concept and the natural elements employed.

Results from the different investigations reported in this thesis are published in journals and conferences. Some are currently submitted and under review, while others are in draft stages for journal and conference preparations.

6.1 Suggestions for further studies

- To further improve the model performance in the Klang Valley region, caution and systematic planning is needed to collate climate data for model improvement and data assimilation. New studies should be directed towards understanding model performance during intermonsoon seasons.
- A better understanding of buildings and trees/shadings configurations in the tropics is necessary to harness the cooling effect of vegetation to reduce the increase in air temperature associated with urbanisation.

- Physics and dynamics of UCI should be investigated to fully take advantage in urban planning.
- Computational studies using the WRF model should be dedicated in the region to improve wind speed predictions.

Acknowledgement

The author would like to thank the Ministry of Science, Technology and Innovation (MOSTI) of Malaysia for providing financial support for this research work. This work is sponsored under contract number M0056.54.01 and 06-02-12-SF0346. The author also wishes to thank the University of Nottingham for access to the *University of Nottingham High Performance Computing Facility* for part of the numerical calculations. This research work also forms part of The Seven South-East Asian Studies Mission (7-SEAS) under the National Aeronautics and Space Administration (NASA).

References

References

- Agus, Mohad Razali. 1990. "Urbanization and Low-Income Housing in Malaysia: Impact on the Urban Malays." *Journal of Pollution and Social Studies* 2 (2): 205–21.
- Ahamad, Fatimah, Mohd Talib Latif, Rosy Tang, Liew Juneng, Doreena Dominick, and Hafizan Juahir. 2014. "Variation of Surface Ozone Exceedance around Klang Valley, Malaysia." *Atmospheric Research* 139 (March): 116–27. doi:10.1016/j.atmosres.2014.01.003.
- Ahmad, Shaharuddin, Noorazuan Hashim, and Yaakob Mohd Jani. 2009. "Fenomena Pulau Haba Bandar Dan Isu Alam Sekitar Di Bandaraya Kuala Lumpur The Urban Heat Island Phenomenon and the Environmental Issues of Kuala Lumpur City." *Malaysian Journal of Society and Space* 5 (3): 57–67. <http://www.ukm.edu.my/geografia/images/upload/5.2009-3-shahruddin-melayu.pdf>.
- Ahmad, Shaharuddin, Noorazuan Hashim, Yaakob Mohd Jani, Kadaruddin Aiyub, and Muhamad Fahmi Mahmud. 2010. "The Effects of Different Land Uses on the Temperature Distribution in Urban Areas." In *SEAGA 2010-Online Proceedings*, 1–18. Hanoi. <http://seaga.xtreemhost.com/seaga2010/CS4B-Shah.pdf>.
- Ahmed, Adeb Qaid, Dilshan Remaz Ossen, Elmira Jamei, Norhashima Abd Manaf, Ismail Said, and Mohd Hamdan Ahmad. 2015. "Urban Surface Temperature Behaviour and Heat Island Effect in a Tropical Planned City." *Theoretical and Applied Climatology* 119 (3-4). Springer Vienna: 493–514. doi:10.1007/s00704-014-1122-2.
- Anderson, By James R, Ernest E. Hardy, John T. Roach, Richard E. Witmer, James Richard Anderson, Ernest E. Hardy, John T. Roach, Richard E. Witmer, and Dallas L Peck. 1976. *A Land Use And Land Cover Classification System For Use With Remote Sensor Data. U.S. Geological Survey Professional Paper 964. USGS Professional Paper 964*. Vol. 2001. Washington, USA. <http://landcover.usgs.gov/pdf/anderson.pdf>.
- ArcGIS. 2015. "ArcGIS Software." *ESRI*. <https://www.arcgis.com/>.
- Arnfield, A J. 1982. "An Approach to the Estimation of the Surface Radiative Properties and Radiation Budgets of Cities (Columbus, Ohio)." *Physical Geography* 3 (2). The Ohio State Univ., USA.: 97–122. <http://www.scopus.com/inward/record.url?eid=2-s2.0-0020391191&partnerID=40&md5=485b790d51afe6f7aa48a674a01b0d97>

- Arnfield, A John, and C S B Grimmond. 1998. "An Urban Canyon Energy Budget Model and Its Application to Urban Storage Heat Flux Modeling." *Energy and Buildings* 27 (1): 61–68. doi:http://dx.doi.org/10.1016/S0378-7788(97)00026-1.
- Arnfield, a. John. 2003. "Two Decades of Urban Climate Research: A Review of Turbulence, Exchanges of Energy and Water, and the Urban Heat Island." *Int. J. Climatol.* 23 (1). : 1–26. doi:10.1002/joc.859.
- Ashfold, M J, J A Pyle, A D Robinson, E Meneguz, M S M Nadzir, S M Phang, A A Samah, et al. 2015. "Rapid Transport of East Asian Pollution to the Deep Tropics." *Atmos. Chem. Phys.* 15 (6). Copernicus Publications: 3565–73. doi:10.5194/acp-15-3565-2015.
- Ashtiani, Arya, Parham a. Mirzaei, and Fariborz Haghghat. 2014. "Indoor Thermal Condition in Urban Heat Island: Comparison of the Artificial Neural Network and Regression Methods Prediction." *Energy and Buildings* 76 (June). Elsevier B.V.: 597–604. doi:10.1016/j.enbuild.2014.03.018.
- Atkinson, B. W. 2003. "Numerical Modelling of Urban Heat-Island Intensity." *Boundary-Layer Meteorology* 109 (3): 285–310. doi:10.1023/A:1025820326672.
- Awang, M B, a B Jaafar, a M Abdullah, M B Ismail, M N Hassan, R Abdullah, S Johan, and H Noor. 2000. "Air Quality in Malaysia: Impacts, Management Issues and Future Challenges." *Respirology (Carlton, Vic.)* 5 (2): 183–96. doi:DOI: 10.1046/j.1440-1843.2000.00248.x.
- Ayanlade, Ayansina, and O O Jegede. 2015. "Evaluation of the Intensity of the Daytime Surface Urban Heat Island: How Can Remote Sensing Help?" *International Journal of Image and Data Fusion* 6 (4). Taylor & Francis: 348–65. doi:10.1080/19479832.2014.985618.
- Aziz, Noreen Noor Abd, Wan Haslin Aziah Wan Hassan, and Nur Adilah Saud. 2012. "The Effects of Urbanization towards Social and Cultural Changes among Malaysian Settlers in the Federal Land Development Schemes (FELDA), Johor Darul Takzim." *Procedia - Social and Behavioral Sciences* 68 (December): 910–20. doi:http://dx.doi.org/10.1016/j.sbspro.2012.12.276.
- Azmi, Siti Zawiyah, Mohd Talib Latif, Aida Shafawati Ismail, Liew Juneng, and Abdul Aziz Jemain. 2010. "Trend and Status of Air Quality at Three Different Monitoring Stations in the Klang Valley, Malaysia." *Air Quality, Atmosphere, & Health* 3 (1). Dordrecht: Springer Netherlands: 53–64. doi:10.1007/s11869-009-0051-1.
- Balchin, W G V, and Norman Pye. 1947. "A Micro-Climatological Investigation of Bath and the Surrounding District." *Quarterly Journal of the Royal Meteorological Society* 73 (317-318). John Wiley & Sons, Ltd: 297–323. doi:10.1002/qj.49707331706.

- Barlow, J. F., C. H. Halios, S. E. Lane, and C. R. Wood. 2015. "Observations of Urban Boundary Layer Structure during a Strong Urban Heat Island Event." *Environmental Fluid Mechanics* 15 (2). Springer Netherlands: 373–98. doi:10.1007/s10652-014-9335-6.
- Barlow, Janet F. 2014. "Progress in Observing and Modelling the Urban Boundary Layer." *Urban Climate* 10, Part 2 (December). Elsevier Ltd: 216–40. doi:http://dx.doi.org/10.1016/j.uclim.2014.03.011.
- Bellamy, Edward. 1888. *Looking Backward: 2000–1887*. United States of America: Houghton Mifflin. <http://www.sacred-texts.com/utopia/lb/index.htm>.
- Bigon, Liora. 2012. "'Garden City' in the Tropics? French Dakar in Comparative Perspective." *Journal of Historical Geography* 38 (1). Elsevier Ltd: 35–44. doi:10.1016/j.jhg.2011.07.005.
- Bohnenstengel, S I, S Evans, P A Clark, and S E Belcher. 2011. "Simulations of the London Urban Heat Island." *Quarterly Journal of the Royal Meteorological Society* 137 (659). John Wiley & Sons, Ltd.: 1625–40. doi:10.1002/qj.855.
- Bowler, Diana E., Lisette Buyung-Ali, Teri M. Knight, and Andrew S. Pullin. 2010. "Urban Greening to Cool Towns and Cities: A Systematic Review of the Empirical Evidence." *Landscape and Urban Planning* 97 (3): 147–55. doi:10.1016/j.landurbplan.2010.05.006.
- Brown, Michael J, and Michael D Williams. 1998. "An Urban Canopy Parameterization for Mesoscale Meteorological Models." In *AMS 2nd Urban Environment Conference*, 10A.1–10A.5. Albuquerque, New Mexico, USA: American Meteorological Society. <http://library.lanl.gov/cgi-bin/getfile?00418760.pdf>.
- Bunnell, Tim. 2002. "Multimedia Utopia? A Geographical Critique of High-Tech Development in Malaysia's Multimedia Super Corridor." *Antipode* 34 (2): 265–95. doi:10.1111/1467-8330.00238.
- Cao, Meichun, and Zhaohui Lin. 2014. "Impact of Urban Surface Roughness Length Parameterization Scheme on Urban Atmospheric Environment Simulation." *Journal of Applied Mathematics* 2014 (ID 267683): 1–14. doi:10.1155/2014/267683.
- Caruso, Geoffrey, Jean Cavailhès, Dominique Peeters, Isabelle Thomas, Pierre Frankhauser, and Gilles Vuidel. 2015. "Greener and Larger Neighbourhoods Make Cities More Sustainable! A 2D Urban Economics Perspective." *Computers, Environment and Urban Systems* 54 (November): 82–94. doi:http://dx.doi.org/10.1016/j.compenvurbsys.2015.06.002.
- Chang, Chi-Ru, and Ming-Huang Li. 2014. "Effects of Urban Parks on the Local Urban Thermal Environment." *Urban Forestry & Urban Greening* 13 (4): 672–81. doi:http://dx.doi.org/10.1016/j.ufug.2014.08.001.
- Chen, Fei, and Jimy Dudhia. 2001. "Coupling an Advanced Land Surface–

Hydrology Model with the Penn State–NCAR MM5 Modeling System. Part I: Model Implementation and Sensitivity.” *Monthly Weather Review* 129 (4): 569–85. doi:10.1175/1520-0493(2001)129<0569:CAALSH>2.0.CO;2.

- Chen, Fei, Zavisă Janjić, and Kenneth Mitchell. 1997. “Impact of Atmospheric Surface-Layer Parameterizations in the New Land-Surface Scheme of the NCEP Mesoscale Eta Model.” *Boundary-Layer Meteorology* 85 (3). Kluwer Academic Publishers: 391–421. doi:10.1023/A:1000531001463.
- Chen, Fei, H Kusaka, M Tewari, J W Bao, and H Hirakuchi. 2004. “Utilizing the Coupled WRF/LSM/Urban Modeling System with Detailed Urban Classification to Simulate the Urban Heat Island Phenomena over the Greater Houston Area.” In *Fifth Conference on Urban Environment*, 9.11. https://ams.confex.com/ams/AFAPURBBIO/techprogram/paper_79765.htm.
- Chen, Fei, Hiroyuki Kusaka, Robert Bornstein, Jason Ching, C. S. B. Grimmond, Susanne Grossman-Clarke, Thomas Loridan, et al. 2011. “The Integrated WRF/urban Modelling System: Development, Evaluation, and Applications to Urban Environmental Problems.” *International Journal of Climatology* 31 (2): 273–88. doi:10.1002/joc.2158.
- Chen, Fei, Kenneth Mitchell, John Schaake, Yongkang Xue, Hua-Lu Pan, Victor Koren, Qing Yun Duan, Michael Ek, and Alan Betts. 1996. “Modeling of Land Surface Evaporation by Four Schemes and Comparison with FIFE Observations.” *Journal of Geophysical Research: Atmospheres* 101 (D3): 7251–68. doi:10.1029/95JD02165.
- Chen, Feng, Xuchao Yang, and Weiping Zhu. 2014. “WRF Simulations of Urban Heat Island under Hot-Weather Synoptic Conditions: The Case Study of Hangzhou City, China.” *Atmospheric Research* 138 (March). Elsevier B.V.: 364–77. doi:<http://dx.doi.org/10.1016/j.atmosres.2013.12.005>.
- Chen, Liang, and Oliver W. Frauenfeld. 2015. “Impacts of Urbanization on Future Climate in China.” *Climate Dynamics*. Springer Berlin Heidelberg, 1–13. doi:10.1007/s00382-015-2840-6.
- Chen, Y, W M Jiang, N Zhang, X F He, and R W Zhou. 2009. “Numerical Simulation of the Anthropogenic Heat Effect on Urban Boundary Layer Structure.” *Theoretical and Applied Climatology* 97 (1-2). Springer: 123–34. doi:10.1007/s00704-008-0054-0.
- Chin, Ho Siong. 2006. “Putrajaya – Administrative Centre of Malaysia - Planning Concept and Implementation-.” In *Sustainable Urban Development and Governance Conference at SungKyunKwan University Seoul*, 1–20. Seoul, Korea. http://eprints.utm.my/6622/1/HoChinSiong2006_Putrajaya-AdministrativeCentreOfMalaysia.pdf.
- Chng, Loi Kok, Ahmad Makmom Abdullah, Wan Nor Azmin Sulaiman, and Mohammad Firuz Ramli. 2010. “The Effects of Improved Land Use on

the Meteorological Modeling in Klang Valley Region Malaysia.” *EnvironmentAsia* 3 (special issue): 117–23. <http://www.tshe.org/ea/pdf/vol3s p117-123.pdf>.

- Choo, Chi Seck, and M Taylor. 1986. “Business Organizations, Labour Demand and Industrialization in Malaysia.” In *Industrialization and Labour Force Processes: A Case Study of Peninsular Malaysia*, edited by T. G. McGee, 141–77. The Research School of Pacific Studies, Australian National University.
- Chou, Shih-hung. 2011. “An Example of Vertical Resolution Impact on WRF-Var Analysis.” *Electronic Journal of Operational Meteorology*, no. May: EJ05. <http://www.nwas.org/ej/pdf/2011-EJ5.pdf>.
- Chow, Winston T L, and Matthias Roth. 2006. “Temporal Dynamics of the Urban Heat Island of Singapore.” *International Journal of Climatology* 2260: 2243–60. doi:10.1002/joc.1364.
- Chu, Peter C. 2003. “Hydrostatic Correction for Sigma Coordinate Ocean Models.” *Journal of Geophysical Research* 108 (C6): 3206. doi:10.1029/2002JC001668.
- Cox, R, B L Bauer, and T Smith. 1998. “A Mesoscale Model Intercomparison.” *Bulletin of the American Meteorological Society* 79 (2): 265–83. doi:10.1175/1520-0477(1998)079<0265:AMMI>2.0.CO;2.
- Davis, Kingsley. 1955. “The Origin and Growth of Urbanization in the World.” *American Journal of Sociology*. doi:10.1086/221602.
- Dewan Bandaraya Kuala Lumpur. 2000. “Kuala Lumpur Structure Plan 2020.” *Land Use and Development Strategy*. <http://www.dbkl.gov.my/pskl2020/english/index.htm>.
- Dodman, D. 2009. “Blaming Cities for Climate Change? An Analysis of Urban Greenhouse Gas Emissions Inventories.” *Environment and Urbanization* 21 (1): 185–201. doi:10.1177/0956247809103016.
- DOE. 2013. “Hourly Surface Observational Data.” *Malaysian Department of Environment*. <http://www.doe.gov.my/>.
- Dudhia, Jimy. 1989. “Numerical Study of Convection Observed during the Winter Monsoon Experiment Using a Mesoscale Two-Dimensional Model.” *Journal of the Atmospheric Sciences* 46 (20). American Meteorological Society: 3077–3107. doi:10.1175/1520-0469(1989)046%253C3077:NSOCOD%253E2.0.CO;2.
- . 2011. *WRF Modeling System Overview*. NCAR & UCAR. http://www2.mmm.ucar.edu/wrf/users/tutorial/201107/WRF_Overview_Dudhia.ppt.pdf.
- Dudhia, Jimy, Song-You Hong, and Kyo-Sun Lim. 2008. “A New Method for Representing Mixed-Phase Particle Fall Speeds in Bulk Microphysics Parameterizations.” *Journal of the Meteorological Society of Japan* 86A: 33–44. doi:10.2151/jmsj.86A.33.

- Ek, M. B. 2003. "Implementation of Noah Land Surface Model Advances in the National Centers for Environmental Prediction Operational Mesoscale Eta Model." *Journal of Geophysical Research* 108 (D22): 8851. doi:10.1029/2002JD003296.
- Elgin, Ceyhun, and Cem Oyvat. 2013. "Lurking in the Cities: Urbanization and the Informal Economy." *Structural Change and Economic Dynamics* 27 (December): 36–47. doi:http://dx.doi.org/10.1016/j.strueco.2013.06.003.
- Elsayed, Ilham. 2012a. *Effects of Urbanization on the Urban Heat Island of Kuala Lumpur City: UHI As A Global Issue Kl & Urbanization Research Method Data & Findings Analysis & Synthesis Conclusion*. LAP LAMBERT Academic Publishing.
- . 2012b. *Effects of Urbanization on the Urban Heat Island of Kuala Lumpur City*. Saarbrücken, Germany: LAP LAMBERT Academic Publishing. <https://www.lap-publishing.com/catalog/details//store/gb/book/978-3-8484-8039-5/effects-of-urbanization-on-the-urban-heat-island-of-kuala-lumpur-city>.
- Elsayed, Ilham S.M. 2012. "Mitigation of the Urban Heat Island of the City of Kuala Lumpur, Malaysia." *Middle-East Journal of Scientific Research* 11 (11): 1602–13. doi:10.5829/idosi.mejsr.2012.11.11.1590.
- Emmanuel, Rohinton, and Eduardo Krüger. 2012. "Urban Heat Island and Its Impact on Climate Change Resilience in a Shrinking City: The Case of Glasgow, UK." *Building and Environment* 53 (July). Elsevier Ltd: 137–49. doi:10.1016/j.buildenv.2012.01.020.
- Enete, I. C, M. E Awuh, and S Amawa. 2014. "Assessment of Health Related Impacts of Urban Heat Island (UHI) in Douala Metropolis, Cameroon." *International Journal of Environmental Protection and Policy* 2 (1): 35–40. doi:10.11648/j.ijepp.20140201.15.
- EPA. 2009. "Reducing Urban Heat Islands : Compendium of Strategies - Green Roofs." Edited by and Barry Zalph, Ryan Bell, Robert Berghage, Hitesh Doshi, Robert Goo, David Hitchcock, Megan Lewis, Tom Liptan, Karen Liu, Greg McPherson, Dave Nowak, Steven Peck, Katrin Scholz-Barth, Jeff Sonne, Benjamin Taube, Linda Velazquez, Kathy Wolf, Jim Yarbrough. *Environmental Protection Agency*. <http://www.epa.gov/heatisland/mitigation/greenroofs.htm>.
- Feng, Jin-Ming, Yong-Li Wang, Zhu-Guo Ma, and Yong-He Liu. 2012. "Simulating the Regional Impacts of Urbanization and Anthropogenic Heat Release on Climate across China." *Journal of Climate* 25 (20). American Meteorological Society: 7187–7203. doi:10.1175/JCLI-D-11-00333.1.
- Fire and Disaster Management Agency of Japan, 2011. "Fire and Disaster Management Agency of Japan, 2011."
- Folland, C K, T R Karl, J R Christy, R A Clarke, G V Gruza, J Jouzel, M E Mann, J Oerlemans, M J Salinger, and S W Wang. 2001. *Climate Change 2001 IPCC Third Assessment Report: Observed Climate Variability and*

Change. http://www.grida.no/climate/ipcc_tar/wg1/pdf/tar-02.pdf.

- Fujibe, Fumiaki. 2009. "Detection of Urban Warming in Recent Temperature Trends in Japan." *International Journal of Climatology* 29 (11): 1811–22. doi:10.1002/joc.1822.
- Gaffin, S R, C Rosenzweig, R Khanbilvardi, L Parshall, S Mahani, H Glickman, R Goldberg, R Blake, R B Slosberg, and D Hillel. 2008. "Variations in New York City's Urban Heat Island Strength over Time and Space." *Theoretical and Applied Climatology* 94 (1-2). Springer-Verlag: 1–11. doi:10.1007/s00704-007-0368-3.
- Gambero, Daniele. 2013. *Greater KL / Klang Valley Conurbation Poised for a Booming Long Lasting Growth*. https://www.academia.edu/7922760/Greater_KL_and_Klang_Valley_a_conurbation_poised_for_a_booming_growth.
- Gee, Terry Mc. 2011. "The Urbanization Transition in Malaysia in the Twenty-First Century." *Akademika* 81 (2): 109–21. [http://www.ukm.my/penerbit/akademika/ACROBATAKADEMIKA81-2/81\(2\)Chap11-locked.pdf](http://www.ukm.my/penerbit/akademika/ACROBATAKADEMIKA81-2/81(2)Chap11-locked.pdf).
- Geiger, Rudolf. 1965. "The Climate near the Ground. Translation of the 4th German Edition." *Harvard University Press, Cambridge*, 611pp 306: 375–99.
- Giannaros, Theodore M, Dimitrios Melas, Ioannis A Daglis, Iphigenia Keramitsoglou, and Konstantinos Kourtidis. 2013. "Numerical Study of the Urban Heat Island over Athens (Greece) with the WRF Model." *Atmospheric Environment* 73 (0): 103–11. doi:10.1016/j.atmosenv.2013.02.055.
- Gloyne, R W, and Rudolf Geiger. 1967. "The Climate near the Ground by Rudolf Geiger." *Science Progress (1933-)* 55 (217). Science Reviews 2000 Ltd.: 141–43 CR – Copyright 1967 Science Reviews. doi:10.2307/43419625.
- Goto, K, K Yabe, and N Araki. 2004. "Estimation of Maximum Demand Sensitivity to the Temperature for Long-Term Power Demand Forecast." In *Technical Meeting of Power and Energy Division*, 13–21. Japan: The Institute of Electrical Engineers of Japan.
- Grimmond, C S B, and T R Oke. 1999a. "Evapotranspiration Rates in Urban Areas." In *Impacts of Urban Growth on Surface Water and Groundwater Quality*, 235–43.
- Grimmond, C. S B. 2006. "Progress in Measuring and Observing the Urban Atmosphere." *Theoretical and Applied Climatology*. doi:10.1007/s00704-005-0140-5.
- Grimmond, C. S. B., and T. R. Oke. 1999b. "Heat Storage in Urban Areas : Local-Scale Observations and Evaluation of a Simple Model." *Journal of Applied Meteorology* 38 (7): 922–40. doi:10.1175/1520-0450(1999)038<0922:HSIUAL>2.0.CO;2.

- Grimmond, Sue U E. 2007. "Urbanization and Global Environmental Change: Local Effects of Urban Warming." *The Geographical Journal* 173 (1): 83–88. doi:10.1111/j.1475-4959.2007.232_3.x.
- Grossman-Clarke, Susanne, Yubao Liu, Joseph a. Zehnder, and Jerome D. Fast. 2008. "Simulations of the Urban Planetary Boundary Layer in an Arid Metropolitan Area." *Journal of Applied Meteorology and Climatology* 47 (3): 752–68. doi:10.1175/2007JAMC1647.1.
- Gsella, A., A. de Meij, A. Kerschbaumer, E. Reimer, P. Thunis, and C. Cuvelier. 2014. "Evaluation of MM5, WRF and TRAMPER Meteorology over the Complex Terrain of the Po Valley, Italy." *Atmospheric Environment* 89 (June). Elsevier Ltd: 797–806. doi:http://dx.doi.org/10.1016/j.atmosenv.2014.03.019.
- Gullick, John Michael. 2003. *A History of Negri Sembilan*. Malaysian Branch of the Royal Asiatic Society.
- Haaland, Christine, and Cecil Konijnendijk van den Bosch. 2015. "Challenges and Strategies for Urban Green-Space Planning in Cities Undergoing Densification: A Review." *Urban Forestry & Urban Greening* 14 (4): 760–71. doi:http://dx.doi.org/10.1016/j.ufug.2015.07.009.
- Hadi, Abdul Samad, Shaharudin Idris, Abdul Hadi harman Shah, and Ahmad Fariz Mohamed. 2011. "Critical Urbanisation Transitions in Malaysia: The Challenge of Rising Bernam to Linggi Basin Extended Mega Urban Region." *Akademika* 81 (2): 11–21. http://www.ukm.my/penerbit/akademika/ACROBATAKADEMIKA81-2/81(2)Chap2-locked.pdf.
- Hamdi, Rafiq, Piet Termonia, and Pierre Baguis. 2011. "Effects of Urbanization and Climate Change on Surface Runoff of the Brussels Capital Region: A Case Study Using an Urban Soil–vegetation–atmosphere-Transfer Model." *International Journal of Climatology* 31 (13). John Wiley & Sons, Ltd.: 1959–74. doi:10.1002/joc.2207.
- Han, Lijian, Weiqi Zhou, Weifeng Li, and Li Li. 2014. "Impact of Urbanization Level on Urban Air Quality: A Case of Fine Particles (PM_{2.5}) in Chinese Cities." *Environmental Pollution* 194 (November): 163–70. doi:http://dx.doi.org/10.1016/j.envpol.2014.07.022.
- Hashim, Omairi Bin, Fadlun Bin Mak Ujud, Shamsul Bahrin Bin Rahmat, Akashah Bin Makjizat, Puan Norzita Binti Razak, Ab Rahim Bin Md Junoh, Jamal Bin Nasir Ali, et al. 2012. *Putrajaya Low Carbon Green City Initiatives Report*. Putrajaya, Malaysia. http://www.ppj.gov.my/cpnavigation/general/Putrajaya_LowCarbonGreenCity_Initiatives_December_2012.pdf.
- Hashim, Jamal Hisham, Mukundan Sugunan Pillay, Zailina Hashim, Shamsul Bahari Shamsudin, Kazal Sinha, Zaman Huri Zulkifli, Khew Swee Lian, et al. 2004. *A Study of Health Impact and Risk Assessment of Urban Air Pollution in the Klang Valley, Malaysia*. http://www.wpro.who.int/environmental_health/documents/docs/UKM_R

eport.pdf.

- Hathway, E.A., and S. Sharples. 2012. "The Interaction of Rivers and Urban Form in Mitigating the Urban Heat Island Effect: A UK Case Study." *Building and Environment* 58 (December): 14–22. doi:10.1016/j.buildenv.2012.06.013.
- Hebbert, Michael. 2014. "Climatology for City Planning in Historical Perspective." *Urban Climate* 10, Part 2 (December): 204–15. doi:http://dx.doi.org/10.1016/j.uclim.2014.07.001.
- Heilig, Gerhard K, and United Nations. 2012. *World Urbanization Prospects: The 2011 Revision. United Nations, Department of Economic and Social Affairs (DESA), Population Division, Population Estimates and Projections Section, New York.* http://esa.un.org/unpd/wpp/ppt/CSIS/WUP_2011_CSIS_4.pdf.
- Heisler, Gordon M, and Anthony J Brazel. 2010. "The Urban Physical Environment: Temperature and Urban Heat Islands." In *Urban Ecosystem Ecology*, ed, 13210:29–56. American Society of Agronomy, Crop Science Society of America, Soil Science Society of America. doi:10.2134/agronmonogr55.c2.
- Henderson, J Vernon, and Anthony J Venables. 2009. "The Dynamics of City Formation." *Review of Economic Dynamics* 12 (2): 233–54. doi:http://dx.doi.org/10.1016/j.red.2008.06.003.
- HEW, Cheng Sim. 2003. "The Impact of Urbanization on Family Structure: The Experience of Sarawak, Malaysia." *Sojourn: Journal of Social Issues in Southeast Asia* 18 (1). Institute of Southeast Asian Studies (ISEAS): 89–109. doi:10.2307/41308003.
- Hill, R D. 1995. "THE IMPACT OF URBANIZATION ON RURAL-URBAN LINKAGES IN THAILAND AND MALAYSIA." *Asian Geographer* 14 (1). Routledge: 28–44. doi:10.1080/10225706.1995.9683998.
- Hirschman, Charles. 1976. "Recent Urbanization Trends in Peninsular Malaysia." *Demography* 13 (4). Springer-Verlag: 445–61. doi:10.2307/2060502.
- Hong, Seungbum, Venkat Lakshmi, Eric E. Small, Fei Chen, Mukul Tewari, and Kevin W. Manning. 2009. "Effects of Vegetation and Soil Moisture on the Simulated Land Surface Processes from the Coupled WRF/Noah Model." *Journal of Geophysical Research* 114 (D18): D18118. doi:10.1029/2008JD011249.
- Hong, Song You, Yign Noh, and Jimy Dudhia. 2006. "A New Vertical Diffusion Package with an Explicit Treatment of." *MONTHLY WEATHER REVIEW* 134 (9): 2318–41. doi:http://dx.doi.org/10.1175/MWR3199.1.
- Hong, Song-You, Jimy Dudhia, and Shu-Hua Chen. 2004. "A Revised Approach to Ice Microphysical Processes for the Bulk Parameterization of Clouds and Precipitation." *Monthly Weather Review* 132 (1): 103–20. doi:10.1175/1520-0493(2004)132<0103:ARATIM>2.0.CO;2.

- Howard, Ebenezer. 1898. *Garden Cities of To-Morrow*. Edited by F. J. Osborn. *An Introductory Essay by Lewis Mumford*. 2nd ed. London, United Kingdom: Swan Sonnenschein & Co. <http://urbanplanning.library.cornell.edu/DOCS/howard.htm>.
- Howard, Luke. 1818a. *The Climate of London: Deduced from Meteorological Observations, Made at Different Places in the Neighbourhood of the Metropolis*. Vol. 1. London, UK: W. Phillips, sold also by J. and A. Arch. http://www.urban-climate.org/documents/LukeHoward_Climate-of-London-V1.pdf.
- . 1818b. *The Climate of London*. Vol. 1. London: W. Phillips, sold also by J. and A. Arch. http://urban-climate.com/wp3/wp-content/uploads/2011/04/LukeHoward_Climate-of-London-V1.pdf.
- . 1820. *The Climate of London: Deduced from Meteorological Observations Made in the Metropolis and at Various Places Around It, Volume 2*. 2nd ed. London: Nabu Press (Reproduced March 4, 2010).
- Hu, Xiao-Ming, John W. Nielsen-Gammon, and Fuqing Zhang. 2010. “Evaluation of Three Planetary Boundary Layer Schemes in the WRF Model.” *Journal of Applied Meteorology and Climatology* 49 (9). American Meteorological Society: 1831–44. doi:10.1175/2010JAMC2432.1.
- Hua, L J, Z G Ma, and W D Guo. 2008. “The Impact of Urbanization on Air Temperature across China.” *Theoretical and Applied Climatology* 93 (3–4). Springer-Verlag: 179–94. doi:10.1007/s00704-007-0339-8.
- Huang, Jianping, Chenhong Zhou, Xuhui Lee, Yunxuan Bao, Xiaoyan Zhao, Jimmy Fung, Andreas Richter, Xiong Liu, and Yiqi Zheng. 2013. “The Effects of Rapid Urbanization on the Levels in Tropospheric Nitrogen Dioxide and Ozone over East China.” *Atmospheric Environment* 77 (October): 558–67. doi:<http://dx.doi.org/10.1016/j.atmosenv.2013.05.030>.
- Hushak, Leroy J. 1975. “The Urban Demand for Urban-Rural Fringe Land.” *Land Economics* 51 (2). University of Wisconsin Press: 112–23 CR – Copyright © 1975 The Board of Re. doi:10.2307/3145580.
- Ibrahim, Illyani, and Azizan Abu Samah. 2011. “Preliminary Study of Urban Heat Island: Measurement of Ambient Temperature and Relative Humidity in Relation to Landcover in Kuala Lumpur.” In *2011 19th International Conference on Geoinformatics*, 1–5. Shanghai: IEEE. doi:10.1109/GeoInformatics.2011.5981068.
- IPCC. 2007. *Climate Change 2007: Synthesis Report - An Assessment of the Intergovernmental Panel on Climate Change*. Edited by R K Pachauri and A Reisinger. IPCC. Vol. 446. Synthesis Report. Valencia, Spain: IPCC. <http://library.wur.nl/WebQuery/wurpubs/396456>.
- . 2013. *Climate Change 2013: The Physical Science Basis. Contribution of Working Group I to the Fifth Assessment Report of the Intergovernmental Panel on Climate Change - Summary for Policymakers*. Edited by Stocker T.F., D. Qin, G.-K. Plattner, M. Tignor,

S.K. Allen, J. Boschung, A. Nauels, Y. Xia, V. Bex, and P.M. Midgley. Cambridge, United Kingdom and New York, NY, USA.: Cambridge University Press.
http://www.climatechange2013.org/images/report/WG1AR5_SPM_FINAL.pdf.

- Jamhari, Anas Ahmad, Mazrura Sahani, Mohd Talib Latif, Kok Meng Chan, Hock Seng Tan, Md Firoz Khan, and Norhayati Mohd Tahir. 2014. "Concentration and Source Identification of Polycyclic Aromatic Hydrocarbons (PAHs) in PM10 of Urban, Industrial and Semi-Urban Areas in Malaysia." *Atmospheric Environment* 86 (April): 16–27. doi:<http://dx.doi.org/10.1016/j.atmosenv.2013.12.019>.
- Jauregui, E. 1990. "Influence of a Large Urban Park on Temperature and Convective Precipitation in a Tropical City." *Energy and Buildings* 15 (3–4): 457–63. doi:[http://dx.doi.org/10.1016/0378-7788\(90\)90021-A](http://dx.doi.org/10.1016/0378-7788(90)90021-A).
- Jenkins, Amber. 2009. "The Ups and Downs of Global Warming." *NASA Global Climate Change: Facts*. <http://climate.nasa.gov/news/175/>.
- Jiang, Lei, Lixin Lu, Lingmei Jiang, Yuanyuan Qi, and Aqiang Yang. 2014. "Impact of a Detailed Urban Parameterization on Modeling the Urban Heat Island in Beijing Using TEB-RAMS." *Advances in Meteorology* 2014 (ID-602528): 1–11. doi:10.1155/2014/602528.
- Jiang, Xiaoyan, Christine Wiedinmyer, Fei Chen, Z.-L. Zong-Liang Yang, and Jeff C.-F. Chun-Fung Lo. 2008. "Predicted Impacts of Climate and Land Use Change on Surface Ozone in the Houston, Texas, Area." *Journal of Geophysical Research* 113 (D20): D20312. doi:10.1029/2008JD009820.
- Jiang, Yitong, Peng Fu, and Qihao Weng. 2015. "Assessing the Impacts of Urbanization-Associated Land Use/Cover Change on Land Surface Temperature and Surface Moisture: A Case Study in the Midwestern United States." *Remote Sensing* 7 (4). Multidisciplinary Digital Publishing Institute: 4880–98. doi:10.3390/rs70404880.
- Jin, Menglin, Robert E Dickinson, and Da Zhang. 2005. "The Footprint of Urban Areas on Global Climate as Characterized by MODIS." *Journal of Climate* 18 (10). American Meteorological Society: 1551–65. doi:10.1175/JCLI3334.1.
- Johnson, W B, F L Ludwig, W F Dabberdt, and R J Allen. 1973. "An Urban Diffusion Simulation Model for Carbon Monoxide." *Journal of the Air Pollution Control Association* 23 (6). Atmospheric Sci. Lab., Stanford Res. Inst., Menlo Park, Calif. 94025, United States: 490–98. <http://www.scopus.com/inward/record.url?eid=2-s2.0-0015637637&partnerID=40&md5=6c0d419fd7caa661f81967da97c70433>
- Jones, P. D., D. H. Lister, and Q. Li. 2008. "Urbanization Effects in Large-Scale Temperature Records, with an Emphasis on China." *Journal of Geophysical Research* 113 (D16): D16122. doi:10.1029/2008JD009916.
- Juneng, Liew, Mohd Talib Latif, and Fredolin Tangang. 2011. "Factors

- Influencing the Variations of PM10 Aerosol Dust in Klang Valley, Malaysia during the Summer.” *Atmospheric Environment* 45 (26). Elsevier Ltd: 4370–78. doi:10.1016/j.atmosenv.2011.05.045.
- Jusuf, Steve Kardinal, and Wong Nyuk Hien. 2009. “Study on Air Temperature Distribution and Its Correlation with Sky View Factor in a Green Singapore Estate.” In *The Seventh International Conference on Urban Climate*.
- Kain, John S. 2004. “The Kain–Fritsch Convective Parameterization: An Update.” *Journal of Applied Meteorology* 41 (1): 170–81. doi:10.1175/1520-0450(2004)043<0170:TKCPAU>2.0.CO;2.
- Kalnay, Eugenia, and Ming Cai. 2003. “Impact of Urbanization and Land-Use Change on Climate.” *Nature* 423 (6939): 528–31. doi:10.0138/nature01649.
- Karl, Thomas R, Richard W Knight, and Neil Plummer. 1995. “Trends in High-Frequency Climate Variability in the Twentieth Century.” *Nature* 377 (6546): 217–20. <http://dx.doi.org/10.1038/377217a0>.
- Karl, Thomas R., Henry F. Diaz, and George Kukla. 1988. “Urbanization: Its Detection and Effect in the United States Climate Record.pdf.” *Journal of Climate* 1: 1099–1123. doi:[http://dx.doi.org/10.1175/1520-0442\(1988\)001<1099:UIDAEI>2.0.CO;2](http://dx.doi.org/10.1175/1520-0442(1988)001<1099:UIDAEI>2.0.CO;2).
- Kennedy, C, S Pincetl, and P Bunje. 2011. “The Study of Urban Metabolism and Its Applications to Urban Planning and Design.” *Environmental Pollution* 159 (8–9): 1965–73. doi:<http://dx.doi.org/10.1016/j.envpol.2010.10.022>.
- Kennedy, Christopher, John Cuddihy, and Joshua Engel-Yan. 2007. “The Changing Metabolism of Cities.” *Journal of Industrial Ecology* 11 (2): 43–59. doi:10.1162/jie.2007.11107.
- Kennedy, Heather. 2000. *The ESRI Press Dictionary of GIS Terminology*. Edited by Michael Karman and Gary Amdahl. California: ESRI Press, Redlands, California. http://www.watermicro-eclass.net/cms/wp-content/uploads/GIS_TERMINOLOGY.pdf.
- Kho, Lim, and Tay Low. 1998. *Plants of Putrajaya Wetlands*. Putrajaya, Malaysia: Eigenverlag.
- Köhler, Manfred, Marco Schmidt, Friedrich Wilhelm Grimme, Michael Laar, Vera Lúcia de Assunção Paiva, and Sergio Tavares. 2002. “Green Roofs in Temperate Climates and in the Hot-humid Tropics – Far beyond the Aestheticsnull.” *Environmental Management and Health* 13 (4). Emerald: 382–91. doi:10.1108/09566160210439297.
- Kottek, Markus, Jürgen Grieser, Christoph Beck, Bruno Rudolf, and Franz Rubel. 2006. “World Map of the Köppen-Geiger Climate Classification Updated.” *Meteorologische Zeitschrift* 15 (3): 259–63. doi:10.1127/0941-2948/2006/0130.
- Kratzer, Albert. 1956. “The Climate of Cities (Das Stadtklima).” *Air Force*

Cambridge Research Laboratories (Reprinted by IAUC). www.urban-climate.org.

- Kulkarni, MakarandA., Sunil Patil, G V Rama, and P N Sen. 2008. "Wind Speed Prediction Using Statistical Regression and Neural Network." *Journal of Earth System Science* 117 (4). Springer-Verlag: 457–63. doi:10.1007/s12040-008-0045-7.
- Kusaka, H, H Kondo, Y Kikegawa, and F Kimura. 2001. "A Simple Single-Layer Urban Canopy Model for Atmospheric Models: Comparison with Multi Layer and Slab Models." *BoundaryLayer Meteorology* 101 (3). Springer Netherlands: 329–58. doi:10.1023/A:1019207923078.
- Kusaka, Hiroyuki, and Fujio Kimura. 2004. "Coupling a Single-Layer Urban Canopy Model with a Simple Atmospheric Model: Impact on Urban Heat Island Simulation for an Idealized Case." *Journal of the Meteorological Society of Japan* 82 (1): 67–80. doi:10.2151/jmsj.82.67.
- Kuttler, Wilhelm, Stephan Weber, Judith Schonfeld, and Alexandra Hesselschwerdt. 2007. "Urban/rural Atmospheric Water Vapour Pressure Differences and Urban Moisture Excess in Krefeld, Germany." *International Journal of Climatology* 27 (14). John Wiley & Sons, Ltd.: 2005–15. doi:10.1002/joc.1558.
- Lai, Li-Wei, and Wan-Li Cheng. 2009. "Air Quality Influenced by Urban Heat Island Coupled with Synoptic Weather Patterns." *The Science of the Total Environment* 407 (8). Elsevier B.V.: 2724–33. doi:10.1016/j.scitotenv.2008.12.002.
- Landsberg, Helmut. 1973. "The Meteorologically Utopian City." *Bulletin of the American Meteorological Society* 54 (2). American Meteorological Society: 86–89. doi:10.1175/1520-0477(1973)054<0086:TMUC>2.0.CO;2.
- Landsberg, Helmut E. 1981. *The Urban Climate*. 1st ed. International Geophysics. Maryland, College Park, U.S.A: Academic Press. <https://books.google.com.my/books?id=zkkKHIXZGBIC>.
- Laprise, René. 1992. "The Euler Equations of Motion with Hydrostatic Pressure as an Independent Variable." *Monthly Weather Review* 120 (1): 197–207. doi:10.1175/1520-0493(1992)120<0197:TEEOMW>2.0.CO;2.
- Lawrence, Mark G. 2005. "The Relationship between Relative Humidity and the Dewpoint Temperature in Moist Air: A Simple Conversion and Applications." *Bulletin of the American Meteorological Society* 86 (2). American Meteorological Society: 225–33. doi:10.1175/BAMS-86-2-225.
- Legates, David R, and Gregory J McCabe. 1999. "Evaluating the Use of Goodnessoffit Measures in Hydrologic and Hydroclimatic Model Validation." *Water Resources Research* 35 (1): 233–41. doi:10.1029/1998WR900018.
- Li, Dan, Elie Bou-Zeid, Michael Barlage, Fei Chen, and James A Smith. 2013. "Development and Evaluation of a Mosaic Approach in the WRF-Noah

Framework.” *Journal of Geophysical Research* 118 (21): 11918–35. doi:10.1002/2013JD020657.

- Li, Dan, Elie Bou-Zeid, Michael Oppenheimer, and Dan Li and Elie Bou-Zeid and Michael Oppenheimer. 2014. “The Effectiveness of Cool and Green Roofs as Urban Heat Island Mitigation Strategies.” *Environmental Research Letters* 9 (5). IOP Publishing: 55002. doi:10.1088/1748-9326/9/5/055002.
- Li, J, A Mahalov, and P Hyde. 2016. “Impacts of Agricultural Irrigation on Ozone Concentrations in the Central Valley of California and in the Contiguous United States Based on WRF-Chem Simulations.” *Agricultural and Forest Meteorology* 221 (May): 34–49. doi:http://dx.doi.org/10.1016/j.agrformet.2016.02.004.
- Li, Jiawei, Zhiwei Han, and Renjian Zhang. 2011. “Model Study of Atmospheric Particulates during Dust Storm Period in March 2010 over East Asia.” *Atmospheric Environment* 45 (24): 3954–64. doi:http://dx.doi.org/10.1016/j.atmosenv.2011.04.068.
- Li, Xian-Xiang, Tieh-Yong Koh, Dara Entekhabi, Matthias Roth, Jagabandhu Panda, and Leslie K Norford. 2013. “A Multi-Resolution Ensemble Study of a Tropical Urban Environment and Its Interactions with the Background Regional Atmosphere.” *Journal of Geophysical Research: Atmospheres* 118 (17): 9804–18. doi:10.1002/jgrd.50795.
- Li, Xuanli, and Zhaoxia Pu. 2009. “Sensitivity of Numerical Simulations of the Early Rapid Intensification of Hurricane Emily to Cumulus Parameterization Schemes in Different Model Horizontal Resolutions.” *Journal of the Meteorological Society of Japan* 87 (3): 403–21. doi:10.2151/jmsj.87.403.
- Liao, Jingbiao, Tijian Wang, Xuemei Wang, Min Xie, Ziqiang Jiang, Xiaoxian Huang, and Jialei Zhu. 2014. “Impacts of Different Urban Canopy Schemes in WRF/Chem on Regional Climate and Air Quality in Yangtze River Delta, China.” *Atmospheric Research* 145-146 (August). The Authors: 226–43. doi:10.1016/j.atmosres.2014.04.005.
- Liew, Van, M.W, J.G. Arnold, and J.D. Garbrecht. 2003. “Hydrologic Simulation on Agricultural Watersheds: Choosing between Two Models.” *Transactions of the ASAE* 46 (6): 1539–51. doi:10.13031/2013.15643.
- Lin, C, W Chen, S Liu, Y Lius, G Liu, and T Lin. 2008. “Numerical Study of the Impact of Urbanization on the Precipitation over Taiwan.” *Atmospheric Environment* 42 (13): 2934–47. doi:10.1016/j.atmosenv.2007.12.054.
- Lin, Chuan-Yao, Fei Chen, J C Huang, W.-N. W.-C. Chen, Y.-A. Liou, W.-N. W.-C. Chen, and Shaw-C. Liu. 2008. “Urban Heat Island Effect and Its Impact on Boundary Layer Development and Land–sea Circulation over Northern Taiwan.” *Atmospheric Environment* 42 (22): 5635–49. doi:10.1016/j.atmosenv.2008.03.015.
- Liu, Yubao, Fei Chen, Thomas Warner, and Jeffrey Basara. 2006. “Verification

- of a Mesoscale Data-Assimilation and Forecasting System for the Oklahoma City Area during the Joint Urban 2003 Field Project.” *Journal of Applied Meteorology and Climatogoy* 45 (7): 912–29. doi:10.1175/JAM2383.1.
- Liu, Zhifeng, Chunyang He, Yuyu Zhou, and Jianguo Wu. 2014. “How Much of the World’s Land Has Been Urbanized, Really? A Hierarchical Framework for Avoiding Confusion.” *Landscape Ecology* 29 (5). Springer Netherlands: 763–71. doi:10.1007/s10980-014-0034-y.
- Lodhi, M A K, Azman Zainal Abidin, and M Yusof Sulaiman. 1997. “Pollutant Emissions from Fossil Fuel Use in Kuala Lumpur and Environmental Damage.” *Energy Conversion and Management* 38 (3): 213–16. doi:http://dx.doi.org/10.1016/S0196-8904(96)00025-8.
- Lowry, W P. 1977. “Empirical Estimation of Urban Effects on Climate: A Problem Analysis.” *Journal of Applied Meteorology* 16 (2). American Meteorological Society: 129–35. doi:10.1175/1520-0450(1977)016<0129:EEOUEO>2.0.CO;2.
- Lowry, W.P. 1974. “Project METROMEX: Its History, Status, and Future.” *Bulletin of the American Meteorological Society* 55: 87–88.
- Lundy, Christopher C, Robert L Brown, Edward E Adams, Karl W Birkeland, and Michael Lehning. 2001. “A Statistical Validation of the Snowpack Model in a Montana Climate.” *Cold Regions Science and Technology* 33 (2-3): 237–46. doi:10.1016/S0165-232X(01)00038-6.
- Macedo, Joseli. 2011. “Maringá: A British Garden City in the Tropics.” *Cities* 28 (4): 347–59. doi:http://dx.doi.org/10.1016/j.cities.2010.11.003.
- Maimaitiyiming, Matthew, Abduwasit Ghulam, Tashpolat Tiyp, Filiberto Pla, Pedro Latorre-Carmona, Ümüt Halik, Mamat Sawut, and Mario Caetano. 2014. “Effects of Green Space Spatial Pattern on Land Surface Temperature: Implications for Sustainable Urban Planning and Climate Change Adaptation.” *ISPRS Journal of Photogrammetry and Remote Sensing* 89 (March): 59–66. doi:10.1016/j.isprsjprs.2013.12.010.
- Malaysia Department of Statistics. 2010. “Demographic Report.” *Department of Statistics Malaysia*. <https://www.statistics.gov.my/dosm/index.php>.
- Manning, William J. 2011. “Urban Environment: Defining Its Nature and Problems and Developing Strategies to Overcome Obstacles to Sustainability and Quality of Life.” *Environmental Pollution* 159 (8–9): 1963–64. doi:http://dx.doi.org/10.1016/j.envpol.2011.04.002.
- Marais, E A, D J Jacob, K Wecht, C Lerot, L Zhang, K Yu, T P Kurosu, K Chance, and B Sauvage. 2014. “Anthropogenic Emissions in Nigeria and Implications for Atmospheric Ozone Pollution: A View from Space.” *Atmospheric Environment* 99 (0): 32–40. doi:http://dx.doi.org/10.1016/j.atmosenv.2014.09.055.
- Marcotullio, Peter J., Ademola K. Braimoh, and Takashi Onishi. 2008. “The Impact of Urbanization on Soils.” In *Land Use and Soil Resources*, 201–

50. Springer Netherlands.

- Mark, Joshua J. 2014. "Urbanization." *Ancient History*. <http://www.ancient.eu/urbanization/>.
- Martilli, Alberto, Alain Clappier, and Mathias W. W. Rotach. 2002. "An Urban Surface Exchange Parameterisation for Mesoscale Models." *Boundary-Layer Meteorology* 104 (2). Kluwer Academic Publishers: 261–304. doi:10.1023/A:1016099921195.
- Martins, João P A, Rita M Cardoso, Pedro M M Soares, Isabel F Trigo, Margarida Belo-Pereira, Nuno Moreira, and Ricardo Tomé. 2015. "The Summer Diurnal Cycle of Coastal Cloudiness over West Iberia Using Meteosat/SEVIRI and a WRF Regional Climate Model Simulation." *International Journal of Climatology*, August. John Wiley & Sons, Ltd, n/a – n/a. doi:10.1002/joc.4457.
- Masron, Tarmiji, Usman Yaakob, Norizawati Mohd Ayob, and Aimi Shamimi Mokhtar. 2012. "Population and Spatial Distribution of Urbanisation in Peninsular Malaysia 1957-2000." *Geografia: Malaysian Journal of Society and Space* 8 (2). Faculty of Social Sciences and Humanities, UKM, Bangi: 20–29.
- Masson, Valéry. 2000. "A Physically-Based Scheme for the Urban Energy Budget in Atmospheric Models." *Boundary Layer Meteorology* 94 (3). Kluwer Academic Publishers: 357–97. doi:10.1023/A:1002463829265.
- McCarthy, Mark P., Martin J. Best, and Richard A. Betts. 2010. "Climate Change in Cities due to Global Warming and Urban Effects." *Geophysical Research Letters* 37 (9): n/a – n/a. doi:10.1029/2010GL042845.
- McGrath, Matt. 2014. "Global Warming Slowdown 'Could Last Another Decade.'" *BBC News: Science and Environment*, August 21. <http://www.bbc.com/news/science-environment-28870988>.
- Memon, Rizwan Ahmed, Dennis Y C Leung, Liu Chunho, Ahmed Memon Rizwan, Leung Y C Dennis, and Chunho Liu. 2008. "A Review on the Generation, Determination and Mitigation of Urban Heat Island." *Journal Of Environmental Sciences* 20 (1). SCIENCE CHINA PRESS: 120–28. doi:10.1016/S1001-0742(08)60019-4.
- Memon, Rizwan Ahmed, Dennis Y C Leung, and Chun-Ho Liu. 2009. "An Investigation of Urban Heat Island Intensity (UHII) as an Indicator of Urban Heating." *Atmospheric Research* 94 (3). Elsevier B.V.: 491–500. doi:10.1016/j.atmosres.2009.07.006.
- Miao, S., F. Chen, Q. Li, and S. Fan. 2010. "Impacts of Urban Processes and Urbanization on Summer Pre-Cipitation: A Case Study of Heavy Rainfall in Beijing on 1 August 2006." *Journal of Applied Meteorology and Climatology* 50: 806–25. doi:<http://dx.doi.org/10.1175/2010JAMC2513.1>.
- Miao, Shiguang, Fei Chen, Margaret A. LeMone, Mukul Tewari, Qingchun Li, and Yingchun Wang. 2009. "An Observational and Modeling Study of Characteristics of Urban Heat Island and Boundary Layer Structures in

Beijing.” *Journal of Applied Meteorology and Climatology* 48 (3). American Meteorological Society: 484–501. doi:10.1175/2008JAMC1909.1.

- Middle, Isaac, Peta Dzidic, Amma Buckley, Dawn Bennett, Marian Tye, and Roy Jones. 2014. “Integrating Community Gardens into Public Parks: An Innovative Approach for Providing Ecosystem Services in Urban Areas.” *Urban Forestry & Urban Greening* 13 (4): 638–45. doi:10.1016/j.ufug.2014.09.001.
- Mills, G. 2006. “Progress toward Sustainable Settlements: A Role for Urban Climatology.” *Theoretical and Applied Climatology* 84 (1-3). Springer-Verlag: 69–76. doi:10.1007/s00704-005-0145-0.
- Mills, Gerald. 2014. “Urban Climatology: History, Status and Prospects.” *Urban Climate* 10, Part 3 (P3). Elsevier: 479–89. doi:http://dx.doi.org/10.1016/j.uclim.2014.06.004.
- Mirzaei, Parham A, and Fariborz Haghighat. 2010. “Approaches to Study Urban Heat Island – Abilities and Limitations.” *Building and Environment* 45 (10): 2192–2201. doi:10.1016/j.buildenv.2010.04.001.
- Mitchell, Kenneth, Mike Ek, Vince Wong, Dag Lohmann, Victor Koren, John Schaake, Qingyun Duan, et al. 2005. *The Community Noah Land-Surface Model (LSM) - User’s Guide Version 2.7.1*. Boulder, Colorado, USA. http://www.ral.ucar.edu/research/land/technology/lsm/noah/Noah_LSM_USERGUIDE_2.7.1.pdf.
- Mlawer, Eli J, J Taubman, Patrick D Brown, Michael J Iacono, and Shepard A Clough. 1997. “Radiative Transfer for Inhomogeneous Atmospheres: RRTM, a Validated Correlatedk Model for the Longwave.” *Journal of Geophysical Research* 102 (D14): 16663–82. doi:doi:10.1029/97JD00237.
- MMD. 2015. “General Climate of Malaysia.” *Malaysian Meteorological Department*. http://www.met.gov.my/index.php?option=com_content&task=view&id=75&Itemid=1089.
- MMM. 2015. “WRF Users Page.” *National Center for Atmospheric Research*. <http://www2.mmm.ucar.edu/wrf/users/>.
- Montoya, Lorena. 2015. “Modelling Urban Crime through Workforce Size: A Test of the Activity Support Concept.” *Environment and Planning B: Planning and Design* 42 (3): 399–414. doi:10.1068/b120068p.
- Moriasi, D N, J G Arnold, M W Van Liew, R L Bingner, R D Harmel, and T L Veith. 2007. “Model Evaluation Guidelines for Systematic Quantification of Accuracy in Watershed Simulation.” *Transactions of the ASABE* 50 (3): 885–900. <http://swat.tamu.edu/media/1312/moriasimodeleval.pdf>.
- Morris, Kenobi Isima. 2016. “Effect of Vegetation and Waterbody on the Garden City Concept: An Evaluation Study Using a Newly Developed City, Putrajaya, Malaysia.” *Computers, Environment and Urban Systems* 58 (July): 39–51. doi.org/10.1016/j.compenvurbsys.2016.03.005.

- Morris, Kenobi Isima, Andy Chan, Siti Aekbal Salleh, Maggie Chel Gee Ooi, Muhammad Yaasiin Oozeer, and Yousif Abdalla Abakr. 2016. "Numerical Study on the Urbanization of Putrajaya and Its Interaction with the Local Climate, over a Decade." *Urban Climate* 16 (June): 1–24. doi:10.1016/j.uclim.2016.02.001.
- Morris, Kenobi Isima, Siti Aekbal Salleh, Andy Chan, Maggie Chel Gee Ooi, Yousif Abdalla Abakr, Muhammad Yaasiin Oozeer, and Michael Duda. 2015a. "Integrating Weather Research and Forecasting Model, Noah Land Surface Model and Urban Canopy Model for Urban Heat Island Effect Assessment." *British Journal of Environment and Climate Change* 5 (3): 231–53. doi:10.9734/BJECC/2015/14923.
- . 2015b. "Computational Study of Urban Heat Island of Putrajaya, Malaysia." *Sustainable Cities and Society* 19 (May): 359–72. doi:10.1016/j.scs.2015.04.010.
- Moser, Sarah. 2010. "Putrajaya: Malaysia's New Federal Administrative Capital." *Cities* 27 (4). Elsevier Ltd: 285–97. doi:http://dx.doi.org/10.1016/j.cities.2009.11.002.
- Murphy, Allan H. 1995. "The Coefficients of Correlation and Determination as Measures of Performance in Forecast Verification." *Weather and Forecasting* 10 (4). American Meteorological Society: 681–88. doi:10.1175/1520-0434(1995)010<0681:TCOCAD>2.0.CO;2.
- Murphy, Allan H. 1988. "Skill Scores Based on the Mean Square Error and Their Relationships to the Correlation Coefficient." *Monthly Weather Review* 116: 2417–24. doi:http://dx.doi.org/10.1175/1520-0493(1988)116<2417:SSBOTM>2.0.CO;2.
- Myrup, Leonard O. 1969. "A Numerical Model of the Urban Heat Island." *Journal of Applied Meteorology* 8 (6): 908–18. doi:10.1175/1520-0450(1969)008<0908:ANMOTU>2.0.CO;2.
- NCAR. 2015. "NCAR Command Language (NCL)." *UCAR*. doi:10.5065/D6WD3XH5.
- NCEP. 2000. "National Centers for Environmental Prediction/National Weather Service/NOAA/U.S. Department of Commerce. 2000, Updated Daily." *NCEP FNL Operational Model Global Tropospheric Analyses, Continuing from July 1999*. Boulder, CO: Research Data Archive at the National Center for Atmospheric Research, Computational and Information Systems Laboratory. doi:10.5065/D6M043C6.
- NCEP, and DTC. 2015. "WRF-NMM Users Page | DTC." *DTC*. http://www.dtcenter.org/wrf-nmm/users/.
- NCEP, NOAA, U.S. DOC, NWS, and National Weather Service National Centers for Environmental Prediction NOAA, U.S. Department of Commerce. 2000. "NCEP FNL Operational Model Global Tropospheric Analyses, Continuing from July 1999." Boulder, CO, CO: Research Data Archive at the National Center for Atmospheric Research, Computational and Information Systems Laboratory. doi:10.5065/D6M043C6.

- Netcdf4excell. 2014. "NetCDF4Excel Add-In." <https://code.google.com/p/netcdf4excell/>.
- New World Encyclopedia. 2010. "Urbanization." *New World Encyclopedia*. http://www.newworldencyclopedia.org/entry/Urbanization#cite_note-8.
- Newman, P. W. G. 1999. "Sustainability and Cities: Extending the Metabolism Model." *Landscape and Urban Planning* 44 (4): 219–26. doi:10.1016/S0169-2046(99)00009-2.
- Nieuwolt, S. 1966. "The Urban Microclimate of Singapore." *Journal of Tropical Geography* 22: 30–37.
- Niu, Guo-Yue, Zong-Liang Yang, Kenneth E. Mitchell, Fei Chen, Michael B. Ek, Michael Barlage, Anil Kumar, et al. 2011. "The Community Noah Land Surface Model with Multiparameterization Options (Noah-MP): 1. Model Description and Evaluation with Local-Scale Measurements." *Journal of Geophysical Research* 116 (D12): D12109. doi:10.1029/2010JD015139.
- Norton, Briony A., Andrew M. Coutts, Stephen J. Livesley, Richard J. Harris, Annie M. Hunter, and Nicholas S.G. Williams. 2015. "Planning for Cooler Cities: A Framework to Prioritise Green Infrastructure to Mitigate High Temperatures in Urban Landscapes." *Landscape and Urban Planning* 134 (February): 127–38. doi:10.1016/j.landurbplan.2014.10.018.
- Nunez, M, and T R Oke. 1977. "ENERGY BALANCE OF AN URBAN CANYON." *Journal of Applied Meteorology* 16 (1): 11–19. <http://www.scopus.com/inward/record.url?eid=2-s2.0-0017439691&partnerID=40&md5=e2c5544466e74a13e76cd13da73e2512>.
- Nuss, Kevin Matthew. 2011. "Tool for Geogrid Output: WTOOLS." In *NCAR WRF Users Workshop*, Extended abstract 11. Boulder, Colorado, USA: NCAR/MMM. http://www2.mmm.ucar.edu/wrf/users/workshops/WS2011/ExtendedAbstracts2011/P3_Nuss_ExtendedAbstract_11.pdf.
- Oke, T R. 1976. "The Distinction between Canopy and Boundary-layer Urban Heat Islands." *Atmosphere* 14 (4). Taylor & Francis: 268–77. doi:10.1080/00046973.1976.9648422.
- . 1981. "Canyon Geometry and the Nocturnal Urban Heat Island: Comparison of Scale Model and Field Observations." *Journal of Climatology* 1 (3). Dept of Geography, The Univ. of British Columbia, Vancouver, B.C., Canada.: 237–54. <http://www.scopus.com/inward/record.url?eid=2-s2.0-0019675029&partnerID=40&md5=0ed0789da426a217a4fb4eda90cb4358>.
- . 1982. "The Energetic Basis of the Urban Heat Island." *Quarterly Journal of the Royal Meteorological Society* 108 (455). John Wiley & Sons, Ltd: 1–24. doi:10.1002/qj.49710845502.

- . 1984. “Towards a Prescription for the Greater Use of Climatic Principles in Settlement Planning.” *Energy and Buildings* 7 (1): 1–10. doi:[http://dx.doi.org/10.1016/0378-7788\(84\)90040-9](http://dx.doi.org/10.1016/0378-7788(84)90040-9).
- . 1995. “The Heat Island of the Urban Boundary Layer: Characteristics, Causes and Effects.” In *Wind Climate in Cities SE - 5*, edited by Jack E. Cermak, Alan G. Davenport, Erich J. Plate, and Domingos X. Viegas, 277:81–107. NATO ASI Series. Springer Netherlands. doi:10.1007/978-94-017-3686-2_5.
- . 2006. “Towards Better Scientific Communication in Urban Climate.” *Theoretical and Applied Climatology* 84 (June): 179–90. doi:10.1007/s00704-005-0153-0.
- . 2009. “Chandler, TJ 1965: The Climate of London. London: Hutchinson, 292 Pp.” *Progress in Physical Geography* 33 (3). SAGE Publications: 437–42.
- Oke, Tim R. 2006. *INITIAL GUIDANCE TO OBTAIN REPRESENTATIVE METEOROLOGICAL OBSERVATIONS AT URBAN SITES*. World Meteorological Organization. <https://www.wmo.int/pages/prog/www/IMOP/publications/IOM-81/IOM-81-UrbanMetObs.pdf>.
- Oke, Timothy R. 1988. *Boundary Layer Climates*. 2nd ed. London: Routledge.
- Oke, TR R. 1973. “City Size and the Urban Heat Island.” *Atmospheric Environment Pergamon Press* 7 (8). Elsevier: 769–79. doi:10.1016/0004-6981(73)90140-6.
- Okita, T. 1960. “Estimation of Direction of Air Flow from Observation of Rime Ice.” *Journal of Meteorology Society of Japan* 38 (4): 207–9. https://www.jstage.jst.go.jp/browse/jmsj/38/4/_contents.
- Onishi, Akio, Xin Cao, Takanori Ito, Feng Shi, and Hidefumi Imura. 2010. “Evaluating the Potential for Urban Heat-Island Mitigation by Greening Parking Lots.” *Urban Forestry & Urban Greening* 9 (4). Elsevier GmbH.: 323–32. doi:10.1016/j.ufug.2010.06.002.
- Ooyama, Katsuyuki V. 1990. “A Thermodynamic Foundation for Modeling the Moist Atmosphere.pdf.” *Journal of the Atmospheric Sciences* 47 (21): 2580–93.
- Oozeer, Muhammad Yaasiin, Andy Chan, Maggie Chel-Gee Ooi, Antonio Mauricio Zarzur, Santo Valentin Salinas, Boon-Ning Chew, Kenobi Isima Morris, and Wee-Kang Choong. 2016. “Numerical Study of the Transport and Convective Mechanisms of Biomass Burning Haze in South-Southeast Asia.” *Aerosol and Air Quality Research*, 1–14. doi:10.4209/aaqr.2015.07.0461.
- OriginLab. 2013. “OriginPro Statistical Software.” *OriginLab Corporation*. <http://www.originlab.com/index.aspx?go=Products/OriginPro>.
- Othman, Jamal, Mazrura Sahani, Mastura Mahmud, and Md Khadzir Sheikh Ahmad. 2014. “Transboundary Smoke Haze Pollution in Malaysia:

Inpatient Health Impacts and Economic Valuation.” *Environmental Pollution* 189 (June): 194–201.
doi:<http://dx.doi.org/10.1016/j.envpol.2014.03.010>.

- Otte, Tanya L, Avraham Lacser, Sylvain Dugpont, and Jason K. S. Ching. 2004. “Implementation of an Urban Canopy Parameterization in a Mesoscale Meteorological Model.” *Journal of Applied Meteorology* 43 (2002): 1648–65. doi:<http://dx.doi.org/10.1175/JAM2164.1>.
- Papangelis, Giorgos, Maria Tombrou, Aggeliki Dandou, and Themis Kontos. 2012. “An Urban ‘green Planning’ Approach Utilizing the Weather Research and Forecasting (WRF) Modeling System. A Case Study of Athens, Greece.” *Landscape and Urban Planning* 105 (1-2). Elsevier B.V.: 174–83. doi:10.1016/j.landurbplan.2011.12.014.
- Parker, David E. 2010. “Urban Heat Island Effects on Estimates of Observed Climate Change.” *Wiley Interdisciplinary Reviews: Climate Change* 1 (1). John Wiley & Sons, Inc.: 123–33. doi:10.1002/wcc.21.
- Parker, David E. 2006. “A Demonstration That Large-Scale Warming Is Not Urban.” *Journal of Climate* 19: 2882–95. doi:<http://dx.doi.org/10.1175/JCLI3730.1>.
- Perini, Katia, and Adriano Magliocco. 2014. “Effects of Vegetation, Urban Density, Building Height, and Atmospheric Conditions on Local Temperatures and Thermal Comfort.” *Urban Forestry & Urban Greening* 13 (3). Elsevier GmbH.: 495–506. doi:10.1016/j.ufug.2014.03.003.
- Pichelli, E, R Ferretti, M Cacciani, A M Siani, V Ciardini, and T Di Iorio. 2014. “The Role of Urban Boundary Layer Investigated with High-Resolution Models and Ground-Based Observations in Rome Area: A Step towards Understanding Parameterization Potentialities.” *Atmospheric Measurement Techniques* 7 (1): 315–32. doi:10.5194/amt-7-315-2014.
- Pidwirny, M. 2006. “Introduction to Applied Climatology.” In *Fundamentals of Physical Geography*, 2nd ed. <http://www.physicalgeography.net/fundamentals/7w.html>.
- Priyadarsini, Rajagopalan, Wong Nyuk Hien, and Cheong Kok Wai David. 2008. “Microclimatic Modeling of the Urban Thermal Environment of Singapore to Mitigate Urban Heat Island.” *Solar Energy* 82 (8): 727–45. doi:10.1016/j.solener.2008.02.008.
- Qaid, Adeb, and Dilshan R Ossen. 2015. “Effect of Asymmetrical Street Aspect Ratios on Microclimates in Hot, Humid Regions.” *International Journal of Biometeorology* 59 (6). Springer: 657–77. doi:10.1007/s00484-014-0878-5.
- Qu, Ruijie, Xiaolin Cui, Haiming Yan, Enjun Ma, and Jinyan Zhan. 2013. “Impacts of Land Cover Change on the Near-Surface Temperature in the North China Plain.” *Advances in Meteorology* 2013: 1–12. doi:10.1155/2013/409302.
- Rahman, Siti Rahmah A., Sharifah S. Norkhadijah, Muhammad F. Ramli,

- Mohd T. Latif, Emilia Z. Abidin, and Sarva M. Praveena. 2015. "The Assessment of Ambient Air Pollution Trend in Klang Valley, Malaysia." *World Environment* 5 (1): 1–11. doi:10.5923/j.env.20150501.01.
- Rajagopalan, Priyadarsini, Kee Chuan Lim, and Elmira Jamei. 2014. "Urban Heat Island and Wind Flow Characteristics of a Tropical City." *Solar Energy* 107 (September). Elsevier Ltd: 159–70. doi:10.1016/j.solener.2014.05.042.
- Ren, Guoyu, and Yaqing Zhou. 2014. "Urbanization Effect on Trends of Extreme Temperature Indices of National Stations over Mainland China, 1961–2008." *Journal of Climate* 27 (6). American Meteorological Society: 2340–60. doi:10.1175/JCLI-D-13-00393.1.
- Ren, Guoyu, Yaqing Zhou, Ziyang Chu, Jiangxing Zhou, Aiyang Zhang, Jun Guo, and Xuefeng Liu. 2008. "Urbanization Effects on Observed Surface Air Temperature Trends in North China." *Journal of Climate* 21 (6). American Meteorological Society: 1333–48. doi:10.1175/2007JCLI1348.1.
- Rosenfeld, Arthur H, Hashem Akbari, Joseph J Romm, and Melvin Pomerantz. 1998. "Cool Communities: Strategies for Heat Island Mitigation and Smog Reduction." Edited by R King Michael. *Energy and Buildings* 28 (1). Academic Press: 51–62. doi:10.1016/S0378-7788(97)00063-7.
- Roth, Matthias. 2007. "Review of Urban Climate Research in (Sub)tropical Regions." *International Journal of Climatology* 27 (14). John Wiley & Sons, Ltd.: 1859–73. doi:10.1002/joc.1591.
- Runnalls, K. E., and T. R. Oke. 2006. "A Technique to Detect Microclimatic Inhomogeneities in Historical Records of Screen-Level Air Temperature." *Journal of Climate* 19 (6): 959–78. doi:http://dx.doi.org/10.1175/JCLI3663.1.
- Salamanca, Francisco, Alberto Martilli, Mukul Tewari, and Fei Chen. 2010. "A Study of the Urban Boundary Layer Using Different Urban Parameterizations and High-Resolution Urban Canopy Parameters with WRF." *Journal of Applied Meteorology and Climatology* 50 (5). American Meteorological Society: 1107–28. doi:10.1175/2010JAMC2538.1.
- Salleh, S A, Z Abd Latif, A Chan, K I Morris, M C G Ooi, and W M N Wan Mohd. 2015. "Weather Research and Forecast (WRF) Model Modification of Land Surface Albedo Simulations for Urban Near Surface Temperature." *The 2015 International Conference on Space Science and Communication (IconSpace2015)*. Langkawi, Malaysia: IEEE, 243–47. doi:10.1109/IconSpace.2015.7283787.
- Salleh, S A, Z Abd Latif, W M N Wan Mohd, and A Chan. 2012. "Albedo Pattern Recognition and Time-Series Analyses in Malaysia." *Int. Arch. Photogramm. Remote Sens. Spatial Inf. Sci.* XXXIX-B7 (July). Copernicus Publications: 235–40. doi:10.5194/isprsarchives-XXXIX-B7-235-2012.

- Salleh, Siti Aekbal, Zulkiflee Abd.Latif, Wan Mohd. Naim Wan Mohd, Andy Chan, Siti Aekbal, Zulkiflee Abd, Wan Mohd. Naim Wan Mohd, and Naim Wan. 2013. "Factors Contributing to the Formation of an Urban Heat Island in Putrajaya , Malaysia." *Procedia - Social and Behavioural Sciences* 00 (UE-004): 1-11. doi:10.1016/j.sbspro.2013.11.086.
- Salleh, Siti Aekbal, Nur Suhaili Mansor, Zaharah Yusoff, and Rabiatul Adawiyah Nasir. 2012. "The Crime Ecology: Ambient Temperature vs. Spatial Setting of Crime (Burglary)." *Procedia - Social and Behavioral Sciences* 42: 212-22. doi:http://dx.doi.org/10.1016/j.sbspro.2012.04.184.
- Sani, Sham. 1972. "Some Aspects of Urban Micro-Climate in Kuala Lumpur West Malaysia." *Akademika* 1. Universiti Kebangsaan Malaysia: 85-94.
- . 1973. "Observations on the Effect of a City Form and Functions on Temperature Patterns." *Journal of Tropical Geography* 36: 60-65.
- . 1980. *The Climate of Kuala Lumpur-Petaling Jaya Area, Malaysia : A Study of the Impact of Urbanization on Local Climate within the Humid Tropics*. Bangi, [Selangor] : Universiti Kebangsaan Malaysia Press, 1980. <https://search.library.wisc.edu/catalog/999549452602121>.
- . 1983. "INADVERTENT ATMOSPHERIC MODIFICATION BY URBANIZATION WITH SPECIAL REFERENCE TO TEMPERATURE: A CASE OF KOTA KINABALU, SABAH." *Kajian Etnografi Sabah: Laporan* 3. Universiti Kebangsaan Malaysia: 61.
- . 1984. "Urban Development And Changing Patierns Of Night Time Temperatures In The Kuala Lumpur-Petaling Jaya Area Malaysia." *Jurnal Teknologi* 5 (1): 27-35. doi:10.11113/jt.v5.937.
- . 1986. "Temperatures in Kuala Lumpur and the Merging Kelang Valley Conurbation, Malaysia." *Report Prepared for UNESCO under the Ecoville Project Coordinated by the Institute of Advanced Studies, University of Malaya*.
- . 1990. "Urban Climatology in Malaysia: An Overview." *Energy and Buildings* 15 (1-2): 105-17. doi:http://dx.doi.org/10.1016/0378-7788(90)90121-X.
- . 1991a. "Urban Climate Studies in Malaysia and Their Relevance to Urban Planning and Air Quality Management in the Humid Tropics." *Ilmu Alam* 20. Dept. of Geography, National University of Malaysia: 3-20.
- . 1991b. "The State of the Malaysian Environment and Its Outlook for the 1990s." *Akademika* 38 (1).
- . 1993. "Urbanisation and Air Quality in Malaysia." *Akademika* 42 (1): 159-80. <http://ejournals.ukm.my/akademika/article/view/3162/2006>.
- . 1994. "Urbanization and the Environment." In *Proceedings of the Conference on Malaysian Development Experience: Changes and Challenges*. National Institute of Public Administration Publication, Kuala Lumpur, 456-504.

- . 1998. “Industrialization and Environment in Malaysia: Issues and Challenges.” In *APEC*, 242–65.
- Santamouris, M. 2014. “Cooling the Cities – A Review of Reflective and Green Roof Mitigation Technologies to Fight Heat Island and Improve Comfort in Urban Environments.” *Solar Energy* 103 (May). Elsevier Ltd: 682–703. doi:10.1016/j.solener.2012.07.003.
- Santhi, C, J G Arnold, J R Williams, W A Dugas, R Srinivasan, and L M Hauck. 2001. “VALIDATION OF THE SWAT MODEL ON A LARGE RWER BASIN WITH POINT AND NONPOINT SOURCES1.” *JAWRA Journal of the American Water Resources Association* 37 (5). Blackwell Publishing Ltd: 1169–88. doi:10.1111/j.1752-1688.2001.tb03630.x.
- Satterthwaite, D. 2009. “The Implications of Population Growth and Urbanization for Climate Change.” *Environment and Urbanization* 21 (2): 545–67. doi:10.1177/0956247809344361.
- Schlünzen, K. Heinke, and Jack J. Katzfey. 2003. “Relevance of Sub-Grid-Scale Land-Use Effects for Mesoscale Models.” *Tellus A* 55 (3). Blackwell Publishing Ltd.: 232–46. doi:10.1034/j.1600-0870.2003.00017.x.
- Schneider, a, M a Friedl, and D Potere. 2009. “A New Map of Global Urban Extent from MODIS Satellite Data.” *Environmental Research Letters* 4 (4): 044003. doi:10.1088/1748-9326/4/4/044003.
- Shaharuddin, A., M. H. Noorazuan, and A. Noraziah W. Takeuchi. 2014. “The Effects of Urban Heat Islands on Human Comfort: A Case of Klang Valley Malaysia.” *Global Journal on Advances Pure and Applied Sciences* 2: 1–8. <http://www.world-education-center.org/index.php/paas/article/viewArticle/3099>.
- Shahbaz, Muhammad, Nanthakumar Loganathan, Rashid Sbia, and Talat Afza. 2015. “The Effect of Urbanization, Affluence and Trade Openness on Energy Consumption: A Time Series Analysis in Malaysia.” *Renewable and Sustainable Energy Reviews* 47 (July): 683–93. doi:http://dx.doi.org/10.1016/j.rser.2015.03.044.
- Shahidan, Mohd Fairuz, Phillip J. Jones, Julie Gwilliam, and Elias Salleh. 2012. “An Evaluation of Outdoor and Building Environment Cooling Achieved through Combination Modification of Trees with Ground Materials.” *Building and Environment* 58 (December). Elsevier Ltd: 245–57. doi:10.1016/j.buildenv.2012.07.012.
- Shashua-bar, L, and M E Hoffman. 2000. “Vegetation as a Climatic Component in the Design of an Urban Street An Empirical Model for Predicting the Cooling Effect of Urban Green Areas with Trees.” *Energy and Buildings* 31: 221–35.
- Shashua-Bar, Limor, and Milo E. Hoffman. 2004. “Quantitative Evaluation of Passive Cooling of the UCL Microclimate in Hot Regions in Summer, Case Study: Urban Streets and Courtyards with Trees.” *Building and Environment* 39 (9): 1087–99. doi:10.1016/j.buildenv.2003.11.007.

- Shashua-Bar, Limor, David Pearlmutter, and Evyatar Erell. 2009. "The Cooling Efficiency of Urban Landscape Strategies in a Hot Dry Climate." *Landscape and Urban Planning* 92 (3–4): 179–86. doi:<http://dx.doi.org/10.1016/j.landurbplan.2009.04.005>.
- Shem, Willis, and Marshall Shepherd. 2009. "On the Impact of Urbanization on Summertime Thunderstorms in Atlanta: Two Numerical Model Case Studies." *Atmospheric Research* 92 (2): 172–89. doi:<http://dx.doi.org/10.1016/j.atmosres.2008.09.013>.
- Shuid, Syafiee. 2004. "Urbanization and Housing in Kuala Lumpur City Centre: Issues and Future Challenges." In *19th EAROPH WORLD PLANNING AND HOUSING CONGRESS*, 1–14. Melbourne, Australia. <http://irep.iium.edu.my/4159/1/earoph2004.pdf>.
- Singh, W Suparta and R Rahman and M S J. 2014. "Monitoring the Variability of Precipitable Water Vapor over the Klang Valley, Malaysia during Flash Flood." *IOP Conference Series: Earth and Environmental Science* 20 (1): 12057. doi:10.1088/1755-1315/20/1/012057.
- Skamarock, W. C., J. B. Klemp, J. Dudhia, D. O. Gill, D. M. Barker, M. G. Duda, X.-Y. Huang, W. Wang, and J. G. Powers. 2008. *A Description of the Advanced Research WRF Version 3. NCAR Technical Note. NCAR Technical Note NCAR/TN-475+STR*. Boulder, Colorado, USA: National Center for Atmospheric Research: Mesoscale and Microscale Meteorology Division. doi:10.5065/D68S4MVH.
- Skamarock, William C., and Joseph B. Klemp. 2008. "A Time-Split Nonhydrostatic Atmospheric Model for Weather Research and Forecasting Applications." *Journal of Computational Physics* 227 (7): 3465–85. doi:10.1016/j.jcp.2007.01.037.
- Soh, Mazlan Bin Che. 2012. "Crime and Urbanization: Revisited Malaysian Case." *Procedia - Social and Behavioral Sciences* 42: 291–99. doi:<http://dx.doi.org/10.1016/j.sbspro.2012.04.193>.
- Steeneveld, G.J., S. Koopmans, B.G. Heusinkveld, and N.E. Theeuwes. 2014. "Refreshing the Role of Open Water Surfaces on Mitigating the Maximum Urban Heat Island Effect." *Landscape and Urban Planning* 121 (January): 92–96. doi:10.1016/j.landurbplan.2013.09.001.
- Stewart, I. D., and T. R. Oke. 2012. "Local Climate Zones for Urban Temperature Studies." *Bulletin of the American Meteorological Society* 93 (12): 1879–1900. doi:10.1175/BAMS-D-11-00019.1.
- Stull, R B. 1988. "An Introduction to Boundary Layer Meteorology." *Book* 13: 666. doi:10.1007/978-94-009-3027-8.
- Sullivan, William C, Olin M Anderson, and Sarah Taylor Lovell. 2004. "Agricultural Buffers at the Rural–urban Fringe: An Examination of Approval by Farmers, Residents, and Academics in the Midwestern United States." *Landscape and Urban Planning* 69 (2–3): 299–313. doi:<http://dx.doi.org/10.1016/j.landurbplan.2003.10.036>.

- Sundborg, Å. 1950. "Local Climatological Studies of the Temperature Conditions in an Urban Area." *Tellus* 2 (3). Blackwell Publishing Ltd: 222–32. doi:10.1111/j.2153-3490.1950.tb00333.x.
- Taha, Haider. 1997. "Urban Climates and Heat Islands: Albedo, Evapotranspiration, and Anthropogenic Heat." *Energy and Buildings* 25 (2). Elsevier: 99–103. doi:10.1016/S0378-7788(96)00999-1.
- TCPA. 2011. *Re-Imagining Garden Cities for the 21st Century: Benefits and Lessons in Bringing Forward Comprehensively Planned New Communities*. Hertfordshire, England, UK. http://www.tcpa.org.uk/data/files/reimagining_garden_cities_final.pdf.
- Tehrany, Mahyat Shafapour, Biswajeet Pradhan, and Mustafa Neamah Jebur. 2013. "Remote Sensing Data Reveals Eco-Environmental Changes in Urban Areas of Klang Valley, Malaysia: Contribution from Object Based Analysis." *Journal of the Indian Society of Remote Sensing* 41 (4): 981–91. doi:10.1007/s12524-013-0289-9.
- Terjung, Werner H. 1976. "Climatology for Geographers." *Annals of the Association of American Geographers* 66 (2). Taylor & Francis, Ltd. on behalf of the Association of American Geographers: 199–222. doi:10.2307/2562466.
- Terjung, Werner H, and Stella S-F. Louie. 1974. "A Climatic Model of Urban Energy Budgets." *Geographical Analysis* 6 (4). Blackwell Publishing Ltd: 341–67. doi:10.1111/j.1538-4632.1974.tb00519.x.
- Tewari, Mukul, Fei Chen, Hiroyuki Kusaka, and Shiguang Miao. 2007. *Coupled WRF / Unified Noah / Urban-Canopy Modeling System*. Boulder CO, Japan.
- Thani, Sharifah Khalizah Syed Othman, Nik Hanita Nik Mohamad, and Sharifah Mastura Syed Abdullah. 2013. "The Influence of Urban Landscape Morphology on the Temperature Distribution of Hot-Humid Urban Centre." *Procedia - Social and Behavioral Sciences* 85 (September). Elsevier B.V.: 356–67. doi:10.1016/j.sbspro.2013.08.365.
- Tomlinson, Charlie J, Lee Chapman, John E Thornes, and Christopher J Baker. 2011. "Including the Urban Heat Island in Spatial Heat Health Risk Assessment Strategies: A Case Study for Birmingham, UK." *International Journal of Health Geographics* 10 (1). BioMed Central Ltd: 42. doi:10.1186/1476-072X-10-42.
- Tong, Hua, Andrew Walton, Jianguo Sang, and Johnny C.L. Chan. 2005. "Numerical Simulation of the Urban Boundary Layer over the Complex Terrain of Hong Kong." *Atmospheric Environment* 39 (19): 3549–63. doi:10.1016/j.atmosenv.2005.02.045.
- United Nations. 2014. "Current World Population." *United Nations Department of Economics and Social Affairs*. http://www.geohive.com/earth/population_now.aspx.
- Varikoden, Hamza, B Preethi, A A Samah, and C A Babu. 2011. "Seasonal

Variation of Rainfall Characteristics in Different Intensity Classes over Peninsular Malaysia.” *Journal of Hydrology* 404 (1–2): 99–108. doi:http://dx.doi.org/10.1016/j.jhydrol.2011.04.021.

- Vidrih, B., and S. Medved. 2013. “Multiparametric Model of Urban Park Cooling Island.” *Urban Forestry & Urban Greening* 12 (2): 220–29. doi:10.1016/j.ufug.2013.01.002.
- Wang, Shaojian, Chuanglin Fang, Xingliang Guan, Bo Pang, and Haitao Ma. 2014. “Urbanisation, Energy Consumption, and Carbon Dioxide Emissions in China: A Panel Data Analysis of China’s Provinces.” *Applied Energy* 136 (December): 738–49. doi:http://dx.doi.org/10.1016/j.apenergy.2014.09.059.
- Wang, Shuyu, Congbin Fu, Helin Wei, Yun Qian, Zhe Xiong, Jinming Feng, Deming Zhao, et al. 2015. “Regional Integrated Environmental Modeling System: Development and Application.” *Climatic Change* 129 (3-4). Springer Netherlands: 499–510. doi:10.1007/s10584-013-0973-3.
- Wang, W., D. Barker, J. Bray, C. Bruyere, M. Duda, J. Dudhia, D. Gill, J. Michalakes, S. Rizvi, and X. Zhang. 2012. *User’s Guide for Advanced Research WRF (ARW) Modeling System Version 3.4, Mesoscale and Microscale Meteorology Division - National Center for Atmospheric Research (MMN-NCAR)*.
- Wang, Xuemei, Jingbiao Liao, Jian Zhang, Chong Shen, Weihua Chen, Beicheng Xia, and Tijian Wang. 2014. “A Numeric Study of Regional Climate Change Induced by Urban Expansion in the Pearl River Delta, China.” *Journal of Applied Meteorology and Climatology* 53 (2). American Meteorological Society: 346–62. doi:10.1175/JAMC-D-13-054.1.
- Weaver, David B, and Laura J Lawton. 2001. “Resident Perceptions in the Urban–Rural Fringe.” *Annals of Tourism Research* 28 (2): 439–58. doi:http://dx.doi.org/10.1016/S0160-7383(00)00052-9.
- Widodo, Johannes. 2012. “Urban Environment and Human Behaviour: Learning from History and Local Wisdom.” *Procedia - Social and Behavioral Sciences* 42: 6–11. doi:http://dx.doi.org/10.1016/j.sbspro.2012.04.161.
- Wijeyesekera, Devapriya Chitral, Noor Affida, Raffika Binti, Mohamad Nazari, Sin Mei Lim, Mohd Idrus, Mohd Masirin, and John Walsh. 2012. “INVESTIGATION INTO THE URBAN HEAT ISLAND EFFECTS FROM ASPHALT PAVEMENTS.” *OIDA International Journal of Sustainable Development* 5 (6): 97–118.
- Wilks, Daniel S. 2006. *Statistical Methods in the Atmospheric Sciences*. Edited by RENATA DMOWSKA, DENNIS HARTMANN, and H. THOMAS ROSSBY. 2nd Editio. Oxford, UK: INTERNATIONAL GEOPHYSICS SERIES.
- Willmott, Cort J. 1981. “On the Validation of Models.” *Physical Geography* 2 (2): 184–94. doi:10.1080/02723646.1981.10642213.

- Willmott, Cort J. 1982. "Some Comments on the Evaluation of Model Performance." *Bulletin of the American Meteorological Society* 63 (11): 1309–13. doi:10.1175/1520-0477(1982)063<1309:SCOTEO>2.0.CO;2.
- Willmott, Cort J., Steven G. Ackleson, Robert E. Davis, Johannes J. Feddema, Katherine M. Klink, David R. Legates, James O'Donnell, and Clinton M. Rowe. 1985. "Statistics for the Evaluation and Comparison of Models." *Journal of Geophysical Research* 90 (C5): 8995. doi:10.1029/JC090iC05p08995.
- Winfield, G. F. 1973. "The Impact of Urbanization on Agricultural Processes." *The ANNALS of the American Academy of Political and Social Science*.
- WMO. 2015. "World Meteorological Organization: World Weather Information Service." *WMO*. <http://www.worldweather.org/en/home.html>.
- Wolman, Abel. 1965. "THE METABOLISM OF CITIES." *Scientific American* 213: 179–90. doi:10.1038/scientificamerican0965-178.
- Wong, Nyuk Hien, and Chen Yu. 2005. "Study of Green Areas and Urban Heat Island in a Tropical City." *Habitat International* 29 (3). Elsevier: 547–58. doi:10.1016/j.habitatint.2004.04.008.
- Yaakob, U, T Masron, and F Masami. 2010. "Ninety Years of Urbanization in Malaysia: A Geographical Investigation of Its Trends and Characteristics." *Journal of Ritsumeikan Social Science and Humanity* 4: 79–101. http://www.ritsumei.ac.jp/acd/re/k-rsc/hss/book/pdf/vol04_05.pdf.
- Yang, Xinyan. 2013. "Temporal Variation of Urban Surface and Air Temperature." University of Hong Kong. <http://hub.hku.hk/handle/10722/195964>.
- Yao, Xiaowei, Zhanqi Wang, and Hua Wang. 2015. "Impact of Urbanization and Land-Use Change on Surface Climate in Middle and Lower Reaches of the Yangtze River, 1988–2008."
- Yusoff, Mariney Mohd. 2007. "Plans, People and Floods : The Problems of Urbanisation in the Klang Valley, Malaysia." The University of Leeds. <http://etheses.whiterose.ac.uk/id/eprint/3749>.
- Yusuf, Yusuf Ahmed, Biswajeet Pradhan, and Mohammed O. Idrees. 2014. "Spatio-Temporal Assessment of Urban Heat Island Effects in Kuala Lumpur Metropolitan City Using Landsat Images." *Journal of the Indian Society of Remote Sensing* 42 (4): 829–37. doi:10.1007/s12524-013-0342-8.
- ZenTech. 2010. "World Climate Guide." *ZenTech*. <http://www2m.biglobe.ne.jp/ZenTech/English/Climate/>.
- Zhang, Biao, Gao-di Xie, Ji-xi Gao, and Yang Yang. 2014. "The Cooling Effect of Urban Green Spaces as a Contribution to Energy-Saving and Emission-Reduction: A Case Study in Beijing, China." *Building and Environment* 76 (June): 37–43. doi:10.1016/j.buildenv.2014.03.003.

- Zhang, Da-Lin, Yi-Xuan Shou, and Russell R. Dickerson. 2009. "Upstream Urbanization Exacerbates Urban Heat Island Effects." *Geophysical Research Letters* 36 (24): L24401. doi:10.1029/2009GL041082.
- Zhang, Da-Lin, Yi-Xuan Shou, Russell R. Dickerson, and Fei Chen. 2011. "Impact of Upstream Urbanization on the Urban Heat Island Effects along the Washington–Baltimore Corridor." *Journal of Applied Meteorology and Climatology* 50 (10). American Meteorological Society: 2012–29. doi:10.1175/JAMC-D-10-05008.1.
- Zhang, Kaixuan, Rui Wang, Chenchen Shen, and Liangjun Da. 2010. "Temporal and Spatial Characteristics of the Urban Heat Island during Rapid Urbanization in Shanghai, China." *Environmental Monitoring and Assessment* 169 (1-4). Springer Netherlands: 101–12. doi:10.1007/s10661-009-1154-8.
- Zhang, Ning, Zhiqiu Gao, Xuemei Wang, Yan Chen, Z. Gao G., Xuemei Wang, and Y. Chen. 2010. "Modeling the Impact of Urbanization on the Local and Regional Climate in Yangtze River Delta, China." *Theoretical Applied Climatology* 102 (3-4). Springer Vienna: 331–41. doi:10.1007/s00704-010-0263-1.
- Zhao, Nan. 2012. *Evaluation of Chengdu's Garden City Project by Ebenezer Howard's Garden City Theory*. USA: University of Oregon. https://scholarsbank.uoregon.edu/xmlui/bitstream/handle/1794/12631/Nan_Zhao_Exit_Project.pdf?sequence=1.
- Zhou, Liming, Robert E Dickinson, Yuhong Tian, Jingyun Fang, Qingxiang Li, Robert K Kaufmann, Compton J Tucker, and Ranga B Myneni. 2004. "Evidence for a Significant Urbanization Effect on Climate in China." *Proceedings of the National Academy of Sciences of the United States of America* 101 (26). National Academy of Sciences: 9540–44. doi:10.1073/pnas.0400357101.

Appendix

Appendix

Appendix 1. namelist.wps

```
&share
wrf_core = 'ARW',
max_dom = 3,
start_date = '2011-09-22_00:00:00', '2011-09-22_00:00:00', '2011-09-22_00:00:00', '2011-01-30_12:00:00',
end_date = '2011-09-24_18:00:00', '2011-09-24_18:00:00', '2011-09-24_18:00:00', '2011-02-15_18:00:00',
interval_seconds = 21600,
io_form_geogrid = 2,
opt_output_from_geogrid_path = '/home/ezakm2/kenobi/',
debug_level = 0,
/
&geogrid
parent_id = 1,1,2,3,
parent_grid_ratio = 1,3,3,3,
i_parent_start = 1,29,25,100,
j_parent_start = 1,28,25,28,
e_we = 79,67,55,91,
e_sn = 77,67,55,106,
geog_data_res = 'modis_30s+2m','modis_30s+30s','modis_30s+30s','modis_30s+30s',
dx = 2700,
dy = 2700,
map_proj = 'mercator',
ref_lat = 2.927,
ref_lon = 101.69,
truelat1 = 2.927,
truelat2 = 0,
stand_lon = 101.69,
geog_data_path = '/home/WRF_DATA/kenobi/geog',
opt_geogrid_tbl_path = '/home/ezakm2/kenobi/',
ref_x = 39.5,
ref_y = 38.5,
/
&ungrib
out_format = 'WPS',
prefix = 'FILE',
/
&metgrid
fg_name = 'FILE',
io_form_metgrid = 2,
opt_output_from_metgrid_path = '/home/ezakm2/kenobi/',
opt_metgrid_tbl_path = '/home/ezakm2/kenobi/',
/
&mod_levs
press_pa = 201300, 200100, 100000,
          95000, 90000,
          85000, 80000,
          75000, 70000,
          65000, 60000,
          55000, 50000,
          45000, 40000,
          35000, 30000,
          25000, 20000,
          15000, 10000,
          5000, 1000
/
&domain_wizard
grib_vtable = 'Vtable.GFS',
dwiz_name = putrajaya_eva
dwiz_desc = 3-nested_domain
dwiz_user_rect_x1 = 1565
dwiz_user_rect_y1 = 467
dwiz_user_rect_x2 = 1605
dwiz_user_rect_y2 = 514
dwiz_show_political = true
dwiz_center_over_gmt = true
dwiz_latlon_space_in_deg = 10
dwiz_latlon_linecolor = -8355712
dwiz_map_scale_pct = 12.5
dwiz_map_vert_scrollbar_pos = 207
dwiz_map_hORIZ_scrollbar_pos = 1047
dwiz_gridpt_dist_km = 2.7
dwiz_mpi_command =
dwiz_tcvitals = null
dwiz_bigmap = Y
/
```

Appendix 2. Some sections of the GEOGRID.TBL

```

# See options.txt for a (somewhat up to date) list of the
# options that may be specified here.
=====
name = HGT_M
  priority = 1
  dest_type = continuous
  df_dx=SLPX
  df_dy=SLPY
  smooth_option = smth-desmth_special; smooth_passes=1
  fill_missing=0.
  interp_option = 30s:average_gcell(4.0)+four_pt+average_4pt
  interp_option = 2m:four_pt
  interp_option = 5m:four_pt
  interp_option = 10m:four_pt
  interp_option = default:four_pt
  rel_path= 30s:topo_30s/
  rel_path= 2m:topo_2m/
  rel_path= 5m:topo_5m/
  rel_path= 10m:topo_10m/
  rel_path= default:topo_2m/
=====
name=LANDUSEF
  priority=1
  dest_type=categorical
  z_dim_name=land_cat
  landmask_water = modis_30s:17 # Calculate a landmask from this field
  landmask_water = modis_lakes:17,21 # Calculate a landmask from this field
  landmask_water = usgs_lakes:16,28 # Calculate a landmask from this field
  landmask_water = nlcd2006:17 # Calculate a landmask from this field
  landmask_water = default:16 # Calculate a landmask from this field
  dominant=LU_INDEX
  interp_option = nlcd2006:nearest_neighbor
  interp_option = ssib_10m:four_pt
  interp_option = ssib_5m:four_pt
  interp_option = modis_30s:nearest_neighbor
  interp_option = 30s:nearest_neighbor
  interp_option = usgs_lakes:nearest_neighbor
  interp_option = modis_lakes:nearest_neighbor
  interp_option = 2m:four_pt
  interp_option = 5m:four_pt
  interp_option = 10m:four_pt
  interp_option = default:four_pt
  rel_path= nlcd2006:nlcd2006_ll_30s/
  rel_path= ssib_10m:ssib_landuse_10m/
  rel_path= ssib_5m:ssib_landuse_5m/
  rel_path= modis_30s:modis_landuse_2011_33class_30s/ ; directory replaced to solved with 33 class
  rel_path= 30s:landuse_30s/
  rel_path= usgs_lakes:landuse_30s_with_lakes/
  rel_path= modis_lakes:modis_landuse_21class_30s/
  rel_path= 2m:landuse_2m/
  rel_path= 5m:landuse_5m/
  rel_path= 10m:landuse_10m/
  rel_path= default:landuse_2m/
=====
; ; ;
; ; ;
; ; ;
; ; ;
=====
#name=URB_PARAM
# priority=1
# dest_type=continuous
# fill_missing = 0.
# z_dim_name=num_urb_params
# interp_option=default:nearest_neighbor
# rel_path=default:NUDAPT44_1km/
=====

```

Appendix 3. Sample of *Vtable* file used in this research

```

GRIB1|Level|From |To |meterid |meterid |meterid |GRIB2|GRIB2|GRIB2|GRIB2|
Param|Type |Level1|Level2| Name | Units | Description |Discp|Catgy|Param|Level|
-----+-----+-----+-----+-----+-----+-----+-----+-----+-----+-----+
11 | 100 | * | | TT | K | Temperature | 0 | 0 | 0 | 100 |
33 | 100 | * | | UU | m s-1 | U | 0 | 2 | 2 | 100 |
34 | 100 | * | | VV | m s-1 | V | 0 | 2 | 3 | 100 |
52 | 100 | * | | RH | % | Relative Humidity | 0 | 1 | 1 | 100 |
7 | 100 | * | | HGT | m | Height | 0 | 3 | 5 | 100 |
11 | 105 | 2 | | TT | K | Temperature at 2 m | 0 | 0 | 0 | 103 |
52 | 105 | 2 | | RH | % | Relative Humidity at 2 m | 0 | 1 | 1 | 103 |
33 | 105 | 10 | | UU | m s-1 | U at 10 m | 0 | 2 | 2 | 103 |
34 | 105 | 10 | | VV | m s-1 | V at 10 m | 0 | 2 | 3 | 103 |
1 | 1 | 0 | | PSFC | Pa | Surface Pressure | 0 | 3 | 0 | 1 |
2 | 102 | 0 | | PMSL | Pa | Sea-level Pressure | 0 | 3 | 1 | 101 |
144 | 112 | 0 | 10 | SM000010 | fraction | Soil Moist 0-10 cm below grn layer (Up) | 2 | 0 | 192 | 106 |
144 | 112 | 10 | 40 | SM010040 | fraction | Soil Moist 10-40 cm below grn layer | 2 | 0 | 192 | 106 |
144 | 112 | 40 | 100 | SM040100 | fraction | Soil Moist 40-100 cm below grn layer | 2 | 0 | 192 | 106 |
144 | 112 | 100 | 200 | SM100200 | fraction | Soil Moist 100-200 cm below gr layer | 2 | 0 | 192 | 106 |
144 | 112 | 10 | 200 | SM010200 | fraction | Soil Moist 10-200 cm below gr layer | 2 | 0 | 192 | 106 |
11 | 112 | 0 | 10 | ST000010 | K | T 0-10 cm below ground layer (Upper) | 0 | 0 | 0 | 106 |
11 | 112 | 10 | 40 | ST010040 | K | T 10-40 cm below ground layer (Upper) | 0 | 0 | 0 | 106 |
11 | 112 | 40 | 100 | ST040100 | K | T 40-100 cm below ground layer (Upper) | 0 | 0 | 0 | 106 |
11 | 112 | 100 | 200 | ST100200 | K | T 100-200 cm below ground layer (Bottom) | 0 | 0 | 0 | 106 |
11 | 112 | 10 | 200 | ST010200 | K | T 10-200 cm below ground layer (Bottom) | 0 | 0 | 0 | 106 |
91 | 1 | 0 | | SEAICE | proprtn | Ice flag | 10 | 2 | 0 | 1 |
81 | 1 | 0 | | LANDSEA | proprtn | Land/Sea flag (1=land, 0 or 2=sea) | 2 | 0 | 0 | 1 |
7 | 1 | 0 | | SOILHGT | m | Terrain field of source analysis | 0 | 3 | 5 | 1 |
11 | 1 | 0 | | SKINTEMP | K | Skin temperature (can use for SST also) | 0 | 0 | 0 | 1 |
65 | 1 | 0 | | SNOW | kg m-2 | Water equivalent snow depth | 0 | 1 | 13 | 1 |
| 1 | 0 | | SNOWH | m | Physical Snow Depth | 0 | 1 | | 1 |
-----+-----+-----+-----+-----+-----+-----+-----+-----+-----+-----+
#
# For SNOWH, NCEP starts with the AFWA snow depth analysis and converts it to a water-equivalent.
# For some reason, NCEP uses a different ratio in the GFS/GDAS than in the NAM and that which is assumed in WRF.
# Therefore, we need to adjust SNOW and compute SNOWH in ungrib.

```

Appendix 4. Reduced section of the METGRID.TBL

```

=====
name=ST
    z_dim_name=num_st_layers
    derived=yes
# IF
    fill_lev = 10 : ST000010(200100)
    fill_lev = 40 : ST010040(200100)
    fill_lev = 100 : ST040100(200100)
    fill_lev = 200 : ST100200(200100)
# ELSE IF
    fill_lev = 10 : ST000010(200100)
    fill_lev = 35 : ST010035(200100)
    fill_lev = 100 : ST035100(200100)
    fill_lev = 255 : ST100255(200100)
# ELSE IF
    fill_lev = 10 : ST000010(200100)
    fill_lev = 200 : ST010200(200100)
# ELSE
    fill_lev = 7 : ST000007(200100)
    fill_lev = 28 : ST007028(200100)
    fill_lev = 100 : ST028100(200100)
    fill_lev = 255 : ST100255(200100)
=====
name=SM
    z_dim_name=num_sm_layers
    derived=yes
# IF
    fill_lev = 10 : SM000010(200100)
    fill_lev = 40 : SM010040(200100)
    fill_lev = 100 : SM040100(200100)
    fill_lev = 200 : SM100200(200100)
# ELSE IF
    fill_lev = 10 : SM000010(200100)
    fill_lev = 35 : SM010035(200100)
    fill_lev = 100 : SM035100(200100)
    fill_lev = 255 : SM100255(200100)
# ELSE IF
    fill_lev = 10 : SM000010(200100)
    fill_lev = 200 : SM010200(200100)
# ELSE
    fill_lev = 7 : SM000007(200100)
    fill_lev = 28 : SM007028(200100)
    fill_lev = 100 : SM028100(200100)
    fill_lev = 255 : SM100255(200100)
=====
;      ;      ;      ;
;      ;      ;      ;
;      ;      ;      ;
=====
name=T0
    interp_option=four_pt+average_4pt+search
    masked=land
    interp_mask=landmask(1)
    missing_value=200.
    fill_missing=-20.
=====

```

Appendix 5. Reduced section of the namelist.input file

```

&time_control
run_days      = 0,
run_hours     = 0,
run_minutes   = 0,
run_seconds   = 0,
start_year    = 2011, 2011, 2011, 2011,
start_month   = 09, 09, 09, 01,
start_day     = 22, 22, 22, 30,
start_hour    = 00, 00, 00, 12,
start_minute  = 00, 00, 00, 00,
start_second  = 00, 00, 00, 00,
end_year      = 2011, 2011, 2011, 2011,
end_month     = 09, 09, 09, 02,
end_day       = 24, 24, 24, 24,
end_hour      = 18, 18, 18, 18,
end_minute    = 00, 00, 00, 00,
end_second    = 00, 00, 00, 00,
interval_seconds = 21600
input_from_file = .true., .true., .true., .true.,
history_interval = 180, 60, 60, 60,
frames_per_outfile = 1000, 1000, 1000, 1000,
restart        = .false.,
restart_interval = 5000,
io_form_history = 2
io_form_restart = 2
io_form_input   = 2
io_form_boundary = 2
debug_level     = 0
io_form_auxinput4 = 2,
auxinput4_inname = "vrflowinp_d01"
auxinput4_interval = 360,
/
&domains
time_step      = 30,
time_step_fract_num = 0,
time_step_fract_den = 1,
max_dom       = 3,
e_we          = 79, 67, 55, 91,
e_sn          = 77, 67, 55, 106,
e_vert        = 32, 32, 32, 38,
num_soil_layers = 4,
sf_urban_physics = 1, 1, 1, 1,
num_land_cat   = 33,
sst_update     = 0,
tmn_update     = 1,
sst_skin       = 1,
bucket_mm      = 100.0,
maxiens = 1,
maxens = 3,
maxens2 = 3,
maxens3 = 16,
ensdim = 144,
/
; ; ; ; ; ; ;
/

&grib2
/

&namelist_quilt
nio_tasks_per_group = 0,
nio_groups = 1,
/

```

Appendix 6. Sample of ncl script for determining model nearest grid to a location on ground

```

load "$NCARG_ROOT/lib/ncarg/nclscripts/csm/gsn_code.ncl"
load "$NCARG_ROOT/lib/ncarg/nclscripts/csm/gsn_csm.ncl"
load "$NCARG_ROOT/lib/ncarg/nclscripts/csm/contributed.ncl"
load "$NCARG_ROOT/lib/ncarg/nclscripts/wrf/WRFUserARW.ncl"

;-----
; This function is not currently being used.
;-----
function wrf_map_resources_fix(a,res2)
begin
  res2 = wrf_map_resources(a,res2)
  res2@tmYRON      = True
  res2@tmXTOn     = True
  res2@mpUSStateLineThicknessF = 1.0
  res2@mpUSStateLineColor = "Black"
  res2@mpPerimLineColor = "Black"
  res2@mpNationalLineThicknessF = 1.0
  res2@mpNationalLineColor = "Black"
  res2@mpLimbLineThicknessF = 1.0
  res2@mpLimbLineColor = "Black"
  res2@mpGeophysicalLineThicknessF = 1.0
  res2@mpGeophysicalLineColor = "Black"
  return(res2)
end

;-----
; Main code
;-----
begin
; dir = "../Data/WRF/"
; a = addfile(dir+"wrfout_d03_2012-07-12_12:00:00","r")

a = addfile("wrfout_d03_2011-09-22_00:00:00","r")
xlat = a->XLAT(0,,:)
xlon = a->XLONG(0,,:)

latval = 2.917 ; The lat of the position in degrees
lonval = 101.599 ; The longitude of the desired position in degrees
;-----
Other part of script left
;-----
; Attach the recalculated lat/lon marker. This should be in
; exact same location as calculated lat/lon marker.
;
mkres@gsMarkerIndex = 6 ; outlined square
mkres@gsMarkerColor = "purple"
txres@txFontColor = mkres@gsMarkerColor
dum9 = gsn_add_polymarker(wks,plot_old,latlon_old(0),latlon_old(1),mkres)
dum10 = gsn_add_polymarker(wks,plot_new,latlon_new(0),latlon_new(1),mkres)
txres@txJust = "CenterRight"
dum11 = gsn_add_text(wks,plot_old,"Calculated ",latlon_old(0),latlon_old(1),txres)
dum12 = gsn_add_text(wks,plot_new,"Calculated ",latlon_new(0),latlon_new(1),txres)

;
;calculating the corresponding grid point of the lat and lon.
;
draw(plot_old) ; This draws the map and all the attached stuff
frame(wks)
draw(plot_new)
frame(wks)

end

```

WRFARW basic governing equations

Appendix 7. WRF basic equations

WRFARW (hereinafter ARW) solver integrates the compressible, nonhydrostatic (with a hydrostatic option) prognostic equations cast in flux form using variables that have conservation properties (conserve mass, momentum, entropy, and scalars), following the Ooyama (1990) philosophy. Formulated equations are adapted using Laprise (1992) terrain-following hydrostatic-pressure vertical coordinate denoted by η and defined as

$$\eta = \frac{(p_h - p_{ht})}{\mu}, \quad \text{where } \mu = p_{hs} - p_{ht}. \quad (1)$$

p_h is the hydrostatic component of the pressure, and p_{hs} and p_{ht} refer to values along the surface and top boundaries, respectively. It is noteworthy that the vertical coordinate definition of (1), proposed by Laprise (1992), is the traditional coordinate σ employed in many hydrostatic atmospheric models (Chu 2003). Values of η vary from 1 at the surface to 0 at the upper boundary of the model domain (see Fig. 0:1). η coordinate is also called a mass vertical coordinate

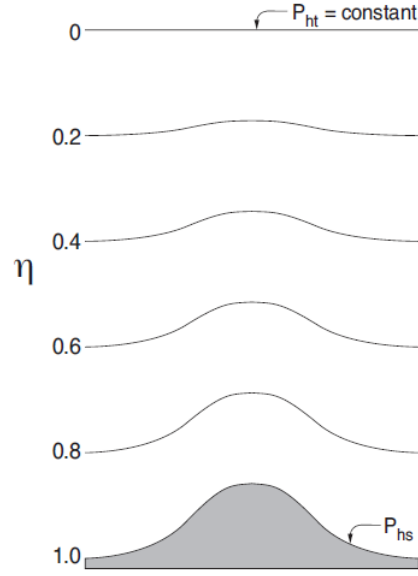


Fig. 0:1. Depiction of the ARW η coordinate system (Skamarock et al. 2008)

$\mu(x, y)$ represents the mass per unit area within the column in the model domain at (x, y) . Thus the appropriate flux form variables are

$$V = \mu v = (U, V, W), \Omega = \mu \dot{\eta}, \Theta = \mu \dot{\theta}. \quad (2)$$

$v = (u, v, w)$ are the covariant velocities in the two horizontal and vertical directions, respectively, while $\omega = \dot{\eta}$ is the contravariant ‘vertical’ velocity and θ is the potential temperature. Hence, the flux form of the Euler equations using the variables defined above become,

$$\partial_t U + (\nabla \cdot Vu) - \partial_x(p\phi_\eta) + \partial_\eta(p\phi_x) = F_u, \quad (3)$$

$$\partial_t V + (\nabla \cdot Vv) - \partial_y(p\phi_\eta) + \partial_\eta(p\phi_y) = F_v, \quad (4)$$

$$\partial_t W + (\nabla \cdot Vw) - g(\partial_\eta p - \mu) = F_w, \quad (5)$$

$$\partial_t \Theta + (\nabla \cdot V\theta) = F_\Theta, \quad (6)$$

$$\partial_t \mu + (\nabla \cdot V) = 0, \quad (7)$$

$$\partial_t \phi + \mu^{-1}[(V \cdot \nabla \phi) - gW] = 0, \quad (8)$$

where the non-conserved variables $\phi = gz$ (the geopotential), p (pressure), and $\alpha = 1/\rho$ (the inverse density). The diagnostic relationship for the inverse density is shown in (9),

$$\partial_{\eta}\phi = -\alpha\mu, \quad (9)$$

and the equation of state

$$p = p_0(R_a\theta/p_0\alpha)^{\gamma}. \quad (10)$$

Note, from (3) to (10), the subscripts x , y and η denote differentiation,

$$\nabla \cdot Va = \partial_x(Ua) + \partial_y(Va) + \partial_{\eta}(\Omega a), \quad \text{and} \quad \nabla \cdot Va = U\partial_x a + V\partial_y a + \Omega\partial_{\eta} a,$$

where a represents a generic variable $\gamma = c_p/c_v = 1.4$ is the ratio of the heat capacities for dry air, while R_a is the gas constant for dry air, and p_0 the reference pressure, with a typical value of 0.1 MPa. The terms F_u , F_v , F_w and F_{θ} , are the forcing terms resulting from model physics, turbulent mixing, spherical projections, and the earth's rotation.

The prognostic equations from (3) to (8) are expressed in the conservative form except for (8) which is the material derivative of the definition of the geopotential. Equation (8) could also be expressed in flux form but is rather ignored because of lack of any advantage in doing so since $\mu\phi$ is not a conserved quantity. It should be noted that the relation for hydrostatic balance (9) is a diagnostic relation that is formally part of the coordinate definition and does not represent a constraint on the solution. In the hydrostatic counterpart to the nonhydrostatic equations, (9) replaces the vertical momentum equation (5) and becomes a constraint on the solution. Adapting same Euler equations cast in the flux form for the inclusion of moisture on the ARW calculations yielded (11),

$$p = p_0(R_d\theta_m/p_0\alpha_d)^\gamma, \quad (11)$$

where $\alpha = \alpha_d(1 + q_v + q_c + q_r + q_i + \dots)^{-1}$ is the inverse density taking into account the full parcel density, while α_d is the inverse density of the dry air ($1/\rho_d$). q_* are the mixing ratios (i.e., mass per mass of dry air) for water vapour, cloud, rain, ice, etc. Also, $\theta_m = \theta(1 + (R_v/R_d)q_v) \approx \theta(1 + 1.61q_v)$.

The above equations are excerpt from the NCAR ARW technical note, and for more details and other physical variables cast in the flux form and calculated by the ARW model, the NCAR WRFARW Technical note (Skamarock et al. 2008) should be consulted.